NASA TECHNICAL REPORT

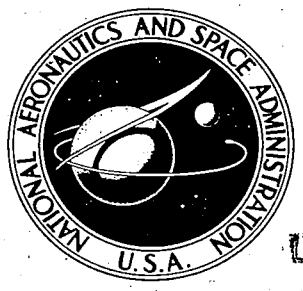

NASA TR R-233

NASA TR R-233

SYNCOM ENGINEERING REPORT

VOLUME I

by Syncom Projects Office

Goddard Space Flight Center
Greenbelt, Md.

NATIONAL AERONAUTICS AND SPACE ADMINISTRATION • WASHINGTON, D. C. • MARCH 1966

SYNCOM ENGINEERING REPORT

VOLUME I

By Syncom Projects Office

Goddard Space Flight Center
Greenbelt, Md.

NATIONAL AERONAUTICS AND SPACE ADMINISTRATION

For sale by the Clearinghouse for Federal Scientific and Technical Information
Springfield, Virginia 22151 – Price $2.00

ABSTRACT

This report is first of a planned series of reports on the Syncom Satellite System. It is an engineering report covering the satellite, the communications ground stations and the telemetry and control ground stations. This report covers a description of each of the Syncom Satellite System Subsystems in addition to their operation and performance. The time period covered by this report is from launch through the first one hundred fifty days in orbit. The material contained in this report was furnished by the Hughes Aircraft Co., El Segundo, California, the United States Army Satellite Communications Agency, Fort Monmouth, New Jersey, and the Goddard Space Flight Center, Greenbelt, Maryland.

CONTENTS

SYNCOM ENGINEERING REPORT

VOLUME I

Prepared by the
Syncom Projects Office
Goddard Space Flight Center

CHAPTER I

INTRODUCTION

Syncom, the world's first active repeater synchronous orbit communications satellite, was developed by the Hughes Aircraft Company under the direction of the Goddard Space Flight Center. The prime objectives of the Syncom program were to:

a) Gain early experience with a communications satellite in synchronous orbit,

b) Develop a communications satellite of moderate bandwidth with simple reliable attitude and period control systems,

c) Develop readily transportable ground support facilities,

d) Develop the capability of launching satellites into a 24-hour orbit using existing launch vehicles with additional apogee-boost propulsion capability,

e) Determine the communications systems' performance parameters, in a design configuration capable of relaying with high quality two voice modulated carriers (either FM or PCM/PM) between widely separated terminals,

f) Obtain scientific data on space propagation,

g) Test the life of communications satellite components at the 24-hour orbit altitude, and

h) Obtain data from the quantitative effects of earth triaxiality (asymmetry around its spin axis) on the synchronous orbit.

The spacecraft was designed to be launched by the Thor-Delta vehicle, and incorporates a solid propellant apogee motor for changing the highly elliptical transfer orbit to an in plane, circular synchronous orbit. The design of the spacecraft is described in Chapter II.

The telemetry and command ground control stations are furnished by Hughes Aircraft Company. The primary station for spacecraft control and receipt of telemetry data during the launch and orbital period was aboard the USNS Kingsport at Lagos. A station at Johannesburg, South Africa, served as a backup to the Lagos station during the launch and orbit adjustment period. After orbital adjustment was completed, principal control was assigned to a telemetry and command station location at Lakehurst.

Communications ground stations and communications experimentation, including evaluation, were provided by the U. S. Army Satellite Communications Agency. One communication ground station was located aboard the USNS Kingsport, anchored in the port of Lagos, Nigeria, during the launch phase. The other principal station was located at Lakehurst, New Jersey. A station at Fort Dix, New Jersey, was used as a backup to the Lakehurst station. Equipment for measuring range and range rate was supplied by the Goddard Space Flight Center. This equipment was used in conjunction with the prime ground communications stations. A description of the communications ground is presented in Chapter II.

Syncom II was successfully launched on 26 July 1963 from Cape Canaveral. The satellite has been adjusted to a true synchronous orbit with the orbital node at 55 deg. W longitude and has been oriented to place the satellite spin axis perpendicular to the orbital plane. All systems and functions of the satellite have been proven out and found to be normal with only minor exceptions.

Satellite tracking was done by three methods: Johannesburg Minitrack station tracking of the spacecraft telemetry carrier signal; communications station tracking of the spacecraft communications signal; and telemetry and command station tracking of the spacecraft telemetry signal. The Minitrack data were used for initial orbit determination. The communication station tracking data (range and range rate) were the most accurate and provided a determination of spacecraft spin axis orientation. Telemetry and command station tracking was less precise than other methods, and was used as a backup.

Chapter III of this report provides a history of Syncom launch and orbital maneuvers. A detailed discussion and tabulated results of each maneuver and a comparison of predicted versus actual results are presented.

The overall objectives of the Syncom program as previously outlined have been met: the feasibility of a spin-stabilized, synchronous orbit, active communications satellite has been demonstrated. Orbital control has been achieved without difficulty. The launch by the Thor-Delta booster from AMR and apogee motor boost resulted in the expected near-synchronous orbit. Velocity corrections and spacecraft orientation have been made by the spacecraft control subsystem in a predicted manner.

The results of communications experiments have been excellent. High quality voice signals have been transmitted with signal-to-noise ratios up to 40 db. Photographs have been transmitted by facsimile with a resolution greater than that of standard television. The main communication ground stations have been able to lock on to the spacecraft beacon signals at elevation angles less than 1/2 degree. Chapter IV of this report discusses the communications experiments results.

Spacecraft performance, all systems, is presented in Chapter V. All systems aboard the spacecraft were functioning properly at the time of this report. The spacecraft life in orbit of over 2 years, barring an unforeseen component failure, has been predicted based on the solar array performance. Degradation of the solar array due to radiation damage, if the predictions are correct, will cause the power available from the array to drop below that required for communication transponder operation in approximately 2 to 5 years.

CHAPTER II

SYNCOM SYSTEM DESCRIPTION

GENERAL SYSTEM DESCRIPTION

The Syncom system is comprised of the Syncom spacecraft in a synchronous orbit, communications ground stations, and telemetry and command ground stations. While not properly identifiable as a part of the Syncom communication system, a computing facility for determination of proper orbit correction data is a necessary adjunct to the system during certain critical orbit adjustment periods.

A basic block diagram of the overall Syncom system is shown in Figure II-1. The most commonly used mode of voice communication is full duplex in which each ground station transmits a

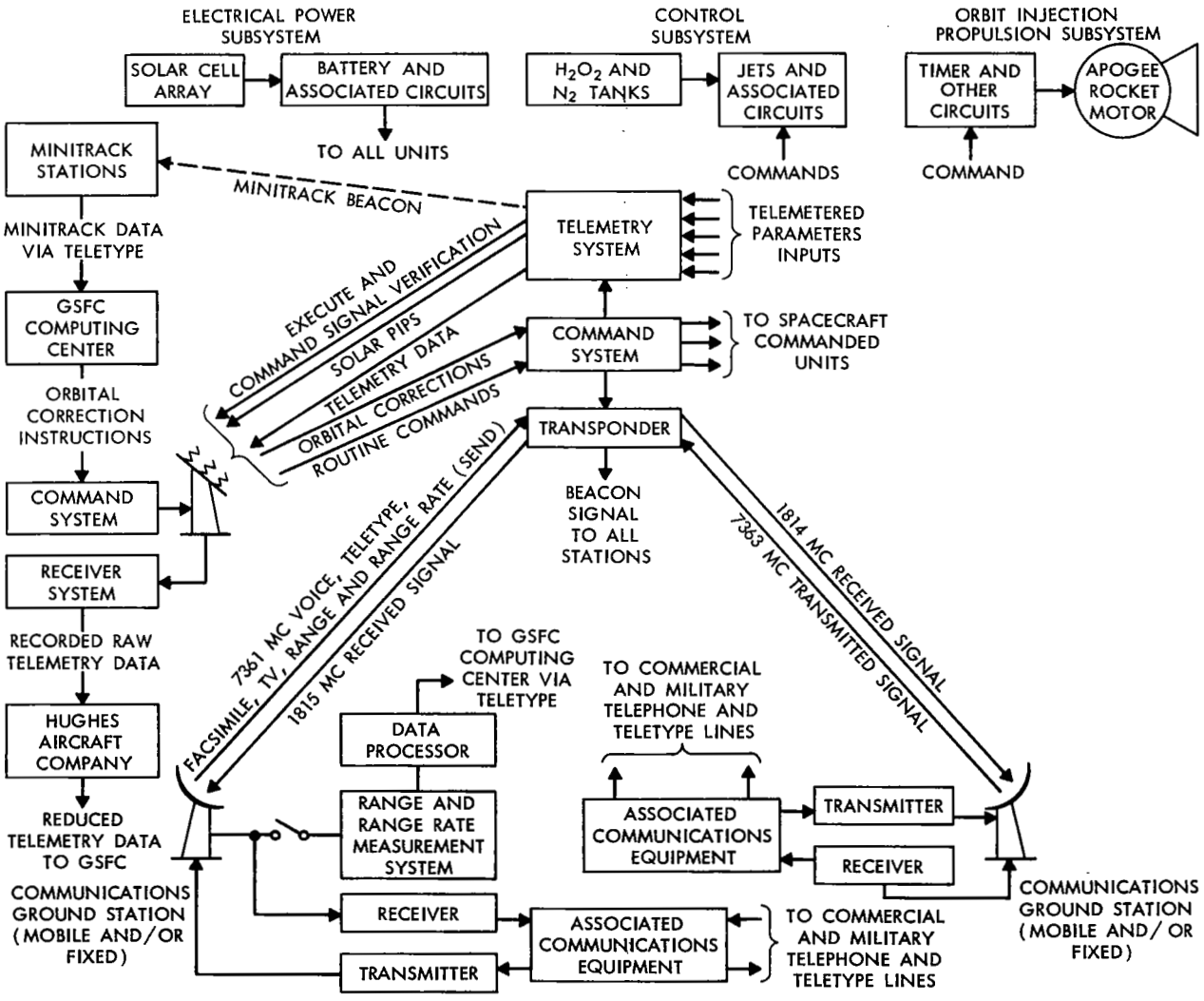

Figure II-1—Syncom system block diagram.

frequency modulated signal to the spacecraft at about 7.4 Gc. This signal is translated in frequency to about 1.8 GC at the spacecraft and retransmitted. The signal is received by the appropriate ground station and demodulated. Teletype and facsimile signals are also commonly transmitted. A beacon signal transmitted from the spacecraft is used by the ground stations for antenna tracking and as a reference signal in making range rate measurements. Range and range rate measurements are made by modulating the carrier with a series of tones and measuring the phase and time of reception of the received signals. Range and range rate data supplements minitrack data for Syncom orbit determinations.

The ground stations currently in use are both fixed and mobile, and employ parabolic antenna diameters varying from 60 feet down to 10 feet. Most of the communications traffic and experiments are conducted using 60-foot and 30-foot diameter antennas, although 10-foot antennas are used for some purposes.

SPACECRAFT DESCRIPTION

The objective of the Syncom program was to demonstrate the feasibility of a spin-stabilized, synchronous orbit, active communications satellite. The choice by NASA of the Thor-Delta vehicle as the booster dictated that the spacecraft be small and light in weight. Also, the spacecraft orbit is necessarily inclined, since weight and space allowances did not exist for a device to eliminate the orbital inclination resulting from a launch from Cape Kennedy. The resulting spacecraft design met this objective successfully. Even though space and weight allowances were quite restrictive, redundancy of functional subsystems was achieved with a resultant increase in reliability. The spacecraft consists of a structure housing five major components.

The communications subsystem provides capability for demonstrating voice, facsimile, teletype, and television transmission. The subsystem consists of one narrow-band and one wide-band transponder, two traveling-wave tubes, and the folding coaxial slotted array antenna with its associated electronic components. The telemetry and command subsystems provide capability for receiving operational commands and transmitting data on spacecraft operation and orbital position. The subsystems consist of electronic equipment and the four whip antennas. The control subsystem provides equipment for adjusting the spacecraft position and attitude. The subsystem consists of a cold gas (nitrogen) unit, a hydrogen peroxide unit, seven sun sensors, an apogee motor ignition timer, an accelerometer, and a nutation damper. The power subsystem provides electrical power for spacecraft operation, and consists of solar cells and batteries with associated regulators and control devices. The solid propellant apogee motor provides the spacecraft with the necessary additional velocity at apogee to change the orbit from an elliptical transfer orbit to a circular orbit which is approximately synchronous.

Structure

The spacecraft consists of two structural units. The outer structure supports the solar panels, the majority of the electronics, and the control subsystem. An inner structure supports the apogee motor and the remaining electronics. The spacecraft is shown in Figure II-2, and the general arrangement is shown in Figure II-3.

The outer structure attaches four honeycomb solar panels to a cylindrical support ring with four lightweight stiffening ribs located 90 degrees apart, providing the attachment to the inner structure.

To satisfy the requirement that the ratio of the roll moment of inertia to the pitch moment of inertia be at least 1.10, the electronic equipment is packaged in small units and equally distributed as far out from the spin axis as possible. To avoid attaching the units directly to the solar panels, a component mounting bulkhead is provided. This consists of an octagonal box section and two thin bulkheads attached to the inner structural tube and the four stiffening ribs. A pair of

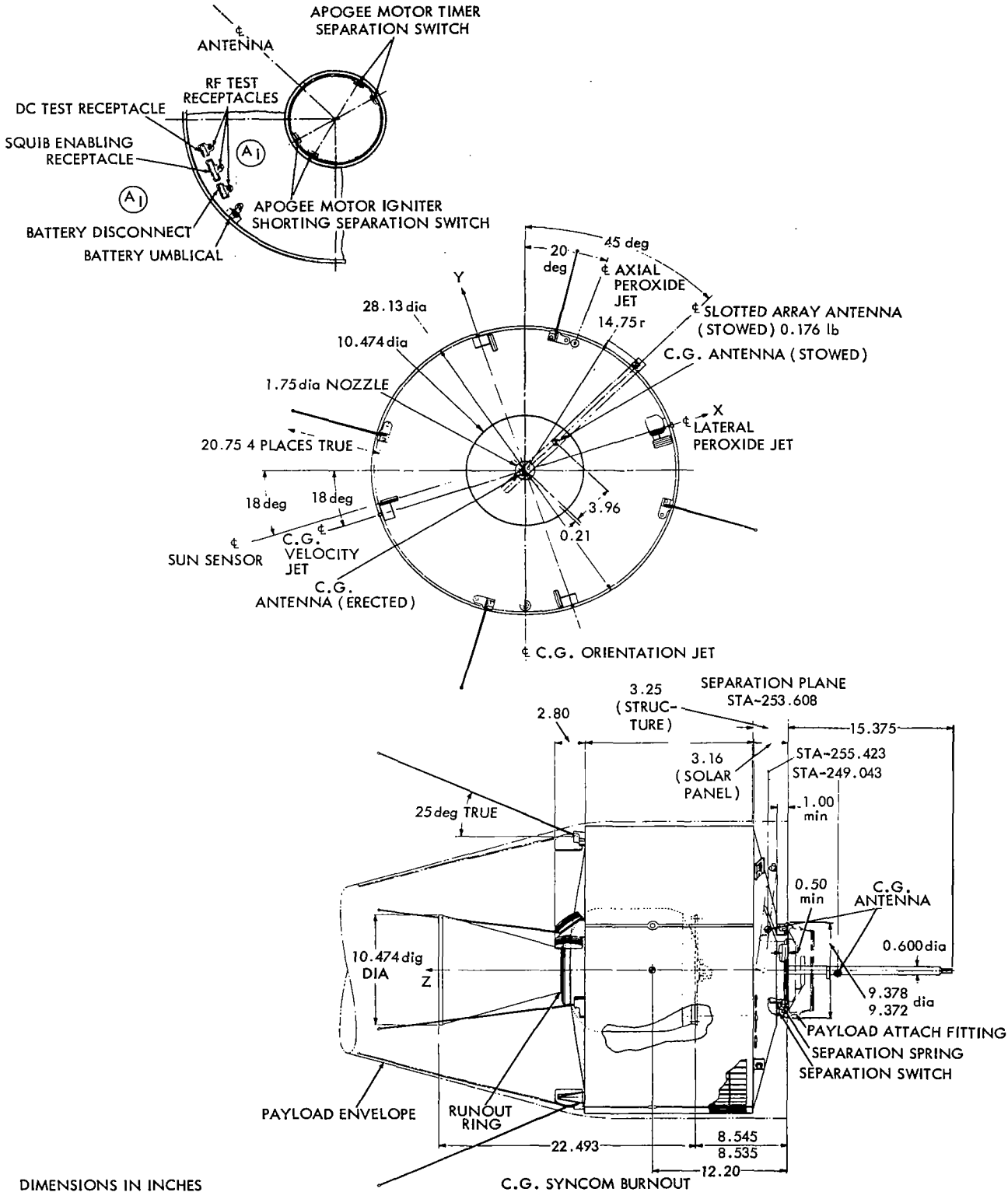

DIMENSIONS IN INCHES

Figure II-2.

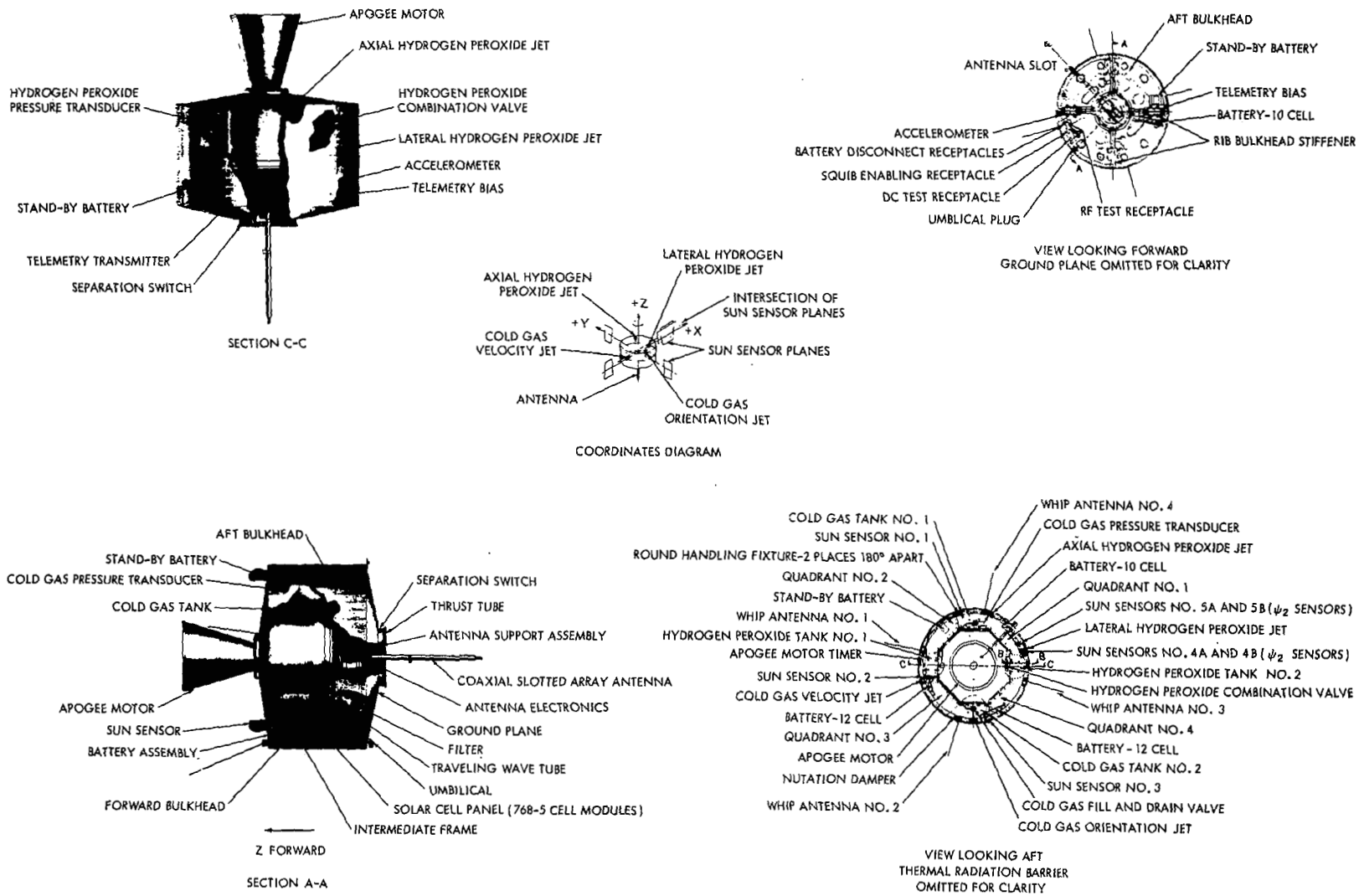
APOGEE MOTOR
AXIAL HYDROGEN PEROXIDE JET
HYDROGEN PEROXIDE PRESSURE TRANSDUCER
HYDROGEN PEROXIDE COMBINATION VALVE
LATERAL HYDROGEN PEROXIDE JET
ACCELEROMETER
TELEMETRY BIAS
STAND-BY BATTERY
TELEMETRY TRANSMITTER
SEPARATION SWITCH
SECTION C-C
AFT BULKHEAD
STAND-BY BATTERY
ANTENNA SLOT
TELEMETRY BIAS
BATTERY-10 CELL
ACCELEROMETER
RIB BULKHEAD STIFFENER
BATTERY DISCONNECT RECEPTACLES
SQUIB ENABLING RECEPTACLE
DC TEST RECEPTACLE
UMBLICAL PLUG
RF TEST RECEPTACLE
VIEW LOOKING FORWARD
GROUND PLANE OMITTED FOR CLARITY
LATERAL HYDROGEN PEROXIDE JET
AXIAL HYDROGEN PEROXIDE JET
+Z
+Y
+X
INTERSECTION OF SUN SENSOR PLANES
COLD GAS VELOCITY JET
SUN SENSOR PLANES
ANTENNA
COLD GAS ORIENTATION JET
COORDINATES DIAGRAM
AFT BULKHEAD
STAND-BY BATTERY
COLD GAS PRESSURE TRANSDUCER
SEPARATION SWITCH
COLD GAS TANK
THRUST TUBE
ANTENNA SUPPORT ASSEMBLY
COAXIAL SLOTTED ARRAY ANTENNA
APOGEE MOTOR
ANTENNA ELECTRONICS
SUN SENSOR
GROUND PLANE
BATTERY ASSEMBLY
FILTER
TRAVELING WAVE TUBE
UMBILICAL
FORWARD BULKHEAD
SOLAR CELL PANEL (768-5 CELL MODULES)
INTERMEDIATE FRAME
Z FORWARD
SECTION A-A
COLD GAS TANK NO. 1
SUN SENSOR NO. 1
ROUND HANDLING FIXTURE-2 PLACES 180° APART
QUADRANT NO. 2
STAND-BY BATTERY
WHIP ANTENNA NO. 1
HYDROGEN PEROXIDE TANK NO. 1
APOGEE MOTOR TIMER
SUN SENSOR NO. 2
COLD GAS VELOCITY JET
BATTERY-12 CELL
QUADRANT NO. 3
APOGEE MOTOR
NUTATION DAMPER
WHIP ANTENNA NO. 2
WHIP ANTENNA NO. 4
COLD GAS PRESSURE TRANSDUCER
AXIAL HYDROGEN PEROXIDE JET
BATTERY-10 CELL
QUADRANT NO. 1
SUN SENSORS NO. 5A AND 5B (ψ_2 SENSORS)
LATERAL HYDROGEN PEROXIDE JET
SUN SENSORS NO. 4A AND 4B (ψ_2 SENSORS)
HYDROGEN PEROXIDE TANK NO. 2
HYDROGEN PEROXIDE COMBINATION VALVE
WHIP ANTENNA NO. 3
QUADRANT NO. 4
BATTERY-12 CELL
COLD GAS TANK NO. 2
SUN SENSOR NO. 3
COLD GAS FILL AND DRAIN VALVE
COLD GAS ORIENTATION JET
VIEW LOOKING AFT
THERMAL RADIATION BARRIER
OMITTED FOR CLARITY

Figure II-3.

cylindrical support rings, fore and aft, completes the outer structure. The forward ring carries the sun sensors, whip antenna, apogee motor timer, orientation jets, and the forward ends of the solar panels. The aft ring supports batteries and the aft ends of the solar panels. The octagonal frame mounts the electronic units, the cold gas tank, the hydrogen peroxide tanks, the nutation damper, and the velocity jets.

The inner structure consists of a machined magnesium ring with the payload attach fitting for mounting to the Delta third stage on one end and provisions for mounting the apogee motor on the opposite end. To allow for thermal expansion of the motor case, the motor is cantilevered from the forward end of the motor case using a four-lug mounting arrangement. Easy access to the attach nuts makes the alignment of the motor relatively simple.

Provisions were made to install the coaxial slotted array antenna and its associated electronic package within the inner ring structure. The traveling-wave tubes are attached to the back of two of the stiffening ribs, and the telemetry transmitters attach to the other two ribs. A ground plane on the aft end of a thermal radiation barrier on the forward face of the structure completes the enclosure of the components.

The general arrangement in Figure II-3 shows that accessibility to all of the units within the mounting frame is obtained by removing the appropriate solar panel. Removal of the ground plane gives access to the traveling-wave tubes and telemetry transmitters. The apogee motor timer is exposed by removing the radiation barrier. The communications antenna and its electronics may be removed as a unit without any disassembly of the spacecraft. The nitrogen and the hydrogen peroxide fill-and-drain fittings are accessible through ports in the radiation barrier. Further, a number of electrical tests points are accessible with a minimum of disassembly.

Weight and Balance

The total weight, center of gravity, and mass moments of inertia about the roll and pitch axes of the spacecraft at separation from the booster, at apogee motor burnout, at hydrogen peroxide burnout, and after expenditure of all stored nitrogen are given in Table II-1.

Table II-1

Spacecraft Weight Analysis

PARAMETER	WEIGHT (pounds)	CENTER OF GRAVITY Z-Z (inches)	MOMENT OF INERTIA		
			ROLL (slug-feet^2)	PITCH (slug-feet^2)	RATIO OF ROLL TO PITCH
Final orbit condition*	78.81	11.80	1.84	1.42	1.30
Total at hydrogen peroxide burnout*	80.71	11.81	1.89	1.47	1.29
Total at apogee burnout*	85.64	11.83	2.02	1.50	1.35
Payload at launch**	146.86				
Air buoyancy effect	0.06				
Payload at separation*	146.92	12.79	2.27	1.80	1.26

*Weight in vacuum

**As weighed in air.

Thermal Design

Adequate temperature control was achieved by proper selection of the solar absorptance and infrared emittance of the external surfaces of the spacecraft and by proper insulation of the subsystem equipment. Feasibility of this design concept was demonstrated by detailed thermal analysis.

Spacecraft Subsystems

Communications Subsystem

At the spacecraft, the signals from the ground are received by an antenna with a pattern which is symmetrical about the satellite spin axis.

These signals are supplied to two receivers of which only one is operating at any one time, the desired one being selected by command. One receiver is wide-band with a bandwidth of 5 ± 0.5 mc between half-power points. It consists of a mixer, a local oscillator, an IF amplifier, and a limiter amplifier. The other receiver is narrow-band with two channels, each 0.5 mc wide, with channel center frequencies separated by 1.725 mc. This receiver consists of a mixer, a local oscillator, an IF amplifier, two filters of 0.5 mc bandwidth separated in frequency by 1.725 mc, and two limiters, one following each channel.

When simultaneous two-way narrow-band communication takes place (duplex operation) over the wide-band channel, two signal channels are passed through the wide-band amplifier and its limiter. They then modulate the transmitter and are transmitted with power levels approximately proportional to their received signal level. The number of carriers which can be handled on the wide-band system is dependent on the bandwidth apportionment between signals. When duplex operation is used on the narrow-band receiver, the two signal channels operate on the two separated IF channels and each signal passes through its separate IF amplifier-limiter prior to transmitter modulation. Therefore, the transmitted signals will be about equal whether or not the received signal levels are equal. Each channel contains a squelch circuit, so that when a channel is not receiving a signal, the noise contribution of that channel is greatly reduced. Following the receiver limiters, the outputs are mixed with a reference signal to provide a frequency translated low-level output with carrier frequency at approximately 1800 mc. These 1800-mc outputs of the receivers are connected to a single hybrid network, the outputs of which are, in turn, connected to the two traveling-wave tube transmitters. Either traveling-wave tube may be selected by command for use with either the narrow-band or the wide-band transmitter, but the receivers and transmitters are interlocked so that only one receiver and one transmitter may be activated at any instant, a turn-on command to either receiver or transmitter automatically turning off the other receiver or transmitter.

The reference signal derived through frequency multipliers from the receiver master oscillator is also transmitted and is used on the ground as an input to the equipment for range and range-rate determination. The signal may also be used as a beacon for tracking the spacecraft with the ground communication system equipment. The output of the transmitter is about two watts. The power subsystem is designed to permit operation of the transponder at 100 percent duty cycle (except in eclipse) whether or not the batteries are operative.

The transmitting antenna consists of a coaxial slot array on the spin axis. The gain of this antenna is approximately 6 db and the pattern is independent of angle about spin axis. The antenna beam is a "pancake" with its plane perpendicular to the spin axis and is about 25 degrees wide. In operation, the spin axis of the satellite is perpendicular to the plane of the orbit, and the "pancake" beam, therefore, encompasses the earth at all times.

Command Subsystem

The command subsystem consists of receivers, decoders, and an antenna unit shared with the telemetry subsystem. The antenna consists of two pairs of whips connected through baluns to the two inputs of a hybrid. The two outputs of hybrid correspond to the two polarization modes of the whips acting as a turnstile system. Each output is connected to a diplexer and each diplexer provides 148-mc command signals to a receiver and accepts 136-mc telemetry transmission from a telemetry transmitter. The two command receivers are identical, parallel units each with mixer, IF amplifier, and AM detector. The detector outputs of the two receivers provide audio output tones recovered from the modulation on the command transmission from the ground. Each command receiver is associated with one of the two redundant command decoders. Either receiver/decoder can exercise complete command control of the spacecraft.

The audio signals are applied to two redundant groups of three tone-operated channels. Power is applied continuously to one channel in each group and upon receipt of the correct audio tone, this channel turns power on to the other two channels in that group. Then the desired command can be inserted by sending a predetermined number of pulses from the ground at a second audio frequency. The command is verified through the telemetry system and then execution is accomplished by sending a tone on the third channel. Functions accomplished by the command system include turning communication transponder, telemetry carrier, and telemetry modulation on and off; selection of communication transmitter, communication receiver, telemetry transmitter, and encoder to be used; and all necessary control system functions. The logic of the command subsystem has been designed to achieve complete flexibility and reasonable security with a minimum number of channels.

Telemetry Subsystem

The telemetry subsystem comprises the antenna (shared with the command subsystem), two transmitters, each with its associated encoder, and the signal conversion elements. The 1.25-watt, 136-mc transmitter is phase-modulated by a subcarrier which, in turn, is frequency-modulated by a time-division-multiplexed modulator which samples the amplitude of the various sensor signals. Certain critical control signals bypass the time-division-multiplexed modulator and are permitted to phase-modulate the telemetry transmitter directly. Each transmitter and its associated encoder is one of a redundant pair, each pair operating at a unique frequency. In the normal modes of spacecraft operation, only one of the transmitter-encoder subsystems is permitted to function at one time, the power to the other subsystem being automatically turned off when the other is turned on. On command, an encoder may be disconnected, thereby removing the telemetry modulation and leaving the telemetry carrier to serve as a tracking beacon for the Minitrack network. During the early flight phases, Minitrack data was furnished to the Goddard Space Flight Center where it was used in computing the spacecraft orbit.

Sixteen channels of time-multiplexed data are telemetered. Included in these data are temperatures of selected points in the spacecraft, solar string voltage, nitrogen and hydrogen peroxide tank pressures, stored but unexecuted commands, battery voltage, power bus voltage, and reference voltages.

Unmultiplexed data transmitted include responses to all "execute" signals, solar sensor "pips", and all gas jet actuations whether sent from the ground control equipment or from the on-board control subsystem.

Orbit Injection Propulsion

The Syncom orbit injection propulsion subsystem supplies the boost necessary to inject the spacecraft into a nominally synchronous, circular orbit, after the vehicle has reached the apogee of a transfer orbit at the required altitude. The spacecraft was launched into the transfer orbit by the three-stage Delta vehicle.

The propulsion subsystem consists of a single solid-propellant rocket motor. This motor imparted a velocity increment of 4696 fps to the spacecraft, which initially weighed 146.8 pounds. The following parameters apply to this motor:

Specific impulse	274.2 seconds
Propellant weight	60.5 pounds
Case and nozzle weight (including provision for attachment)	10.5 pounds
Motor weight	71.0 pounds
Diameter	12.0 inches
Payload	75.8 pounds

The required performance and objectives given above are met by the JPL rocket engine designated the Starfinder which was used for the launch.

Control Subsystem

The control subsystem consists of the components necessary to establish the desired longitude, to control the orbital velocity to synchronous, and to orient the satellite spin axis from boost attitude to operating attitude. The subsystem consists of a pulsed-jet hydrogen peroxide propulsion unit for coarse velocity control, a pulsed-jet cold-gas unit for fine velocity control and for orientation, solar sensors, and control circuits. A timer for firing the apogee motor and an accelerometer for indicating firing are parts of the control subsystem.

Electrical Power Subsystem

The electrical power subsystem consists of silicon solar cells, a nickel-cadmium battery, combined voltage regulators and switches, and an auxiliary telemetry battery. The subsystem is capable of supplying approximately 25 watts without drain on the battery when the satellite is not shadowed by the earth. The solar cells are arrayed on the external cylindrical surface. In the operating configuration, the sunline is within 25 degrees of normal to the axis of the cylinder, a condition met by suitable choice of launch time.

GROUND STATIONS

Telemetry and Command Stations

The primary station for command, control, and receipt of telemetry data during the launch period was located aboard the USNS Kingsport. During the launch period, a station at Johannesburg, South Africa, served as a backup for the primary station. After orbital adjustments were completed, principal control was assigned to a station located at Lakehurst, New Jersey.

Satellite Tracking

The spacecraft may be tracked in its orbit by the Minitrack network and by the communication stations. The telemetry transmitter carrier may be tracked by the Minitrack network stations to obtain coordinate data in standard Minitrack form. The telemetry transmitter was turned on prior to launch so that it could be tracked during the launch period. The minitrack data from the Johannesburg station was used at the Goddard Space Flight Center for initial orbit determinations.

When the transponder is turned on, the communication stations with their narrow-beamed antennas and range and range rate measuring equipment can track the spacecraft accurately. The communication stations are designed to measure polarization angle of the received signal. This

information is useful in the determination of spacecraft spin axis orientation. The spacecraft also may be tracked with the telemetry receiving subsystem. However, the broad-beam pattern of the telemetry receiving subsystem precludes the use of these data for precise location work.

Syncom Telemetry and Command Station Equipment Description

A brief functional description of the telemetry and command ground control stations is given in the overall system description. The station equipment, whether installed in one of the 8' × 30' air transportable trailers or aboard the USNS Kingsport, is essentially the same functionally and operationally, the only difference being the equipment arrangement to best satisfy the operational requirements of the station. The purpose of this section is to describe the equipment at each ground station necessary to satisfy these functional station requirements.

The ground station consists of the following subsystems: Antenna, transmitter, receiver, recording, and control console. The control console includes the synchronous controller, command encoding equipment, telemetry decoding equipment, oscilloscope, and coded time generator (see Figures II-4 and -5).

Antenna Subsystem

The telemetry and command antenna array consists of one 148-mc cross-polarized yagi surrounded by eight 136-mc, cross-polarized yagis, all mounted on top of a 14-foot tower which houses the drive and control mechanisms. Operation is performed from a remote control panel.

The command antenna consists of one cross-polarized, seven-element yagi cut to a center frequency of 148.26 mc located in the center of the mounting platform. The antenna has two outputs with means for selecting left- or right-hand circular polarization and vertical or horizontal plane polarization.

The telemetering array consists of eight cross-polarized, seven-element yagis cut to a center frequency of 136.47-mc, mounted on the platform in a square perimeter around the command antenna. The horizontal and vertical outputs of these eight antennas are fed through two line filters which reject the 148.26-mc command frequency and pass the 136.47-mc telemetering frequency to a preamplifier. A coax switch assembly controlled by a polarization selector on the control panel provides selection of the following polarizations, separately or together: left-hand circular, right-hand circular, vertical, horizontal, slant left, and slant right.

The antenna mounting platform is supported by a pair of rocker arms secured to the ends of a shaft extending from the cage that houses the elevation drive equipment. The cage is mounted on an azimuth bearing shaft supported by bearings at the top of a 14-foot tower and on a platform in the tower incorporating the azimuth drive equipment. Elevation rotation is ± 80 degrees from zenith, and the azimuth rotation is ± 280 degrees from 0-degree setting.

Power to rotate the mount is supplied by hydraulic actuators. The hydraulic pressure to operate these actuators is supplied by a motor-driven pump equipped with a fluid reservoir and the necessary electrically-operated control valves to rotate the mount in either direction. Each drive is equipped with automatic electric brakes and rotational limit switches. Synchronizers indicate the pointing angle of the antenna array to an accuracy of ± 1 degree.

Command Transmitter

The Hughes-fabricated 3 kilowatt command transmitter consists of the following subsystems: Crystal oscillator, multiplier chain, power amplifier, modulator, driver amplifier, and power supplies.

A Butler type temperature-controlled fundamental crystal oscillator with a frequency stability better than 0.0005 percent generates a signal that is applied to a multiplier chain consisting of a

frequency tripler, doubler, and another tripler. The multiplier chain, in turn, drives a straight-through neutralized buffer operating at a power level of up to 250 watts at the transmitting frequency of 148.26 mc. The buffer output is adjustable to optimize the RF drive requirements of the final amplifier tetrode. Audio control tones from the command panel feed the modulator-driver which consists of a preamplifier, phase inverter and an audio driver. The output power travels through a directional coupler which operates both as a forward and a reflected power meter. Protective circuitry has been incorporated to prevent catastrophic failure from loss of cooling or other vital functions. In addition, full metering of all stages has been provided for ease of operation.

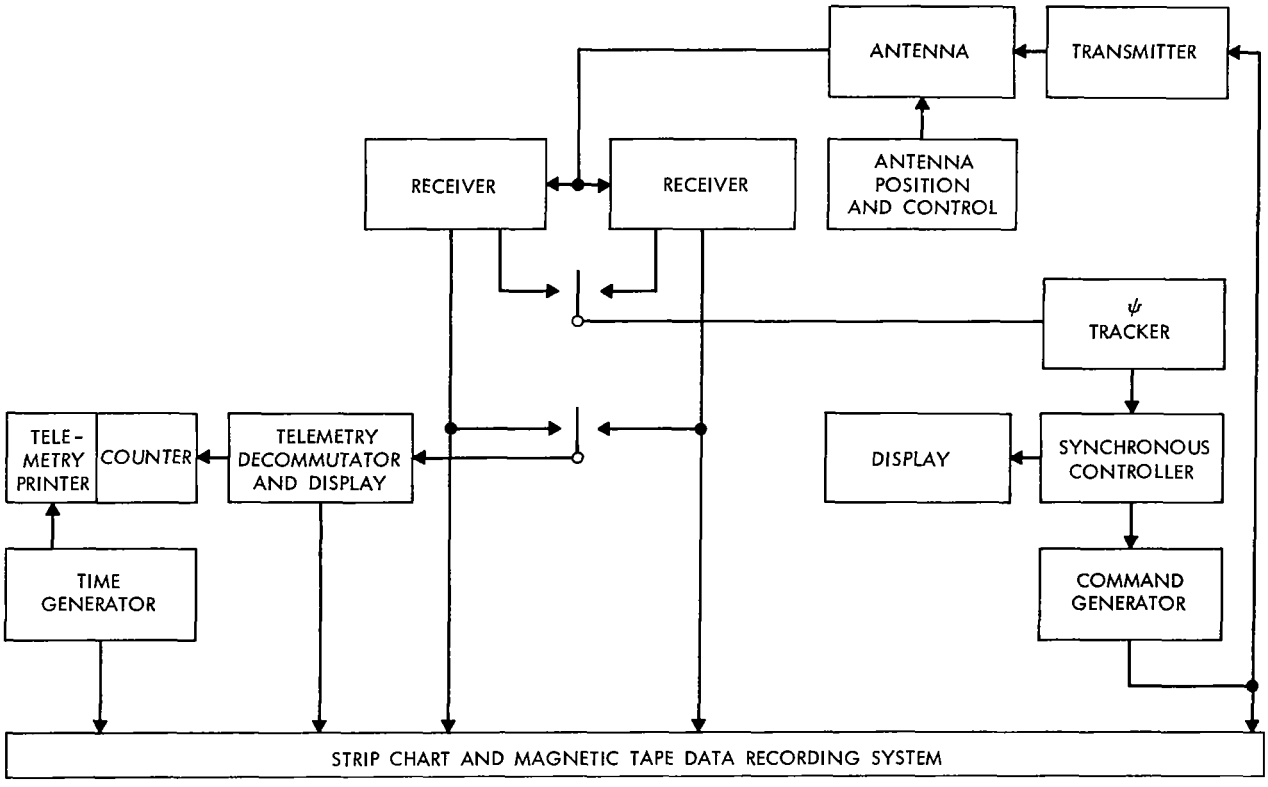

Figure II-4—Simplified diagram of telemetry and command ground station.

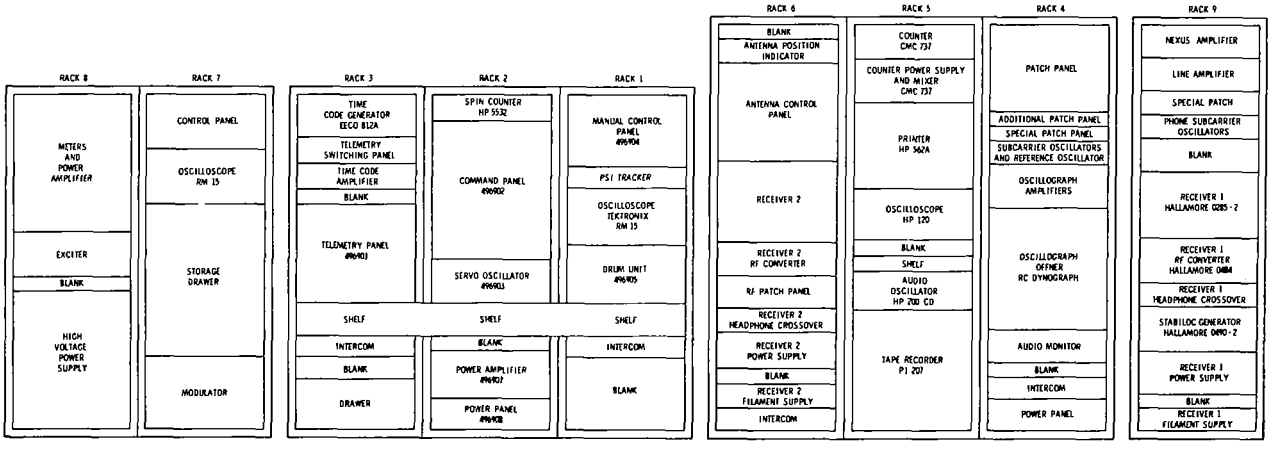

Figure II-5—Telemetry and command station general arrangement.

Telemetry Receivers

The receivers contain all the necessary circuitry to receive and detect phase-stable telemetry signals in the 136- to 137-mc band. The receivers employ a narrow-band second-order phase-locked loop which provides a highly efficient technique for receiving phase-stable signals in the presence of wideband noise by means of coherent detection. The basic Lear Siegler, Inc., receivers have been modified by Hughes to enhance operation and to provide additional data outputs. The incoming signal from the antenna-mounted low-noise figure preamplifier is mixed with the multiplied output of a VCO in the RF converter unit which produces an output signal at approximately 30 mc. This signal is then amplified in a 30-mc IF strip in the detector unit and coupled to a second mixer/amplifier utilizing a crystal-controlled oscillator which produces an output at 6.6 mc. The output of the second mixer-amplifier is coupled to a 6.6-mc phase detector which has an output proportional to the phase angle between the 6.6-mc signal and the 6.6-mc reference oscillator. Outputs from the 6.6-mc reference oscillator are coupled to four (4) phase detectors, one of which is part of the phase-locked loop. The action of the loop filter under locked conditions with an unmodulated signal results in a minimum output from the phase detector in the loop as well as the PM data detector. This causes the output of the AM phase detector to be maximum because of the 90-degree shift in the reference to this phase detector. The PM data detector is used to recover the phase-modulated telemetry data while the PM loop detector is used to detect phase error output. This phase error output is coupled to the loop filter which, in turn, controls the frequency of the voltage-controlled oscillator (VCO). The AM phase detector is used to obtain signal strength. The VCO operates at a frequency which is a submultiple of the local oscillator injection frequency. This VCO output is then coupled to the multiplier in the preamplifier converter unit to produce a local oscillator signal which is equal to the signal frequency plus 30 mc.

Solar pulse information is recovered from the received signal through the use of a phase compressor and a linear phase filter. The solar pulse information directly phase-modulates the telemetry carrier in addition to the telemetry information, resulting in a peak deviation of approximately 2.4 radians. This is beyond the detection capabilities of a normal phase detector. To recover the solar pulse data, a phase compressor-detector was developed by Hughes. Phase compression is accomplished by shifting the reference oscillator phase with the phase detector output in a manner that decreases the effective deviation at the phase detector. After first passing the 6.6-mc IF output through a 4-kc filter to remove the telemetry data, the solar pulse information is fed to the phase compressor unit. Here the solar pulses are compared to the phase-shifted reference oscillator output, and the detected result is coupled to the linear phase filter, which is a 300-cycle low-pass filter.

Ground Control Equipment Console

The control console contains the necessary equipment to control the operation of the spacecraft and monitor received spacecraft telemetry data. It consists of four basic units: the synchronous controller, command encoding equipment, telemetry decoding equipment and auxiliary equipment.

The synchronous controller generates signals to pulse the spacecraft control jets synchronously in order to orient and impart velocity increments to the spacecraft. To do this, the controller uses a mechanical rotating drum and a position servo that acts to bring the master-trigger from the rotating drum contacts into time synchronism with the pip from the solar sensors of the spacecraft, causing the drum to rotate in synchronism with the spacecraft.

Spacecraft and drum synchronism is accomplished by generating an error signal proportional to the magnitude and direction of displacement between a trigger from the drum position and a trigger from the spacecraft position. This error signal is integrated to obtain a control voltage which controls the drive frequency of the drum in order to reduce the position error.

Rotating cams in the drum generate three pulses. These cams rotating in synchronism with the spacecraft generate pulses of a specific time duration and occur at a predetermined point in the spacecraft rotation. The command trigger pulse occurring in delayed synchronism with the solar sensor pulse is adjustable to start and stop within any points of the rotation of the spacecraft. An adjustable delay set into the system compensates for the time required for the signal to reach the spacecraft. The delayed command trigger gates the execute signal from the command system so that the gas jets in the spacecraft will be opened and closed at the proper time during orbital corrections. The master trigger pulse is generated in delayed synchronism with the solar sensor pulse; the delay being equal to the time delay required for the solar sensor pulse to travel from the spacecraft to the drum unit. This trigger is used in the synchronous controller servo to control the speed of the drum. The ψ_2 trigger pulse is adjusted to occur in synchronism with the ψ_2 pulse from the sun sensor. Since the angle between the spacecraft spin axis and the sunline is a known function of the delay between the ψ solar sensor pulse and the ψ_2 solar sensor pulse, the angle can be calculated. The delay adjustment for the ψ_2 trigger is directly calibrated in degrees to show this angle.

The psi tracker provides psi pulse position memory by generating late and early gates which are synchronized to the received solar pulses. The late gate is used to trigger the sweep of the drum servo display oscilloscope by providing a clean reconstructed psi pulse for purposes of synchronizing the drum unit to the received solar pulses.

The command encoding equipment generates specific frequencies, in pulsed form, to modulate the command transmitter. The signals are transmitted to the spacecraft and control its operation. During actual operation, the command equipment also monitors the command signal, the confirm signal from the spacecraft, and the status and operating time of spacecraft units, and counts the actuations of the gas jets. The command equipment consists of four items: The subcarrier oscillator, the command control, the mixer, and display unit.

The subcarrier oscillator consists of three crystal oscillators and a modular count-down circuit to provide the system with 8.673, 7.7, 11.024, and 9.745 kc signals. The command control converts the frequencies into pulses of specific time duration to command the operation of the spacecraft functions. Either of the first two frequencies (8.673 or 7.7 kc) can be used to form a gate into the spacecraft command system so that a command signal can pass through one of the two channels into the spacecraft register. Selection of the frequency and the spacecraft channel is made when the "Enable 1" or the "Enable 2" switch is depressed on the command panel.

The control panel can give the spacecraft any one of 32 commands. When the proper switch is depressed, the modular binary counter automatically gates the 11.024-kc signal to produce a series of pulses (with the proper number and specified time duration of pulses and spaces) to command the spacecraft. To simplify the procedure for the operator, 32 switches, each representing a separate command and properly labeled, are mounted on the panel.

The last frequency (9.745 kc) is used for the "Execute" signal. After the command has been received by the spacecraft and passed into the register, the command will not be obeyed until the "Execute" signal is received. A pulse of 9.745-kc energy will be gated when the "Execute" switch is depressed. A series of pulses can then be generated automatically by the drum unit to activate the spacecraft gas jets in the pulsed mode of operation. These outputs are passed to the mixer block and to the indicators for further use. The mixer receives the signals generated by command control and mixes the three signals into one complex waveform used to modulate the command transmitter.

The display unit contains indicators, counters, and timers. Indicators in the form of lights display the status of the spacecraft units currently in operation, and also show which commands are in process. Command verification is received by telemetry and also displayed. The timers and counters show the operational time on the spacecraft components and count the times the gas jets were pulsed.

The telemetry decoding equipment is designed to receive the demodulated output from the ground station telemetry receiver and convert it into usable information which is displayed on the panel-mounted meters and used in the command equipment and in the synchronous controller. The telemetry equipment consists of five basic items: The filtering unit, the pip indicator, the discriminator, decommutation unit, and display meters.

The filtering unit has three filters that separate the three bands of audio information carried by the carrier frequency. The first filter is a low-pass filter (±150 cps) to separate the solar sensor pulses; the second is a bandpass filter (9.745 ± 0.150 kc) to separate the controller and solenoid/squib pulses; and the third is a bandpass filter (14.5 ± 1.1 kc) to separate the remainder of the signals. The output from the low-pass filter (solar sensor pulses) is the input to the pip indicator. The output from the 9.745-kc filter (controller and solenoid/squib pulses) is detected and fed to an adding network in the servo-oscillator panel (in preparation for display on an oscilloscope) and also to the command panel for verification of the command signal. The 14.5-kc output of the ground telemetry receiver is fed to the discriminator. The pip indicator consists of two neon bulbs that blink in synchronism with the received solar sensor pulses (ψ and ψ_2). The discriminator, of the phase-locked loop variety, converts the frequency-modulated 14.5-kc signal to a series of analog voltages which are fed to the strip chart recorder and to the decommutator. The VCO output of the discriminator is used to drive the counter-printer instrumentation.

The decommutator circuits form a series of gates synchronized with the output from the spacecraft by the "Sync Calib" signal. These gates separate, or decommutate, the 14 channels of information carried by the 14.5-kc frequency signal. The output from the decommutator is used to energize the timers, counters, and status lights on the command panel and also to drive the display meters on the telemetry panel. Separate display meters are also provided for each of the 11 telemetry channels. The display meters, driven by the output from the decommutator, are peak-reading devices and present a dc voltage in analog form on meter faces calibrated to read directly the pressures, temperatures and other information.

Several items of equipment are included in this group. A Tektronix RM15 oscilloscope is used to present accurate information on synchronism of the drum unit and spacecraft rotation. A Hewlett Packard 5532 Counter is used for an accurate quick-look indication of the spacecraft spin speed. The console also contains a time code generator which has a visual indication as well as electrical outputs for time encoding of the strip chart recorder, magnetic tape recorder, and the printer.

Recording System

The recording system includes a hot-wire chart recorder, a magnetic tape recorder, a digital printer, and several items of associated equipment.

The Offner Electronics strip chart recorder is a standard 8-channel recorder and is used to record such functions as time, decommutated telemetry, receiver AGC and signal strengths, and control signals from the synchronous controller.

The Precision Instruments magnetic tape recorder is used for permanent storage of all received spacecraft telemetry data, transmitted command signals, time, receiver AGC and signal strengths, a reference frequency, and voice label. The recorder has record and reproduce capabilities for both FM and direct record modes.

A standard Hewlett Packard model 562A digital printer is used in conjunction with a CMC electronic counter, a telemetry switching panel, and the EECO time code generator to provide accurate quick-look information of spacecraft telemetry, capability for continuous monitoring of any particular telemetry channel, and an easily read permanent record of spacecraft data.

Communications Ground Stations Resource Requirements

The communications ground stations are provided by the Department of Defense through the U. S. Army Satellite Communication Agency (SATCOM). Transmitted power may be varied from 0 to 20 kw at approximately 7400 mc. Voice signals are angle-modulated on the carrier. Maximum RF bandwidth is approximately 100 kc. Reception of the beacon signal at approximately 1800 mc provides for angle tracking. A low-noise receiver and detector are used for receiving the communication signals. The Syncom system also has a means for measuring range and range rate which uses the spacecraft communication subsystem as a transponder. The ground station portion of the range and range-rate equipment is supplied by NASA.

One communication station is aboard the USNS Kingsport, which was anchored in the port of Lagos, Nigeria during the first few weeks preceding and following the launch. The other principal communication station is located at Lakehurst, New Jersey. Stations are also located at Fort Dix, New Jersey and Camp Roberts, California. The ground stations at Fort Dix and Camp Roberts are equipped with 60-foot diameter parabolic antennas, while 30-foot antennas are installed aboard the USNS Kingsport and at the Lakehurst station. The geographical positions of the communication stations are shown in Figure II-6. Figure II-7 contains photographs of the station.

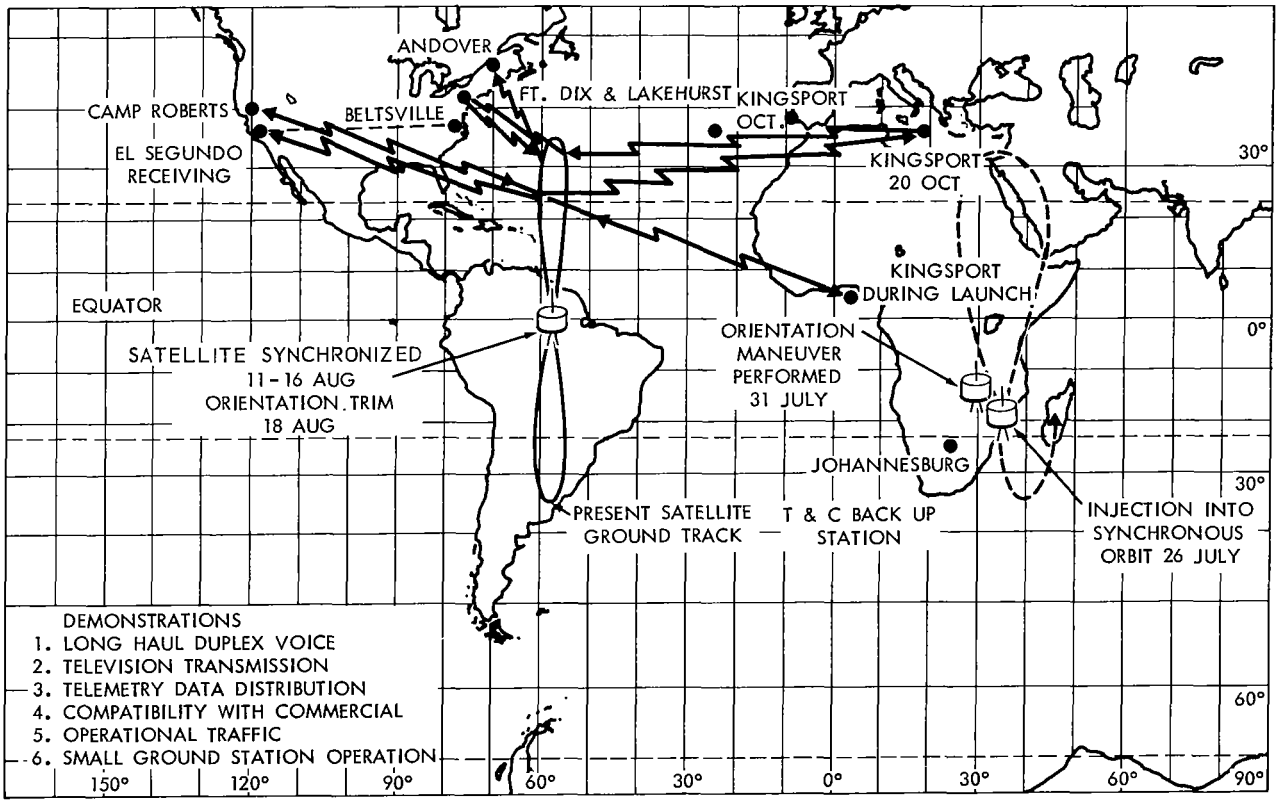

Figure II-6—Geographical locations of communication stations.

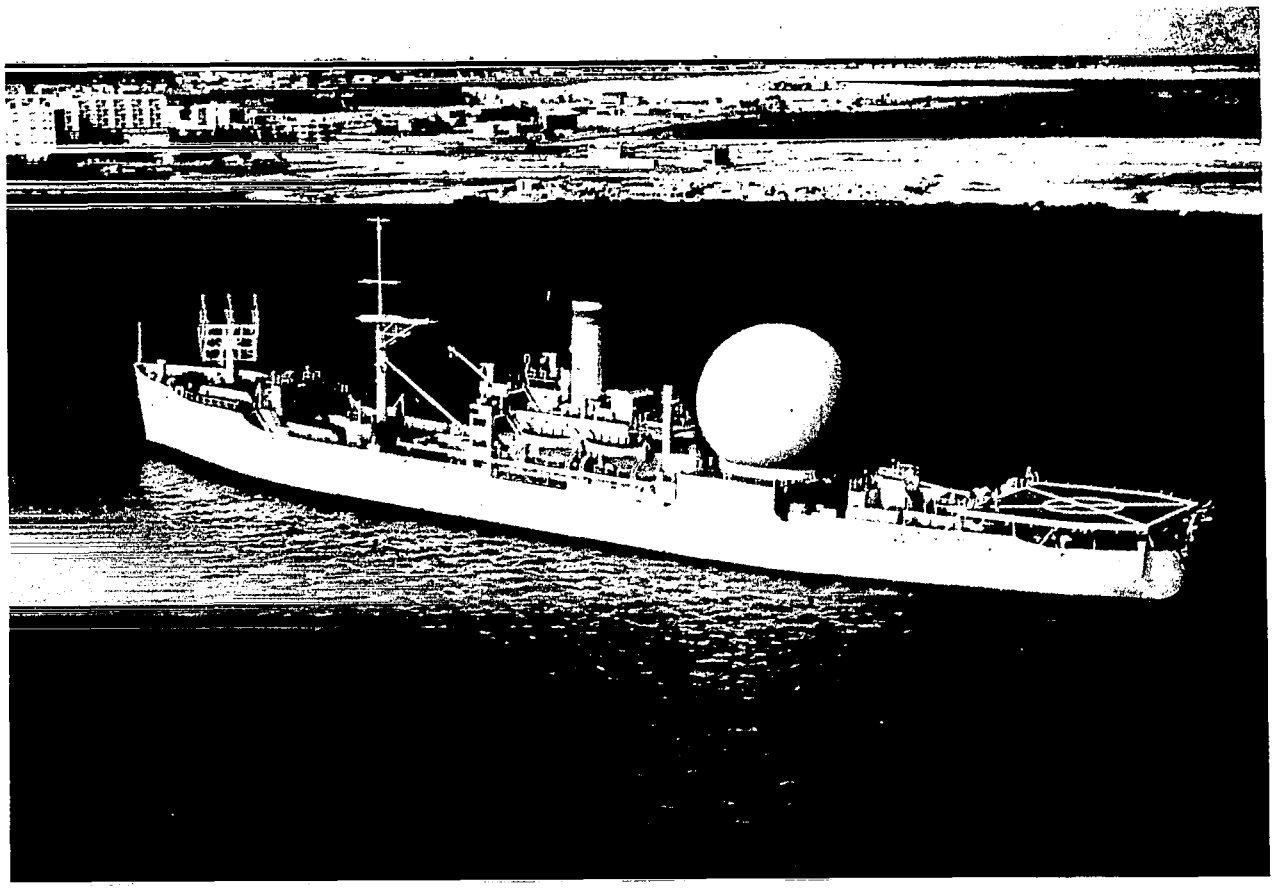

Figure II-7—U. S. Army Satellite Communications Agency's surface complex for NASA'S Syncom.

Satellite Communications Test Operations Center

Communications tests of NASA's Syncom satellite are managed from the Army SATCOM Agency's Satellite Communications Test Operations Center, an information coordinating and communications test control facility wherein data will be received, filtered, and displayed for use in coordinating test operations. Prior to actual operations with the satellite, SATCOM Agency participation with NASA involved the joint planning of the cooperative system test and the organization and operation of the communications test program. These responsibilities include the following tasks relative to test planning: preparation of a coordinated Experiment Test Plan to define the technical spacecraft and communications test to be performed during orbital operation; and preparation of material pertinent to operation of communications tests for inclusion in the Operations Plan.

Detailed data describing the Satellite Communications Test Operations Center follows:

SYSTEM	DISPLAYS
Telemetry	42-item capability on Display Board which can be updated at 8-second intervals over a teletype line.

SYSTEM	DISPLAYS
	During early phases of program, was used to display quick-look communication experiment data.
Television	5 channel, closed circuit 21-monitor units; Channels 1 and 2 connected to plotting boards; 3 and 4 connected to internal and incoming teletype printers; 5 is connected to a commercial tuner.
Telephone	Multiple line 2/4 wire call director system, types of signaling; direct ringing, selective ringing, coded dialing, and direct dialing.
Time	Digital read-out timing systems: Universal Time, System Time, Countdown Time and Countup Time; systems driven by a short duration, 1000 cycle per second sine wave keyed once a second. Accuracy of 1 part in 10^6 per day.
Display Panels	3 double-sided, 3 ft by 7 ft rotatable, w/both back and edge variable intensity lighting. Contains launch and test information on map and graph type formats placed behind plexiglass panels.
Support and Equipment Maintenance Room	Contains circuit patching facilities, teletype printers and circuits, magnetic tape recorders, plotting and drafting boards and related equipment.

USNS Kingsport Shipboard Terminal Equipment

The SATCOM terminal aboard the USNS Kingsport was converted for Syncom use by modification of existing ADVENT facilities and the addition of pertinent equipment. These facilities, comprising ground communications equipment and a 30-foot diameter parabolic antenna, are augmented by the Syncom range, range rate, and polarization measuring system. The ship terminal is capable of transmitting at a maximum of 20 kw power level. A Syncom telemetry and command station is also aboard. Refer to Figure II-8.

Detailed data describing this terminal follows:

COMMUNICATIONS AND TRACKING ANTENNA

Type:	Solid skin paraboloid reflector
Reflector Size:	30-ft diameter
Reflector Material:	Aluminum
Weight:	48,000 lb
Drives:	Amplidyne powered direct drive motors
Stabilization:	3 axes
Axis Travel Limits:	Traverse = ± 25 degrees Elevation = -15 degrees to +135 degrees Train = 360 degrees continuous
Radome:	Pressurized 53-ft hypalon coated dacron
Tracking Accuracy:	± 0.05 degrees

SYSTEM STRUCTURE	USNS Kingsport, 11,000-ton, 455-ft former Victory ship w/10,000 mile range at 15 knots sustained speed.

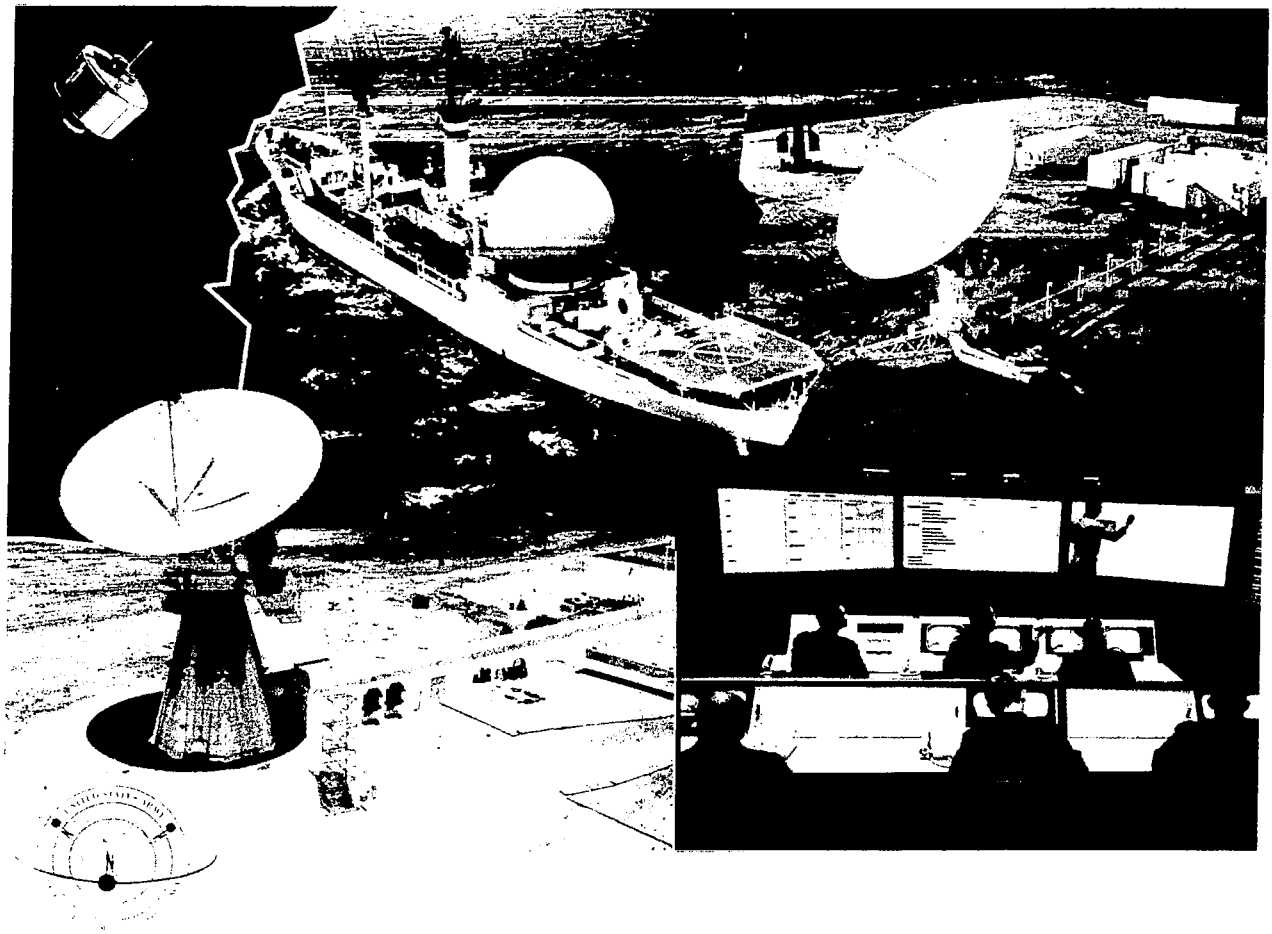

Figure II-8—USNS Kingsport.

Operating Personnel:	60 Navy project personnel, 15 civilian technicians, and ship's crew of 66 MSTS
Location:	On station at sea

SATELLITE COMMUNICATION SYSTEMS

Transmitter:	One FM, SHF (7300 mc nominal), 20-kw output w/frequency stabilization of 1 part in 10^6.
Receiver:	One UHF (1800 mc nominal), w/selectable IF bandwidth of 10, 40 and 100 kc, operating at a system noise temperature of 200° K.
Antenna:	Prime focus horn feed. SHF feed is RHC; UHF feed is interchangeable - RHC or linear polarized; spiral scan automatic tracking, with reflector surface tolerance of 0.0625 inches for outer zone and 0.0313 inches for center zone; 1st side lobe attenuation (UHF and SHF) of 20 db; transmitting gain of 53 db, receiving gain of 40 db. Will operate as temperatures of +12° to +122° F.

COMMUNICATIONS CAPACITY	An analog input of baseband bandwidths of 4, 20 and 50 kc.

TRACKING SYSTEM	Double conversion AM superheterodyne receiver with AFC, AGC, swept 2nd IF, post-detection narrowing and amplification, target acquisition, and switchable mission-dependent parameters.
POWER SOURCE	Ship's generators which produce 600 kw vac.

Air-Transportable Terminals Mark I

There are two primary transportable terminals, each of which constitutes a complete Syncom communications ground station, with the additional capability for measuring range, range rate, and antenna polarization angles. The range and range rate equipment is included in the communication vans. The complete system is comprised of 8 vans (trailers) to accommodate and transport the equipment: An antenna trailer, a receiver van, a high power transmitter van, an operations van, a power control van, and three engine-generator vans. Three additional vehicles are used for service, i.e., a maintenance and spare parts van, an antenna transport trailer, and a service platform. At the site, the trailers are interconnected to form an integrated system by means of cables and transmission lines. All trailers and vans are air-transportable in C124 and C133 aircraft. The station is manned by U. S. Army Strategic Communications Command personnel who were given the required special training. Refer to Figure II-9.

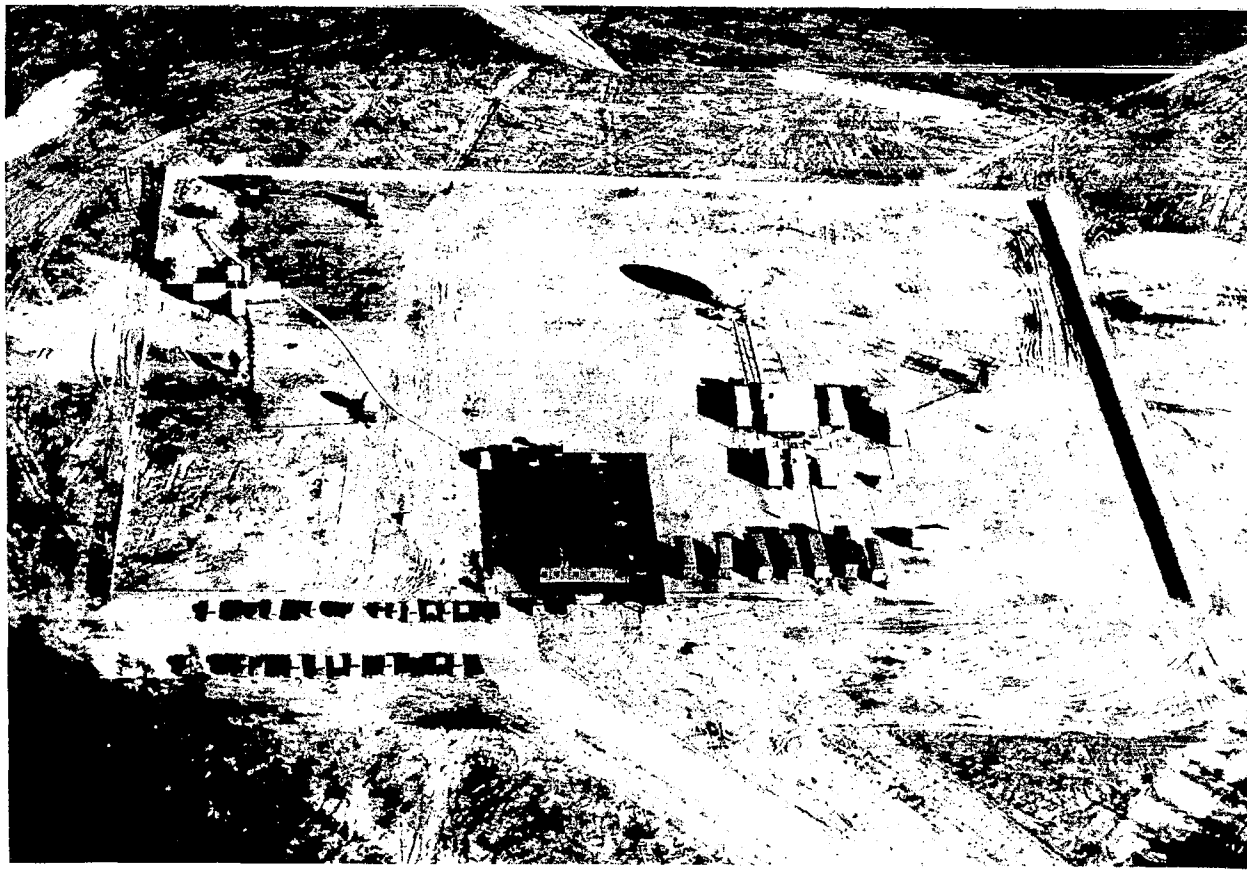

Figure II-9—Syncom System Antennas, Lakehurst.

Detailed data describing the Air Transportable Satellite Communications Terminal (Mark I) at Lakehurst, New Jersey follow:

ANTENNA

Type:	Solid skin honeycomb paraboloid reflector
Reflector Size:	30 feet
Reflector Material:	Aluminum
Weight:	50,000 pounds
Drives:	Electro-mechanical
Axis Travel Limits:	Elevation = -5 degrees to +185 degrees azimuth = continuous 360 degrees
Radome:	None
Tracking Accuracy:	± 0.05 degrees

SYSTEM ARRAY — 11 vans and trailers plus 2 additional vehicles for telemetry and command

Operating Personnel:	12 men communications, 5 men T&C
Assembly:	12 men, 2 days for communications stations
Ambient Operating Temperature Range:	-25 degrees to +130 degrees F
Location:	Lakehurst, N. J. Naval Air Station
Contractors:	Bendix Radio Division - communications Hughes Aircraft - T&C Goodyear Aircraft Corp. - antenna (Sub to BRD)

SATELLITE COMMUNICATIONS SYSTEMS

Transmitter:	One FM, SHF (7300 mc nominal), 20 kw output w/frequency stabilization of 1 part in 10^6.
Receiver:	One UHF parametric amplifier (1800 mc nominal) w/selectable IF bandwidths of 10, 40, and 100 kc, operating at a system noise temperature of 200°K at elevation angle of 7.5 degrees.
Antenna:	Prime focus horn feeds-SHF feed is RHC polarized, UHF is linear polarized conical scan, automatic tracking, with reflector surface tolerance of 0.065 inches maximum, 1st side lobe attenuation of 22.5 db nominal, both UHF and SHF, receiving gain 42 db nominal, transmitter gain 54 db nominal.
Communications Capacity:	An analog input of baseband bandwidths of 4, 20, and 50 kc.

TRACKING SYSTEM — Double conversion AM superheterodyne receiver, with AFC, AGC, swept 2nd IF, post-detection narrowing and amplification, target acquisition, and switchable mission-dependent parameters.

TELEMETRY SYSTEM — 2 watt satellite transmitter, PAM/FM/PM modulation, VHF (138 mc), satellite antenna gain = -4.5 db; ground antenna gain = +23 db; telemetry rate of 4 channels per second.

POWER SOURCES — 3 vans w/diesel engine generators capable of 200 kw at 266/460 volt, 3 phase for communications system.

Fixed Ground Stations (Ft. Dix, N. J. and Camp Roberts, Cal.)

The SATCOM terminals at Fort Dix and Camp Roberts were originally constructed for the ADVENT program and later modified to include a Syncom communications capability but no Syncom range, range rate, or polarization measurement equipment. This modification was performed by the addition of demodulator equipment for narrow band FM operation without compromising the digital capability.

Detailed data describing these terminals follow:

ANTENNA TYPE	Solid skin, honeycomb paraboloid reflector
Reflector Size:	60 feet
Reflector Material:	Aluminum
Weight:	190 tons
Drives:	Electro-mechanical
Axis Travel Limits:	Elevation = -5 degrees to +185 degrees azimuth = continuous 360 degrees
Radome:	None
Tracking Accuracy:	± 0.024 degrees
SYSTEM STRUCTURE	65-ft steel antenna tower on concrete foundation 30-ft deep by 84-ft in diameter, w/reflector atop pedestal base and bridge superstructure; 200-ft long covered passageway to 6,000 sq ft Operations Building.
Operating Personnel:	25 to 30 (single shift basis)
System-Operating Temperatures:	constant (air-conditioned station)
Locations:	Fort Dix, New Jersey and Camp Roberts, California
Prime Contractors:	Sylvania Electric Products (antenna and station construction) Bendix Systems Division (communications equipment) Philco Corp. (TT&C equipment)

SYNCOM RANGE AND RANGE RATE SYSTEM

The Syncom Range and Range Rate Tracking system is a ground system which provides range, range rate, and other tracking and auxiliary data necessary to support the NASA Goddard Space Flight Center (GSFC) Syncom Communications Satellite Program. The system is designed so that it may be used at remotely located stations around the world. The equipment is mounted in racks which can be secured inside a trailer or on a ship so as to provide a transportable system. Overall rack height is slightly greater for shipboard use than for trailer use. For shipboard use (system 1), blank panels are used across the top of racks 1 through 5 to provide overall rack size compatibility. The transmitter exciter unit forms a part of this system, however, it is remotely located. The Syncom Range and Range Rate (RARR) System utilizes the following elements of the Syncom Communication Subsystem:

a) Ground Transmitter
b) Antenna
c) Receiver Preamplifier
d) Satellite Transponder and Antenna

The RARR system measures range and range rate of a Syncom type communications repeater satellite. Range measurements are accomplished by measuring the transit delay experienced by an ensemble of modulated tones impressed on an RF carrier. Range rate is measured by appropriate Doppler shift techniques. The Syncom ground station produces reference square waves and coherent ranging tones (square waves) from a tone generator. The tones are synchronized to a digital clock reference, and are adjusted in phase so that, at a known time, all tones have a simultaneous zero crossing. The tones are then combined, modulated on a carrier, and transmitted at a prescribed carrier frequency. This transmitted signal is received by a transponder in the satellite, and after suitable frequency translation, retransmitted to the ground station. In addition, a multiple of the satellite local oscillator frequency is also transmitted to the ground station for Doppler purposes. The outputs of the ground receiving subsystem are fed to extraction units (one for range and one for Doppler) which provide range and range rate information to the two digital recording channels. The Doppler extraction technique uses the carrier plus local oscillator signal to generate Doppler information, while the range extraction technique uses the sidetone information to generate range information. Range tone square waves of 500 kc, 100 kc, 20 kc, 4 kc, 800 cps, 160 cps, 32 cps, and 8 cps are provided by a unit in the digital area called the range tone and reference pulse generator (RTPG). Switches are provided on the digital data processor rack so that the operator may select the highest received tone (500 kc or 100 kc or 20 kc) and lowest received tone (160 cps or 32 cps or 8 cps) to be used in extracting the range information.

Functional Description

The Syncom Range and Range Rate System is a single-station ground-to-satellite-to-ground tracking system which measures the range and range rate of the Syncom satellite. Tracking data is available in the launch, suborbital, and orbital phases. The system described herein requires the use of an external transmitter power amplifier, antenna, and receiver RF preamplifier. These elements are common to the Syncom Ground Communications Equipment. The system description is divided into three subsystems: a) Range, b) Range Rate, and c) Digital Data Processing. Each subsystem is illustrated in Figure II-10.

Range Subsystem

Syncom satellite range measurements start with generation of the basic crystal oscillator frequency in the Transmitter Oscillator (TO) unit. This frequency is multiplied and then phase modulated with a composite range tone baseband (comprised of four to eight phase-related frequencies) generated by the range tone circuits. The modulated signal is next sent to the Transmitter Exciter unit which further multiplies the signal for use in the ground transmitter. The transmitter power amplifies the output of the exciter unit and transmits the X-band modulated carrier to the satellite. At the satellite, the received carrier is frequency-translated and retransmitted at S-band to the ground receiving station. At the receiving station the range tones are demodulated from the carrier, transformed to a stop-pulse, and sent to a range counter (R-counter). The R-counter previously received a start-pulse derived from the range tones, at which time it began counting a clock frequency. Upon receipt of the stop-pulse, the R-counter stops counting. Range of the satellite is calculated from the R-counter time measurement, which is actually the resultant time delay between ground transmission of the range tones and receipt of the satellite retransmitted range tones. Digital data processing circuits convert the R-counter output along with inputs containing other pertinent information to a form suitable for driving a teletype tape punch machine. Range data and other pertinent information is punched in the tape and then read out on a teletype machine.

Analog phase meters and an eight channel Analog (chart) Recorder provide an alternate or standby method of measuring and recording range data. Phase difference between the individual transmitted and received tones is recorded as an analog voltage for analyst interpretation.

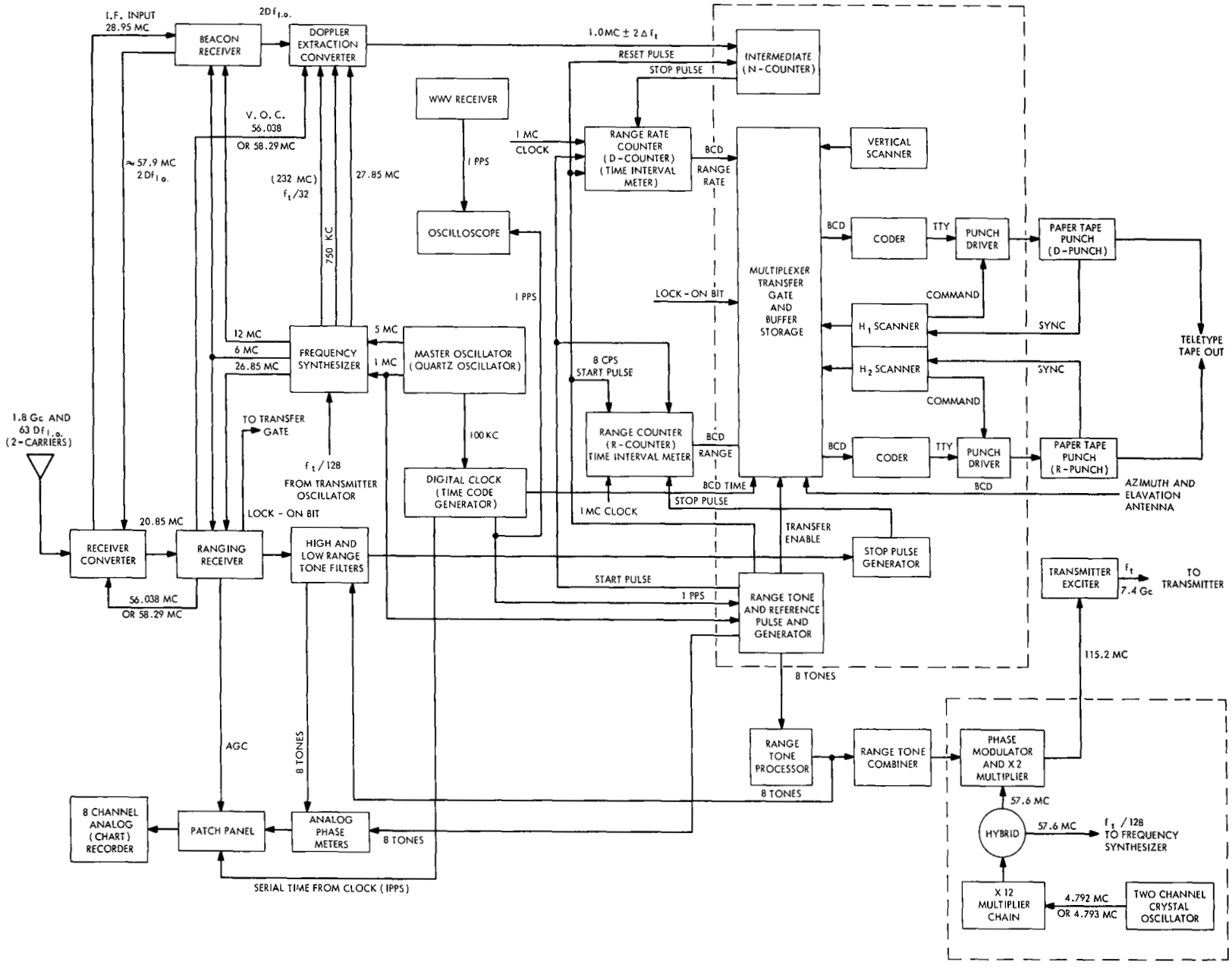

Figure II-10—Syncom range and range rate system, functional block diagram.

Transmitting Section

The satellite range measurement process begins in the Transmitter Oscillator unit with generation of one of two basic frequencies in a crystal oscillator. The two frequencies correspond to the two channels of the satellite transponder, and the channel selection is an operator function. The nominal 4.79 mc output is processed through several multiplier stages increasing the basic frequency twelve times to approximately 57.6 mc. This output is fed to a hybrid isolation transformer which routes the 57.6 mc to the Frequency Synthesizer unit (for use in extracting the Doppler signal) and also to a phase modulator. In the phase modulator, 57.6 mc is modulated with the Range Tone Combiner composite range tone output (detailed in the Range Tone Modulation portion of this description). The modulated output is next multiplied by a times two multiplier to a nominal 115.2 mc and sent to the Transmitter Exciter (TE) unit, where further multiplication increases the frequency to approximately 7.4 Gc. This output is sent to a transmitter which transmits the nominal 7.4 Gc modulated carrier to the satellite via the ground antenna. The satellite in turn translates the received signal and retransmits the modulated carrier at approximately 1.8 Gc back to the ground where it enters the receiving system via the same antenna.

Range of the satellite is next determined by appropriate ranging circuits. These circuits measure transit time delay between the ground transmission and received satellite retransmission. A more detailed explanation of the received range transmission is described in the Processing of Received Satellite Range Transmission portion of this discussion.

Range Tone Modulation

The range tone modulation portion of the range subsystem is used to produce a composite range tone baseband (composed of four to eight range tones). As previously described, the 7.4 Gc carrier is modulated by the composite range tone baseband which, in turn, is transmitted to the satellite. Initially the range tone process begins with a 1-mc output from a quartz oscillator (Master Oscillator). This output is fed to a range tone and reference pulse generator (located in the Digital Data Processing subsystem) which employs a series of binary counting circuits to divide the 1-mc into the following separate frequencies: a) 500 kc, b) 100 kc, c) 20 kc, d) 4 kc, e) 800 cps, f) 160 cps, g) 32 cps, h) 8 cps, i) 4 cps, j) 2 cps, and k) 1 cps. The three lowest frequencies are used to synchronize the acquisition and tape punch rates, whereas the eight higher frequencies are employed as range tones. All eight output range tones are applied to the Range Tone Processor. This unit consists of bandpass filters and balanced modulators which convert the eight square waves to sine waves. In addition, the four lower range tones (single sideband) modulate a 4-kc subcarrier (becoming 4.008 kc, 4.032 kc, 4.160 kc, and 4.8 kc) to enhance the eventual tone detection process. The range tone outputs are sent to the High and Low Range Tone Filters as reference frequencies (explained in the Processing of Received Satellite Transmission portion of this description) and also to the Range Tone Combiner. This unit contains resolvers and individual amplifiers which introduce an optimum phase relationship between all individual tone frequencies. This optimum phase relationship defines a specific wave front used in determining transit time delay between transmitted and received range tones. The Range Tone Combiner also contains summing circuitry which combines the individual phase-shifted frequencies into a composite output. The summing circuitry contains provisions for deleting certain tones if they are not desired, and for adjusting the individual amplitudes of the tones prior to summing. The composite tone output is sent to the Transmitter Oscillator unit to modulate the multiplied basic crystal oscillator frequency (previously detailed in the Transmitting Section description).

Another operation pertinent to range tone modulation is synchronization of the system to a standard time base. Initially the time base starts with a 100-kc output from the Master Oscillator. This frequency is applied to a Time Code Generator (Digital Clock) which generates a 1 PPS timing pulse and sends it to the range tone and reference pulse generator. The 1 PPS output from the range tone and reference pulse generator is automatically made to coincide with the Digital Clock 1 PPS. The time base can be checked and/or synchronized to WWV by comparing the WWV receiver 1 PPS output with the Digital Clock 1 PPS output on an oscilloscope, and adjusting the latter as required.

Processing of Received Satellite Range Transmission

The satellite receives a 7.4 Gc modulated signal (carrier and composite range frequency tone) from the ground transmitter. This signal is translated to another frequency and retransmitted at approximately 1.8 Gc (along with a multiple of the satellite local oscillator) back to the ground receiving station. The transmission is received at the antenna and sent through a broad band parametric amplifier to the Receiver Converter unit. A Receiver Converter multiplier chain multiplies the voltage controlled oscillator (VCO) signal from the Ranging Receiver from approximately 58 mc to approximately 1.8 Gc, after which it is mixed with the received satellite transmission. The resultant 20.85 mc mixer output is fed to the Ranging Receiver. In the receiver, this signal is amplified and heterodyned with a 26.85-mc reference frequency from the Frequency Synthesizer unit. The resultant 6-mc output is amplified and compared in a phase detector with a 6-mc reference frequency from the Frequency Synthesizer. Any phase difference between the two signals results in a correction voltage which is applied to the VCO to control the VCO operating frequency. In this manner, the VCO operating frequency is locked to and controlled by the satellite transmitted ranging channel carrier frequency. When locked to the ranging carrier, the modulation is recovered by a phase detector circuit. High and Low Range Tone Filters accept the demodulated receiver output and separate the composite range tone baseband into its individual frequency components. The lower range tones, which had previously been single sideband modulated on to the 4-kc tone prior to transmission, are translated back down to their original frequencies. Prior to acquisition of the satellite transmitted signal by the Ranging Receiver, the tone tracking filters are locked on to the reference tones from the Range Tone Processor to assure that the filters are operating near their proper frequency.

Upon acquisition of the satellite transmitted signal, the 100 kc sidetone phase delay to the spacecraft and return is measured to an accuracy of 1 percent by controlling the 100 kc phase-locked loop (thus the deviation of the phase of the 100-kc signal and the phase-locked frequency is less than 3.6 degrees). This accuracy equals 1 count of 10 mc, which in turn is equivalent to a resolution of 0.1 microsecond in range time or to a resolution of ±15 meters in range. The lower range tones of 20 kc, 4 kc, 800 cps, 160 cps, 32 cps, and 8 cps are controlled so that their individual phases do not vary more than ± 36 degrees, which resolves the ambiguity of the next higher tone to the whole cycle.

The demodulated tones (from 4 to 8 depending on which ones are in use) are shaped into pulses and routed to individual flip-flops in the Stop Pulse Generator located in the Digital Data Processor unit. The low tone return pulse sets the low tone flip-flop which enables the next higher tone flip-flop. In a similar manner, each subsequent flip-flop is enabled by the set condition of the previous flip-flop. Since the phase relation of the tones is previously adjusted, the flip-flops are reset in sequence from the lowest tone chosen. When the highest tone chosen has reset its respective flip-flop, a pulse is generated which is used as the stop pulse to the Range Counter (R-counter). This is a commercial time interval meter that counts 10 mc (obtained by internally multiplying the 1-mc output from an ultrastable Master Oscillator). During the range transmission process, the Range Tone and Reference Pulse Generator sends a start-pulse (derived from the reference square wave output that also resets the R-counter) which may occur every 1/8 of a second. This pulse starts the R-counter 10-mc count which continues until receipt of the stop-pulse which stops the frequency count. Operating time of the R-counter coincides with total transit time required for the range frequency tones to be transmitted from the ground and then returned by the satellite. The shorter the distance between ground station and satellite, the lower the count on the R-counter. Conversely, a greater distance would produce a higher R-counter count. Range of the satellite is calculated from the R-counter measurement which is actually the resultant time delay between ground transmission of the range tones and receipt of the satellite retransmitted range tones. Digital data processing circuits convert the binary coded decimal (BCD) output from the R-counter along with inputs containing other pertinent information to a form suitable for driving a teletype Paper Tape Punch machine. Range data and other pertinent information are punched in the tape and then read out on a teletype machine. A more detailed explanation of range readout is described in the Digital Data Processing Subsystem portion of this description.

Analog phase meters and an eight channel Analog (chart) Recorder are used as a back up method of measuring and recording range data. By using the square wave output of each range tone to set a flip-flop, a measure of relative range is obtained. The output of the flip-flop is a pulse whose width is dependent on the transit time and at a PRF equal to the tone being examined. As the range (and hence transit time) increases from zero, the pulse width of the flip-flop output increases until it equals entire period (i.e., the reciprocal) of that tone. As the range is further increased, the pulse width immediately drops to zero and starts to increase again. The recorder thus presents ambiguous range as measured by each range tone, and the ambiguities must later be resolved by the operator. For recording pusposes, the flip-flop output is integrated (by charging a capacitor) and converted into a DC voltage proportional to phase delay. This phase delay is presented on a hot stylus recording. For reasons of flexibility, a patched system of connecting the recorder is used.

Range Rate Subsystem

Range rate is established by measuring two-way Doppler shift resulting from a transmission to the satellite in motion and a subsequent retransmission back to the ground station. The sequence of operations which result in range rate information are:

a) Ground station transmits a very stable frequency to satellite in motion.
b) Satellite translates the received signal to another frequqncy and then retransmits this frequency back to the ground station along with a multiple of the satellite local oscillator frequency.
c) Ground station receives and processes transmitted satellite frequency and local oscillator frequency through appropriate Doppler extraction circuits.
d) Doppler extraction output is routed through data processing circuits which automatically compute and read out range rate data.

The crystal controlled satellite local oscillator is not highly stabilized. This eliminates stability circuits and components; thereby minimizing power consumption and weight in the satellite. Doppler extraction circuits are used to compensate for possible satellite transmission frequency instabilities and still maintain range rate information.

Two-Way Doppler Transmission

The carrier of the ground transmitter is used in the mixer operations for the range rate measurements. It is derived from one of two ultrastable oscillators, the one used depending on frequency selection. The carrier and the ranging sidetones are received at the spacecraft transponder, which acts as a booster amplifier and translates the spectrum down to either 1814.069 or 1815.794 mc from 7361.275 or 7363.000 mc, respectively (Figures II-11 and II-12).

The receivers at the tracking station receive the transmitted carrier frequency from the ground transmitter minus 192 times the satellite total oscillator frequency for the range tone frequency. For the beacon frequency they receive 63 times the satellite local oscillator frequency. The receivers provide initial mixing and phase locking to the transmitted carrier frequency and beacon frequency. This produces a difference frequency equal to the sum of the following:

a) The satellite local oscillator frequency.
b) The one-way Doppler shift of the carrier in the 7.3 Gc range.
c) The one-way Doppler shift of the ground-transmitted carrier frequency minus 192 times the satellite local oscillator frequency.
d) The one-way Doppler shift of 63 times the satellite local oscillator frequency.
e) The satellite local oscillator drift.
f) The Doppler frequency (Figure II-13).

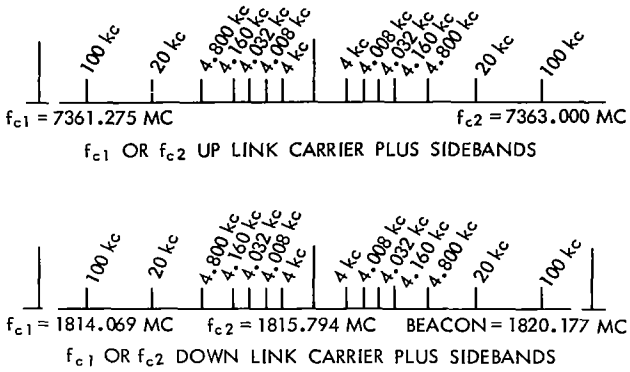

Figure II-11—Spectra.

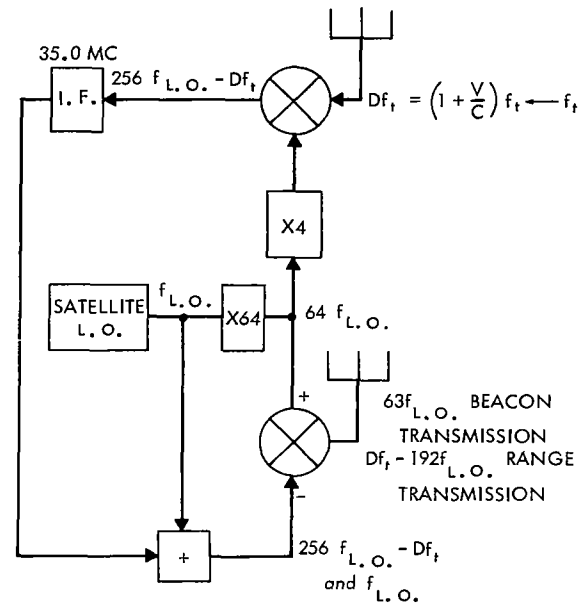

Figure II-12—Spacecraft transponder.

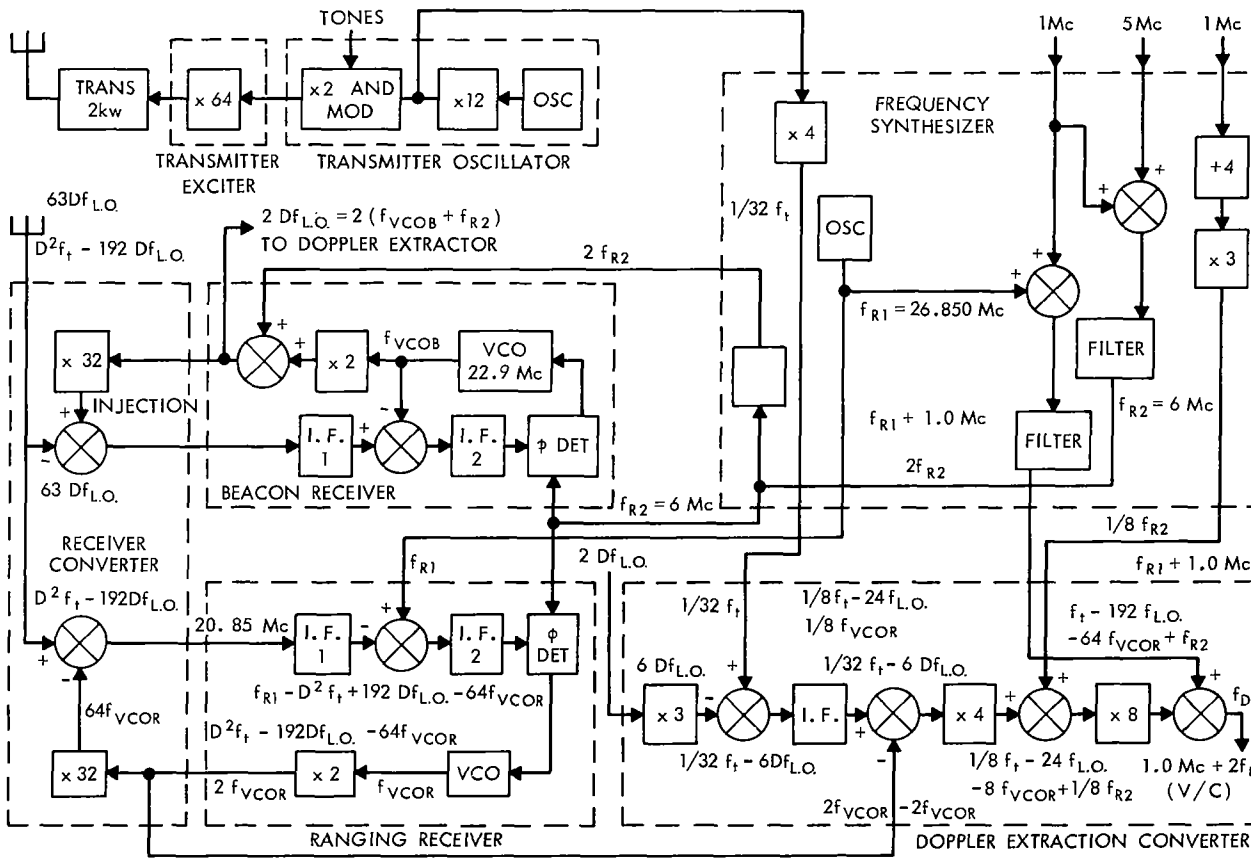

Figure II-13—Receivers and Doppler extraction process (f_{vcor} is the frequency of the VCO in the ranging receiver and f_{vcob} is the frequency of the VCO in the beacon receiver).

The ranging frequency (ground-transmitted carrier frequency minus 192 times the satellite local oscillator frequency) is converted by utilizing phase-locked oscillators for carrier and range tone detection.

The Doppler extractor mixes the outputs of both receivers to remove all satellite local oscillator drifts and produces the two-way Doppler shift of the transmitted carrier impressed on a bias frequency of 1 mc (Figure II-13). The 1-mc biased Doppler is fed to a digital unit of the Doppler extractor which counts at a 10-mc rate in a second time interval unit for a period of 81924 counts of the 1-mc biased frequency ± the Doppler frequency.

Doppler Extraction Process

The Doppler Extraction Converter Unit (also referred to as Doppler Extractor) is used to extract two way Doppler information. The Doppler extractor consists of mixers, multipliers, and amplifiers. The Doppler shifted satellite LO frequency ($2Df_{L.O.}$) is applied to the Doppler extractor along with various reference frequencies from the Frequency Synthesizer unit. The beacon frequency, $2Df_{L.O.}$, (D is the Doppler-shifted frequency) is multiplied by 3 in the first multiplier (Figure II-13) to produce $6Df_{L.O.}$, which is mixed with $(1/32)\ f_t$ to yield $(1/32)\ f_t - 6Df_{L.O.}$. This output is mixed with $2f_{vcor}$ (f_{vcor} is the frequency of the VCO in the ranging receiver) to produce $(1/32)\ f_t - 6Df_{L.O.} - 2f_{vcor}$ which is then multiplied by 4 to give the output at the times 4 multiplier of $(1/8)\ f_t - 24f_{L.O.} - 8f_{vcor}$. This signal is mixed with $(1/8)\ f_{R2}$ (750 kc) to produce $(1/8)\ f_t - 24f_{L.O.} - 8f_{vcor} + 1/8f_{R2}$. This is subtracted from f_{R1} + 1 mc (f_{R1} = 27.85 mc) to obtain an output of 1.0 mc $\pm 2f_t(v/c)$. This Doppler Extractor output is 1 mc ± 2 times the change in carrier due to Doppler Shift, (1.0 mc $\pm 2f_t$) or a frequency between approximately 700 kc and 1.3 mc. Adding 1 mc to the output allows the read-out equipment to detect the sign of the Doppler shift. For the Syncom frequencies, 1 cycle of Doppler shift is equivalent to a range rate of approximately 0.05 meters per second. Refer to Figure II-12.

Range Rate Measurements

The Doppler extractor output is applied to intermediate binary counting circuits (referred to as Intermediate Counter or N-Counter) which count the incoming Doppler frequency until reaching a count of 81925. At this time, the N-counter sends a stop-pulse to a commercial time interval meter (referred to as Range-Rate or D-Counter). The D-counter counts 10-mc obtained by internally multiplying the 1-mc output from an ultrastable Master Oscillator. During the range rate transmission process, the range tone and reference pulse generator sends out a start-pulse (derived from the 8 cps square wave output that also resets the N and D-counters) which may occur every 1/8 of a second. This pulse starts the D-counter to continuously count 10 mc until receipt of the stop-pulse which stops the frequency count. If the Doppler frequency is greater than 1 mc (satellite moving toward a ground station), the N-counter will reach 81925 faster; thereby sending out a stop-pulse sooner and stopping the D-counter at a lower count. Conversely a Doppler frequency lower than 1 mc (satellite moving away from ground station) will require more time to reach a 81925 N count; thereby stopping the D-counter at a higher count. Range rate may be calculated from the D-counter measurement by the operator or an external computer. Digital data processing circuits convert the binary coded decimal (BCD) D-counter output data into a form suitable for driving a teletype Paper Tape Punch machine. Range rate data is punched in the tape and then read out on a teletype machine. A more detailed explanation of range rate readout is described in the Digital Data Processing Subsystem portion of this description.

Data Processing Subsystem

The digital equipment generates the range tones and timing signals required for transmission and the necessary equipment for recording received data in both analog and digital form. There are two digital tape punches plus a backup 8-channel Analog (chart) Recorder. The Master Oscillator and count-down circuitry (range tone and reference pulse generator) generate the basic

frequencies for the entire system. This comprises the data sampling reference pulses, the ranging tone frequencies, and a 1 PPS signal. The Time Code Generator (Digital Clock) in conjunction with the Master Oscillator generates 1 PPS signals which are used to synchronize the system to a standard time base. Periodically, the digital clock 1 PPS may be synchronized with the WWV receiver output by means of the oscilloscope and hence, the whole system will become synched to WWV. Range and range rate extraction units generate the start and stop pulses defining the intervals during which the Time Interval Meters (R and D counters) count to produce range and range rate information. The 1-mc clock input to the counters is multiplied by 10 within the counters to provide time increments of 0.1 microseconds. The Analog phase meters, in conjunction with the Analog (chart) Recorder, are used as a backup to the range subsystem to present the phase difference between transmitted and received tones of each range tone frequency. Ranging receiver AGC and time information also may be recorded by the Analog (chart) Recorder. The Digital Data Processor contains multiplexing units to assemble the range, range rate, elevation, azimuth, time, and other data. Data is processed, formatted in binary coded decimal (BCD) code, multiplexed and converted to teletype (TTY) code, and then punched into a paper tape in a standard TTY 5 band code.

Digital Data Processor Operation

The Digital Data Processor range tone and reference pulse generator, stop pulse generator, and intermediate-counter (N-counter), were previously described in the Range Subsystem and Range Rate Subsystem descriptions. BCD information from the Range (R-counter), Range Rate or Doppler Counter (D-counter), digital clock, and antenna (azimuth and elevation) are sent to the transfer and buffer storage unit. The BCD outputs from the time interval meters (R and D counters) are transferred to the buffer storage in order to free the counters for the measurement of the next range and Doppler time intervals. Following transfer of the BCD outputs from the counters, the counters are reset to zero and await the next START pulse from the range tone and reference pulse generator. The transfer gate and buffer storage unit transfers out information through a coder. The coder changes the BCD code to TTY code suitable for driving a teletype Paper Tape Punch. Information is presented to the tape punches by the H_1 and H_2 scanners via the punch drivers. The tape punch command presentation rate is controlled by feeding a sync pulse back into the scanner. There are two tape punches along with associated drivers, scanners, and coders. Both tape punches and associated units are employed when necessary to rapidly punch information on the tape. The punch rate is controllable to 1, 2, 4, or 8 horizontal scans (12 characters) per second for each tape punch. Complete information pertaining to range, range rate, time, antenna (azimuth and elevation) and receiver lock-on information (establishes if both receivers were locked on to the appropriate carriers) is punched in the tape along with other identifying information. The punched tape must be fed through a teletype machine in order to type out the information.

CHAPTER III

LAUNCH AND ORBITAL MANEUVERS

The prelaunch activity at AMR is directed toward compatibility checks with the boost vehicle; confidence checks and final preparation on the flight spacecraft for launch. The center of the AMR operation is established in the spacecraft laboratory in Building AE. This building houses system test equipment which is used to check the flight spacecraft for both readiness and compatibility with the boost vehicle hardware. A prototype spacecraft is utilized to insure that the checkout equipment is compatible with the flight spacecraft.

The prototype spacecraft is delivered to AMR with adequate lead time to make the necessary qualification checks on the test equipment as well as confirming the installations and qualifying the r.f. links between the spacecraft laboratory and the sites remote from the laboratory such as the NASA/DAC (Douglas Aircraft Co.) spin balance area and the launch area.

PRELAUNCH ACTIVITY

The prototype spacecraft was delivered to the NASA/DAC spin balance area on 8 July, installed on an inert third stage and mounted on the launch vehicle at Pad 17A for participation in the F-minus-10 day (RFI) tests. After the successful completion of this test the prototype was returned to the spacecraft laboratory.

The flight spacecraft was delivered to the spacecraft laboratory on 10 July. During the on-arrival test, command receiver sensitivity was seriously degraded when adjacent whip antennas were disconnected. This test was made with hardline connections from the test equipment to the spacecraft. The problem was more pronounced when telemetry transmitter 2 was operating with adjacent whips disconnected. An investigation of the telemetry transmitter spectrum under this condition revealed an abnormal spike at approximately 150 mc. With all whips connected, the spectrum appeared normal. From these observations, the telemetry transmitter was considered possibly to be at fault, and a replacement transmitter was temporarily substituted. This did not correct the problem. The problem could not be duplicated on the prototype spacecraft. Since this condition would not occur except in the case of loss of two adjacent whips, a decision was made to consider the spacecraft satisfactory for launch.

The spacecraft was delivered to NASA/DAC spin balance area on 13 July, and the apogee motor was installed and aligned with no problem. The spacecraft was weighed by Douglas personnel and installed on the flight third stage. A check made on the spacecraft separation switches showed that at least one switch was not closing properly and the spacecraft was lifted from the third stage. The four switches on the spacecraft thrust ring interface were checked, and one switch was found to require more than the normal amount of leaf travel before it activated. The leaf was replaced on this switch as well as on one other questionable switch and the spacecraft was reinstalled on the third stage.

The dynamic balance of the third stage/spacecraft was completed on 15 July, and the assembly was delivered to Pad 17A and mated to the booster on 17 July.

During the F-minus-6 day tests on the booster vehicle, noise appeared on the booster second stage pitch telemetry channel. During subsequent testing, this condition re-occurred and also appeared at a lower magnitude on the yaw channel. The problem was isolated to the position potentiometers on the actuators. A decision was made to change both actuators. Only one actuator was available and a second could not be delivered until 19 July. This necessitated a slip of the All-Systems Test until 22 July with launch on 24 July.

The F-minus-3 day All-Systems Test was conducted and successfully completed on 22 July.

The F-minus-1 day tests on the spacecraft and vehicle were completed as scheduled on 23 July.

The launch day countdown was initiated at 1751 EST on 23 July. During the first spacecraft functional test at 2103 EST, a transponder oscillation was noted when the wideband transponder was on. The problem could not be definitely isolated; therefore, at 0112 EST on 24 July the launch was postponed. An investigation of the flight spacecraft and prototype indicated that the oscillations were created by feedback from the communications antenna to the antenna electronics when the communications antenna was in its folded position as mounted on the third stage. This condition did not exist, however, during earlier tests in this same configuration. Using the prototype spacecraft, it was demonstrated that these oscillations would disappear when the communications antenna was erected to its normal operating position coincident with the spacecraft spin axis. Tests were conducted on the flight model using metallic foil to shield the communications antenna to reduce the coupling to the antenna electronics. These corroborative data confirmed that the behavior was abnormal due to feedback from the antenna to the interior elements of the transponder and, so, unique to the payload arrangement in the booster and not a problem after payload separation from the booster third stage. The launch was rescheduled for 0932 EST on 25 July.

The F-minus-0 countdown was initiated at 1700 EST on 24 July but was interrupted at 1900 EST for a previously scheduled launch at nearby Complex 31. The countdown resumed at 2305 EST and proceeded normally until 0505 EST on 25 July. At this point it was noted that the first stage yaw gyro was drifting at a rate of 22 degrees per hour. The countdown proceeded with another drift gyro check scheduled at T-minus-20 minutes. The drift rate check at T-minus-20 minutes indicated a drift of 54 degrees per hour. The drift rate could not be corrected; the launch was postponed at 0956 EST on 25 July, and rescheduled for 0933 EST on 26 July.

A decision was made to leave the spacecraft telemetry system on until the countdown was resumed at approximately 0100 EST on 26 July to monitor the pressure in the spacecraft hydrogen peroxide unit. This monitoring operation was conducted with the system test equipment telemetry readout console in the spacecraft laboratory. No change in pressure was noted during the monitoring period. The spacecraft telemetry system was turned off at 0045 EST 26 July.

The countdown was reinitiated at 0105 EST on 26 July. At 0145, during the sequence for turning on the spacecraft wide band receiver for a spacecraft transponder check, the axial hydrogen peroxide jet was inadvertently fired. This firing resulted from a procedural error in the operation of the ground equipment.

When the axial jet fired, the nozzle plug was blown out. A thorough investigation revealed no damage to the spacecraft, third stage or spin table from the nozzle plug. A vacuum pump was connected to the axial jet at 0215 EST to remove any residual peroxide around the valve seat. The vacuum pump was removed at 0300 EST. The third stage/spacecraft fairing installation commenced at this time on schedule.

The countdown proceeded normally to lift-off at 0933 EST with no further problems.

SATELLITE ACQUISITION AFTER LIFTOFF

Spacecraft telemetry system 1 was on at liftoff and yielded data to the GSFC Satellite Tracking Station and the Building AE tracking station at the Cape until the spacecraft disappeared beyond the rf horizon at T +415 seconds (415 seconds after liftoff). All data were normal at this time.

At Antigua, the tracking system acquired the spacecraft telemetry signal at T +240 seconds and then lost the signal at T+770 seconds. The spacecraft telemetry data from Antigua indicated that spacecraft separation from the third stage occurred between T+529 and T+533 (nominal T + 531). These telemetry data were relayed from Antigua by RF link and were received at the Cape Telemetry Receiving Site 2 in real time.

Ascension Island acquired the spacecraft at T+780 seconds and monitored it continuously until well after apogee motor firing. Telemetry data from Ascension Island were transmitted to the Cape in real time with good results.

The USNS Kingsport acquired the spacecraft telemetry at approximately T+15 minutes and monitored the data continuously through apogee motor firing.

The Johannesburg telemetry and command station acquired the spacecraft telemetry at approximately T+18 minutes, monitored this signal through apogee motor firing, and was capable of monitoring until the spacecraft was in its westward drift orbit approximately two weeks later.

From lift off, through the powered flight phase, to payload separation, all programmed events occurred on schedule. Vehicle performance was nominal. Minor corrections were required by the BTL second stage guidance system but were within the capability of the system.

Third stage spin up occurred as scheduled at T+210 seconds. The third stage spin rate at second stage/third stage separation was 147.5 rpm. The spin rate decreased to 145.5 rpm at third stage burnout. (T+411 seconds).

After the initial acquisition of the spacecraft by the Kingsport a telemetry status report was taken and the data indicated that all systems were normal. At that time the Kingsport became capable of tracking the spacecraft continuously. The spacecraft communication transponder was commanded "On" and the first utilization occurred at approximately T+25 minutes for polarization angle and range and range rate measurements. These data are used for spacecraft attitude determination and to supplement the orbital data gathered by the Minitrack system, respectively.

Following the range and range rate measurements, a voice and music message, of approximately five minutes duration, was transmitted from the Kingsport to the spacecraft; the spacecraft to ground return signal was received by the Kingsport. Immediately following the voice and music, a ten-minute message of tones and other modulation was transmitted to measure the performance characteristics of the spacecraft. Successful performance was achieved in all test categories. The spacecraft transponder was commanded off by the Kingsport at T+91 minutes.

At approximately T+170 minutes the spacecraft transponder was commanded "On" and another series of experiments was conducted with completely satisfactory results. These experiments were completed and the transponder was commanded "Off" at T+230 minutes.

Throughout the remainder of the transfer orbit, Minitrack data, polarization angle measurements, and range and range rate measurements were processed by GSFC. This information was processed for a precise determination of the transfer orbit and establishing the optimum firing time for the spacecraft apogee motor. Calculations made, based upon the available transfer orbit data, indicated a near nominal transfer orbit; therefore, it was decided that the apogee motor firing would be accomplished by the pre-set spacecraft timer rather than by ground command.

APOGEE MOTOR IGNITION

Apogee motor ignition occurred at T+5 hours 33 minutes. The motor burn time was a nominal 20.2 seconds. Spacecraft acceleration was measured by the spacecraft accelerometer. The tracking station located at Olifantsfontain, South Africa (which is one of twelve in a world wide network operated by the Smithsonian Astrophysical Observatory under a NASA grant) photographed the firing with a Baker-Nunn Camera having a 20 inch focal length at f. 1. The photographs taken are shown in Figure III-1. Exposure time for each frame was six seconds. Just after ignition (Photo No. 1) the firing is still only a dot (arrow on the print) but subtends 3 minutes of arc or about 19 miles. At burnout (Photo No. 5) the plume was 66 miles long and 33 miles wide.

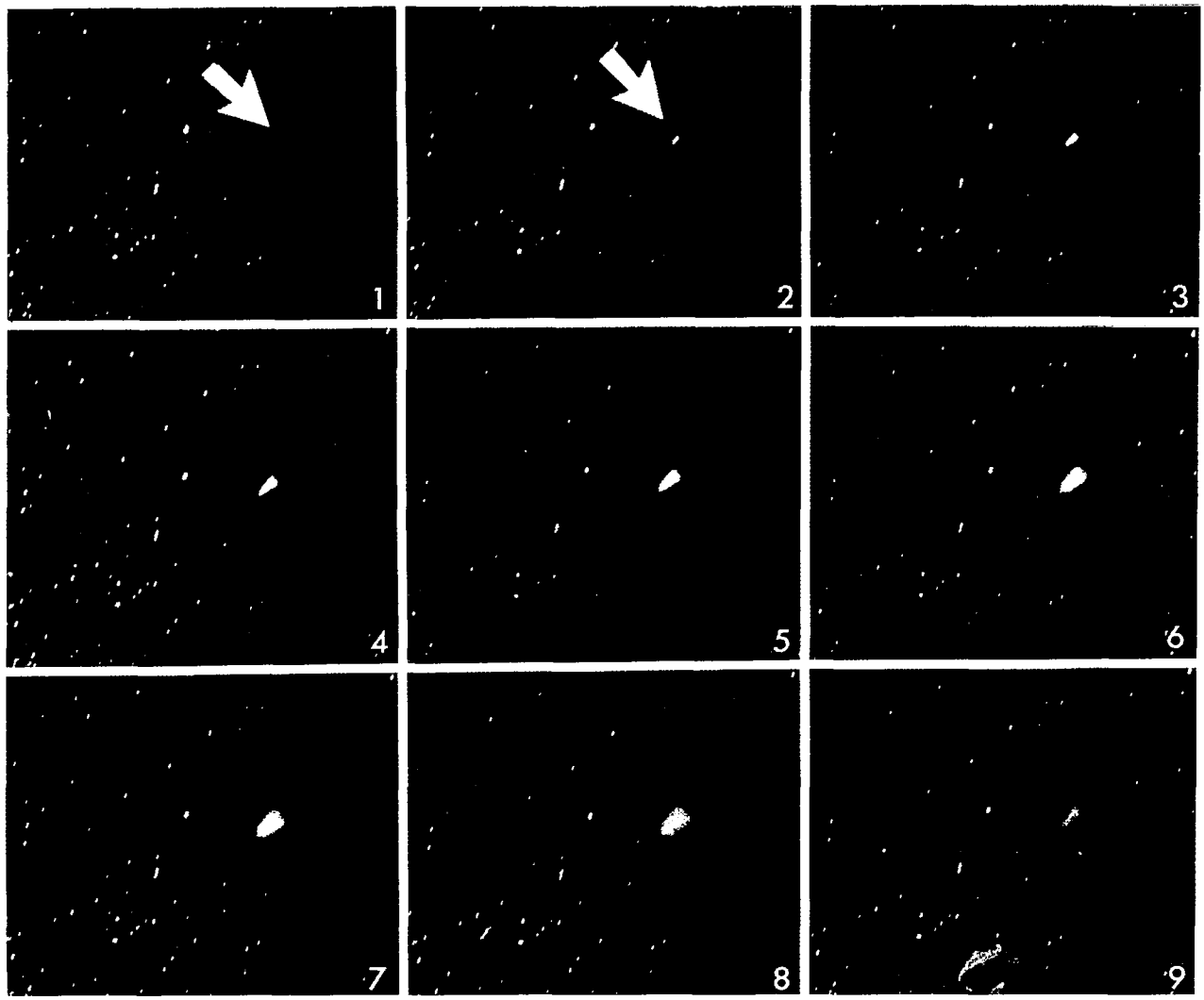

Figure III-1—Apogee motor firing sequence.

ORBITAL PERFORMANCE CONCLUSIONS

The following information, based on preliminary analysis, summarizes the orbits, maneuvers, and control subsystem performance for Syncom II:

a) The spacecraft was synchronized at the desired 55°W longitude,

b) The spin axis was maneuvered to within 1 degree of the desired direction,

c) The transfer orbit and apogee motor boost were near nominal; no mission degradation resulted from small deviations from predicted parameters,

d) All of the orbit control modes functioned properly,

e) All orbit maneuvers were successful,

f) The specific impulses obtained from the control subsystem were correct,

g) There were propellant flow-rate calibration errors, but these errors did not degrade mission results,

h) Orbit determination and prediction are limitations on the evaluation of small corrections (velocity corrections of 1 fps, for example), and

i) Attitude determination within short intervals of time is limited by polarization angle measurements.

Definition of Orbital Parameters

Parameters which are referred to by symbols or groups of alphabetic characters are defined in the following sections.

Spacecraft Flight Parameters

In Figure III-2, the spacecraft flight parameters have been referred to a coordinate system where the x axis lies in the Greenwich meridian and the equatorial plane at the epoch; the y axis is 90° east, and the z axis is chosen to form a right handed system.

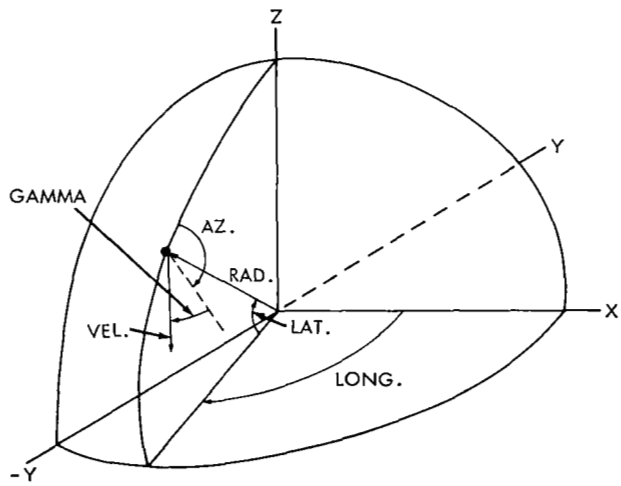

Figure III-2—Spacecraft flight parameters.

Lat.	Geocentric latitude (+ north)
Long.	Longitude (+ west)
Rad.	Radius from the center of the earth
Vel.	Inertial velocity
Gamma	Vertical flight path angle of the velocity vector (positive if the spacecraft is moving away from the earth)
Az.	Azimuth angle of the velocity vector (0 degrees to the north and increasing to the east)

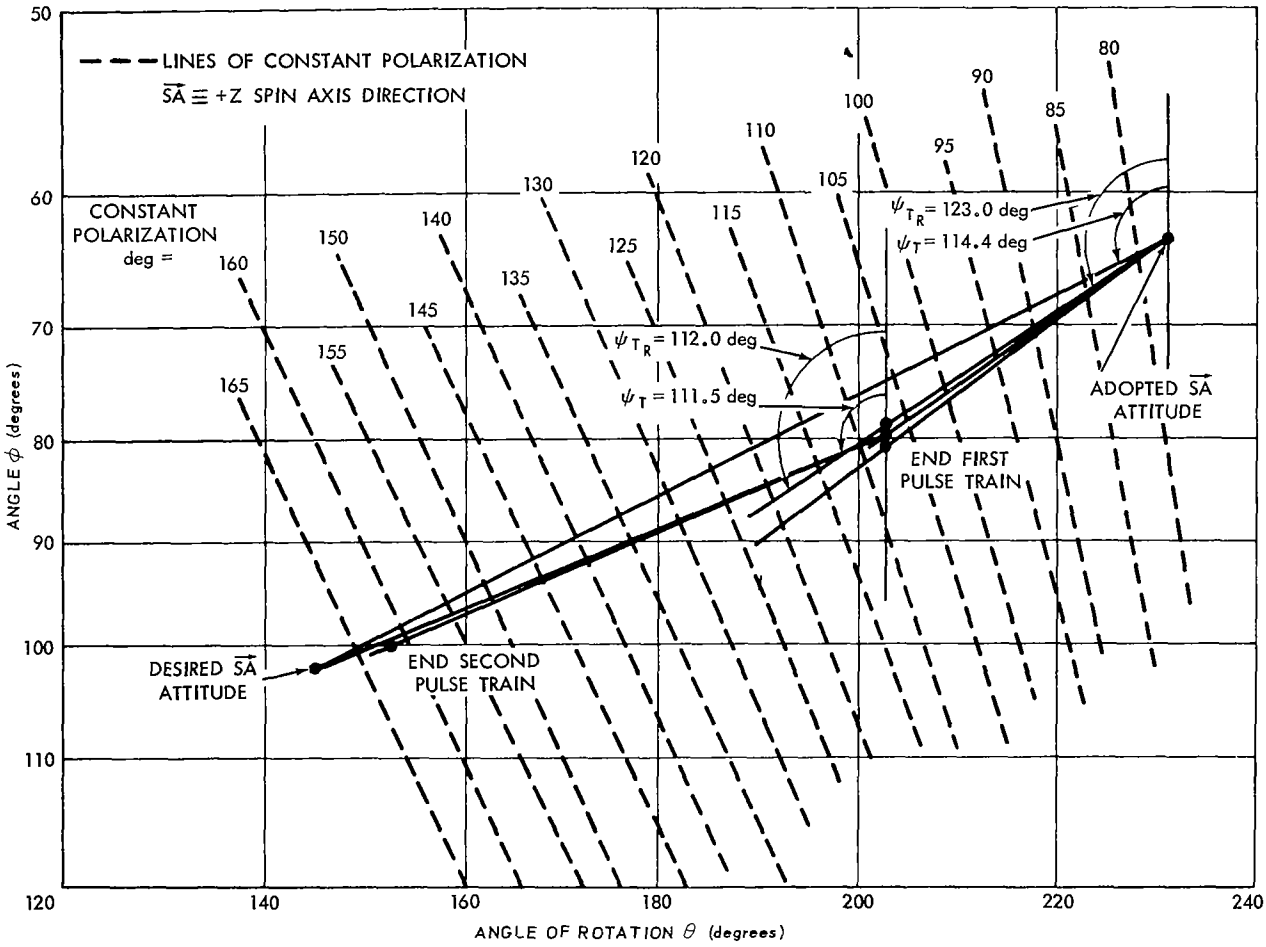

Figure III-3—Mercator plot of reorientation maneuver.

Other Parameters

Constant Polarization Lines	Those lines along which the +z spin axis would precess with no change in polarization angle if an indicated ψ_T were applied. ψ_T is measured from a meridian (vertical line) on the chart to a dashed line. See Figure III-3.
Dec.	Declination of the +z spin axis direction (Figure III-4)
e	Eccentricity of the orbit
I_{sp}	Specific impulse, seconds
$(I_{sp})_{eff}$	Effective specific impulse, corrected for pulsed operation
Number pulses	Number of times the control jet was opened and closed for a maneuver

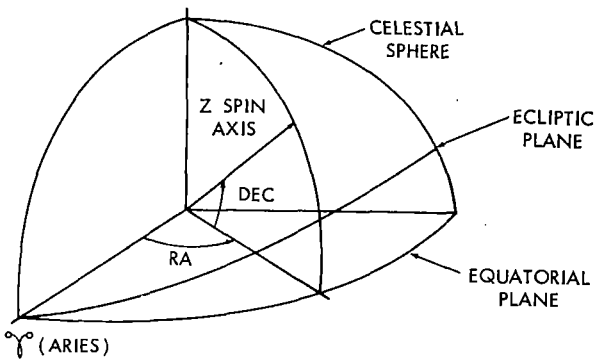

Figure III-4—Declination and right ascension.

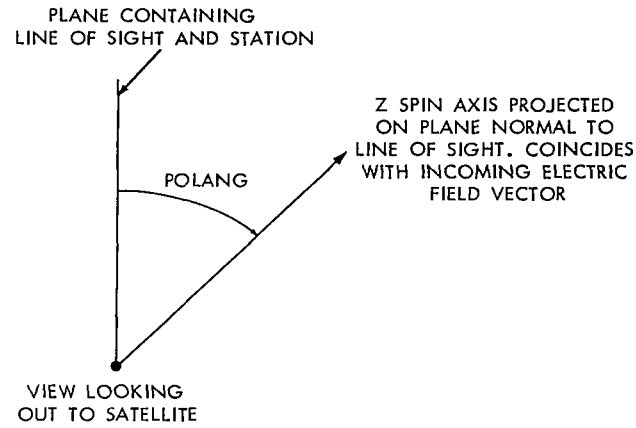

Figure III-5—Polarization angle.

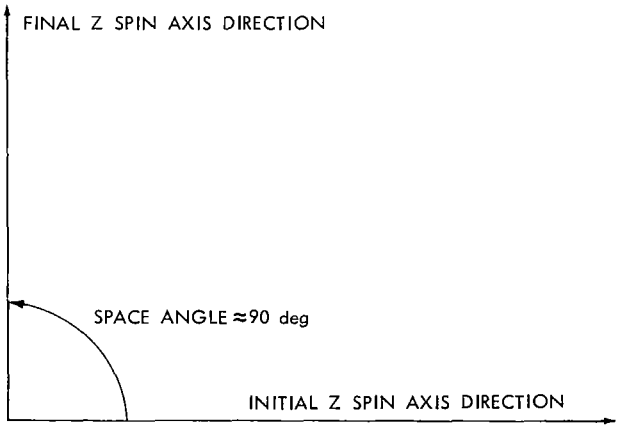

Figure III-6—Precession angle.

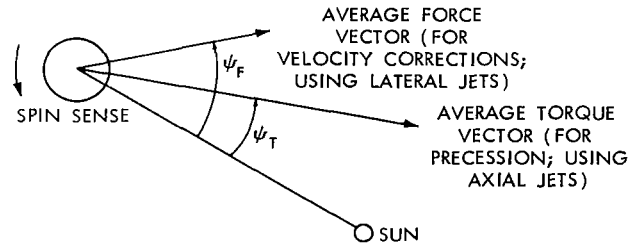

Figure III-7—Precession phase.

POLANG	Polarization angle; the angle, measured about the line of sight, between the vertical plane containing the line of sight and the plane of polarization of the transponder signal (plane of electric vector and line of sight). If the polarization is vertical, the polarization angle is zero; if the plane of polarization is rotated clockwise from the vertical as seen from the station, the polarization angle is positive. POLANG has a range of -180 to +180 degrees, as Hughes takes into account the sense of direction of the spin axis, which is not observable in polarization angle measurements (Figure III-5).
Precession angle	Space angle through which the spin axis was precessed (Figure III-6).
Precession phase	ψ_T the angle, from the projection of the sunline on the plane normal to the spin axis, to the average precession torque vector (positive in the sense of spin). Figure III-7 is a view of Syncom II with the +z spin axis pointing out of the paper.
Pulsing time	Total time required for a maneuver
RA	Right ascension of the +z spin axis direction (Figure III-4)
Resulting drift	Difference in longitude on two successive passes of the ascending node (i.e., when the subsatellite point crosses the equator, traveling from south to north); this quantity is positive if the drift is to the west

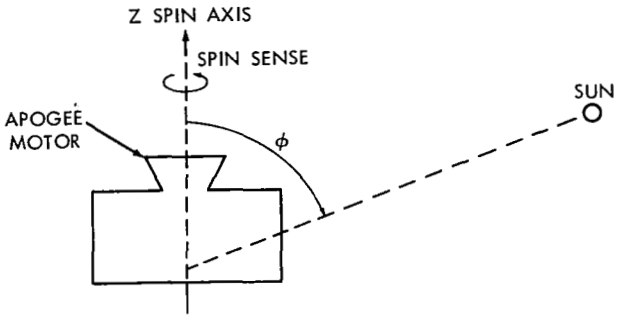

Figure III-8—Spin axis.

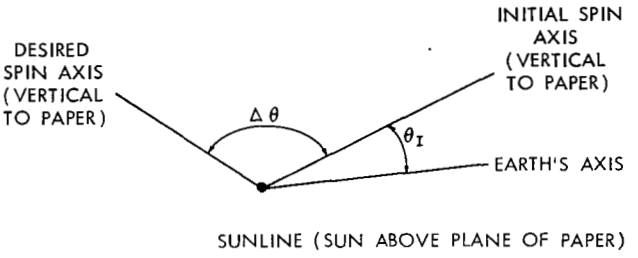

Figure III-9—Angle of rotation.

Spin axis (attitude)	+z spin axis direction (i.e., the axis of rotation); the +z axis is directed toward the apogee motor end of the satellite (see Figure III-8).
Δ(drift)	Change in drift rate (prior to and after a maneuver)
Δ_V	Velocity increment, fps
$\lvert\Delta V\rvert$	Magnitude of a velocity increment
ΔW	Amount of mass loss, pounds
θ	Angle of rotation, about the sunline, of the +z spin axis relative to a plane defined by the sunline and the axis of the earth (Figure III-9).
ϕ	Angle between the +z spin axis direction and the sunline (Figure III-8)
ϕ_I	Initial ϕ
ϕ_F	Final ϕ
ψ_2	Spin phase angle between solar sensor pips; analytically, $\psi_2 \triangleq \sin^{-1}\left[\tan 35°/\tan \phi\right]$
ψ_D	Angle defining spacecraft geometry and time delays in the electronic circuits. Example: (ψ_D) force $H_2O_2 \cong 180 + 30 + 30 = 240$ degrees 180 degrees accounts for the direction of the applied force using the H_2O_2 lateral jet, relative to the ψ solar sensor. 30 degrees accounts for turning the jet on 30 degrees before the average applied force. 30 degrees accounts for estimated 30 milliseconds time delay.
ψ_T	Theoretical precession phase angle
ψ_{T_R}	Observed precession phase angle
ω	Argument of perigee

Control Subsystem Geometry

The geometry of the hydrogen peroxide unit is shown in Figure III-10 and the geometry of the nitrogen unit is shown in Figure III-11.

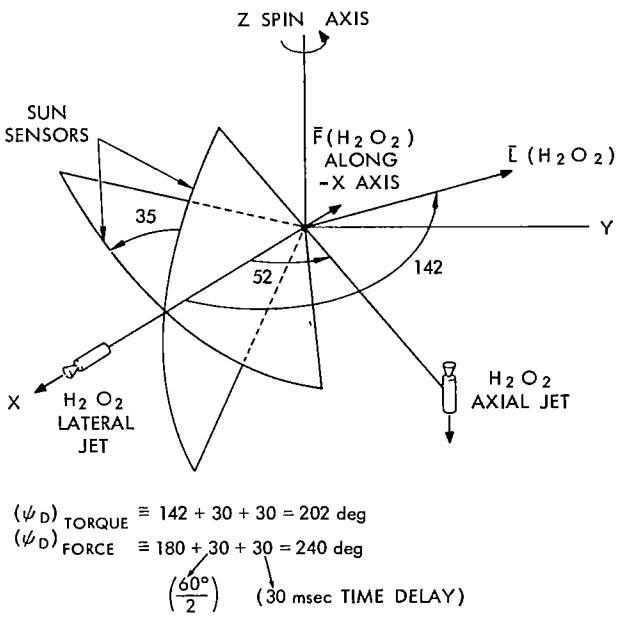

Figure III-10—Hydrogen peroxide unit geometry.

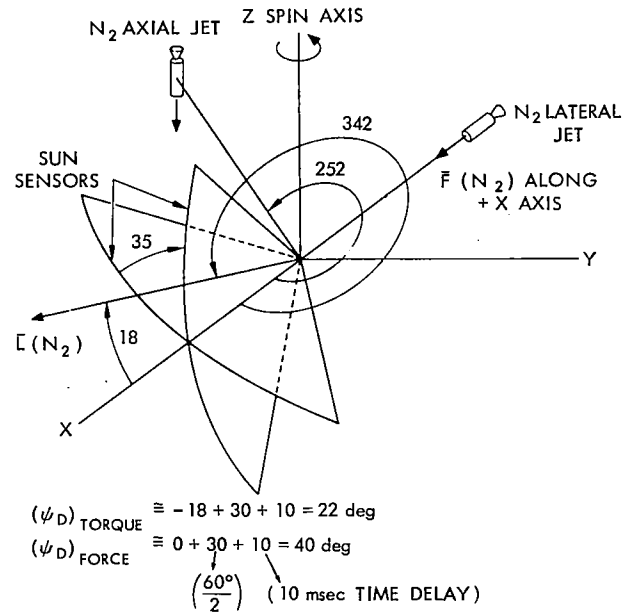

Figure III-11—Nitrogen unit geometry.

SUMMARY OF MANEUVERS

This discussion summarizes all of the maneuvers which were made with Syncom II through January 15, 1964. All results presented are based on preliminary analysis; a definitive analysis will be made when definitive vectors are received from Goddard Space Flight Center (GSFC).

Since the spin axis (+z) direction was generally believed to be known within at least 5 degrees, with the primary uncertainty in the direction perpendicular to the sunline, orbital maneuver calculations were performed using both the best estimates of spin axis right ascension and declination and also one or more alternate solutions. This was done to determine the sensitivities of important parameters (i.e., ΔV, eccentricity, etc.) with relation to the thrust directions which would be realized by considering various spacecraft attitudes. In general, the required maneuver procedures did not depend significantly on spin axis direction, and the procedures were based on the best available solution for spin axis attitude.

Transfer Orbit

On 26 July, Epoch* $14^h 40^m 00^s$ Z the Thor-Delta boost vehicle placed Syncom II in a near nominal transfer orbit. The velocity increment imparted by the third stage was approximately 30 fps $(2/3\sigma)$ low; otherwise the transfer orbit was nominal. The resulting inclination and eccentricity, which can be derived from the actual flight parameters listed in Table III-1, were, respectively, 33.14 degrees and 0.732718.

*The tabulated flight parameters are derived for an epoch which has been chosen (for convenience) to be 9 seconds after actual third-stage burnout.

Table III-1

Flight Parameters

PARAMETER	LATITUDE ° N	LONGITUDE ° W	RADIUS (n. mi.)	VELOCITY (fps)	GAMMA (degrees)	AZIMUTH (degrees)	DEGREES
Nominal*	21.798	63.439	3559.85	33,604.69	0.236	115.385	68.4
Bell Telephone Laboratories	21.868	63.621	3557.89	33,633.66	0.022	115.301	
Actual**	21.829	63.586	3559.587	33,669.97	0.061	115.577	69.0

*Predicted by Douglas Aircraft Company prior to flight.

**Flight parameters derived at liftoff +280 minutes and used to determine when to fire the apogee motor.

The Bell Telephone Laboratory (BTL) tracking data collected during second-stage powered flight of the Thor-Delta were reduced to corresponding flight parameters by GSFC and Hughes and are presented here. The calculation was based on nominal third-stage performance. The "actual" flight parameters were determined at the GSFC from range, range-rate, azimuth, elevation, and Minitrack direction cosine data collected at Lagos, Nigeria, and Johannesburg, South Africa, during the transfer orbit.

Apogee Boost and Resulting Orbit

On 26 July apogee motor ignition took place at $20^h05^m56.54^s$ Z. Apogee motor burnout occurred at $20^h06^m16.74^s$ Z.

As a result of the apogee boost, the spacecraft was placed in a near-synchronous orbit; however, since the transfer orbit was low in energy, the spacecraft was in a low-energy orbit, relative to synchronous energy, and drifted eastward after the apogee boost. The apogee boost was 0.3 percent above nominal and actually improved the resulting orbit. The difference between the resulting inertial velocity and the inertial velocity required for synchronism was approximately 0.6σ ($\approx$68 fps). This was not detrimental since there was more than 3σ of velocity control available in the S/C.

Some of the more pertinent parameters for the maneuver are shown in Table III-2.

Axial Jet Correction (Hydrogen Peroxide)

On 27 July, $19^h10^m00^s$ to $19^h12^m20^s$ Z* Axial Jet Correction was initiated because the spacecraft was placed in the initial near-synchronous orbit with the first ascending nodal crossing occurring at 38° East Greenwich, and because the satellite was drifting eastward at a rate of 7 degrees per orbit, the hydrogen peroxide axial jet control unit was utilized (in the continuous mode) during the designated time interval, which was one orbit period subsequent to the apogee motor boost, to initiate a westward drift toward the desired final longitude of 55° West Greenwich. The predicted westward drift rate of 6.1 degrees per orbit was selected to keep the final eccentricity to a reasonable value, yet bring the satellite on station at 55° W in a reasonable length of time. The specific impulse was correct, but the control system calibration was in error; hence, the flow rate was over

*The difference between the GMTs presented here and in the following discussion represents the total time required to complete the designed maneuver.

estimated and the resulting ΔV was less than expected, resulting in a lower drift rate than was predicted. The lower drift rate did not degrade the overall mission results; it simply meant that it would take slightly longer to bring the satellite on station with a smaller eccentricity in the final orbit. Parameters of interest are tabulated in Table III-3.

Table III-2

Maneuver Parameters

PARAMETER	ΔV (fps)	RESULTING DRIFT (deg/orbit)	INCLINATION (degrees)	e	ω (degrees)	RA (degrees)	DEC. (degrees)
Predicted (liftoff +280^m elements)	4696.1	-8.87		0.02880	127.7	178.929*	-23.357*
Actual**	4712.1**	-7.03	33.05	0.02844	180.8	180.17**	-23.45**
Difference	16.0	1.84		-0.00036	-18.9	1.24***	-0.10***

Note: Initial spacecraft weight: 146.92 pounds
Final spacecraft weight: 85.64 pounds
ΔW: 61.28 pounds

*Based upon attitude derived from BTL data.

**The actual parameter values (ΔV, RA, and Dec.) are derived from the Hughes VINCEV (velocity increment evaluation) computer program. The VINCEV program calculates the magnitude and direction of the imparted ΔV required to transfer from one orbit to another, based on knowledge of the orbital elements before and after a velocity correction.

***The total deviation in boost direction from the derived BTL attitude was 1.14 degrees.

Table III-3

Axial Jet Correction Parameters

PARAMETER	ΔV, (fps)	RESULTING DRIFT (deg/orbit)	INCLINATION (degrees)	e	ω (degrees)	RA (degrees)	DEC. (degrees)	ΔW (pounds)	ISP, (seconds)
Predicted*	124	6.1		†	†	180.17 ‡	-23.45	2.067	157
Predicted**	107.5	4.21		0.01329	63.88	180.17 ‡	-23.45	1.80	157
Actual	109.8	4.53	33.05	0.01305	61.74	177.62	-23.49	1.80	160

*Based on jet on-time.

**Based on the observed pressure drop.

† The predicted (based on jet on-time) e and ω are not presented since the desired drift rate was a compromise between two selected values.

‡ These values were derived from the direction of apogee motor boost.

Reorientation (Axial Hydrogen Peroxide Jet)

On 31 July, at 20^h40^m to 21^h07^mZ reorientation occurred since 24-hour communication capability was desired as soon as practicable, and since the incident angle of the sun's rays was increasing relative to normal incidence on the solar panels and thereby causing a decline in power output, an early reorientation maneuver of the +z spin axis was designed to direct the axis parallel to the southward normal to the orbit plane; before the maneuver, the +z spin axis direction was nearly in the plane of the orbit. In the desired direction (RA = 47.92 degrees: Dec. = 56.95 degrees) maximum gain of the spacecraft antenna is achieved in the direction of the earth at all times.

Since the spacecraft was drifting less rapidly to the west before the maneuver than was desired, it was decided to reorient the axis of rotation at the time in the orbit when a maximum increase in westward drift would result because of jet impulse. This approach required that additional propellant be expended to synchronize the spacecraft at 55° W longitude; however, there was more than sufficient fuel on board to meet all objectives.

Two pulse trains were designed to complete the maneuver, the first to establish correct directional maneuvering and the second to maneuver the spacecraft to the desired orientation. As a result of the maneuver, the following conclusions were reached:

a) ψ_D was as much as 7 degrees more than predicted, and

b) After correction based on the low flow rate observed in the previous maneuver, it was concluded that the flow rate data were good for pulsed operation.

Accurate reorientation is limited by the accuracy of POLANG measurements.

Table III-4 summarizes the more interesting parameters.

A Mercator plot of the reorientation maneuver similar to that actually used at the time the maneuver was executed is shown in Figure III-3. At the end of the first pulse train Figure III-3 shows three dots on a vertical line. The top dot represents location of the spin axis after precession as observed by Hughes personnel at the control site in Nigeria. The lowest dot represents the position as determined by Hughes personnel at GSFC. The middle dot represents the mean value used to obtain ψ_T for the second pulse train.

At the end of the second pulse train, as indicated on Figure III-3, the test conductor at GSFC realized that 90 degrees of precession had probably not been achieved; however, because exact positioning was not required at that time, he terminated the maneuver to determine the attitude of the spacecraft more exactly.

With the spacecraft in the resulting attitude, determined to be within approximately 8.5 degrees of the desired direction, 24-hour communications with the satellite were realized at Lagos, Nigeria.

Effect of Reorientation on Orbit

Table III-5 shows the more interesting parameters which were influenced as a result of reorientation. It is considered unlikely that the magnitude and direction of the "actual" ΔV are "real." One possible explanation for the large discrepancy between predicted and actual ΔV is that there may be errors in the orbital data which were used to derive the "actuals."

Table III-4

Axial Jet Reorientation Parameters

PARAMETER	PULSING TIME, (seconds)	NUMBER OF PULSES	PRECESSION ANGLE, (degrees)	PRECESSION PHASE, (degrees)	Ø1 (degrees)	ØF (degrees)
FIRST PULSE TRAIN						
Predicted	56	135	30*	114.3	64.0	76.4
Actual	56	135	29-31**	122-124	64.3†	79.5-80.5
SECOND PULSE TRAIN						
Predicted	87	211	54*	113.2‖	79.5-80.5	101.2
Actual	87	215	52-53**	112.5	79.5-80.5	100.1

*Calibration data were corrected based on the previous maneuver.

**33 and 51.8 degrees were calculated from the propellant expended for (Isp) eff = 111 seconds.

† The 0.3 degree difference in predicted versus actual Ø1 is a consequence of the adopted spin axis RA and Dec. prior to the maneuver. Since there was some uncertainty in the +z spin axis direction, the mean values adopted for RA and Dec. were respectively, 180.0 and -23.5 degrees.

‡ The 3 to 4 degree difference in predicted versus actual ØF is a consequence of the observed precession phase angle.

§ A sign error was made in correcting a polarization angle for Faraday rotation during execution of the maneuver; after correcting this error, precession would be predicted as per the above. The second pulse train was designed to complete the 90 degree precession but was insufficient because the duration was based on the incorrect POLANG.

‖ Based upon results of the first pulse train, the precession phase angle was adjusted by 4 degrees for the second pulse train; hence there is better agreement with predicted versus actual.

Table III-5

Parameters Influenced by Reorientation

PARAMETER	ΔV (fps)	Δ (DRIFT) (deg/orbit)	RESULTING DRIFT (deg/orbit)	INCLINATION (degrees)	W (pounds)
Predicted	15.5 (Isp = 119 sec)*	1.30	5.83		0.396
	20.8 (Isp = 160 sec)*	1.74	6.27		0.396
Actual	30.0**	2.29	6.82	33.13	0.40

*Based upon actual ΔW.

**It is assumed, based upon ΔW, that the large discrepancy in ΔV will be reduced (resolved) when definitive orbital elements become available. This assumption is supported by the large angle (≈23 degrees) between the direction of the computed ΔV and the path traversed by the spin axis during the maneuver.

Hydrogen Peroxide Lateral Jet Correction

On 11 August at 16^h00^m00 to $06^h14^m13^s$ Z*, the first velocity correction, in preparation to synchronize the satellite at 55° West Greenwich, was designed to reduce the westward drift rate to a value such that three orbital periods subsequent to the maneuver the spacecraft would be in the optimal position in its orbit to be synchronized at exactly 55°W.

Optimal means that at the time of the subsequent required maneuver a minimal ΔV would be required and after the maneuver a minimum eccentricity would be realized.

Since ψ_D was incorrect for the hydrogen peroxide axial jet, a revised value of ψ_D for the hydrogen peroxide lateral jet was derived based on the reorientation results. A correction of 6.8 degrees was applied to the previously derived value of ψ_D for the hydrogen peroxide lateral jet. It appears that this correction in the phasing angle for the maneuver should not have been applied. Results from the Hughes VINCEV (Velocity Increment Evaluation) computer program suggest that the direction of ΔV was in error by about 8 degrees in the same direction as the correction for ψ_D; however, since orbital data was only preliminary, these results are not definitive. Some of the more important parameters are listed in Table III-6.

First Nitrogen Pulsed Jet Correction

On 12 August, at 05^h45^mZ to $06^h14^m19^s$Z†, since the westward drift rate had not been sufficiently reduced after the first velocity correction, a second correction was designed and executed during the above GMTs, to reduce the westward drift rate to a value such that three orbital periods subsequent to the maneuver, the spacecraft would be in the optimal position in its orbit to be synchronized at exactly 55°W.

Table III-6

Hydrogen Peroxide Pulsed Jet Correction Parameters

PARAMETER	PULSING TIME (seconds)	ΔV (fps)	RESULTING DRIFT (deg/orbit)	ΔW (pounds)	(I_{sp}) EFF (seconds)*	NUMBER PULSES	INCLINATION (degrees)
Predicted	393**	44.06	2.0	1.03	111	938/906***	
Actual	393	39.3† 37.5‡	2.67	0.91§	106	894(SYNCTV)||	33.12

*Includes a factor of 0.9549; see note (**) under Table III-7.

**The value of the flow rate factor for pulsing operation for axial jet (0.77) is nearly correct for lateral jet; the value of 0.671 presented in calibration reports was in error.

***At a constant spin speed, 938 pulses would have resulted from 393 seconds of total pulsing time; however, because of a decrease in spin speed during the maneuver, it was calculated that 906 pulses were generated.

† This maneuver took approximately 15 minutes to complete because of periodic servo unlock at the ground command and control station.

§ Based on observed pressure drop.

|| SYNCTV is the telemetry and command (T/C) station at Lakehurst, New Jersey.

*This maneuver took approximately 15 minutes to complete because of periodic servo unlock at the ground command and control station.

†The maneuver took approximately 30 minutes to complete, partly because of servo unlock at the ground command and control station.

The magnitude of ΔV required for this maneuver was approximately 0.1 percent of the inertial velocity. Because the ΔV for this and subsequent maneuvers was small in magnitude, and because the orbital data used in the analysis were preliminary, caution should be exercised in attempts to deduce conclusive information from the remainder of this discussion.

Table III-7 gives important first nitrogen pulsed jet correction parameters.

Table III-7

First Nitrogen Pulsed Jet Correction Parameters

PARAMETER	PULSING TIME (seconds)	ΔV (fps)*	RESULTING DRIFT (deg/orbit)	ΔW (pounds)*	(ISP) EFF (seconds)	INCLINATION (degrees)
Predicted	510	13.75	1.189	0.495	(74 X 0.9549) = 70.66**	
Actual	510	12.8-13.1 †	1.31	0.485	67 to 72	33.12
		13.755 ‡				

*There are uncertainties in ΔW and ΔV comparable to the possible effect of calibration data errors.

**The factor of 0.9549 applied to (Isp) is a geometrical consideration resulting from the 60-degree pulse duration using the

$$F_G = \frac{3}{\pi}\int_{-\pi/6}^{\pi/6} \cos x \, dx = \frac{3}{\pi} = 0.9549$$

† Initial evaluation; the angular error was probably < 10 degrees.

‡ A revised evaluation by GSFC.

Second Nitrogen Pulsed Jet Correction

On 15 August, at $05^h20^m00^sZ$ to $06^h06^m22^sZ$*, the westward drift was not reduced to the desired value after the second velocity correction; however, the spacecraft was not maneuvered again until the above date and time. By August 15, the spacecraft had actually passed 55°, so this third velocity correction was designed to change the westward drift to an eastward drift of 0.05 deg/orbit. This rate was chosen because orbital perturbations caused by triaxiality would decrease the eastward drift rate to 0 deg/orbit and cause the spacecraft to drift westward again. When this maneuver was designed, it was predicted that a 40-day cycle time for velocity corrections would result, requiring about 12 fps/year of control.

Because the previous velocity correction was "undershot", and because the magnitude of the required ΔV was again small, an attempt not to undershoot was made by adding 5 percent to the calculated required weight of gas before entering it on the calibration chart. Preliminarily, it appears that about one-half of the 10 percent overshoot which resulted from this maneuver was caused by incorrect evaluation of the previous velocity correction as indicated in Table III-7. The important parameters for the third velocity correction are in Table III-8.

*Because a long time period was required to complete this maneuver, interruptions were scheduled to allow for warming of the nitrogen gas and modification of the pulsing phase angle.

Table III-8

Second Nitrogen Pulsed Jet Correction Parameters

PARAMETER	PULSING TIME (seconds)	ΔV (fps)	RESULTING DRIFT (deg/orbit)	ΔW (pounds)	(I_{sp}) EFF (seconds)	INCLINATION (degrees)
Predicted	924	12.72	-0.05	0.471*	71.5 X 0.9549** = 68.28	
Actual	924	13.97	-0.17	0.502	70.6 (74 nonpulsing)	33.13

*The on-time was based on original calibration for ΔW = 0.471 X 1.05 = 0.495 pounds. 1.05 represents the 5 percent factor introduced in an attempt to avoid undershoot.

**Since the same control jet was used, the factor of 0.9549 is defined as in the first nitrogen velocity correction.

Third Nitrogen Pulsed Jet Correction

On 16 August at 15^h44^m to 15^h46^mZ, since the third velocity correction over-corrected the orbit, another correction was designed and executed at the above date and time to reduce the eastward drift rate. The magnitude of the required ΔV for the maneuver was only 0.01 percent of the inertial velocity and due to the many uncertainties is already discussed, "actual" parameters are not presented. The more important parameters are given in Table III-9.

Table III-9

Third Nitrogen Pulsed Jet Correction Parameters

PARAMETER	PULSING TIME (seconds)	ΔV (fps)	RESULTING DRIFT (deg/orbit)	ΔW (pounds)	(I_{sp}) EFF (seconds)	INCLINATION (degrees)
Predicted	120	1.33	-0.025	0.0488	(72.0 X 0.9549) = 68.7*	
Actual	120	**	(-0.085)	**	**	33.15

*Since the same control jet was used, the factor of 0.9549 is defined as in the first nitrogen velocity correction.

**Not presented because of large uncertainties.

Attitude Correction

On 18 August, at 01^h30^m to $01^h31^m35^s$ Z, since the +z spin axis was about 8.5 degrees from the desired position, the received signal strength at Lakehurst, New Jersey, was degraded during the mid-morning hours (EDST). This was undesirable for communications with Lagos, Nigeria; therefore, the attitude was corrected using the quadrant mode for the nitrogen axial jet control system at the time indicated above.

In addition, since the eastward drift rate was still too high, the time chosen for executing the maneuver was such that a maximum decrease in eastward drift rate would result.

The large and small ellipses in Figure III-12 represent the region the +z spin axis was determined to be within before and after attitude touchup.

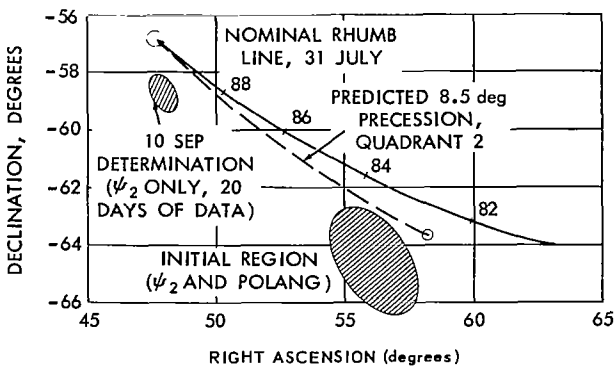

Figure III-12—Spacecraft +z axis directions before and after attitude correction.

To establish the suitability of a single-pulse train in the quadrant mode for the attitude touch-up, the Hughes reorientation computer program was "run backwards" from the target attitude (which differs only slightly from the target as represented by the rhumb line termination point for 31 July), with a precession phase angle 180 degrees from that available in Quadrant 2. The results plotted showed that an 8.5-degree precession using this quadrant would result in the correct final attitude if the initial attitude were within about 1 degree of the best estimate.

Based on the Hughes attitude determination computer program, the +z spin axis was maneuvered to within a degree of the southward normal to the orbit plane. The later results are based on the solar sensor data obtained over an extended time period; the change in the sun's direction over this period gives a more accurate solution (in comparison to early solutions where POLANG measurements were needed to define the attitude).

It should be pointed out that the desired attitude shown in the chart has changed slightly since August 18 because of perturbations on the orbit. The actual +z spin axis direction is nearer the desired direction than is indicated by the chart. The important parameters are listed in Table III-10.

Table III-10

Parameters Showing Effect of Attitude Correction

PARAMETER	PULSING TIME (seconds)	ΔV (fps)	RESULTING DRIFT (deg/orbit)	ΔW (pounds)	(I_{sp}) EFF (seconds)	INCLINATION (degrees)
Predicted	95	1.58	-0.07	0.0581	(68.0 X 0.9003) = 61.22*	
Actual	95	**	-0.037	**	**	33.05 †

*The factor of 0.9003 applied to (Isp) is a geometrical consideration resulting from the 90-degree pulse duration in the quadrant mode.

$$F_G = \frac{2}{\pi} \int_{-\pi/4}^{\pi/4} \cos x \, dx = \frac{2\sqrt{2}}{\pi} = 0.9003$$

**Not presented because of large uncertainties.
† Determined by GSFC on 29 September.

Combined Effect of the Third Nitrogen Velocity Correction and the Attitude Correction

The combined effect of the third nitrogen velocity correction and the attitude correction resulted in the following drift rate changes:

Predicted: 0.157 deg/orbit
Actual: 0.13 deg/orbit

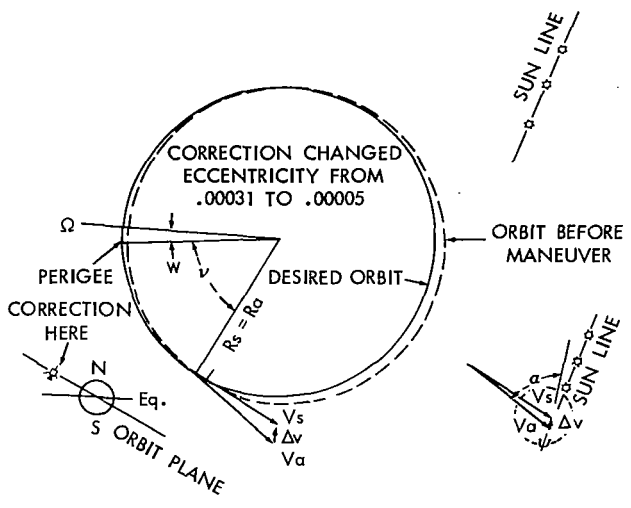

Ω First point of Aries

ω Argument of perigee

ν True anomaly ($\nu = 54.4°$)

R_s Radius of synchronous orbit ($R_s = 22753.3\ \mu$ ini)

R_a Radius at time of maneuver

V_s Desired synchronous velocity ($V_s = 10087.85$ ft/sec)

V_a Velocity before maneuver ($V_a \approx 10088.2$ ft/sec)

α The angle between ΔV and Va ($\alpha = 65°$)

ψ_f The angle between the sunline and the direction of corrective force ($\psi_f = 321°$)

|ΔV| The velocity correction vector ($|\Delta V| = 2.79$ fps)

Figure III-13—Resynchronization maneuver geometry.

Resynchronization Maneuver (Hydrogen Peroxide Lateral Jet)

On 28 November at $00^h24^m00^s$ Z to $00^h24^m31.4^s$ Z, since by November 28, the satellite had drifted to 59° West Greenwich and was drifting at a rate of 0.1 degree per orbit at that time, it was decided by NASA to resynchronize and circularize the orbit simultaneously. Preliminarily, it appears that the maneuver was undershot by 5 to 10 percent, resulting in a westward drift rate of 0.01 degree per orbit. Figure III-13 presents geometry for the maneuver and the more interesting parameters.

SPIN AXIS ORIENTATION

Information relative to spin axis attitude is obtainable from a number of sources including sun sensor data, polarization plane measurements, signal strength measurements, attitude at injection into the transfer ellipse, and comparison of orbits before and after apogee boost to obtain the velocity vector increment at boost. The last two sources of attitude information are peculiar to certain phases of the launch sequence, and the effective use of signal strength data requires a series of measurements over a period of several hours or more. Thus the only general technique for immediate attitude information is the use of a sun angle coupled with a polarization angle, the concept being that the spin axis must simultaneously lie in the plane of polarization and in a conical surface having the satellite-to-sun line as an axis and the sun angle ϕ, as the semi-apex-angle. (ϕ is functionally related to ψ_2, the directly measured angle.) In general, two intersections of a plane and a cone exist, but the proper one can be identified from other considerations.

During reorientation maneuvers, for example, simultaneous measurements of sun angle and polarization angle are required to provide the desired continuous monitoring of the changing spin axis attitude; however, when time permits, either two polarization measurements or two sun angle measurements fix the spin axis attitude, the first case being the intersection of two planes, and the second case being the intersection of two cones. For the relative positions of the earth, sun, and spacecraft to change sufficiently to give a good fix, several hours between polarization measurements and several weeks between sun angle measurements are required.

The accuracy of fixing the spin axis position by two measurements is at best only as good as the accuracy in the two angular data. The sun angles are measurable with errors of about 0.2 degrees, while the errors in polarization angle measurement are about 2.0 degrees. (The polarization

angle error arises from uncertainty in the amount of Faraday rotation of the wave in passing through the ionosphere, as well as from inaccuracy in performing the measurement.) Thus, while two polarization measurements separated by a few hours localize the spin axis within about 2 degrees, an accuracy of location of about 0.2 degrees should be possible using two sun angles. However, this assumes that the spin axis remains stationary during the month or so between sun angle measurements. (The experience of Syncom II indicates that this assumption would be generally valid.)

Except during reorientation maneuvers, it is possible to obtain sun angles, polarization angle, and signal strength data in number ranging from a dozen or so to several hundred, depending on the period of time the spin axis is left undisturbed. To take advantage of such redundant data, a computer program (ATTDET) is used with the IBM 7090 computer to find a maximum likelihood fit to the data, thus locating the spin axis position with an accuracy roughly proportional to the square root of the number of data.

Program ATTDET accepts sun angle data of both types (ϕ and ψ_2), polarization angles, and signal strength data. Each observed value is read into the computer together with the time the measurement was made and an assigned weighting factor. The observed polarization angles (POLANG data) are corrected for Faraday rotation before they are entered into the computer. The magnitude of the correction depends on the integrated electron density in the ionosphere, this varying with the time of day at the observing station, the strength of the earth's magnetic field at the station, and the angle between the local vertical and the line of sight from the observing station to the spacecraft. (Since the launch, ATTDET has been modified to perform these tedious corrections automatically, so that POLANG data can be used as observed. Previously a nominal correction obtained from a computer ephemeris was multiplied by a factor read from a curve for the station's local time of day to arrive at the correction to be applied to the observed POLANG.)

Historical Summary of Spin Axis Attitude

Transfer Orbit

While the number of observed data during the period from launch to apogee boost was small, the attitude determined therefrom was very close to all of three independent values available for this period, namely the nominal attitude predicted in the DTO analysis, the attitude obtained from BTL data, and lastly, the attitude derived from a comparison or orbits before and after apogee boost (i.e., from the vector velocity increment at boost). There four attitudes are summarized in Table III-11.

Table III-11

Spin Axis Attitude During Transfer Orbit

DATA SOURCE	SARA* (degrees)	SADEC** (degrees)
Nominal	181.535	-23.895
Derived from BTL Data	178.929	-23.357
Derived from Velocity Increment at Apogee Boost	180.169	-23.452
Computed Using ATTDET at T +280 minutes	179.502	-25.151
*Spin axis right ascension **Spin axis declination		

The data available for input to ATTDET numbered 22, of which 4 were POLANG measurements, 14 were ψ_2 data, and 4 were ϕ angles (these having been read from the synchronous control dial simultaneously with 4 of the ψ_2 data). The position of the sun was such that the sun sensor data, which are about ten times as accurate as the POLANG data, served primarily to determine the spin axis right ascension, while the spin axis declination was determined almost entirely by the POLANG data. Therefore, the spin axis right ascension as given by ATTDET should be considered the definitive value, while the spin axis declination so computed can only be said to be consistent with the other values within the probable error.

Apogee Boost to First Reorientation

During the period of about 23 hours between apogee boost and the axial jet correction, 3 POLANG and 64 ψ_2 data were observed. Before the first reorientation maneuver four days later, an additional 39 POLANG and 261 ψ_2 data were observed. The spin axis attitudes determined from these data are given in Table III-12; they did not differ significantly from those of Table III-11.

Table III-12

Spin Axis Attitudes Between Apogee Boost and Final Reorientation

PARAMETER	SARA (degrees)	SADEC (degrees)
Attitude between Apogee Boost and Axial Jet Velocity Correction (based on 3 POLANG and 64 ψ_2 data)	178.98 ± .74	-25.86 ± .92
Attitude between Axial Jet Correction and First Reorientation (based on 39 POLANG and 261 ψ_2 data)	180.07 ± .20	-24.87 ± .25

A spin axis right ascension of 180.0° and declination of -23.5° were adopted as the initial attitude on which to base the reorientation calculations. The desired final attitude was the south-pointing normal to the orbit plane, this having a right ascension of 47.92° and a declination of -56.95°. (For details of the reorientation, see the discussion relating to Figure III-9).

First Reorientation to Second Reorientation

Four velocity corrections were made during the interval between the first and the second reorientation maneuvers, thus producing five orbits and dividing the interval into five time periods. The first of these lasted nearly eleven and a half days, the next two about a day each, while the last two each lasted about one day and ten hours.

A total of 118 usable POLANG data and 539 sun angle data was recorded during the long period between the reorientation and the first velocity correction. Because the ATTDET program in use at that time could accommodate a maximum of 256 data, the number of sun angle data was reduced by averaging; these average values were then used with appropriate weighting.

The various spin axis attitudes calculated using all or part of these data are listed in Table III-13. All usable POLANG data came from SYNCST; the SYNTLH POLANG data was observed to be consistently in error, and a check of the antenna revealed that the feed was misaligned (i.e., rotated from the vertical plane) by about ten degrees.

Table III-13
Calculated Spin Axis Attitudes Following First Reorientation and Before the First Velocity Correction

BASIS OF CALCULATION	SARA	FSADEC
2 ψ_2 (averaged) and 87 POLANG data culled from 111 for SYNCST	55.48 ± .28	-64.20 ± .32
111 SYNCST POLANG data alone	56.48 ± .61	-65.44 ± .28
1181 SYNCST POLANG data and 38 selected sun angles (modified ATTDET)	55.73 ± .22	-65.30 ± .24

The first and second attitudes given in Table III-13 were calculated at GSFC using the ATTDET program on the Syncom Computer System tape. The first attitude was considered the definitive attitude for the orbit immediately following the first reorientation. The second attitude, calculated using only POLANG data, served to verify the consistency of the POLANG data. The third attitude was calculated recently using a modified ATTDET program which discounts poor data by assigning little weight to the corresponding residuals and which also finds the optimum Faraday correction for POLANG data. In this case, the best fit results when the Faraday correction is made with the usual sign, but with a magnitude about half that usually used.

On 18 August when the second reorientation maneuver was made, the best estimate of the spin axis attitude was right ascension 56.21 ± 0.36 degrees and declination -64.60 ± 0.80 degrees, this being calculated using nine POLANGS and an average value of the ψ_2 data observed since the last velocity correction, which preceded the reorientation by about thirty-four hours. Thus, within the accuracy afforded by the small number of data reported during this period, no significant overall displacement of the spin axis by the four velocity corrections was apparent.

Orbit After Second Reorientation

Following the second reorientation, no further spacecraft maneuvers were executed until 28 November, giving an undisturbed period of nearly 103 days during which a very large number of data were recorded.

The spin axis attitude during this period has been monitored almost entirely on the basis of sun angle (ψ_2) data because most of the POLANG observations appear to have been improperly made. The ψ_2 data has been processed in its entirety and also by periods of about a month each. The attitudes so calculated are presented in Table III-14. The differences between the three attitudes are not considered significant or to reflect a particular trend.

Conclusions About Satellite Reorientation Maneuvers

The use of polarization angles and sun sensor indications to determine the orientation of the spacecraft spin axis has been demonstrated to be practical and of adequate accuracy for the mission requirements. Certain refinements in the measuring techniques, as discussed below, would be desirable during certain operational phases, notably reorientation maneuvers, and for general convenience but would appear to be mandatory only if precise data for various geophysical studies were sought. For example, any serious investigation of the Faraday effect in the ionosphere would require POLANG data in greater number and of greater accuracy.

Table III-14

Spin Axis Attitude Since Final Reorientation

BASIS OF COMPUTATION	SARA (degrees)	SADEC (degrees)
209 ψ_2 data, 18 August to 25 September	47.71 ± .07	-58.21 ± .08
64 ψ_2 data, 26 September to 22 October	47.03 ± .33	-58.31 ± .12
63 ψ_2 data, 22 October to 22 November	48.23 ± .36	-58.40 ± .04
337 ψ_2 data, 18 August to 22 November (all data used above)	47.60 ± .04	-58.30 ± .03

While both the polarization angle and sun angle data were generally of good quality, experience has shown that a high level of training and skill has been required to realize the best results. Any steps toward automating these measurements, such as direct readout or other means of lessening the burden on the observer, would be desirable.

The basic concept, configuration, and mounting accuracy of the solar sensors appear to be entirely adequate to the requirements, and the overall accuracy of the sun angle measurements has been of the order of one tenth of a degree under good conditions.

The quality of the POLANG data ranged from excellent to unusable, the former being attributed to great care in performing the measurements, to proper technique and understanding of the significance of the measurement, and to proper alignment or calibration of the antenna feed (using an established reference signal of known polarization). A pressing need for an automated or at least improved method for POLANG measurement is indicated if only to reduce the time required for an accurate reading.

Although the use of signal strength data to determine the spin axis attitude, or as an adjunct to POLANG and ψ_2 data, appears to be feasible and is provided for in the computer program ATTDET, no signal strength data from the A-26 launch has been so utilized to date.

COMMUNICATIONS EXPERIMENT DURING LAUNCH

Chronologically, the initial operation of the shipborne terminal, the Kingsport, was in the role of down-range tracking station after the satellite had been injected into the transfer ellipse. Range and range rate data, together with azimuth and elevation angles, had to be acquired and transmitted rapidly by teletype to the Goddard Space Flight Center (GSFC) for transfer orbit calculations.

The first priority objective of Syncom II was to achieve a synchronous orbit using the spinning injection concept. In support of this objective, the ship, moored in the harbor of Lagos, Nigeria, acquired the satellite at launch plus 28 minutes and a minute later was gathering range and range rate data. During the approximate five-hour ascent of the spacecraft toward apogee, two communication tests were performed. The first occurred between 1554Z and 1606Z hours with the spacecraft at a range of approximately 10,000 nautical miles. During this test period, pre-taped music, voice and teletype signals were transmitted through the spacecraft and received aboard the Kingsport. The quality of the music (the National Anthem) as received at the Kingsport was so satisfactory that it was transmitted over a voice circuit passing from Lagos through Kano and thence over the Project Mercury Network to GSFC. The second test was performed between 1801Z and

1814Z hours with the spacecraft at a range of approximately 20,000 nautical miles. Once again music, voice and teletype signals were successfully transmitted through the spacecraft and received at the Kingsport. The performance obtained during the transfer orbit indicated, that prior to injection into a synchronous orbit, the satellite transponder had survived the launch and was performing in an excellent manner.

RANGE AND RANGE RATE CALCULATIONS

Data Description and Data Handling

The description and analysis of data which follow are directly applicable to Syncom I; however, the processing of the data during the launch phase of Syncom II was essentially the same as for Syncom I.

The tracking data presented in this report were acquired by the tracking ship in the harbor of Lagos, Nigeria. They consist of two 15 minute segments, separated by approximately 2 hours and 19 minutes. The first segment was acquired when the satellite height was between 10,000 and 15,000 km. The highest range tone used for making range measurements was 100 kc.

During the second segment of data, the satellite altitude above the earth was between 30,000 and 35,000 km. For the first 5 minutes of this segment the 4 kc tone was used, because of communication problems. The 100 and 20 kc tones were toned off. This provided more power in the lower tones in order to receive ranging data; though the range accuracy was degraded to ± 500 m with the 4 kc tone. The power in the 4 kc tone could not be increased to decrease the phase jitter which is due to the 4.008 kc phase-locked loop locking on the 4 kc tone. After approximately 5 minutes, the 20 kc tone was turned on and the modulation index increased, increasing the power in the 20 kc tone, which decreased the phase jitter of this tone. This tone was used as the highest ranging tone for the rest of this interval. The deviation in range with the 20 kc tone was less than ±20 m.

During the two tracking intervals, 1052 measurements of range data and 945 measurements of range rate data were recorded. At the Goddard Space Flight Center the 1052 points of range data, including the 4 kc data, were smoothed to 68 points of which 55 points were used for final orbital calculations. If the measurements using the 4 kc tone are excluded, only 5 smoothed points were eliminated from the calculations. The 945 points of range rate data received were smoothed to 71 points and all 71 were used in the final orbital calculations.

The data from the system is punched on paper tape for transmission to the Goddard Space Flight Center in the format shown in Figure III-14. The received data are processed in a two-computer operation. The reproduced teletype tape with the data is first processed in the CDC-160 computer which performs the following operations:

a) Computes range in meters from the time of propagation or phase delay of the ranging tones to the spacecraft and return,

b) Computes range rate in m/sec from the time interval required to count "N" cycles of a standard frequency ± the Doppler frequency of the carrier,

c) Reproduces the 30 foot communications antenna angle readout which the system measures to 0.1 degree, and

d) Makes the necessary adjustments to time for the propagation time of the ranging tones to and from the spacecraft, and for the difference in time between the sampling of the time register and the range and range rate registers.

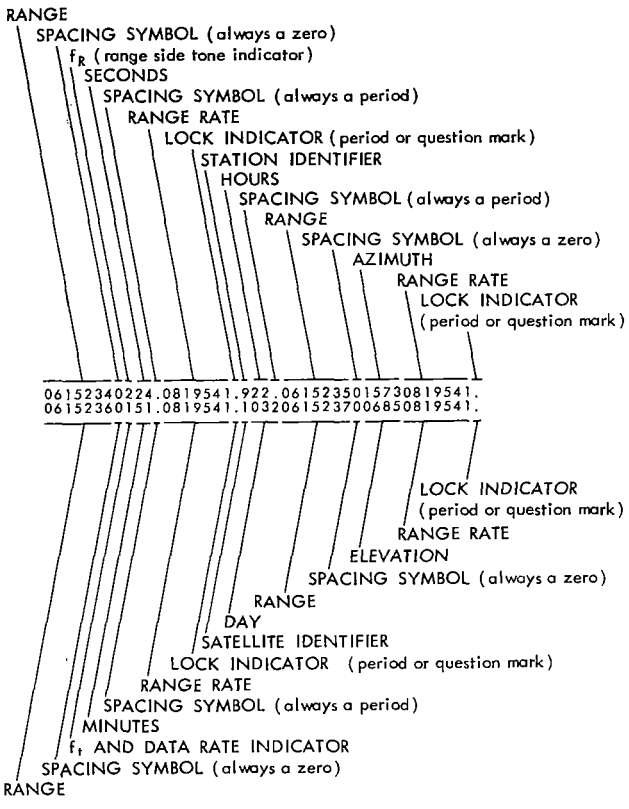

Figure III-14—Data format.

The raw data from the CDC-160 are reproduced on punched cards and magnetic tape for processing by the IBM 7090 or 7094 computer, which uses the punched cards and magnetic tape for an input program. The data are then smoothed by fitting a quadratic or higher degree polynomial to them in the least squares sense. After smoothing, a differential correction program is applied to the data by using either the Brouwer or MCOI orbit generators for calculating the orbital elements and standard deviations.

Data Analysis

Computer Results for Standard Deviations

The MCOI orbit generator was used for the Syncom satellite. It is a numerical integration program that applies a Runge-Kutta Gill Integration Tecynique to the solution of the equations of motion, by assuming a spheroidal earth. The integrated equations of motion include effects due to the principal term and second, third, fourth, and fifth harmonics of the earth's potential, as well as lunar and solar perturbations, drag, and solar radiation. For lunar and solar perturbations the program requires as input, ephemerides' tapes for the sun and moon. Drag effects are computed by assuming an exponential atmosphere with a constant temperature gradient. The standard output is an ephemeris tape giving the position and velocity vectors of the satellite at a given interval of time. The differential correction program uses the position and velocity vectors to calculate the orbital elements and their standard deviations. The standard deviation for Syncom I was 15.49 m in range and 0.05 m/sec in range rate.

The calculated orbital elements used range and range rate data and angular data from the Johannesburg Minitrack station. The range data had a weighting factor of 40, the range rate data had a weighting factor of 24, and the Minitrack data had a weighting factor of 1. Therefore, the orbital elements were heavily influenced by the range and range date data.

The Minitrack data agreed with the calculated orbital elements to 0.12 milliradian or about 25 seconds of arc, which proves that the range, range rate, and Minitrack data agree with the calculated orbital elements.

Analysis of Range and Range Rate Data Over Short Continuous Intervals

For analysis of the range and range rate data over short continuous intervals a polynomial fit was made to the data. It was found that a second degree polynomial best fit the data in all the cases considered. That is;

$$g_k = a_o + a_1 k + a_2 k^2 , \qquad (1)$$

where

$g_k = g(t_k)$, the value of the function at time t_k, the function being either range or range rate,

$k = \dfrac{t_k - t_0}{\Delta t}$ $(k = 0, 1, 2, \cdots, n-1)$;

t_k = the time corresponding to the k^{th} observation,

t_o = the time corresponding to the initial observation,

Δt = the time interval between successive observations.

The total interval over which the data is time continuous is defined by

$$T = t_{n-1} - t_0 .$$

Application of the method of least squares gives the coefficients (a_o, a_1, a_2) and the standard deviation of fit of the polynomial to the data. That is, the normal equations are

$$\begin{bmatrix} \sum_{k=0}^{n-1} g_k \\ \sum_{k=0}^{n-1} k g_k \\ \sum_{k=0}^{n-1} k^2 g_k \end{bmatrix}_{(3\times 1)} = \begin{bmatrix} n & \sum_{k=0}^{n-1} k & \sum_{k=0}^{n-1} k^2 \\ \sum_{k=0}^{n-1} k & \sum_{k=0}^{n=1} k^2 & \sum_{k=0}^{n-1} k^3 \\ \sum_{k=0}^{n-1} k^2 & \sum_{k=0}^{n-1} k^3 & \sum_{k=0}^{n-1} k^4 \end{bmatrix}_{(3\times 3)} \begin{bmatrix} a_0 \\ a_1 \\ a_2 \end{bmatrix}_{(3\times 1)} .$$

In abbreviated matrix form Equation 1 is

$$G_{(k\times 1)} = T_{(k\times 3)} A_{(3\times 1)} , \tag{3}$$

where $k > 3$. The resultant normal equations given by Equation 2, in abbreviated form, are

$$\left[T^T_{(3\times k)} G_{(k\times 1)}\right] (3\times 1) = \left[T^T_{(3\times k)} T_{(k\times 3)}\right] (3\times 3)\, A_{(3\times 1)} . \tag{4}$$

The solution of Equation 4 is given by

$$A_{(3\times 1)} = \left[T^T T\right]^{-1}_{(3\times 3)} \left[T^T G\right]_{(3\times 1)} . \tag{5}$$

From this least squares solution the measure of how well the data fits the assumed ploynomial is given by the value of σ. The meaning of σ is that the probability will be 68.3 percent that all the data fitted to the polynomial will lie in the region bounded by $+\sigma$ and $-\sigma$.

For evaluating σ, use is made of the solution to Equation 2 or 4 as follows:

$$\sigma = \pm \frac{1}{n-3} \left[\sum_{k=0}^{n-1} gk^2 - a_0 \sum_{k=0}^{n-1} g_k - a_1 \sum_{k=0}^{n-1} kg_k - a_2 \sum_{k=0}^{n-1} g_k k^2 \right]^{1/2} \quad (6)$$

where $n > 3$. In matrix form

$$\sigma = \pm \left\{ \frac{1}{n-3} \left[(G^T G) - A^T (T^T G) \right] \right\}^{1/2} , \quad (7)$$

and it is from this point of view that the analysis of range and range rate data is considered here.

Figures III-15 and III-16 are plots of the residuals in the region where the satellite height was between 10,000 and 15,000 km. The highest range tone used in this region was 100 kc. The residuals represent deviations of the raw data from the second degree polynomial fitted to the data in the least squares sense.

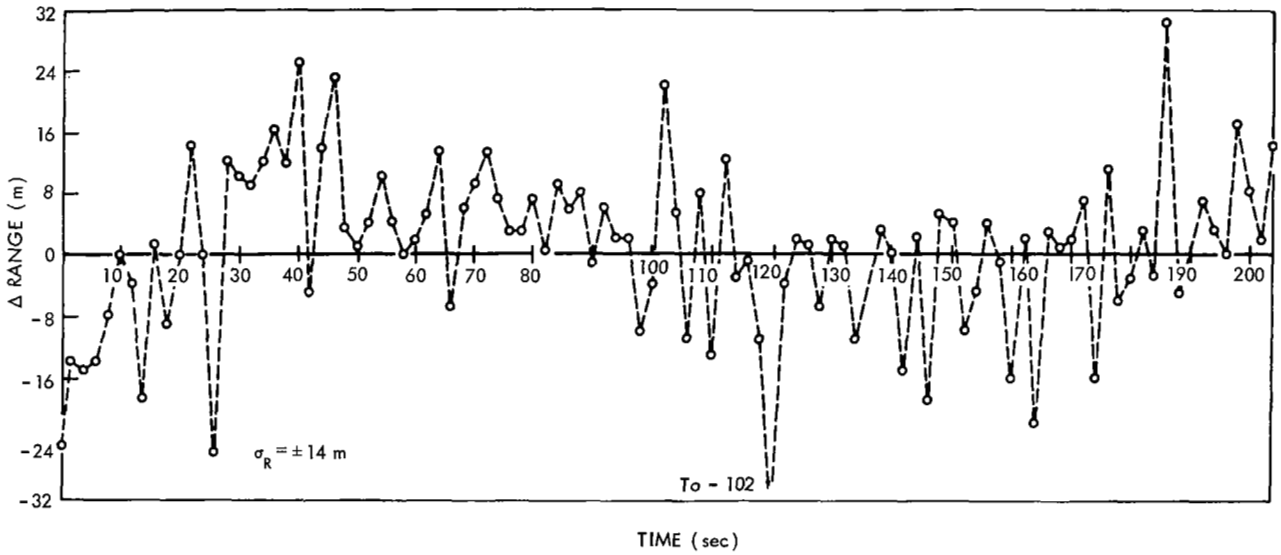

Figure III-15—Data at 10,000 - 15,000 km (100 kc tone range).

Corresponding to Figures III-15 and III-16, the polynomials fitted to the data in the 10,000 to 15,000 km region are

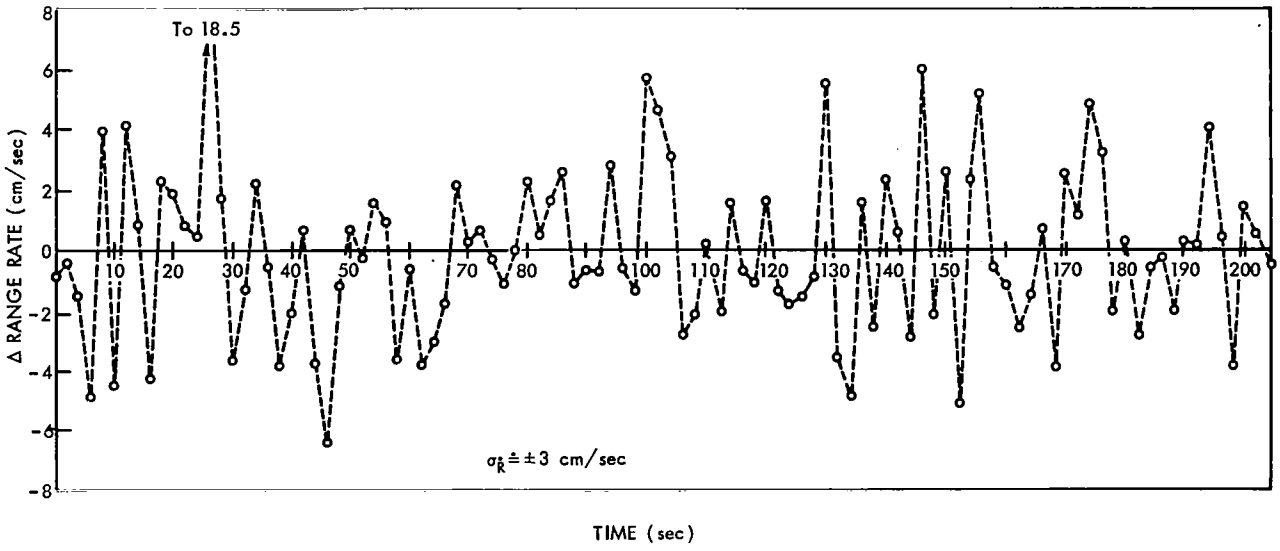

Figure III-16—Data at 10,000 - 15,000 km (range rate).

a) for range (R) data,

$$T = t_{n-1} - t_0 = 206 \text{ sec},$$

$$\Delta t = 2 \text{ sec},$$

$$k = \frac{t_k - t_0}{\Delta t} = 0, 1, 2, \cdots, 103, \tag{8}$$

$$R_k = 13408663.406 + 8937.701k - 1.6413k^2 \text{ (in meters)}$$

$$\sigma R = \pm 14.0\text{m (See Equation 6 or 7), and}$$

b) for range rate ($\dot{R}$) data,

$$T = 206 \text{ sec},$$

$$\Delta t = 2 \text{ sec},$$

$$k = \frac{t_k - t_0}{\Delta t} = 0, 1, 2, \cdots, 103, \tag{9}$$

$$\dot{R}_k = 4467.7189 - 1.6428k + 0.00 \text{ (in meters/sec)},$$

$$\sigma\dot{R} \pm 0.031 \text{ m/sec}.$$

In the 10,000 to 15,000 km region, second degree polynomial fits to the range and range rate data over smaller values of T were also made. For all those intervals of T containing more than 15 data points, the second degree polynomial fitted the data best.

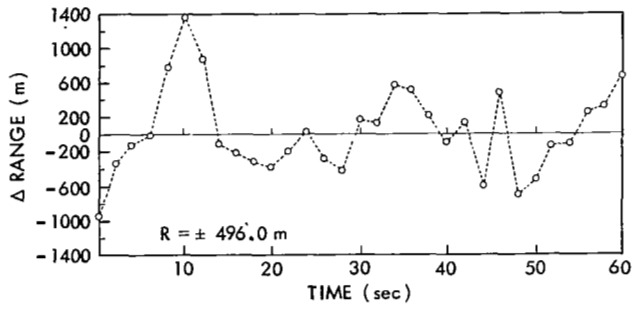

Figure III-17—Data at 30,000 - 35,000 km (4 kc tone range, class a).

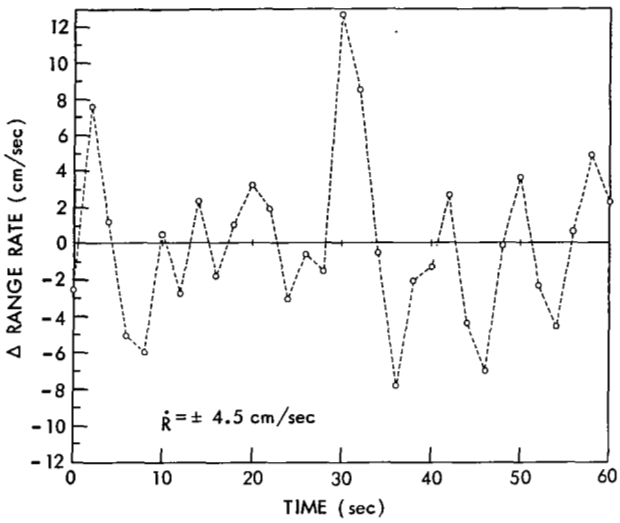

Figure III-18—Data at 30,000 - 35,000 km (range rate, class a).

Range data in the region between 30,000 and 35,000 km must be divided into two classes:

a) data extracted from a 4 kc ranging tone, and

b) data immediately following the above, which were extracted from a 20 kc ranging tone.

The plots of the residuals of the class a data are given in Figures III-17 and III-18 and those of class b data are given in Figures III-19 and III-20. Corresponding to the residual plots, the polynomials fitted to these data are:

a) For class a range data,

$$T = 62 \text{ sec},$$

$$\Delta t = 2 \text{ sec},$$

$$k = \frac{t_k - t_0}{\Delta t} = 0, 1, 2, \cdots, 31, \tag{10}$$

$$R_k = 34902312.641 + 1825.673k - 3.7109k^2 \text{ (in meters)}$$

$$\sigma R = \pm 496.0\text{m} ;$$

b) For class a range rate data,

$$T = 62 \text{ sec},$$

$$\Delta_t = 2 \text{ sec},$$

$$k = \frac{t_k - t_0}{\Delta t} = 0, 1, 2, \cdots, 31, \tag{11}$$

$$\dot{R}_k = 906.5779 - 0.4128k - 0.0002k^2 \text{ (in meters/sec)},$$

$$\sigma\dot{R} = \pm 0.0445 \text{ m/sec} ;$$

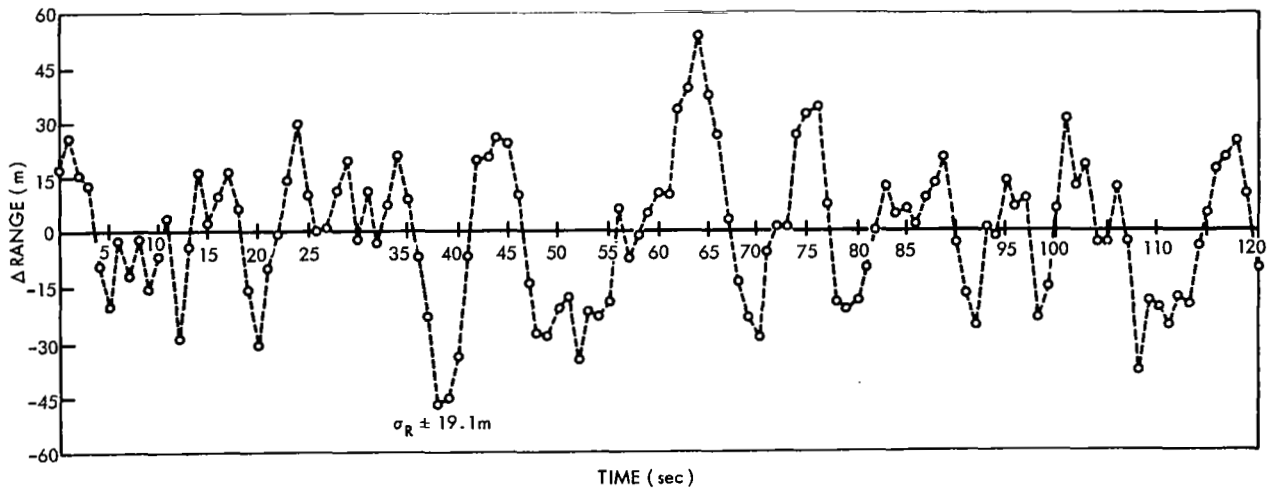

Figure III-19—Data at 30,000 - 35,000 km (20 kc tone range, class b).

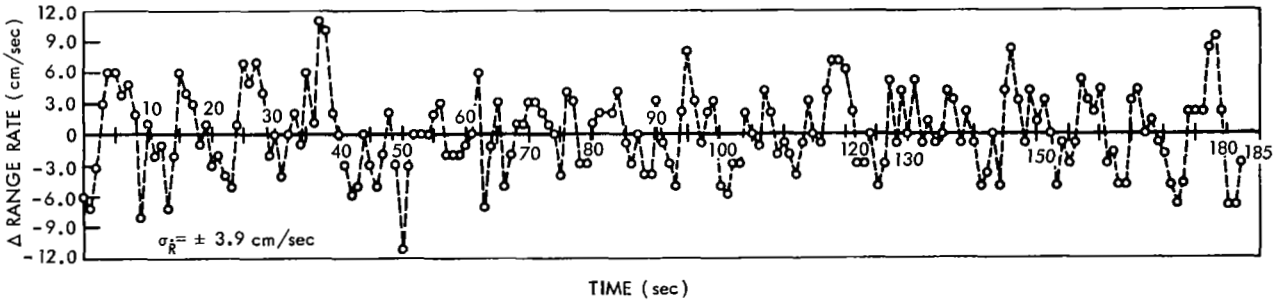

Figure III-20—Data at 30,000 - 35,000 km (range rate, class b).

c) For class b range data,

$$T = 120 \text{ sec} ,$$

$$\Delta_t = 1 \text{ sec} ,$$

$$k = \frac{t_k - t_0}{\Delta t} = 0, 1, 2, \cdots, 120 , \qquad (12)$$

$$R_k = 35647734.938 + 724.109k - 0.0992k^2 \text{ (in meters)}$$

$$\sigma R = \pm 19.1 \text{ m} ;$$

d) For class b range rate data,

$$T = 182 \text{ sec} ,$$

$$\Delta t = 1 \text{ sec} ,$$

$$k = \frac{t_k - t_0}{\Delta t} = 0, 1, 2, \cdots, 182,$$

$$\dot{R}_k = 725.674 - 0.1964k + 0.00001k^2 \text{ (in meters/sec)} ,$$

$$\sigma\dot{R} = \pm 0.039 \text{ m/sec} .$$

Conclusion

It should be noted that, from the standpoint of only the 100 or 20 kc highest range tone data, the precision of a signal measurement is better than ±20 m in range and better than ±0.05 m/sec in range rate for satellite heights between 10,000 and 35,000 km.

Although range measurements were not made with the 100 kc sidetone, the data proves the system's ability to make accurate (±20 m) range measurements using the 20 kc sidetone.

CHAPTER IV

COMMUNICATION TEST RESULTS

INTRODUCTION

Communications via active satellite repeater represents one of the first practical applications of orbiting earth satellites with broad military and commercial application. The feasibility of such communications has been amply demonstrated by the U. S. Army Signal Corps' Projects SCORE and COURIER, by the American Telephone and Telegraph Company's TELSTAR, and by the National Aeronautics and Space Administration's (NASA's) Project RELAY. These satellites orbited at low to medium altitudes, from 115 to 6700 miles above the earth's surface, and offered communication capability for relatively short periods of time being limited to the order of from several minutes to approximately one or two hours by their time in view of ground-based communication stations. The joint NASA-Department of Defense (DOD) Project Syncom offers the most advanced communication capability to date by virtue of its 24-hour orbital period at 22,300 miles altitude, which provides nearly around-the-clock visibility to surface stations within coverage of its antenna pattern. In fact, if Syncom II, the presently orbiting satellite, had been placed in an equatorial orbit instead of one inclined 33 degrees to the earth's equator, it would offer complete 24 hour visibility. The literature is replete with discussion of the relative merits of synchronous vis-a-vis medium altitude communication satellites, and this aspect will not be belabored here.

It is the purpose of this section to describe the data reduction and analysis procedures used for the Syncom II communication experiments and to present the results of the early experiments conducted primarily during the first 90 days of operation.

APPROACH TO EVALUATION

Satellites appear destined to play a major role in long-haul communications and, with advances in technology and communication needs, it is certain that improved systems will be developed and implemented to provide an ever-expanding capacity and improved communications quality, bounded only by economic practicality. The accuracy and cost of preparing meaningful link calculations (alias db budget, power budget, etc.) which are part of the systems engineering for any new system, depend in part on the availability of accurate information on equipment and propagation characteristics. Design choices are similarly dependent upon such knowledge. The importance of obtaining new information on, or confirmation of, quantitative effects of environmental and man-controllable factors on system performance was recognized early in the Syncom program. The large number of variables affecting system performance, including environmental conditions, equipment characteristics, and human factors, led to the decision to evaluate experimental data on a statistical basis, and the test and evaluation phases of the program were planned accordingly.

A statistical analysis of experimental results requires considerable data, especially when the data can be separated as a function of the large number of independent variables contained in the Syncom system such as transmitting surface station, receiving surface station, operating mode, satellite receiver, satellite transmitter, operating channel (radio frequency), satellite position, weather conditions, transmitter power, etc. For the data contained in this section, four operating stations and seven operating modes are included. The accumulation of a large amount of test data is possible for Syncom II because of the long time availability of the satellite. Therefore, it is possible to utilize statistical analysis, including curve-fitting, goodness-to-fit testing, two-variable and multiple regression analysis, frequency distribution, and trend analysis. At the time of preparation of this report, some of these avenues had been explored, and the data are summarized herein, others were just being entered, while still others had not yet been opened.

Experiments and Data

Experiments

The communication experiments performed may be classified into three major groups, viz., demonstration, technical performance, and technical characteristics tests. The demonstration tests, performed primarily with live inputs, were designed to demonstrate qualitatively the system performance and to evaluate those system characteristics, such as the effects of echo and delay, which are best measured through user appraisal. The technical performance tests, performed primarily with input signals derived from prerecorded magnetic tapes to ensure uniform signal input conditions, were intended to measure quantitatively the system communication performance, as a communication link, with resulting data in a form amenable to statistical analysis. The technical characteristics tests, using both live and taped signal inputs, were intended to measure quantitatively the link characteristics with a view toward statistical analysis. Elements of the latter two experiment categories were somewhat intermingled in some of the tests.

In brief, the demonstration experiments included single channel telephony, single and multi-channel teletype, and facsimile tests. The technical performance experiments comprise single and multi-channel telephony, single and multi-channel teletype, simultaneous telephony and teletype, and facsimile tests. The technical characteristics tests encompassed measurements of envelope delay, signal-plus-noise to noise, and voice frequency performance; the last uses the Voice Interference Analysis Set (VIAS), about which more will be presented in later portions of this section.

Data

For system evaluation purposes, the data gathered during the communication experiments may be categorized as primary and supporting data. The primary data consist of magnetic tape recordings of transmitted and received signals (input to the modulator and output of the demodulator); facsimile photographs; Sanborn chart recordings of surface station parameters; and communication experiment logs (which, in telegraph form, are referred to as quick-look data), including supplements thereto. Supporting information comprises weather information, including both weather radar summaries and observations; range and range-rate data, as available; reduced telemetry, particularly values of satellite received signal levels, satellite transmitter power, transponder status (receiver number, TWT number, etc.), and battery and solar cell status; and other information pertinent to system operation, reported by telephone or teletype or recorded in station operating logs.

Data Reduction

General Information

The successful launching, orbit injection, velocity corrections, and reorientation maneuvers of Syncom II made possible the accumulation of vast amounts of test data.

The data reduction system devised for the experimental data is based upon the desire to process large amounts of data, the quality and format of which have a sufficient range of variation to require human interpretation. In addition, information retrieval and reprocessing were required to be such as to permit correlation and other statistical analysis in many different combinations within the body of the data and with corollary and supporting data. Except for those few instances where completely misleading input information was supplied, the system described below has been quite successful.

Data reduction is accomplished in two steps. Preliminary data processing is accomplished at SATCOM and the bulk of the data is reduced at the Franklin Institute Laboratories for Research and Development (FIL), under contract to SATCOM.

Preliminary Data Reduction

Almost all of the preliminary data reduction is done using equipment mounted in the Mobile Test Van. The following are accomplished:

a) Magnetic tape recordings of single-channel teletype signals are played into the Telegraph-Telephone Terminal AN/TCC-14 by means of the Consolidated Electrodynamics Corporation (C. E. C.) GR-2800 Recorder-Reproducer System. The output of the AN/TCC-14 is punched and printed on paper tape with the Teletype Reperforator TT-107B. Simultaneously, during the reversal portions of the teletype messages, teletype distortion is measured using the Teletypewriter Test Set AN/GGM-1 and recorded on data sheets.

b) Magnetic tape recordings of simultaneous telephony and teletype signals are separated by the AN/TCC-14, with the telephony output re-recorded on magnetic tape and the teletype output punched and printed on paper tape. Teletype distortion measurements are made and recorded.

c) Multi-channel telephony signals, recorded on magnetic tape, are demultiplexed with the Telephone Terminal AN/TCC-3 and re-recorded on magnetic tape. Simultaneously, tone distortion and signal-plus-noise to noise measurements, on the recorded test tones, are made and recorded on data sheets.

d) Magnetically recorded eight and sixteen channel teletype signals are demultiplexed by the Telegraph Terminal AN/UCC-1 and the individual channels are punched and printed on paper tape. Teletype distortion measurements are made for each channel.

In addition, the following preliminary data reduction is accomplished at SATCOM, not involving the Mobile Test Van:

a) Special VIAS modulation signals, recorded on magnetic tape, are processed through the VIAS equipment, resulting in measurements of articulation index and corresponding signal-plus-noise to noise measurements. (The significance of the articulation index is discussed later in this section.)

b) Facsimile photographs are evaluated with the assistance of experts from the U. S. Army Research and Development Laboratory for gray scale, resolution, and overall picture quality. Detailed analysis of faults is made and tabulated with the ratings.

Final Data Reduction

The raw data (magnetic recordings, Sanborn charts, etc.), and the results of the preliminary data reduction are sent to FIL for final data reduction, tabulation, plotting, and statistical analysis; additional analysis and all system evaluation are done at SATCOM. The data processing system established at FIL is geared to large volume data handling with quick reaction time for special data reduction and analysis requirements; a flow diagram is shown in Figure IV-1. A description of the data processing procedures employed follows.

As a first step, the Sanborn recordings and daily operational logs, which describe the tests conducted in chronological sequence, together with pertinent station operating data, are scanned to determine the sequence of events to be expected on the magnetic tapes. At the same time, the station operating data indicated on the flow chart are extracted and punched on IBM cards.

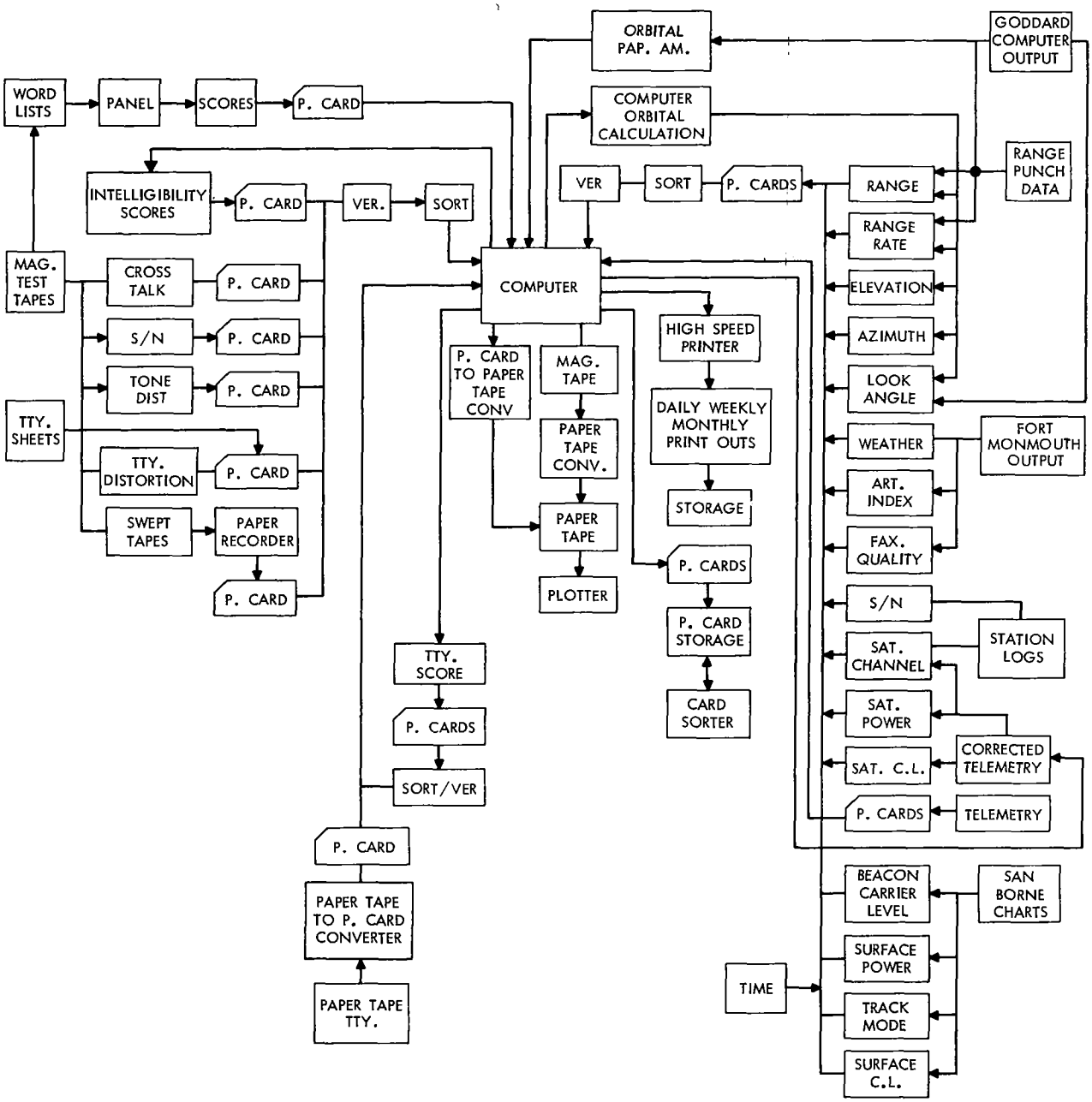

Figure IV-1—Data processing flow chart.

The magnetic tape recordings, on half-inch instrumentation tape, contain a variety of information, depending upon the individual test recorded on each reel. In general, the input to the modulator is recorded on one channel, the output of the demodulator on a second channel, time on a third channel, and announcements by station personnel as to the operating situation (such as a modem code) on a fourth channel. Each tape is played through a C.E.C. GR-2800 Recorder-Reproducer System for measurements; the announcement and time channels are monitored to obtain necessary correlation information. The experiment data are recorded on data sheets and subsequently punched on IBM cards. The measurements made are as follows:

a) Signal-plus-noise and noise measurements are made on the test tones and quiet periods, respectively, recorded for this purpose, using a Ballantine Laboratories Model 320A true rms VTVM. Simultaneously, measurements of tone distortion are made with a Hewlett-Packard Model 330C Distortion Analyzer.

b) The swept tones are fed into the receiving portion of an Acton Laboratories Type 452A Transmission and Delay Measuring Set and simultaneously, through a rectifier, to a Sanborn Model 299 D. C. Amplifier-Recorder. As the tone is swept in frequency, its amplitude is recorded on the Sanborn recorder and its instantaneous frequency is displayed on a front panel meter of the transmission and delay measuring set. At preselected frequencies, pips are recorded on the Sanborn chart by means of a hand-operated switch which results in a calibrated amplitude versus frequency plot.

c) Intelligibility word lists, which are the Harvard phonetically-balanced word lists, are re-recorded on quarter-inch tape via an Ampex 1260 Tape Recorder with a flat frequency response from 20 cps to 20 kc/s. In a specially arranged room, the recordings are played to a listener panel via another Ampex 1260 Tape Recorder through stereophonic Koss SP-3X Head Phones, to each panel member through an individual volume control. The listener panel members write the words as they hear them, phonetically if necessary, and the individual scores, both by word and panel member, are recorded. These scores are reviewed to ensure that the listener panel is fairly homogeneous, with respect to hearing and comprehension abilities, and that none of the words shows a consistently low score indicating a defect in the original recording of the word.

The punched paper tapes containing the standard Fox messages are passed through an IBM 047 Tape-to-Card Printing Punch which has been modified to recognize and punch every pertinent teletype symbol, including figure and character shifts, carriage returns, line feeds, etc., and the messages are reduced to punched IBM cards. This is done to ensure that a single missed character, such as a line feed or figure shift, which could produce the semblances of many errors, is counted as only one error. The teletype distortion measurements, furnished by SATCOM, are punched on IBM cards.

Other data furnished, such as weather, articulation index, and facsimile quality ratings, are punched on IBM cards. Supporting information from orbital calculations and telemetry are obtained from Goddard Space Flight Center (GSFC), or when not available, are computed using orbital and satellite orientation parameters supplied by GSFC and spacecraft status (Telemetry) messages teletyped from the Telemetry and Command Stations.

The punched cards, after verification and sorting by IBM 056 Card Verifiers and 082 Card Sorter, respectively, are fed into a modified UNIVAC I Computer, along with control cards containing information on system configuration keyed to time, i.e., which surface stations were transmitting and which were received at all times during the testing period. The computer performs all arithmetic operations, such as subtracting noise values from corresponding signal-plus-noise measurements to yield signal-plus-noise to noise values. For the teletype messages, the computer compares the Fox messages on the punched cards to the standard Fox messages stored in the memory and counts number of correct characters. This number divided by the total number of characters counted during the transmission, expressed in percent, is then fed out as teletype score; this is later converted to teletype error by subtracting from 100 percent. The computer also formats

instructions for sorting and print-out. Computer outputs are obtained in the form of high-speed print-out, magnetic tape, and punched cards. By means of suitable conversions among magnetic tape, punched cards and punched paper tape, stored data can be retrieved in any desired form. The keys for nine sorting levels are also contained in the stored data so that, with proper instructions to the computer, or with the use of the card sorter, data may be stripped out according to station, operating mode, serial number, test item number, modulator or demodulator data, day, hour, minute, or by specific data type (such as teletype score, signal-plus-noise to noise, etc.). This is necessary for correlation of data or other statistical analysis.

An Electronics Associates, Incorporated (EAI) Model 3500 Dataplotter, operating from punched paper tape input, is used to plot any required data. Plotting at a rate of 300 points per minute, this plotter can be programmed to plot points or curves and to print symbols, axes, and calibration marks. The plotter is coded to plot scatter diagrams for regression analysis and performance curves, both for the reduced test data and for the results of statistical analysis.

TRANSMISSION CHARACTERISTICS

Spacecraft Characteristics

The satellite power amplifier which amplifies both the beacon and communications signals is a traveling wave tube which is preceded by a limiter. In the absence of a communications signal at the input to the satellite, the entire output power appears at the beacon frequency. As the received communication signal level increases in the satellite receiver, the beacon signal is suppressed until the transponder is saturated. (See Figure IV-2.) At this point, further increase in communication signal level does not increase the power output at the communications frequency, and the beacon signal is suppressed no further. It is essential that the communication transfer characteristics of the transponder be known to evaluate communication performance under conditions in which the transponder isn't fully saturated. Since these characteristics were not measured prior to launch, it was attempted to measure them from the surface stations.

The satellite transfer characteristics for channels one and two are shown in Figure IV-2. The characteristics were obtained by varying the up link power and measuring the received communication carrier level at the surface station. From the orbital data during the time of the test, the antenna aspect angle was obtained and used in conjunction with the averaged antenna pattern to determine the relative antenna gain. The surface station received signal level was corrected for the effects of the change in satellite antenna gain. It should be noted that the transfer characteristics are associated with a particular transmitting station, as noted on Figure IV-2. When using any other transmitting station in which the antenna gain and line losses differ from the ones used in obtaining these curves, the transmitter power must be normalized to the transmitting stations used in these tests.

From the transfer characteristics it can be seen that for a *corrected* surface transmitter power greater than 4 db below 10 kw (that is, greater than 4 kw), the satellite transponder is fully saturated and the power in the communication channel doesn't change. For a corrected surface transmitter power less than 4 db below 10 kw (that is, less than 4 kw), the satellite transponder is not fully saturated and thus, the curves can be used to normalize the ground receive signal level to any transmitter power. For the overall Syncom communications evaluation, all data are normalized to a transmitter power of 10 kw. By using measured telemetry data during the time of this test, these curves have been roughly related also to received signal at the satellite. The limited dynamic range of the spacecraft telemetry transducer prohibits the use of the satellite received carrier level channel over the entire range of interest. To correct the transmitter power, the effects of atmospheric attenuation, Δ range loss, satellite antenna gain must be subtracted from the measured transmitter power and this transmitter power must be normalized to eliminate the effects of ground

station transmitting antenna gain and line losses. An example of the use of the transfer characteristics is shown below:

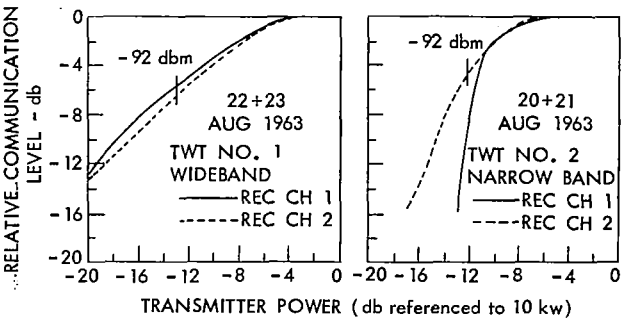

Figure IV-2—Syncom II communication experiment, satellite communication transfer characteristics (referenced to 10 kw ground xmtr power).

Assume a transmitter power of 500 watts--- +56.99 dbm
Assume that Camp Roberts is transmitting
a) Camp Roberts Antenna Gain +59.0 db
b) Line Loss - 2.5 db
Gains and Losses +56.5 db
Camp Roberts antenna gain normalized to the Fort Dix Transmitter = 56.5 -56.5 = 0
Antenna Aspect Angle (Camp Roberts) = 91.28°
a) Satellite Antenna Gain = -.4 db
Ground Station Antenna Elevation Angle 21.70°
a) Atmospheric attenuation (oxygen and water vapor) -.17 db
b) Range Loss -201.71 db
c) △Range Loss = 201.78 -201.00 = -.78 db
Corrected transmitter power +55.64 db
Correction factor obtained from the transfer characteristics to normalize 500 watts to 10 kw = 7.4 db
Measured communication level at 500 watts - 117 dbm
Normalized (10 kw) received carrier level = -117 - (-7.4) = -109.6 dbm
Actual measured received carrier levels on a different day under similar transmission conditions, but the satellite transponder being fully saturated, gives results which are within 2 db of the received carrier obtained by normalization using the transfer characteristics.

The curves of Figure IV-2 also show the crossover point and the input power to the spacecraft at which the beacon and the communication level are equal. Investigation to more accurately determine the crossover point is underway to improve the confidence in these curves.

UHF/SHF Beam Collimation

The power output of the spacecraft beacon is a function of the amplitude of the SHF signal received at the satellite. For example, if there is no input to the spacecraft communications transponder, there will be no evidence of beacon suppression. As the received communications level at the spacecraft increases to threshold and above, the beacon will start to be suppressed. This beacon suppression characteristic, associated with the Syncom spacecraft, leads to a novel technique for checking UHF/SHF beam alignment. This technique is briefly described as follows:

a) With the surface station power output set at zero, the spacecraft is acquired and the antenna locked in azimuth. The received beacon level is recorded on a Sanborn strip chart.

b) The antenna is pulled off the spacecraft in elevation until the received beacon level disappears, then the antenna is swept at a constant rate, in elevation, through the position of the spacecraft and the beacon level recorded on the Sanborn chart. (See Figure IV-3a).

c) The transmitted SHF power is increased in steps of 100, 200 and 400 watts and b. above repeated for each power level. The recorded beacon levels are shown in Figures IV-3b to IV-3d. The point of maximum SHF illumination of the spacecraft will result in a maximum

dip in the recorded beacon level. Therefore, if UHF/SHF beam alignment is perfect (in elevation) the dip in the recorded Sanborn beacon level would occur at the mid point of the beacon plot. The same procedures are repeated with the antenna locked in elevation and swept in azimuth. The resulting beacon level is shown in Figure IV-3e.

Figures IV-3a through IV-c are actual recordings of a collimation test performed at Fort Dix indicating a good UHF/SHF beam alignment.

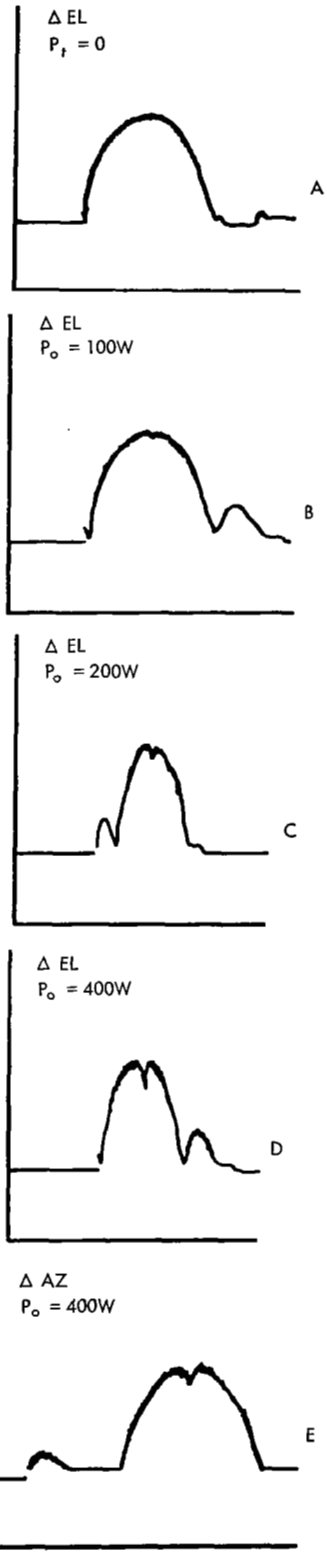

Figure IV-3—UHF/SHF beam collimation.

Link Calculations vs. Data

Spacecraft-to-Ground and Ground-to-Spacecraft

Link Calculations (Spacecraft-to-Ground)

The link calculations prepared prior to launch were based on orbital calculations for a satellite stationed at 24.5° west longitude. Since the satellite was ultimately stationed at approximately 55° west longitude, the calculations required updating. In an effort to be compatible with test data on hand, the predicted down-link communication levels were updated for the periods 1 and 2 October 1963 and 6 and 7 February 1964. The fixed parameter associated with the spacecraft-to-ground link is shown in Table IV-1. Tables IV-2 to IV-7 contain the variable parameter and final predicted communications level for all stations during the time periods mentioned above. The oxygen and water vapor loss was obtained from theoretical calculations shown in Figure IV-4. Spacecraft transmit antenna gain was obtained from Figure IV-5a, on which is plotted average antenna gain versus antenna angle, based on pre-launch antenna range measurements.

Two 24-hour communications level tests were performed on 1 and 2 October 1963 and 6 and 7 February 1964. The radiated power from the ground station throughout both test periods was 10 kw, which was adequate to fully saturate the spacecraft transponder for the entire period of the test and therefore remove from the subsequent analysis any variations associated with the up-link. While all stations (with the exception of Station No. 5 at Greenbelt) were involved in both tests, the fact that the Kingsport was underway off the coast of Spain during the 1 and 2 October period and that an error in the communications level calibration at Fort Dix during the 6 and 7 February period nullified the data for these stations.

The resulting calculated and measured communication and beacon levels are shown in Figures IV-6 to IV-15. The curves for Camp Roberts and Fort Dix show a predicted best and worst case, while the Lakehurst and Kingsport curve contains a single absolute value. This is due to the fact that the Dix and Roberts antennas are circularly polarized and have a 1 db ellipticity loss. This does not apply to the linear polarized antennas at Lakehurst and the Kingsport.

The data on Figures IV-6 to IV-15 reveal that while excellent trend correlation exists between predicted and measured values for

Table IV-1
Syncom Communications Spacecraft-to-Ground Link Fixed Parameters

PARAMETER		SCT/ Lakehurst	FORT DIX			NSCST/LAGOS			CAMP ROBERTS (1)		
		Absolute	Worst Case	Absolute	Best Case	Worst Case	Absolute	Best Case	Worst Case	Absolute	Best Case
Transmitter Power	dbm	+33.0 S		+33.0 S			+33.0 S			+33.0 S	
Cable Loss (etc.)	db	-1.0 M		-1.0 S			-1.0 S			-1.0 S	
Duplex Loss	db	-3.9 C		-3.9 C			-3.9 C			-3.9 C	
Antenna Mismatch Loss	db	-0.2 S		-0.2 S			-0.2 S			-0.2 S	
Receiving Antenna Gain	db	+43.0 M		+47.2 M			+39.5 M			+47.2 M	
Antenna Mismatch Loss	db	0.0 M	-0.1 S		0.0 E	-0.1 S		0.0 E	-0.1 S		0.0 E
Lobing Loss	db	-0.7 M		-1.0 M			-0.8 M			-1.0 M	
Polarization Loss	db	0.0 T		-3.0 M			-0.0 T			-3.0 M	
Elipticity Loss	db	0.0 T	-1.0 M		+1.0 M		0.0 T		-1.0 M		+1.0 M
Parametric Feeding Loss	db	-0.4 M		-0.8 M			-1.3 M			-0.8 M	
Sum of Fixed Losses and Gains	dbw	+69.2 C	+69.2 C		+71.3 C	+65.2 C		+65.3 C	+69.2 C		+71.3 C

Symbols: C — Calculated
M — Measured
E — Estimated
S — Specified
T — Theoretical

(1) Fixed Parameters of Fort Dix Adopted for this Station

all stations, there also does exist variation in magnitude, with the measured values falling both above and below predicted values. Variations between measured and predicted values of communications and beacon levels may result from one or more of the following factors.

a) Reduction in satellite transmitted power.
b) Error in measured versus actual satellite orientation.
c) Accuracies associated with measurement of levels at surface terminal.
d) Propagation losses at low elevation angles deviating from theoretical values.
e) Human factors.
f) Accuracy of surface and spacecraft antenna gain measurements.

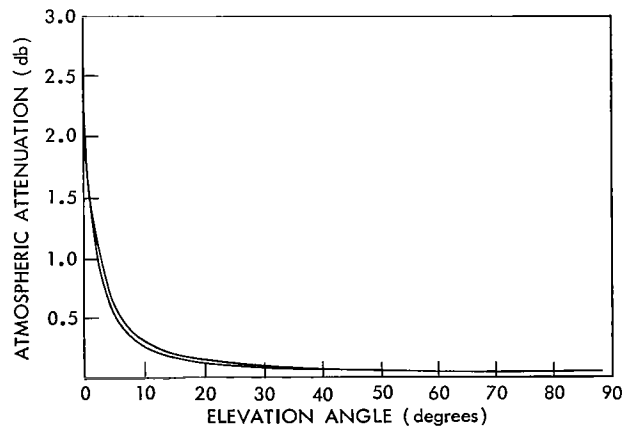

Figure IV-4—Syncom II communication experiment (atmospheric oxygen and unsaturated water vapor).

An examination of Lakehurst data, Figure IV-16, shows that the measured communications level (Curve D) varies from a maximum of -112 dbm (reference to the parametric amplifier) at 0500 Z hours to a minimum of -117.5 dbm at 1900 Z hours. Since the satellite communications transponder is fully saturated, the variation in communications level is primarily due to changes in antenna gain of the satellite, atmospheric attenuation due to combined atmospheric oxygen and unsaturated water vapor at low elevation angles, and the effects of free space loss associated with changes in slant range. These variations are due to the fact that the spacecraft orbit inclination is 33° with respect to the equator and therefore the sub-satellite point traces out a Figure Eight around

Table IV-2

Link Calculations, Spacecraft-to-Ground, Kingsport

TIME	ELEV ANGLE	FREE SPACE LOSS	OXYGEN & WATER VAPOR	SAT ANT GAIN	DUPLEX LOSS	TOTAL VAR LOSS	BEST CASE FIXED GAINS & LOSSES	BEST REVD CARRIER	WORST CASE FIXED GAINS & LOSSES	WORST REVD CARRIER
0000	66.78	-188.85	-.05	4.95	3.90	180.05	65.30	114.75	65.20	114.85
0100	61.80	-188.90	-.05	4.90	3.90	180.15	65.30	114.85	65.20	114.95
0200	55.81	-188.97	-.05	4.80	3.90	180.32	65.30	115.02	65.20	115.12
0300	48.84	-189.06	-.07	4.60	3.90	180.63	65.30	115.33	65.20	115.43
0400	41.15	-189.19	-.08	4.20	3.90	181.17	65.30	115.87	65.20	115.97
0500	33.14	-189.34	-.10	3.70	3.90	181.84	65.30	116.54	65.20	116.64
0600	25.35	-189.50	-.15	3.30	3.90	182.45	65.30	117.15	65.20	117.25
0700	19.44	-189.62	-.18	3.00	3.90	182.90	65.30	117.60	65.20	117.70
0800	12.68	-189.77	-.28	2.70	3.90	183.45	65.30	118.15	65.20	118.25
1000	7.25	-189.89	-.50	2.60	3.90	183.89	65.30	118.59	65.20	118.69
1100	8.10	-189.87	-.40	2.60	3.90	183.77	65.30	118.47	65.20	118.57
1200	11.37	-189.80	-.30	2.80	3.90	183.40	65.30	118.10	65.20	118.20
1300	16.82	-189.62	-.20	3.10	3.90	182.87	65.30	117.57	65.20	117.67
1400	24.06	-189.52	-.15	3.45	3.90	182.32	65.30	117.20	65.20	117.12
1500	32.60	-189.35	-.10	3.80	3.90	181.75	65.30	116.45	65.20	116.55
1600	41.89	-189.18	-.08	4.30	3.90	181.06	65.30	115.76	65.20	115.86
1700	51.34	-189.02	-.06	4.70	3.90	180.48	65.30	115.18	65.20	115.28
1800	60.28	-188.91	-.05	4.80	3.90	180.26	65.30	114.96	65.20	115.06
1900	67.91	-188.84	-.05	4.90	3.90	180.09	65.30	114.79	65.20	114.89
2000	73.18	-188.80	-.05	4.99	3.90	179.96	65.30	114.66	65.20	114.76
2100	75.06	-188.79	-.05	5.00	3.90	179.94	65.30	114.64	65.20	114.74
2200	73.77	-188.79	-.05	5.05	3.90	179.89	65.30	114.59	65.20	114.69
2300	70.65	-188.82	-.05	5.00	3.90	179.97	65.30	114.67	65.20	114.77
2400	66.52	-188.85	-.05	4.95	3.90	180.05	65.30	114.75	65.20	114.85

Table IV-3

Link Calculations, Spacecraft-to-Ground, Lakehurst

TIME	ELEV ANGLE	FREE SPACE LOSS	OXYGEN & WATER VAPOR	SAT LOOK ANGLE	ANT GAIN	DUPLEX LOSS	TOTAL VAR LOSS	FIXED GAINS & LOSSES	REVD CARRIER
0000	66.78	-188.85	-.05	88.82	+4.95	+3.9	-180.05	+69.8	110.25
0100	61.80	-188.90	-.05	88.00	+4.90	+3.9	-180.15	+69.8	110.35
0200	55.81	-188.97	-.05	86.96	+4.80	+3.9	-180.32	+69.8	110.52
0300	48.84	-189.06	-.07	85.79	+4.60	+3.9	-180.63	+69.8	110.83
0400	41.15	-189.19	-.08	84.58	+4.20	+3.9	-181.17	+67.8	111.37
0500	33.14	-189.34	-.10	83.43	+3.70	+3.9	-181.84	+69.8	112.04
0600	25.35	-189.50	-.15	82.43	+3.30	+3.9	-182.45	+69.8	112.65
0700	19.44	-189.62	-.18	81.74	+3.00	+3.9	-182.90	+69.8	113.10
0800	12.68	-189.77	-.28	81.04	+2.70	+3.9	-183.45	+69.8	113.65
0900	8.85	-189.86	-.40	80.71	+2.60	+3.9	-183.76	+69.8	113.96
1000	7.25	-189.89	-.50	80.63	+2.60	+3.9	-183.89	+69.8	114.09
1100	8.10	-189.87	-.40	80.80	+2.60	+3.9	-183.77	+69.8	113.97
1200	11.37	-189.80	-.30	81.22	+2.80	+3.9	-183.40	+69.8	113.60
1300	16.82	-189.67	-.20	82.73	+3.10	+3.9	-182.87	+69.8	113.07
1400	24.06	-189.52	-.15	82.73	+3.45	+3.9	-182.32	+69.8	112.52
1500	32.60	-189.35	-.10	83.57	+3.80	+3.9	-181.75	+69.8	111.95
1600	41.89	-189.18	-.08	84.90	+4.30	+3.9	-181.06	+69.8	111.26
1700	51.34	-189.02	-.06	86.10	+4.70	+3.9	-180.48	+69.8	110.68
1800	60.28	-188.91	-.05	87.24	+4.80	+3.9	-180.26	+69.8	110.46
1900	67.91	-188.84	-.05	88.23	+4.90	+3.9	-180.09	+69.8	110.29
2000	73.18	-188.80	-.05	88.99	+4.99	+3.9	-179.96	+69.8	110.16
2100	75.06	-188.79	-.05	89.44	+5.00	+3.9	-179.94	+69.8	110.14
2200	73.77	-188.79	-.05	89.56	+5.05	+3.9	-179.89	+69.8	110.09
2300	70.65	-188.82	-.05	89.33	+5.00	+3.9	-179.97	+69.8	110.17
2400	66.52	-188.85	-.05	88.78	+4.95	+3.9	- 80.05	+69.8	110.25

Table IV-4

Link Calculations, Spacecraft-to-Ground, Fort Dix

TIME	ELEV ANGLE	FREE SPACE LOSS	OXYGEN & WATER VAPOR	SAT LOOK ANGLE	SAT ANT GAIN	DUPLEX LOSS	TOTAL VAR LOSS	BEST CASE FIXED GAINS & LOSSES	BEST REVD CARRIER	WORST CASE FIXED GAINS & LOSSES	WORST REVD CARRIER
0000	66.78	-188.85	-.05	88.82	+4.95	+3.9	-180.05	+71.3	108.75	+69.2	110.85
0100	61.80	-188.90	-.05	88.00	+4.90	+3.9	-180.15	+71.3	108.85	+69.2	110.95
0200	55.81	-188.97	-.05	86.96	+4.80	+3.9	-180.32	+71.3	109.02	+69.2	111.12
0300	48.84	-189.06	-.07	85.79	+4.60	+3.9	-180.63	+71.3	109.33	+69.2	111.43
0400	41.15	-189.19	-.08	84.58	+4.20	+3.9	-181.17	+71.3	109.87	+69.2	111.97
0500	33.14	-189.34	-.10	83.43	+3.70	+3.9	-181.84	+71.3	110.54	+69.2	112.64
0600	25.35	-189.50	-.15	82.43	+3.30	+3.9	-182.45	+71.3	111.15	+69.2	113.25
0700	19.44	-189.62	-.18	81.74	+3.00	+3.9	-182.90	+71.3	111.60	+69.2	113.70
0800	12.68	-189.77	-.28	81.04	+2.70	+3.9	-183.45	+71.3	112.15	+69.2	114.25
0900	8.85	-189.86	-.40	80.71	+2.60	+3.9	-183.76	+71.3	112.46	+69.2	114.56
1000	7.25	-189.89	-.50	80.63	+2.60	+3.9	-183.89	+71.3	112.49	+69.2	114.69
1100	8.10	-189.87	-.40	80.80	+2.60	+3.9	-183.77	+71.3	112.47	+69.2	114.57
1200	11.37	-189.80	-.30	81.22	+2.80	+3.9	-183.40	+71.3	112.10	+69.2	114.20
1300	16.82	-189.67	-.20	81.87	+3.10	+3.9	-182.87	+71.3	111.57	+69.2	113.67
1400	24.06	-189.52	-.15	82.73	+3.45	+3.9	-182.32	+71.3	111.02	+69.2	113.12
1500	32.60	-189.35	-.10	83.57	+3.80	+3.9	-181.75	+71.3	110.45	+69.2	112.55
1600	41.89	-189.18	-.08	84.50	+4.30	+3.9	-181.06	+71.3	109.76	+69.2	111.86
1700	51.34	-189.02	-.06	86.10	+4.70	+3.9	-180.48	+71.3	109.18	+69.2	111.28
1800	60.28	-188.91	-.05	87.24	+4.80	+3.9	-180.26	+71.3	108.96	+69.2	111.06
1900	67.91	-188.84	-.05	88.23	+4.90	+3.9	-180.09	+71.3	108.79	+69.2	110.89
2000	73.18	-188.80	-.05	88.99	+4.99	+3.9	-179.96	+71.3	108.66	+69.2	110.76
2100	75.06	-188.79	-.05	89.44	+5.00	+3.9	-179.94	+71.3	108.64	+69.2	110.74
2200	73.77	-188.79	-.05	89.56	+5.05	+3.9	-179.89	+71.3	108.59	+69.2	110.69
2300	70.65	-188.82	-.05	89.33	+5.00	+3.9	-179.97	+71.3	108.67	+69.2	110.77
2400	66.52	-188.85	-.05	88.78	+4.95	+3.9	-180.05	+71.3	108.75	+69.2	110.85

Table IV-5

Link Calculations, Spacecraft-to-Ground, Camp Roberts

TIME	ELEV ANGLE	FREE SPACE LOSS	OXYGEN & WATER VAPOR	SAT LOOK ANGLE	SAT ANT GAIN	DUPLEX LOSS	TOTAL VAR LOSS	BEST CASE FIXED GAINS & LOSSES	BEST REVD CARRIER	WORST CASE FIXED GAINS & LOSSES	WORST REVD CARRIER
0000	27.16	-189.46	-.14	89.06	+5.00	+3.9	-180.70	+71.3	109.40	+69.2	111.50
0100	24.05	-189.52	-.15	89.10	+5.00	+3.9	-180.77	+71.3	109.47	+69.2	111.57
0200	21.06	-189.58	-.16	88.89	+4.95	+3.9	-180.89	+71.3	109.59	+69.2	111.69
0300	18.05	-189.64	-.18	88.45	+4.90	+3.9	-181.02	+71.3	109.72	+69.2	111.82
0400	14.77	-189.72	-.24	87.81	+4.85	+3.9	-181.21	+71.3	109.91	+69.2	112.01
0500	11.06	-189.79	-.30	87.03	+4.80	+3.9	-181.39	+71.3	110.09	+69.2	112.19
0600	6.89	-189.90	-.50	86.17	+4.70	+3.9	-181.80	+71.3	110.50	+69.2	112.60
0700	2.47	-190.00	-1.10	85.29	+4.45	+3.9	-182.75	+71.3	111.45	+69.2	113.55
1400	1.504	-190.02	-1.40	82.36	+3.30	+3.9	-184.22	+71.3	112.92	+69.2	115.02
1500	8.06	-189.86	-.42	82.67	+3.40	+3.9	-182.98	+71.3	111.68	+69.2	113.78
1600	15.30	-189.71	-.22	83.19	+3.65	+3.9	-182.38	+71.3	111.08	+69.2	113.18
1700	22.45	-189.55	-.14	83.91	+3.95	+3.9	-181.84	+71.3	110.54	+69.2	112.64
1800	28.64	-189.43	-.13	84.76	+4.25	+3.9	-181.41	+71.3	110.11	+69.2	112.21
1900	33.05	-189.34	-.10	85.71	+4.60	+3.9	-180.94	+71.3	109.64	+69.2	111.74
2000	35.13	-189.30	-.10	86.66	+4.75	+3.9	-180.75	+71.3	109.45	+69.2	111.55
2100	34.93	-189.30	-.10	87.54	+4.85	+3.9	-180.65	+71.3	109.35	+69.2	111.45
2200	33.00	-189.34	-.10	88.27	+4.90	+3.9	-180.64	+71.3	109.34	+69.2	111.44
2300	26.99	-189.46	-.13	89.07	+5.00	+3.9	-180.69	+71.3	109.39	+69.2	111.49
2400	23.89	-189.52	-.14	89.09	+5.00	+3.9	-180.76	+71.3	109.46	+69.2	111.56

Table IV-6

Link Calculations, Spacecraft-to-Ground, Camp Roberts

TIME	ELEV ANGLE	FREE SPACE LOSS	OXYGEN & WATER VAPOR	SAT LOOK ANGLE	SAT ANT GAIN	DUPLEX LOSS	TOTAL VAR LOSS	BEST CASE FIXED GAINS & LOSSES	BEST REVD CARRIER	WORST CASE FIXED GAINS & LOSSES	WORST REVD CARRIER
0000	9.61	-189.85	-.35	82.24	+3.25	+3.9	-183.05	+71.3	111.75	+69.2	113.85
0100	16.75	-189.68	-.20	82.94	+3.50	+3.9	-182.48	+71.3	111.18	+69.2	113.28
0200	23.19	-189.54	-.15	83.86	+3.90	+3.9	-181.89	+71.3	110.59	+69.2	112.69
0300	28.10	-189.44	-.13	84.93	+4.30	+3.9	-181.37	+71.3	110.07	+69.2	112.17
0400	30.85	-189.38	-.11	86.08	+4.70	+3.9	-180.89	+71.3	109.59	+69.2	111.69
0500	31.28	-189.38	-.11	87.21	+4.80	+3.9	-180.79	+71.3	109.49	+69.2	111.59
0600	29.80	-189.40	-.12	88.21	+4.90	+3.9	-180.72	+71.3	109.42	+69.2	111.52
0700	27.13	-189.46	-.13	89.01	+5.0	+3.9	-180.69	+71.3	109.39	+69.2	111.49
0800	23.97	-189.52	-.15	89.55	+5.05	+3.9	-180.72	+71.3	109.42	+69.2	111.52
0900	20.80	-189.59	-.16	89.80	+5.10	+3.9	-180.75	+71.3	109.45	+69.2	111.55
1000	17.78	-189.65	-.20	89.75	+5.10	+3.9	-180.85	+71.3	109.55	+69.2	111.65
1100	14.84	-189.72	-.23	89.41	+5.00	+3.9	-181.05	+71.3	109.75	+69.2	111.85
1200	11.78	-189.81	-.28	88.81	+4.95	+3.9	-181.24	+71.3	109.94	+69.2	112.04
1300	8.38	-189.86	-.40	87.99	+4.90	+3.9	-181.46	+71.3	110.16	+69.2	112.26
1400	4.54	-189.95	-.70	87.03	+4.80	+3.9	-181.95	+71.3	110.65	+69.2	112.75
1500	.378	-190.06	-2.00	85.99	+4.7	+3.9	-183.46	+71.3	112.16	+69.2	114.26
2300	3.09	-189.99	-.90	81.82	+3.10	+3.9	-183.89	+71.3	112.59	+69.2	114.69
2400	10.11	-189.83	-.33	82.29	+3.30	+3.9	-182.96	+71.3	111.66	+69.2	113.76

Table IV-7

Beacon Carrier Levels

	LAKEHURST						KINGSPORT		CAMP ROBERTS				
TIME	TOTAL VAR LOSSES	FIXED GAINS & LOSSES	REVD TRACK LEVEL	FORT DIX GAINS & LOSSES	WORST FORT DIX TRACK LEVEL	BEST FORT DIX TRACK LEVEL	GAINS & LOSSES	TRACK LEVEL	TOTAL VAR LOSSES	WORST CASE GAIN & LOSSES	WORST TRACK LEVEL	BEST GAIN & LOSSES	BEST TRACK LEVEL
0000	-180.05	56.6	123.45	56.00	124.05	121.95	52.00	128.05	180.70	56.00	124.70	58.1	122.60
0100	-180.15	56.6	123.55	56.00	124.15	122.05	52.00	128.15	180.77	56.00	124.77	58.1	122.67
0200	-180.32	56.6	123.72	56.00	124.32	122.22	52.00	128.32	180.89	56.00	124.89	58.1	122.79
0300	-180.63	56.6	124.03	56.00	124.63	122.53	52.00	128.63	181.03	56.00	125.02	58.1	122.92
0400	-181.17	56.6	124.57	56.00	125.17	123.07	52.00	129.17	181.21	56.00	125.21	58.1	123.11
0500	-181.84	56.6	125.24	56.00	125.84	123.74	52.60	129.84	181.39	56.00	125.39	58.1	123.39
0600	-182.45	56.6	125.85	56.00	126.45	124.34	52.00	130.45	181.80	56.00	125.80	58.1	123.70
0700	-182.90	56.6	126.30	56.00	126.90	124.80	52.00	130.90	181.80	56.00	126.75	58.1	124.65
0800	-183.45	56.6	126.85	56.00	127.45	125.35	52.00	131.45					
0900	-183.76	56.6	127.16	56.00	127.76	125.66	52.00	131.76					
1000	-183.89	56.6	127.29	56.00	127.89	125.79	52.00	131.89					
1100	-183.77	56.6	127.17	56.00	127.77	125.67	52.00	131.77					
1200	-183.46	56.6	126.86	56.00	127.46	125.36	52.00	131.40					
1300	-182.87	56.6	126.27	56.00	126.87	124.77	52.00	130.87					
1400	-182.32	56.6	125.72	56.00	126.32	124.22	52.00	130.32	184.22	56.00	128.22	58.1	126.12
1500	-181.75	56.6	125.15	56.00	125.75	123.65	52.00	129.75	182.98	56.00	126.98	58.1	124.88
1600	-181.06	56.6	124.46	56.00	125.06	129.96	52.00	129.06	182.38	56.00	126.38	58.1	124.28
1700	-180.48	56.6	123.88	56.00	124.48	122.38	52.00	128.48	181.84	56.00	125.84	58.1	123.74
1800	-180.26	56.6	123.66	56.00	124.26	122.16	52.00	128.26	181.41	56.00	125.41	58.1	123.31
1900	-180.09	56.6	123.49	56.00	124.09	121.99	52.00	128.09	190.94	56.00	124.94	58.1	122.84
2000	-179.96	56.6	123.36	56.00	123.96	121.86	52.00	127.96	180.75	56.00	124.75	58.1	122.65
2100	-179.94	56.6	123.34	56.00	123.94	121.84	52.00	127.94	180.65	56.00	124.65	58.1	122.55
2200	-179.89	56.6	123.29	56.00	123.89	121.79	52.00	127.89	180.64	56.00	124.64	58.1	122.54
2300	-179.97	56.6	123.37	56.00	123.97	121.87	52.00	127.97	180.69	56.00	124.69	58.1	122.59
2400	-180.05	56.6	123.45	56.00	124.05	121.95	52.00	128.05	180.76	56.00	124.76	58.1	122.66

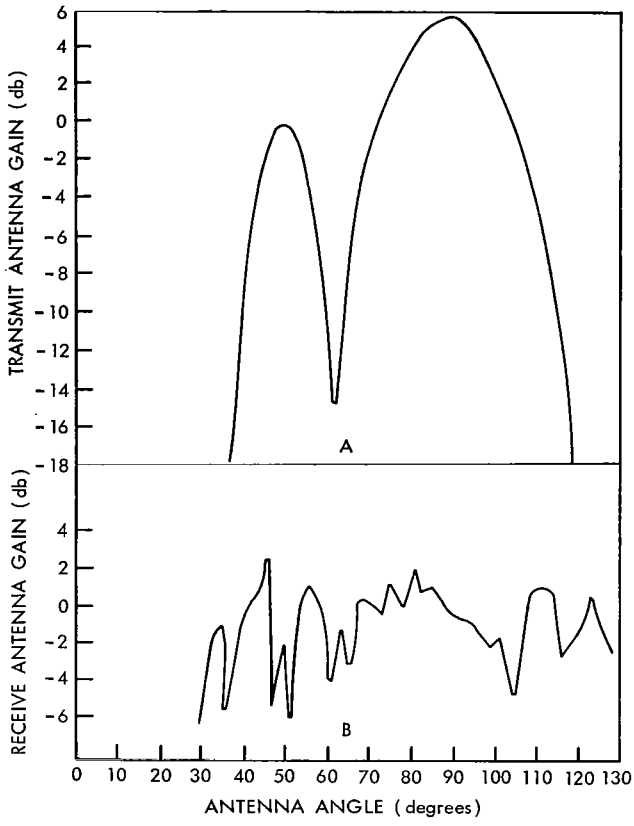

Figure IV-5—Syncom spacecraft transmit and receive antenna gain vs. antenna angle.

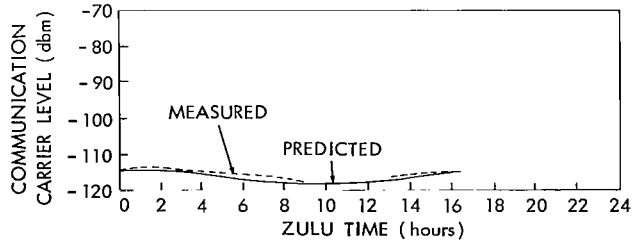

Figure IV-6—Syncom II communication experiment, Kingsport.

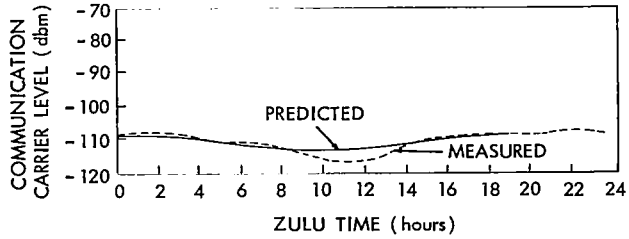

Figure IV-7—Syncom II communication experiment, Lakehurst.

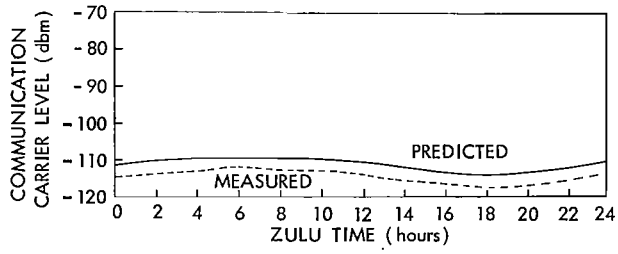

Figure IV-8—Syncom II communication experiment (1 & 2 Oct. 1963), Lakehurst.

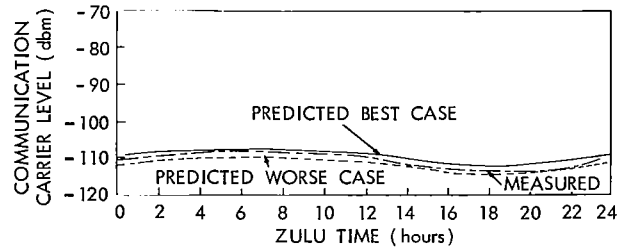

Figure IV-9—Syncom II communication experiment, Fort Dix.

the equator extending from approximately 33° north latitude to 33° south latitude. As the sub-satellite point travels this Figure Eight, the slant range and elevation angle obviously change and the antenna aspect angle (the angle between line-of-sight from the surface terminal and the spacecraft spin axis) will vary. For example, with the spacecraft in an orbit in which the ascending node is located at 55° west longitude, it would present to Lakehurst an antenna aspect angle that varied from approximately 78° to 90° during a 24-hour period. Under the same orbital conditions, it would present to the Kingsport, stationed off the coast of Nigeria, an antenna angle that varied from 83° to 95°. For the specific period of 1 and 2 October 1963, the antenna aspect angle presented to Lakehurst varied from 80.3° to 89.9° twice during the 24-hour period. From Figure IV-5a, it can be seen that this would result in a spacecraft transmit antenna gain variation of approximately 3 db.

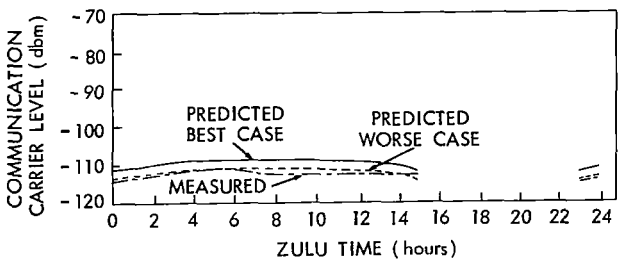

Figure IV-10—Syncom II communication experiment, (1 & 2 Oct 1963), Camp Roberts.

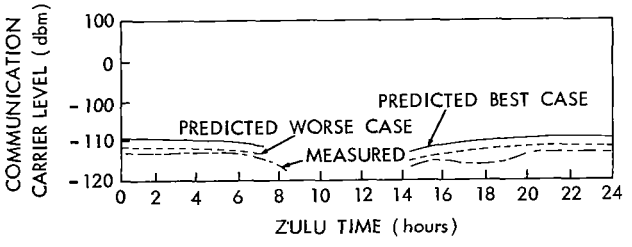

Figure IV-11—Syncom II communication experiment, Camp Roberts.

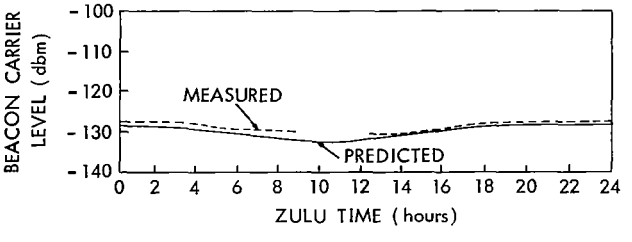

Figure IV-12—Syncom II communication experiment, USNS Kingsport.

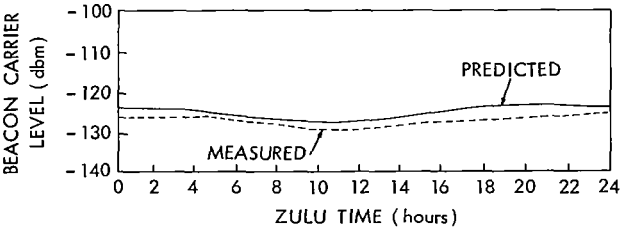

Figure IV-13—Syncom II communication experiment, Lakehurst.

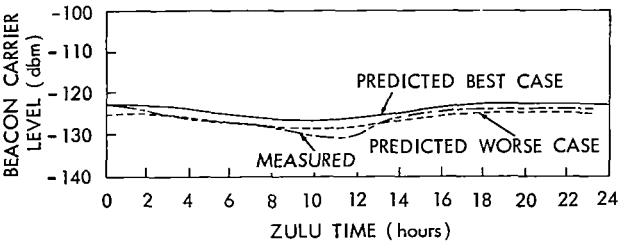

Figure IV-14—Syncom II communication experiment, Fort Dix.

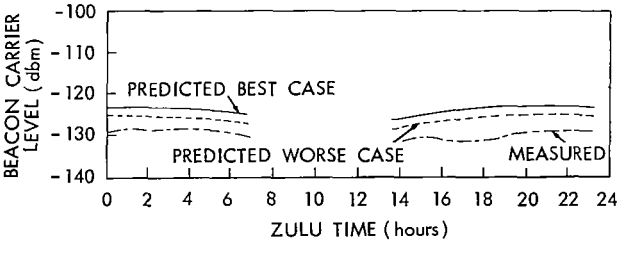

Figure IV-15—Syncom II communication experiment, Camp Roberts.

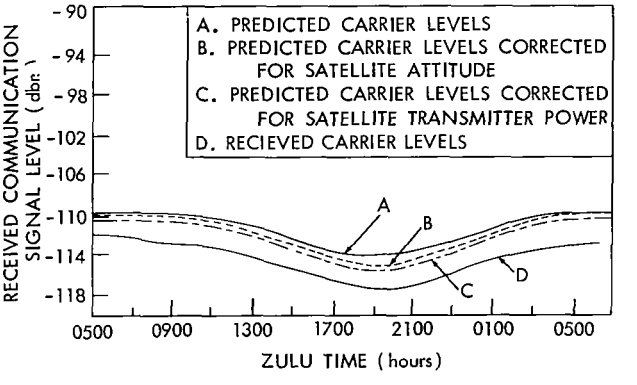

Figure IV-16—Syncom II communication experiment, data taken October 1 and 2.

A comparison of the predicted (Curve A) and measured (Curve D) values of Figure IV-16 indicates that excellent trend correlation exists. However, the measured curve is always lower than the predicted, varying from a minimum of 2 db at 0500Z hours to a maximum of 3.5 db at 1400Z hours. One possible cause for this deviation could be in the accuracy to which communications levels can be measured at the surface stations. The accuracy of this measurement is approximately 2 db with a reset accuracy of 1/2 db. This, therefore, could account for all or part of the 2 db difference occurring at say 0500Z hours

and would be a constant factor throughout the 24-hour test period. This, however, would still leave an approximately 1.5 db difference occurring between 1800Z hours and 2100Z hours unexplained.

An investigation into the position of the satellite during this period of time reveals that it is in the lowest extremes of the southern hemisphere with corresponding long slant ranges, low elevation angle, and poor antenna angles. The poor antenna angle, plus the steepness of the spacecraft transmit antenna gain pattern (Figure IV-5a) at these antenna aspect angles, would point to the possibility that the actual orientation of the spacecraft with respect to the orbital plane is off by a small amount from measured values, possibly one or two degrees. In an effort to add some support to this theory, it was assumed that the spacecraft attitude was off by 1.5° in a direction that would increase the total variation in antenna gain during a 24-hour period. Based on this assumption, new predicted values were calculated and plotted as Curve B, Figure IV-16. A comparison of Curves B and D now reveals that while there is negligible difference between predicted values and measured during the 0500Z to 1100Z time period (where the aspect angle is close to 90° and variations in spacecraft antenna gain is small), the difference at the 1900Z hour period has been reduced by approximately 1 db. A third factor to be considered at this time is that all link calculations were based on a satellite-transmitted power of 33 dbm, whereas the telemetry data during the test period consistently indicated a power level of 32.5 dbm. Applying this correction to Curve B results in Curve C.

A comparison of Curves C and D reveals an approximate 1.8 to 2.5 db difference between measured and predicted values which now fall within the measurement accuracy capabilities of the ground terminal.

The above procedure could be repeated by assuming that the orientation of the spacecraft is off by approximately 2° or more. This would have a tendency of bringing the predicted and measured values closer together. However, it is felt that with all the inaccuracies associated with test equipment calibration, measurement techniques and the ever present human factors, the obtainment of measured values that agree to within 2-3 db of predicted values is considered to provide excellent correlation in evaluation of the Syncom down-link.

A comparison of measured with predicted communications and beacon levels received at Lakehurst, Figures IV-7 and IV-13, for the 6 and 7 February 1964 period reveals a closer correlation than the 1 and 2 October test. A similar analysis would be applicable in explaining the resulting difference between predicted and measured results.

Figure IV-9 shows a comparison of the measured communications levels versus the predicted best and worst case values for the Fort Dix station during the 1 and 2 October test. Overall correlation is obviously excellent. The measured curve stays between the limits of predicted values over the entire 24-hour period, tending to be closer to the predicted best case value until 1300Z hours. During the 1300Z-2400Z hour period, the spacecraft is once again in the southern hemisphere, and if (as assumed above), the spacecraft orientation is off by 1.5°, this could account for the measured value dropping close to the predicted worst case limit during this time period.

Figures IV-6 and IV-12 depict the results of communications and beacon measurements made aboard the Kingsport during the 6 and 7 February 1964 test period. Once again, correlation between measured and predicted values is excellent. The fact that measured values are slightly higher than predicted would tend to indicate that the Kingsport measurement accuracy was on the high, or plus, side. The break in the measured curve during the 0900Z-1200Z hour period was a result of an obstruction directly in the Kingsport's line-of-sight. It should be noted that the Kingsport was docked in the Norfolk Naval Shipyard during this test.

A comparison of the results obtained at Camp Roberts during the 1 and 2 October test period (Figure IV-10) indicate that the measured values either coincide with or were slightly below the predicted worst case value. Since the trend correlation is extremely good, this would indicate that the Roberts measurement accuracy was on the low, or minus, side.

STATION	MAXIMUM			MINIMUM		
	LEVEL	TIME	ELEVATION ANGLE	LEVEL	TIME	ELEVATION
FORT DIX	- 108 dbm	0500Z	71.6°	- 114 dbm	1900Z	6.5°
LAKEHURST	- 112 dbm	0500Z	71.6°	- 117.5 dbm	1930Z	6.5°
CAMP ROBERTS	- 111 dbm	0500Z	31.2°	- 115 dbm	2350	5.3°
USNS KINGSPORT	- 116 dbm	0500Z	17.0° *	- 120 dbm	1730Z	10.0° *

*Approximate figure due to the fact that USNS Kingsport was underway.

Figure IV-17—Syncom maximum & minimum received comm levels, 1-2 Oct 1963, all stations.

It should be noted that the predicted and measured communications levels contained in Figures IV-6 to IV-11 are for the half duplex mode. To obtain the comparable levels for full duplex operation (two channels through the spacecraft transponder), an additional 3.9 db loss must be added. For example, for full duplex operation, the measured communications levels at Fort Dix for the 1 and 2 October 1963 period would vary from a maximum of -111.9 dbm to a minimum of -117.9 dbm. A listing of the maximum and minimum communications levels for all stations during the 1 and 2 October test period is contained in Figure IV-17.

Link Calculations (Ground-to-Spacecraft)

The predicted ground-to-spacecraft link characteristics were updated for the period of 23 August 1963 using various transmitter powers from the Fort Dix Station. The fixed gains and losses for the different stations are shown in Tables IV-8, 9 and 10. Orbital predictions were used to obtain the antenna aspect angles which were used in conjunction with the curves of Figure IV-5B (antenna gain vs antenna aspect angle) to obtain the antenna gain. The predicted ground station antenna elevation angles were also obtained from the orbital data and used in conjunction with Figure IV-18 (free space attenuation vs elevation angle) to obtain the free space loss at 7361 MC. The attenuation due to oxygen and unsaturated water vapor was obtained from Figure IV-4. The sum of the gains and losses was calculated at the various transmitter powers.

Table IV-8

Syncom Communications, Ground-to-Spacecraft Link Fixed Parameters

PARAMETER		SCT/LAKEHURST			SCT/FT. DIX			NSCST/LAGOS			SCT/ROBERTS		
		Worst Case	Absolute	Best Case	Worst Case	Absolute	Best Case	Worst Case	Absolute	Best Case	Worst Case	Absolute	Worst Case
Line Loss	db	-3.0 S		-2.8 C		-2.5 M			1.6 M			-2.5 M	
Antenna Gain	db		+53.4 M			+59.0 M			+53.9 M			+59.0 M	
Antenna Mismatch Loss	db				-0.1 S		0.0 E		-0.1 M		-0.1 S		0.0 E
Radome Loss	db		None			None			-0.2 M			None	
SHF Beam Pointing Loss	db	-2.3 S+M		-0.3	-0.6 S		-0.1 S	-1.1 S		-0.1 S	-0.6 S		-0.1 S
Polarization Loss	db		-3.0 C			-3.0 C			-3.0 C		-0.8 E	-3.0 C	
Ellipticity Loss	db	-0.5 E		+0.5 E	-0.8 E		+0.8 E	-0.5 E		+0.5 E			+0.8 E
Satellite Antenna Mismatch Loss	db		-0.5 M			-0.5 M			-0.5 M			-0.5 M	
Sum of Fixed Losses & Gains	dbw	+44.1 C		+47.3 C	+51.5 C		+53.7 C	+46.9 C		+48.9 C	+51.5 C		+53.7 C

SYMBOLS: C - Calculated
M - Measured
E - Estimated
S - Specified
T - Theoretical
S+M - Specified and Measured
E/M - Estimated Based on Measurements

Table IV-9

Link Calculations, Ground-to-Spacecraft, Fort Dix

TIME	TRANS POWER (kw)	TRANS POWER (dbm)	WORST CASE FIXED GAINS & LOSSES	BEST CASE FIXED GAINS & LOSSES	FREE SPACE LOSS	SAT ANT GAIN	OXYGEN & WATER VAPOR	TOTAL VAR LOSSES	WORST CASE SAT REVD POWER	BEST CASE SAT REVD POWER	MEAS-URED SAT REVD POWER
1035	20	+73.00	+51.50	+53.70	-201.00	-.62	-.05	-201.67	-77.17	-74.97	-84.8
1038	15	+71.76	+51.50	+53.70	-201.01	-.63	-.05	-201.69	-78.43	-76.23	-84.6
1041	11	+70.42	+51.50	+53.70	-201.01	-.64	-.05	-201.70	-79.78	-77.58	-84.8
1044	9	+69.54	+51.50	+53.70	-201.01	-.65	-.05	-201.71	-80.67	-78.47	-85.0
1047	8	+69.03	+51.50	+53.70	-201.01	-.66	-.05	-201.72	-81.19	-78.99	-85.0
1050	6.5	+68.13	+51.50	+53.70	-201.01	-.67	-.05	-201.73	-82.10	-79.90	
1053	4	+66.02	+51.50	+53.70	-201.01	-.68	-.05	-201.74	-84.22	-82.02	-85.2
1056	3	+64.78	+51.50	+53.70	-201.01	-.68	-.05	-201.74	-85.46	-83.26	-86.2
1059	2.5	+63.98	+51.50	+53.70	-201.02	-.68	-.05	-201.75	-86.27	-84.07	-87.0
1107	2	+63.02	+51.50	+53.70	-201.02	-.68	-.05	-201.75	-87.23	-85.03	-88.2
1105	1.5	+61.76	+51.50	+53.70	-201.02	-.68	-.05	-201.75	-88.49	-86.29	-89.0
1108	1.25	+60.97	+51.50	+53.70	-201.02	-.69	-.05	-201.76	-89.29	-87.09	-89.0
1111	1.0	+60.00	+51.50	+53.70	-201.03	-.70	-.05	-201.78	-90.28	-88.08	-89.9
1114	0.9	+59.54	+51.50	+53.70	-201.03	-.65	-.05	-201.73	-90.69	-88.49	-89.8
1117	0.8	+59.03	+51.50	+53.70	-201.03	-.60	-.05	-201.68	-91.15	-88.95	-90.3
1120	0.7	+58.45	+51.50	+53.70	-201.03	-.60	-.05	-201.68	-91.73	-89.53	-90.3
1123	0.6	+57.78	+51.50	+53.70	-201.04	-.55	-.05	-201.64	-92.36	-90.16	-90.8
1126	0.5	+56.99	+51.50	+53.70	-201.04	-.50	-.05	-201.59	-93.10	-90.90	-91.7
1129	0.4	+56.02	+51.50	+53.70	-201.04	-.48	-.05	-201.57	-94.05	-91.85	-92.1
1132	0.3	+54.78	+51.50	+53.70	-201.04	-.45	-.05	-201.54	-95.26	-93.06	
1135	0.2	+53.02	+51.50	+53.70	-201.05	-.40	-.05	-201.50	-96.98	-94.78	
1138	0.1	+50.00	+51.50	+53.70	-201.05	-.40	-.05	-201.50	-100.00	-97.80	

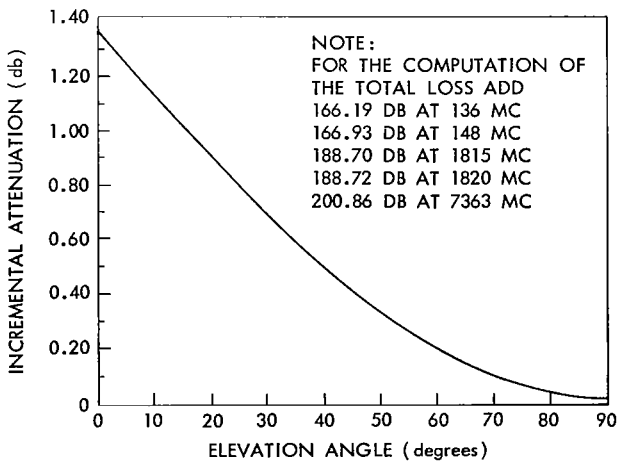

Figure IV-18—Syncom II communication experiment, free space attenuation, free space attenuation vs. elevation angle.

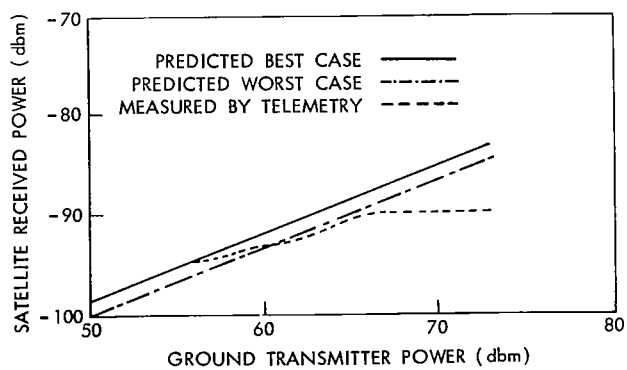

Figure IV-19—Syncom II communication experiment, ground-to-spacecraft link characteristics, Fort Dix transmitting.

Table IV-10

Link Calculations, Carrier-to-Noise, Lakehurst

ELEV ANGLE	K (dbm)	B	T_{sr}	T_{sr}(db)	N_p	TIME	C_p	C/N	PREDICTED S+N/N MODE			MEASURED S+N/N MODE		
									NN	WN	WNFB	NN	WN	WNFB
33.85	198.60	52.74	179°	22.53	-123.33	1500	111.95	11.38	34.3	41.5	42			
38.47	198.60	52.74	178°	22.50	-123.36	1530	111.50	11.86			42	31	35	37
43.18	198.60	52.74	183°	22.62	-123.24	1600	111.26	11.98	34.7	42	42.4			
47.91	198.60	52.74	177°	22.48	-123.38	1630	111.00	12.38				30	35	37
52.58	198.60	52.74	176°	22.46	-123.40	1700	110.68	12.72	35.6	42.2	42.8			
57.10	198.60	52.74	178°	22.50	-123.36	1730	110.50	12.86				31	37	38
61.36	198.60	52.74	180°	22.56	-123.30	1800	110.46	12.84	35.7	42.2	42.8			
65.27	198.60	52.74	177°	22.48	-123.38	1830	110.30	13.08				30	35	36
68.70	198.60	52.74	174°	22.41	-123.45	1900	110.29	13.16	35.8	42.3	43			
71.50	198.60	52.74	177°	22.48	-123.38	1930	110.25	13.13				31	36	36
73.52	198.60	52.74	176°	22.46	-123.40	2000	110.16	13.24	35.8	42.4	43			
74.65	198.60	52.74	176°	22.46	-123.40	2030	110.16	13.24				32	37	38
74.89	198.60	52.74	178°	22.50	-123.36	2100	110.16	13.20	35.8	42.4	43			
74.36	198.60	52.74	174°	22.41	-123.45	2130	110.10	13.35				29	38	36
70.48	198.60	52.74	177°	22.48	-123.38	2200	110.09	13.29	35.8	42.4	43.1			
68.46	198.60	52.74	179°	22.53	-123.33	2230	110.00	13.33				32	37	37
66.22	198.60	52.74	177°	22.48	-123.38	2300	110.17	13.21	35.8	42.4	43			
63.75	198.60	52.74	176°	22.46	-123.40	2330	110.25	13.15				31	37	37
61.04	198.60	52.74	173°	22.38	-123.48	2400	110.25	13.23	35.8	42.4	43			
58.06	198.60	52.74	176°	22.46	-123.40	0030	110.30	13.10				32	37	38
54.82	198.60	52.74	184°	22.65	-123.21	0100	110.35	12.86	35.7	42.2	42.8			
51.34	198.60	52.74	177°	22.48	-123.38	0130	110.50	12.88				32	37	38
47.66	198.60	52.74	179°	22.53	-123.33	0200	110.52	12.81	35.7	42.2	42.8			
43.80	198.60	52.74	179°	22.53	-123.33	0230	110.60	12.73				31	37	37
39.83	198.60	52.74	179°	22.53	-123.33	0300	110.83	12.50	35.5	42.1	42.7			
35.81	198.60	52.74	175°	22.43	-123.43	0330	111.00	12.43				31	37	37
31.80	198.00	52.74	175°	22.43	-123.43	0400	111.37	12.06	34.8	41.9	42.3			
27.87	198.60	52.74	178°	22.50	-123.36	0430	111.60	11.76				31	37	37
24.09	198.60	52.74	178°	22.50	-123.36	0500	112.04	11.32	34.3	41.4	41.8			
20.54	198.60	52.74	175°	22.43	-123.43	0530	112.30	11.13				30.6	27	27.8

Figure IV-19 shows the predicted best case and worst case satellite received power and the actual measured satellite received power reported by telemetry. From these curves, it is seen that the measured received power is within 1 db of the predicted worst case value. Considering the accuracy of the telemetry transducer, this is considered to provide good correlation between predicted and measured values. The measured curve at the higher received powers is due to the lack of dynamic range of the telemetry transducer. Telemetry data at the lower levels of transmitter power were not recorded.

System Noise Characteristics

Signal-Plus-Noise to Noise

As a result of the up and down link evaluations, the variations to be expected in received communications levels over a 24 hour period are well defined. The next step in completing the comparison

evaluation for link characteristics is to determine the degree of correlation existing between signal-plus-noise to noise measurements and predicted values.

During the 24 hour test of 6-7 February 1964, signal-plus-noise to noise measurements were taken at approximately hourly intervals. The result of these measurements taken at Lakehurst, Camp Roberts and the Kingsport for the three narrow baseband modes are shown in Figures IV-20, 21 and 22 a and b, respectively. The predicted values were obtained by first employing the predicted communications levels, Figures IV-6, IV-7 and IV-11 and measured system noise temperature values, Figures IV-32 and 33 to calculate a carrier to noise ratio (188 kc bandwidth) versus time. Then, the FM characteristic curves, Figures IV-23, 24 and 25, were used to determine the corresponding predicted signal-plus-noise to noise values. The FM characteristic curves represent the results of measurements made in the laboratory on the Lakehurst receiver during the design of the ground terminals. Predicted values were not calculated for the Kingsport because system noise temperature values were not available. The results of the predicted values for Lakehurst and Camp Roberts are shown in Figures IV-20 and 21.

An examination of the Lakehurst data, Figure IV-20, reveals that for all three modes the measured values were from 2 to 8 db below predicted levels. In an effort to explain this discrepancy, signal-plus-noise to noise measurements taken during the acceptance testing of the Lakehurst terminal were examined. This revealed that in a ground station loop test employing the power amplifier and transponder simulator, the signal-plus-noise to noise values, Figures IV-26, 27, and 28, leveled off at approximately 31 db for the narrow-narrow mode; 40 db for the wide-narrow with feedback mode, and 41 db for the wide-narrow mode. Further investigation of the same type measurements with the modulator-demodulator connected back-to-back (exclusive of power amplifier and transponder simulator) revealed that the signal-plus-noise did not exhibit a leveling-off effect, but in fact, followed the normal FM characteristics of Figures IV-23, 24, and 25. Therefore, it was concluded that an undesired noise modulation was present on the carrier and was either generated in the ground station exciter-power amplifier combination, or the spacecraft transponder. The difference in leveling off value between the narrow-narrow mode and the wide-narrow mode is due to the difference in deviation. The narrow-narrow mode employs a maximum of 4 kc deviation, while the wide-narrow mode deviates 40 kc. Therefore, the effects of the unwanted residual noise on the carrier would be less for the mode employing the larger deviation.

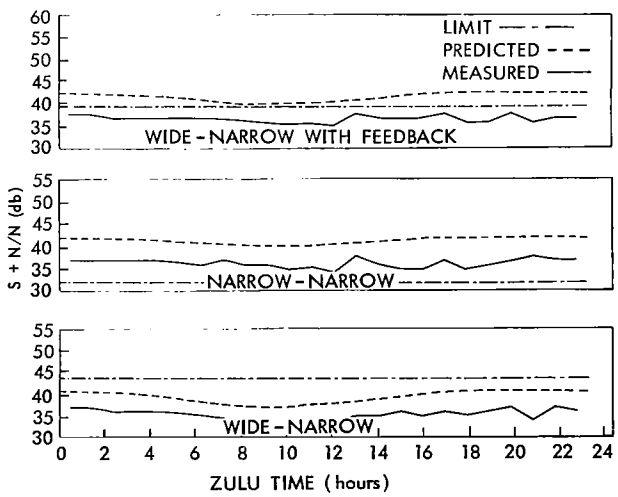

Figure IV-20—Syncom II communication experiment, Lakehurst.

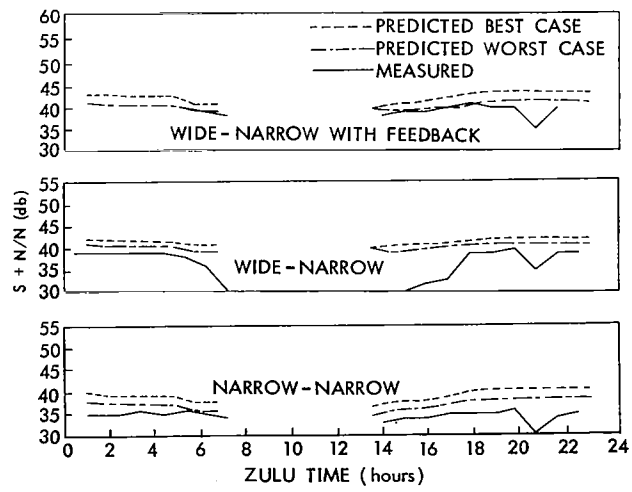

Figure IV-21—Syncom II communication experiment, Camp Roberts.

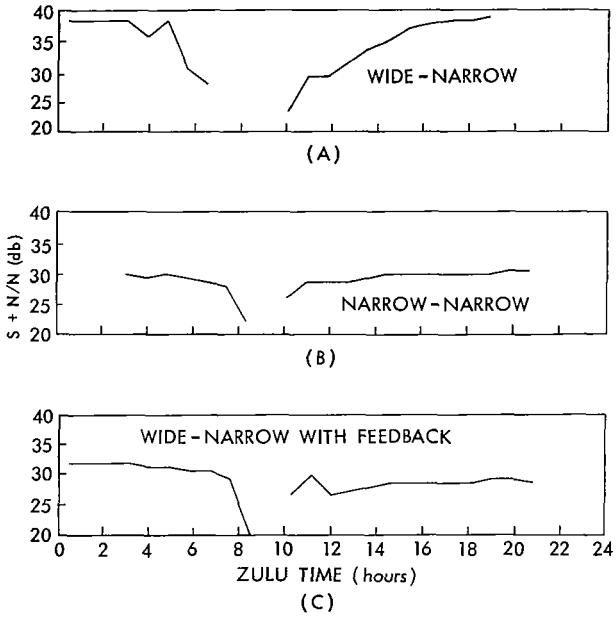

Figure IV-22—Syncom II communication experiment, Kingsport.

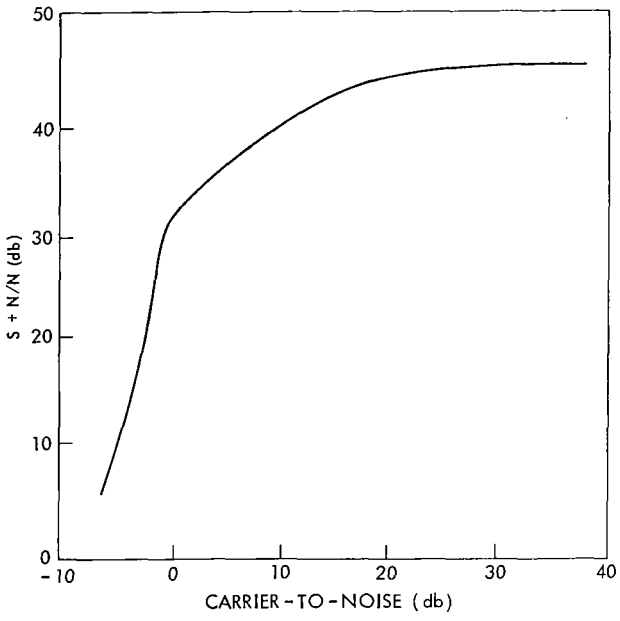

Figure IV-24—Syncom II communication experiment, FM characteristics wide-narrow, Lakehurst.

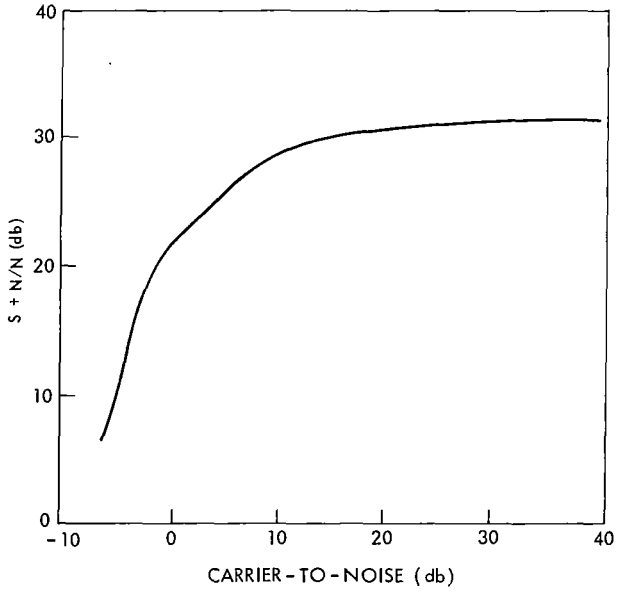

Figure IV-23—Syncom II communication experiment, characteristics narrow-narrow, Lakehurst.

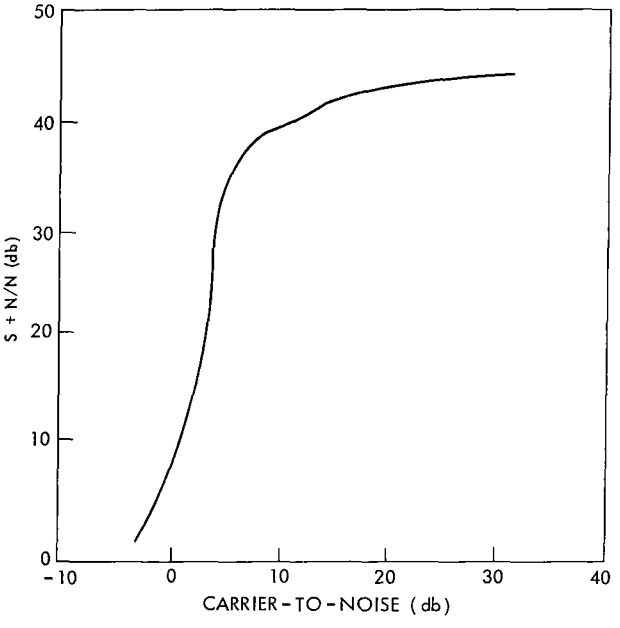

Figure IV-25—Syncom II communication experiment FM characteristics wide narrow with feedback, Lakehurst.

Based on the above, a third curve is added to each mode of Figure IV-20 representing the system limit value. A comparison of the measured and system limit values reveals a much improved correlation which is considered to be within the accuracy of measurement techniques. A similar analysis also applies to Camp Roberts station.

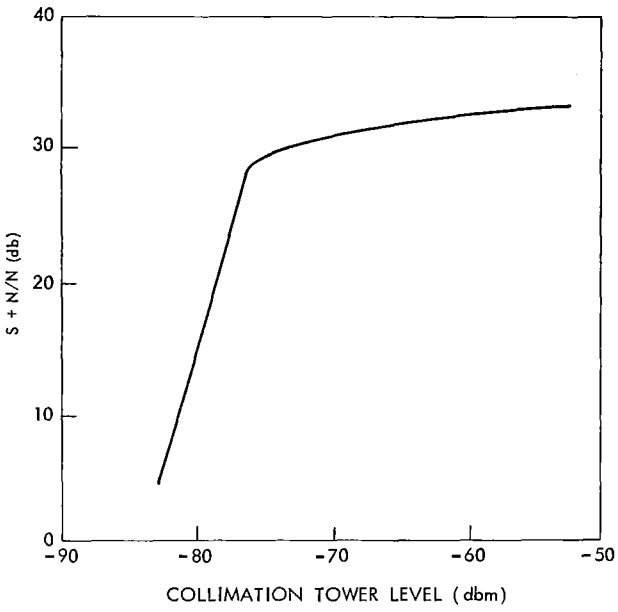

Figure IV-26—Syncom II communication experiment, narrow-narrow, Lakehurst

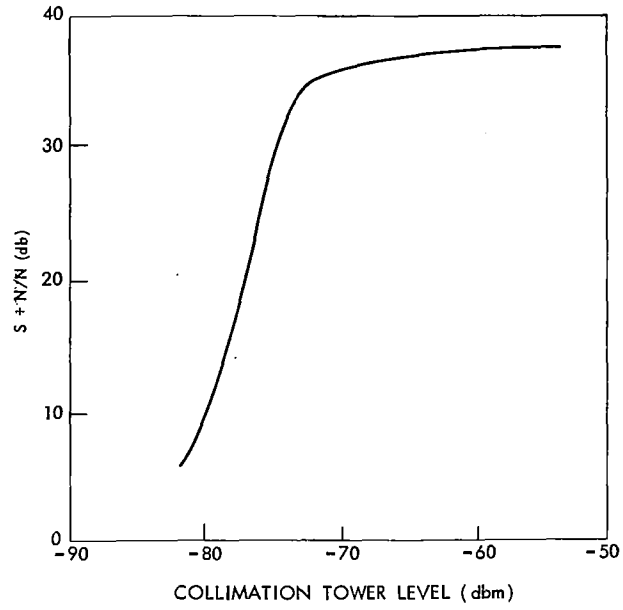

Figure IV-27—Syncom II communication experiment, wide-narrow, Lakehurst.

The leveling-off effect noted above is of importance in that it indicated that any improvement in the down-link power would be nullified from a signal-plus-noise to noise standpoint. In addition, it points out that in the design of future systems required to meet stringent signal-plus-noise to noise standards, the problem of residual noise modulation associated with the ground equipment and spacecraft must be overcome.

Signal-Plus-Noise to Noise Versus Communication Level

Some preliminary results of available signal-plus-noise to noise tests performed by the various stations were tabulated and plotted for the various modes of operation. No attempt was made to disregard extraneous points or to normalize the data. The raw data, as reported, were plotted and a curve fitted to the points using eyeball techniques. In an attempt to provide some degree of confidence in the resulting curves, they were compared with laboratory measurements.

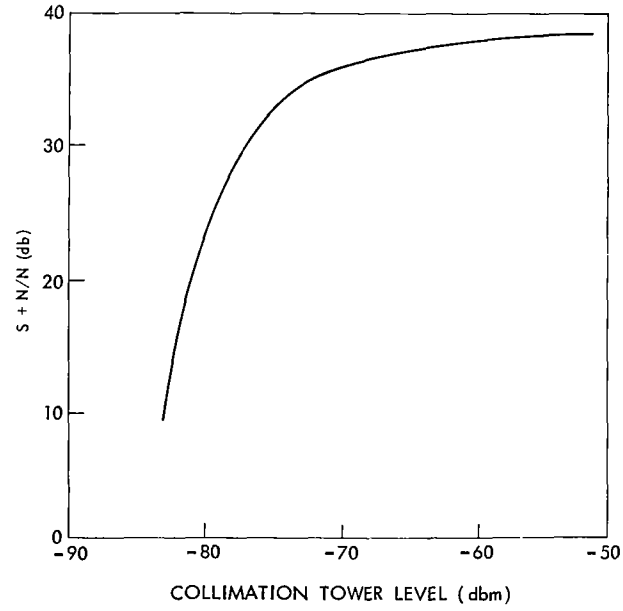

Figure IV-28—Syncom II communication experiment, wide-narrow with feedback, Lakehurst.

Figure IV-29 shows the results of the signal-plus-noise measurements taken at the Lakehurst station for the narrow-narrow and wide-narrow with feedback modes using a 1 kc tone. The plotted points are deliberately shown to indicate the spread associated with the data. Curve B represents

Table IV-11

Link Calculations, Carrier-to-Noise, Camp Roberts

ELEV ANGLE	K (dbm)	B	T_{sr}	$T_{sr(db)}$	N_p	TIME	C_p	C/N	PREDICTED S+N/N MODE			MEASURED S+N/N MODE		
									NN	WN	WNFB	NN	WN	WNFB
17.28	198.60	52.74	175°	22.43	-123.43	0600	112.65	10.78	33.8	41.2	41.5			
14.37	198.60	52.74	179°	22.53	-123.53	0630	112.80	10.53	33.5			30	36	37
11.9	198.60	52.74	187°	22.72	-123.14	0700	113.10	10.04	33	40.8	41			
9.91	198.60	52.74	195°	22.90	-122.96	0730	113.40	9.56	32.6			29.4	37	36.8
8.45	198.60	52.74	187°	22.72	-123.14	0800	113.65	9.49	32.6	40.7	40.5			
7.57	198.60	52.74	195°	22.09	-122.96	0830	113.70	9.26	32.4			29.2	36	36.4
7.30	198.60	52.74	196°	22.92	122.94	0900	113.96	8.98	32.1	40.4	40.1			
7.64	198.60	52.74	205°	23.12	-122.74	0930	114.00	8.74	32			29.4	36	36
8.6	198.60	52.74	196°	22.92	-122.94	1000	114.09	8.85	32	40.3	40			
10.16	198.60	52.74	186°	22.70	-123.16	1030	114.00	9.16	32.3			29.5	35	35.5
12.29	198.60	52.74	183°	22.62	-123.24	1100	113.97	9.27	32.4	40.6	40.4			
14.95	198.60	52.74	186°	22.70	-123.16	1130	113.80	9.36	32.4			28.8	35.4	35.8
18.10	198.60	52.74	191°	22.81	-123.05	1200	113.60	9.45	32.6	40.7	40.5			
21.68	198.60	52.74	184°	22.65	-123.21	1230	113.30	9.91	33			28.6	34.2	35.2
25.62	198.60	52.74	181°	22.58	-123.28	1300	113.07	10.21	33.2	41	41			
29.86	198.60	52.74	182°	22.60	-123.26	1330	112.80	10.46	33.4			30	38	38
34.34	198.60	52.74	183°	22.62	-123.24	1400	112.52	10.72	33.7	41.2	41.3			
38.98	198.60	52.74	178°	22.50	-123.36	1430	112.20	11.16	34.1			30	37	37
43.71	198.60	52.74	178°	22.50	-123.36	1500	111.95	11.41	34.4	41.6	42			

a curve fitted to the measured points shown in the graph. Curve A represents the average results of measurements made in the laboratory on two receivers during design of the ground station equipment. Correlation between measured and laboratory test data for both modes is considered excellent. Figure IV-30 shows a similar set of curves recorded aboard the USNS Kingsport and once again, a comparison of measured versus laboratory values provide good correlation.

Signal-plus-noise to noise measurements taken at Fort Dix for the wide-medium mode with feedback and the wide-wide mode are shown in Figure IV-31. In the wide-medium mode with feedback, measurements were plotted for 2 kc and 20 kc and in the wide-wide mode for 5 kc and 50 kc. The curves for these particular two modes are extremely important and revealing in that they clearly indicated that the Syncom system definitely possesses some 20 kc medium baseband capability, but does not possess any 50 kc wide band potential using the Syncom ground equipment.

System Noise Temperature

The system noise temperature versus time shown in Figures IV-32 and 33 was measured using the "Y" Factor method while the antenna was rotated in accordance with predicted look angles to simulate tracking of the satellite. (The satellite transponder was off during this time.)

To measure the system noise temperature (T_s) using this method, the receiver noise temperature (T_r) was measured. The "Y" Factor for receiver noise temperature measurement is the ratio of the noise measured in the IF amplifier with the noise generator off to the noise measure

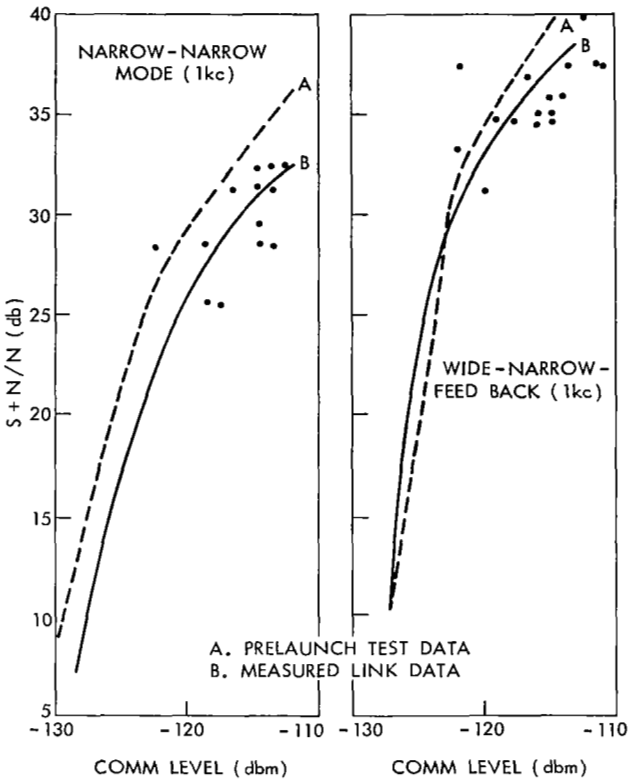

Figure IV-29—Syncom S+N/N vs. received comm level, Lakehurst.

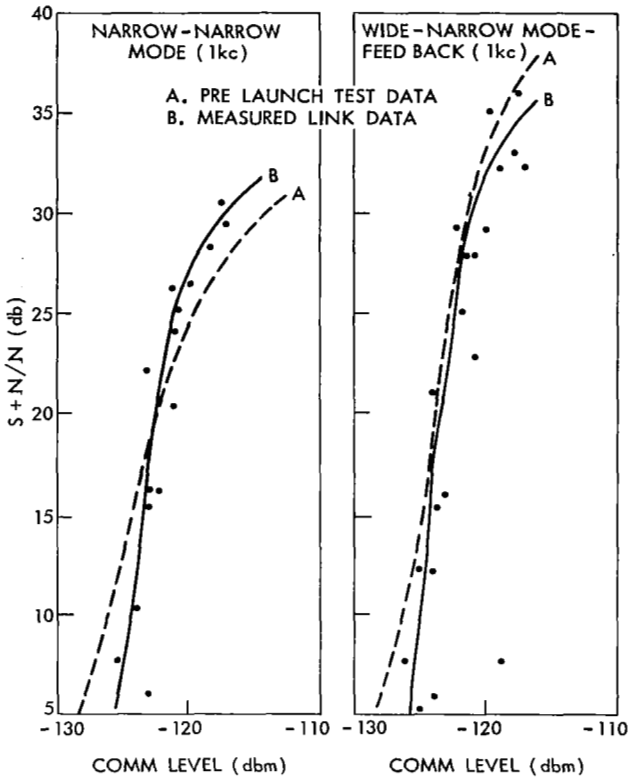

Figure IV-30—Syncom S+N/N vs. received comm level, USNS Kingsport.

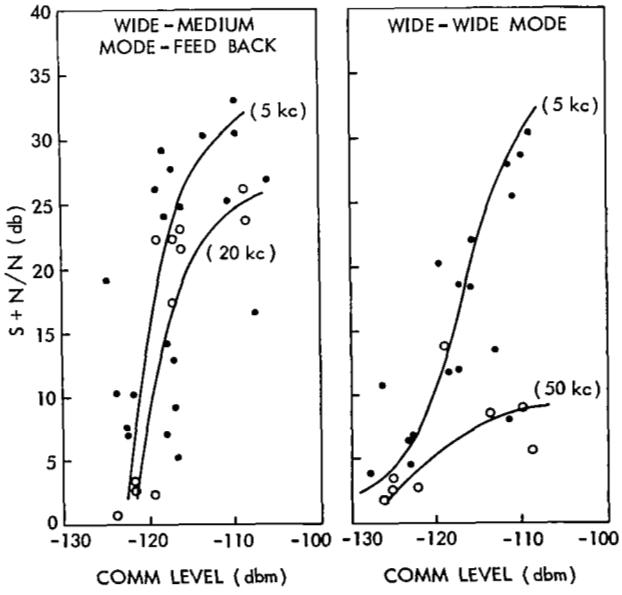

Figure IV-31—Syncom, Fort Dix.

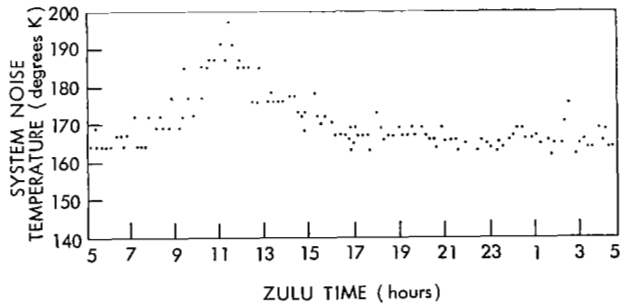

Figure IV-32—Syncom II communication experiment, Lakehurst.

in the IF amplifier with the noise generator on. The receiver noise figure is then determined from a graph of "Y" Factor versus noise figure. The receiver noise temperature is

$$T_r = (NF - 1)\ 290°K\ ,$$

where NF is the receiver noise figure expressed as a power ratio.

To obtain the system noise temperature, the input to the parametric amplifier was connected to a 50 ohm load and a reference in noise level was obtained. The input to the parametric amplifier was then connected to the antenna and the "Y" Factor was measured as the increase of noise in the IF amplifier. The effective noise temperature of the antenna and feed combination (T_e) is

$$T_e = \frac{T_0 + T_r (1 - Y_{pr})}{Y_{pr}},$$

where

$T_0 = 290°K$
T_r = Receiver Noise Temperature
Y_{pr} = "Y" Factor expressed as a power ratio.

The antenna noise temperature was calculated from the equation

$$T_a = L_{1_{pr}} \times T_e - T_0 \left(L_{1_{pr}} - 1\right),$$

where $L_{1_{pr}}$ is the feed line loss expressed as a power ratio.

The system noise temperature was calculated from the equation

$$T_s = T_s + \left(L_{1_{pr}} - 1\right) T_0 + L_{1_{pr}} T_r .$$

The curves in Figure IV-33 also show how the system noise temperature (T_s) varies with antenna elevation angle. It should be noted that the antenna azimuth was also varying during this time since the antenna rotation was simulating satellite track. The peak in system noise temperature at 1840 hours Zulu time is due to the antenna beam pointing into the sun.

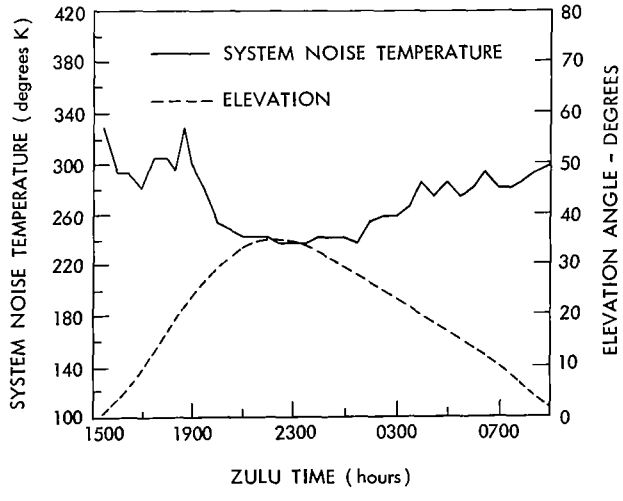

Figure IV-33—Syncom II communication experiment system noise temperature, system noise temperature and elevation angle vs. time, Camp Roberts Station.

Amplitude Response

The amplitude response of the Syncom system was obtained by using an Acton Transmission & Delay Measuring Set at the Fort Dix Terminal. Two swept frequency ranges were employed; 400 to 6000 cycles and 500 to 12000 cycles. The small sweep range permitted a better evaluation of the low frequency response of the different modes. Tests were conducted with the Modulator-Demodulator connected back-to-back, Figure IV-34 and through the spacecraft, Figure IV-35. The Mod-Demod Tests were performed with an equivalent received communications level of -112 dbm and the input to the modulator was held constant at a 0 dbm level. For the spacecraft link the

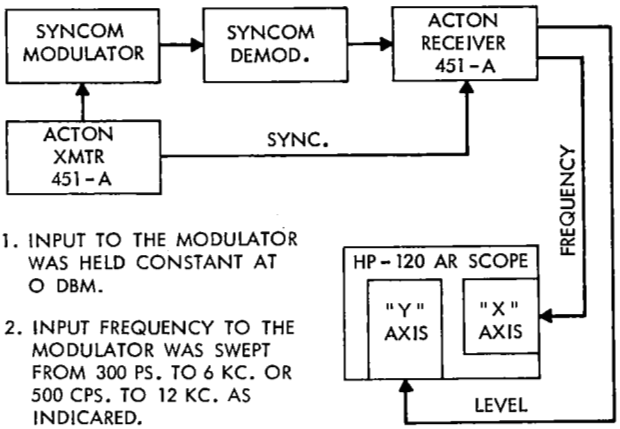

Figure IV-34—Modulator-Demodulator back to back.

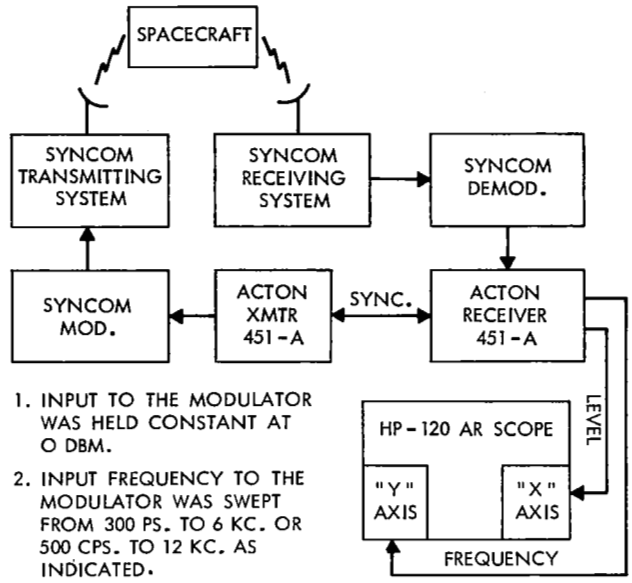

Figure IV-35—System test loop using spacecraft.

power output was 1.25 kw corresponding to a Received Communications Level of -116 dbm. The input to the modulator was zero dbm.

Figures IV-36 thru IV-41 show the comparative results, in the form of oscilloscope pictures, of the back-to-back vs spacecraft test for all seven modes. The frequency was swept from 400 to 6000 cycles. Figure IV-40 shows the results of spacecraft test for modes 4, 5, 6 and 7 with the swept range increased to 12 kc. An evaluation of Figures IV-36 thru IV-39 indicates that the ground terminal equipment essentially establishes the frequency response for all seven modes. In addition, all seven modes suffer from poor low frequency response (below 1 kc) which, as described later in this report, has detrimental effect on multichannel communications. The poor low frequency response is attributed to the video shaper preceding the phase modulator. Figure IV-41 shows response curves for modes 2 and 6 with the video shaper by-passed. It will be noted that not only is the low frequency response greatly improved but the overall response is also improved. The results of these tests indicate that all multichannel communication should be accomplished with the video shaper by-passed. Current and future tests are being performed in this manner.

Spacecraft Antenna Pattern

Before reorientation of the satellite, the satellite antenna lay in the plane of the orbit which resulted in the earth being illuminated twice a day for a period of approximately two hours on each pass. This afforded the opportunity to confirm the spacecraft transmitting antenna pattern through measurement of received signal strength at the surface terminal; in this case, the USNS Kingsport, located in Lagos Harbor, Nigeria. By computing the satellite antenna aspect angle (the angle between the satellite spin axis and the line of sight from the surface terminal to the spacecraft) for the time period of measurement, data were obtained to allow a plot of relative signal strength received versus aspect angle. This was plotted together with the averaged spacecraft antenna pattern based on pre-launch antenna measurements; the averaging of antenna pattern cuts in planes perpendicular to the antenna axis is required due to the spacecraft spin. (Figures IV-42 to IV-46). It will be noted that the patterns are similar in shape; the irregularities in the averaged pattern, particularly the flattening at the peak are probably due to ground or other interference effects during the measurements. Of particular interest is the displacement between the two patterns, indicating a slight error in the satellite orientation parameters. The five patterns measured indicate, in time sequence,

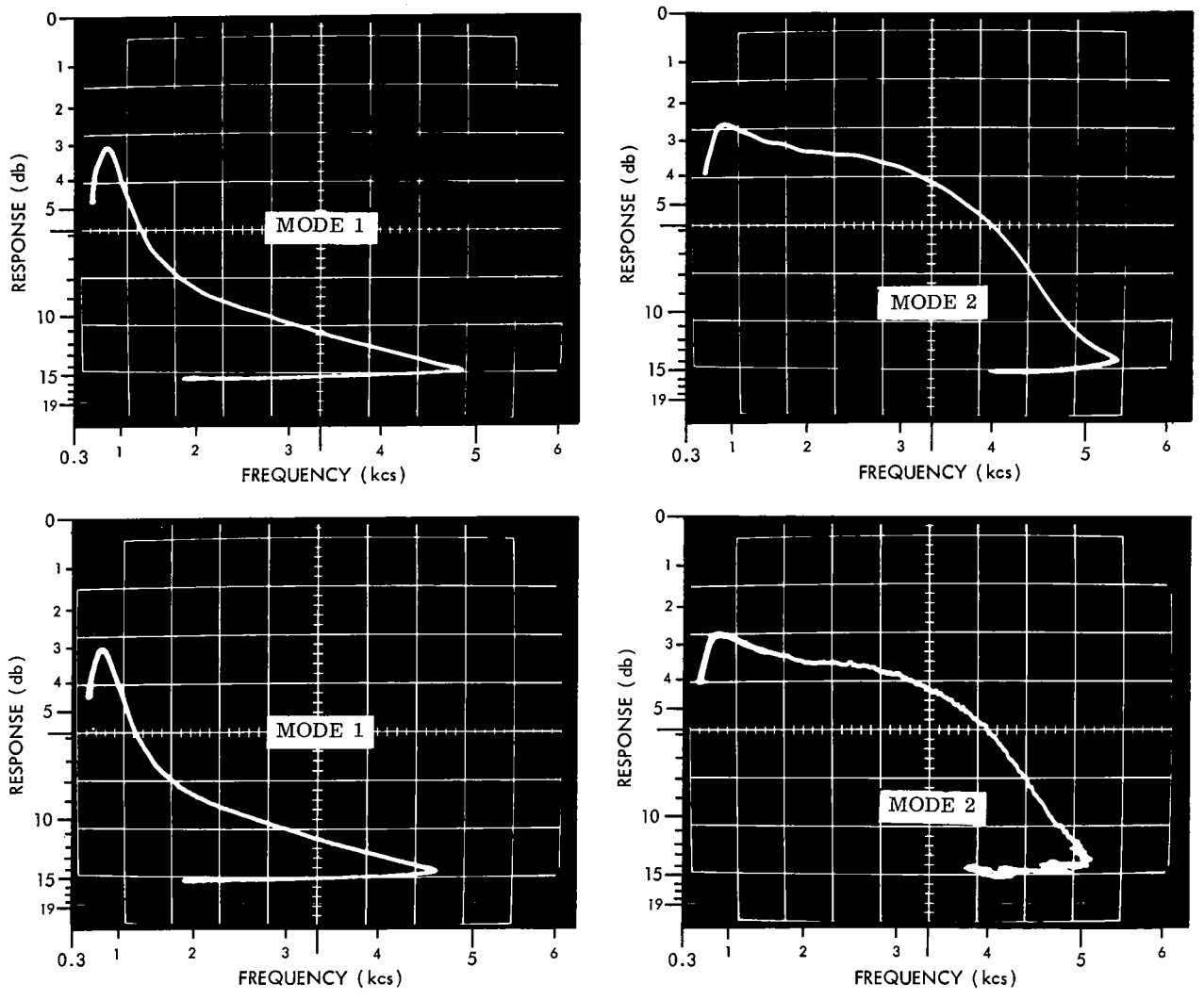

Figure IV-36—Amplitude response of spacecraft communications system voice channel - modes 1 and 2.

almost perfect coincidence at first and then a consistent displacement averaging approximately 1.5 degrees. This figure agrees quite well with post-orientation measurements.

DEMONSTRATIONS AND SPECIAL TESTS

Summary of Demonstrations

In the 1300 plus hours of cumulative communications and range and range rate transmission through the satellite (as of 31 January 1964), well over 1000 special tests and demonstrations have taken place. A detailed breakdown of these tests is outside the scope of this report. The demonstrations have included voice, teletype, facsimile, data, and ranging transmissions.

The capability of the satellite communications terminals to provide a single high quality voice frequency channel through Syncom II has been demonstrated to more than a thousand government

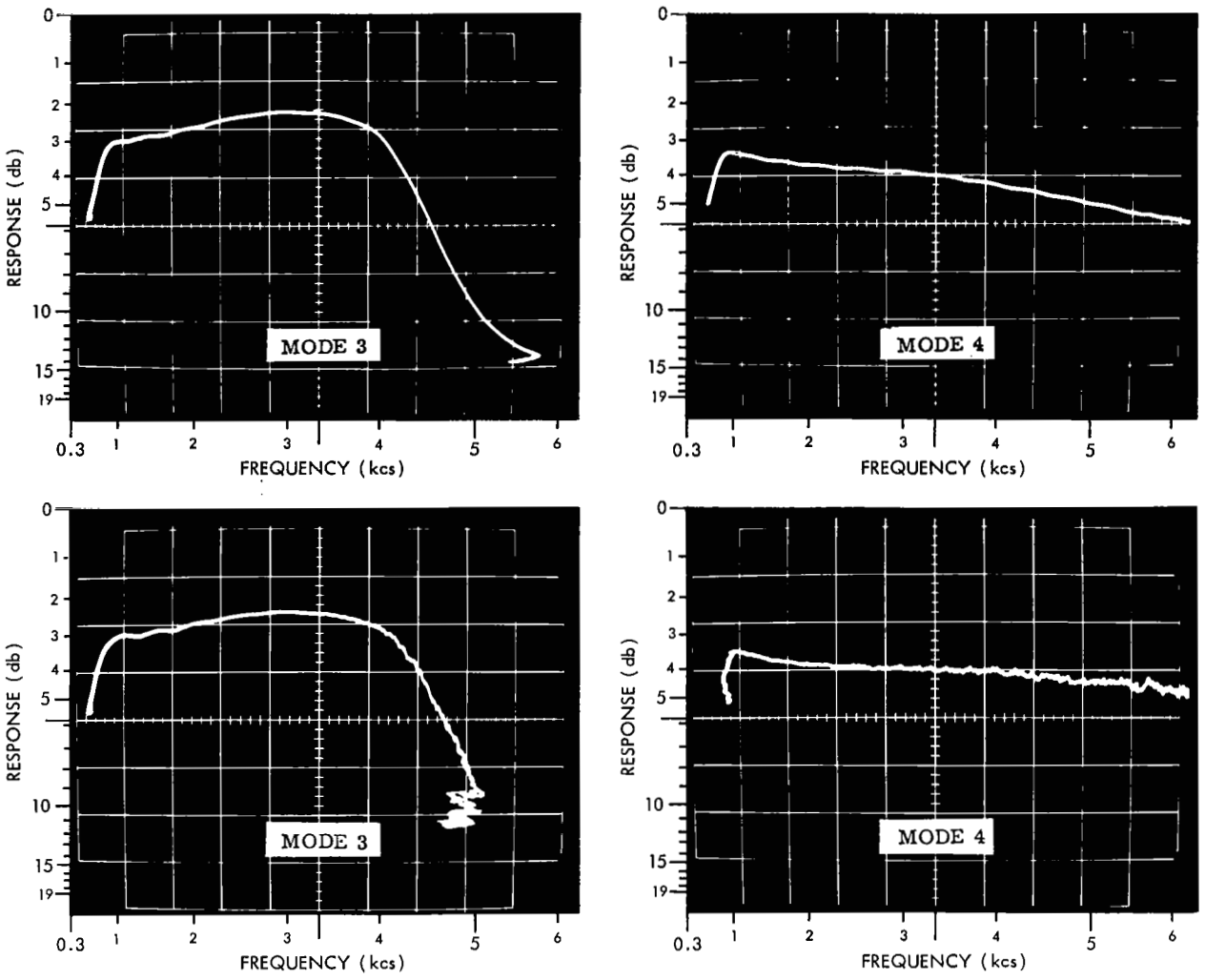

Figure IV-37—Amplitude response of spacecraft communications system voice channel - modes 3 and 4.

and private industry observers and to the delegates of 70 nations attending the Extraordinary Administrative Radio Conference of the International Telecommunications Union. The shipborne terminal and the two transportable terminals designed specifically for Syncom have successfully played a support role as satellite tracking stations in producing range and range rate data. The ship has demonstrated the capability for simultaneously transmitting in a communications mode and in a tracking mode for range and Doppler data acquisition. The three terminals have demonstrated the capability of rapidly converting from the ranging mode to the communications mode.

The Fort Dix, Camp Roberts, and Kingsport earth stations have confirmed what was already established in the TELSTAR 1 tests; that transmission below elevation angles of 7.5 degrees yields degraded results and that operation above 7.5 degrees is free from the selective fading effects characteristic of overland microwave systems.

Syncom's 5 mc bandwidth capability coupled with earth stations with large enough antennas suggested that television was possible. Television was successfully transmitted from Fort Dix to the Bell Laboratories experimental station at Andover.

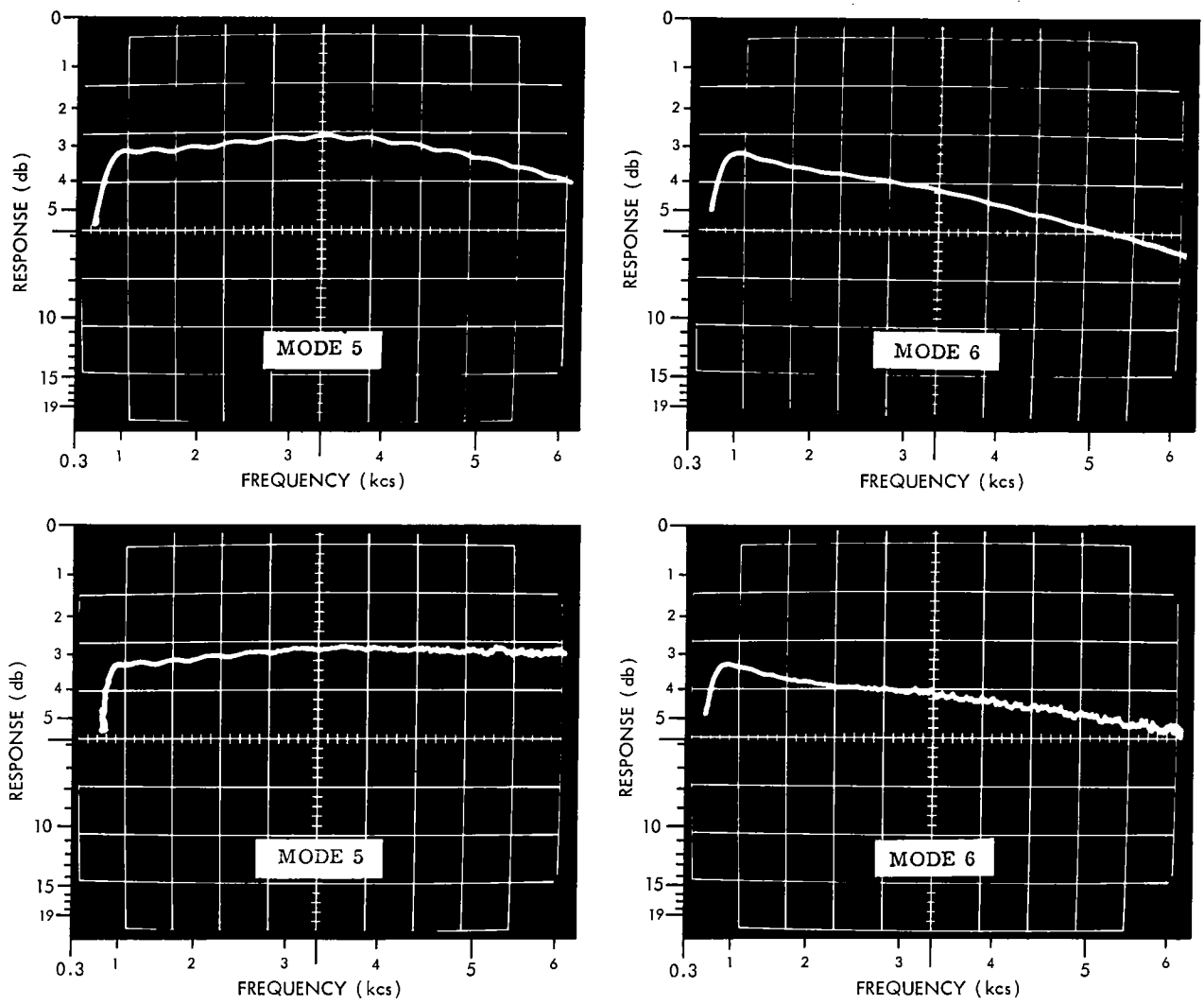

Figure IV-38—Amplitude response of spacecraft communications system voice channel - modes 5 and 6.

Under optimum signal levels, transmission of four voice frequency channels was successfully done, pinpointing an area in which more intensive testing and demonstrations are planned and underway.

Vocoder operation has been successfully conducted through the satellite. The path length delay did not present a problem for vocoder operation.

Multiple access tests have been conducted through Syncom II successfully, using the spread spectrum technique. During these tests, Lakehurst and the Kingsport transmitted to each other on assigned channels, while Camp Roberts was talking to itself on a loop basis. The Kingsport operated successfully at powers lower than 100 watts in making range and range rate measurement, demonstrating that a highly transportable terminal can be built and operate with parabolic antennas 15 feet in diameter.

The real-time transmission of telemetry data through the satellite was demonstrated, and since the telemetry and command station was colocated with the link terminal, the feasibility of a station

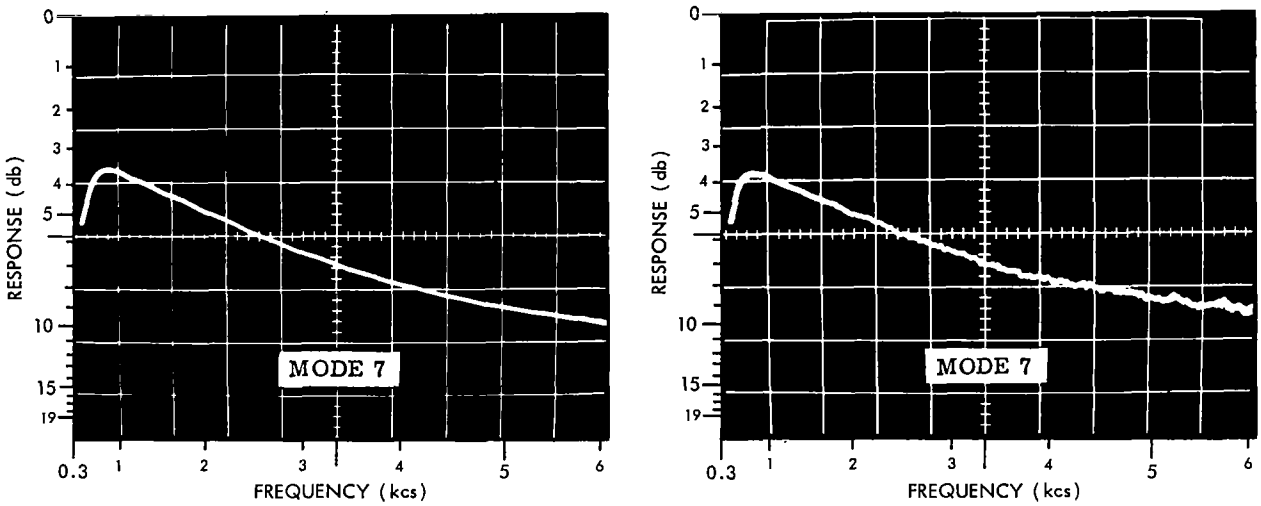

Figure IV-39—Amplitude response of spacecraft communications system voice channel - mode 7.

capable of simultaneous tracking, telemetry reception, and real-time data transmission through a synchronous satellite has also been demonstrated. The slow angular rates and continuous visibility of the satellite make this type of operation possible. This is discussed in detail in the section describing transmission of real time data.

Voice

The first public demonstration of telephone calling over the Syncom link took place on 23 August 1963, when the late President John F. Kennedy spoke from the White House to the Prime Minister of Nigeria. This conversation was the opening feature of a program sponsored by the Voice of America. It was followed by a conversation between Vice-President Lyndon Johnson in the Voice of America studios in Washington, D. C. and the President of the Nigerian Senate. This in turn was followed by other conversations between the United States and Nigerian officials. Immediately following the telephone conversations, an exchange of facsimile pictures was made in which photos of President Kennedy and the Nigerian Prime Minister were exchanged.

On September 20 two significant demonstrations took place:

In one, the world's first telephone call was made through two satellites. The two tandem satellite links started with the ship in Lagos through Syncom to Lakehurst, over Bell System land line to Nutley, New Jersey, thence through Relay I to Brazil. The quality of the voice signals was excellent.

In the other demonstration, President Kennedy's address to the United Nations was beamed through Syncom to a regular broadcast station in Africa and then broadcast over the African Continent.

Television

Television from 22,222 miles out in space was demonstrated as being feasible on 25 September 1963, when the SATCOM terminal at Fort Dix, N. J. picked up channel 3, Philadelphia, on a home receiver and transmitted it through Syncom to the Bell Laboratories experimental earth station at Andover, Maine. The picture was described by Bell Laboratories engineers as being of "motel quality". For this test, which was a special engineering test, a modulator fabricated for use in the Relay satellite program was installed at Fort Dix and wired around the modem usually employed

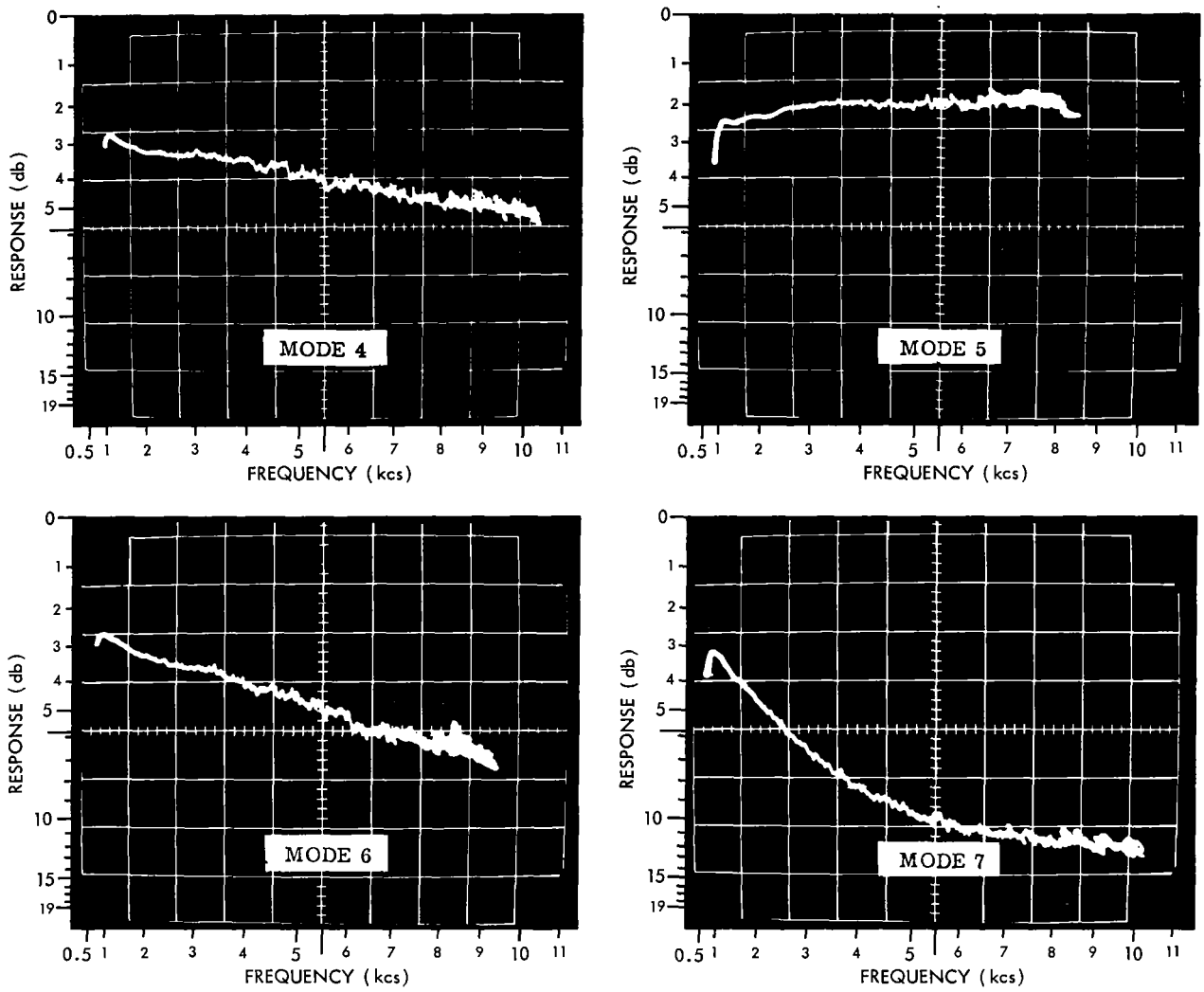

Figure IV-40—Amplitude response of spacecraft communications system voice channel - modes 4, 5, 6, and 7, employing a 12 kc sweep range.

for Syncom. At Andover, the Bell Telephone Laboratories installed a traveling wave maser amplifier specifically designed for operation at the Syncom frequencies.

Aircraft to Ship Via Syncom

In September, after the Kingsport had departed Nigeria, a telephone call was made from a U. S. Navy aircraft over Norfolk, Virginia, using single-side band RF radio through the Navy Communications Station in Washington, D. C. to the Lakehurst terminal to the Kingsport on the high seas. Results were excellent.

Transmittal of Oceanography Data

In a demonstration the oceanographic ship, Geronimo, teletyped temperature and salinity measurements via single side band radio link to the Kingsport. Then it was relayed through Syncom to Lakehurst and thence to a computer center in Washington, D. C. which determined that a gross

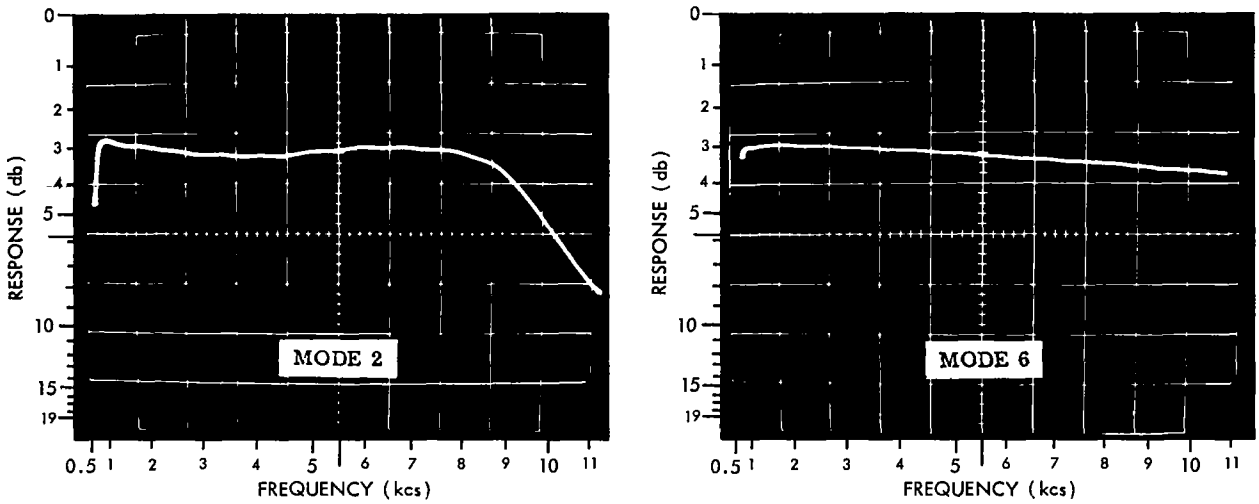

Figure IV-41—Amplitude response of spacecraft communications system voice channel - modes 2 and 6, with the video channel bypassed.

error in the measurements existed, notified the Geronimo via Syncom, enabling the oceanographers to detect and repair an equipment defect.

Washington Hotel Demonstration

During a three day period in late October 1963, two booths were set up in a Washington Hotel, each tied by customer type two-wire lines to a link terminal. The booths were open to the public. More than two hundred persons spoke to each other through Syncom using subscriber telephones and passing through the Bell System Switchboards. Echo suppressors were in operation at each of the two terminals. No echo effects were experienced by any of the talkers.

Demonstration to International Telecommunications Union

In late October 1963, the Kingsport entered a harbor in Spain, tied up to the dock and into a telephone circuit passing through Spain, across France, and into a telephone in the Batiment Electoral in Geneva, Switzerland, where the Extraordinary Administrative Radio Conference of the International Telecommunications Union was held. Meanwhile, in the United States, telephone lines in the Bell System were connected from the U. N. in New York and Headquarters, National Aeronautics and Space Agency to a switchboard at the Goddard Space Flight Center; thence to the link terminal at Lakehurst. For the following 11 days from nine to midnight, Geneva time, delegates to the conference from 70 nations were afforded the opportunity to test voice communications through a synchronous satellite, by talking to their counterparts in Washington and in the U. N. via Syncom. Washington-Geneva Press Conference on 8 November was the vehicle for announcing the decisions reached on the allocation of frequencies for space communications in the coming decade.

24-Hour Autotrack Test

In early September, the Fort Dix terminal locked on Syncom and tracked it for a solid 24 hours. During this period the elevation angles varied from 7 degrees minimum to 70 degrees maximum.

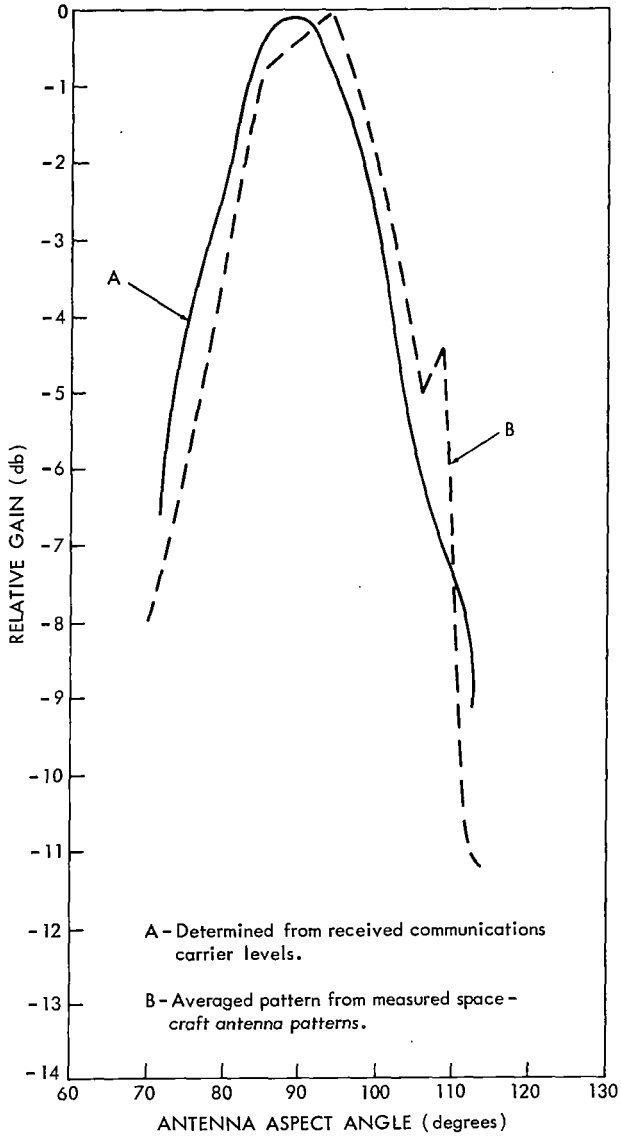

Figure IV-42—Syncom communication experiment, spacecraft antenna pattern, data from measurements made on 28 Jul 63.

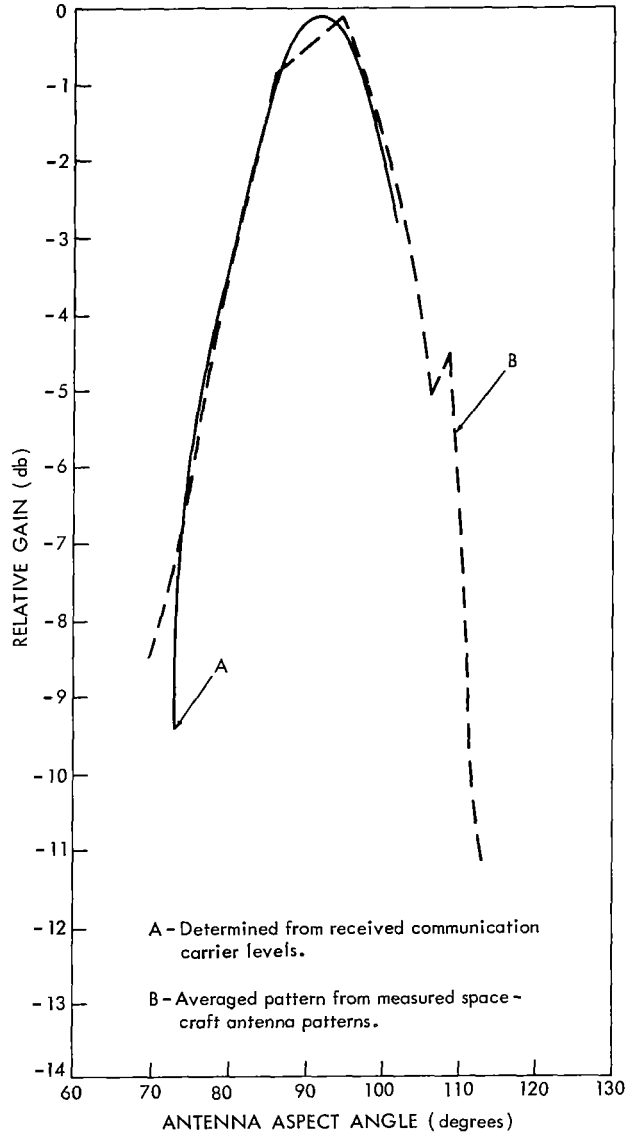

Figure IV-43—Syncom communication experiment, spacecraft antenna pattern, data from measurements made 27 Jul 63.

28-Hour Communications Test at Sea

Ship operations at sea were terminated with a 28-hour continuous communications test. For its return journey the ship was routed so that it would pass directly under the satellite. This routing did result in one zenith pass at sea. During this pass the triaxial antenna maintained solid lock, even though the ship at sea was heaving and rolling. A similar pass also occurred over Lagos on 3 August 1963. The routing put the ship at the northern tip of the "figure 8," so that the 28-hour test was done with the ship north of the figure eight. A most interesting fact related to this test was the large variation in signal strengths at the ship, particularly in those at the extremities of the figure 8. A 6 db reduction with respect to the northernmost point was observed when Syncom was lowest in the southern hemisphere. This is to be expected when one considers

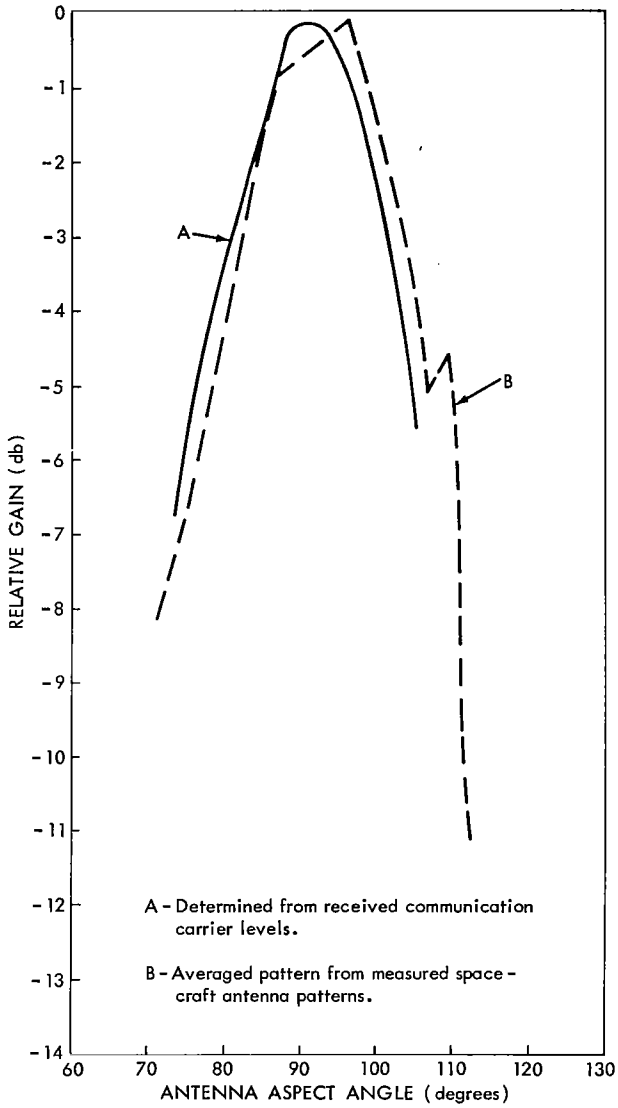

Figure IV-44—Syncom communication experiment, spacecraft antenna pattern, data from measurements made on 29 Jul 63.

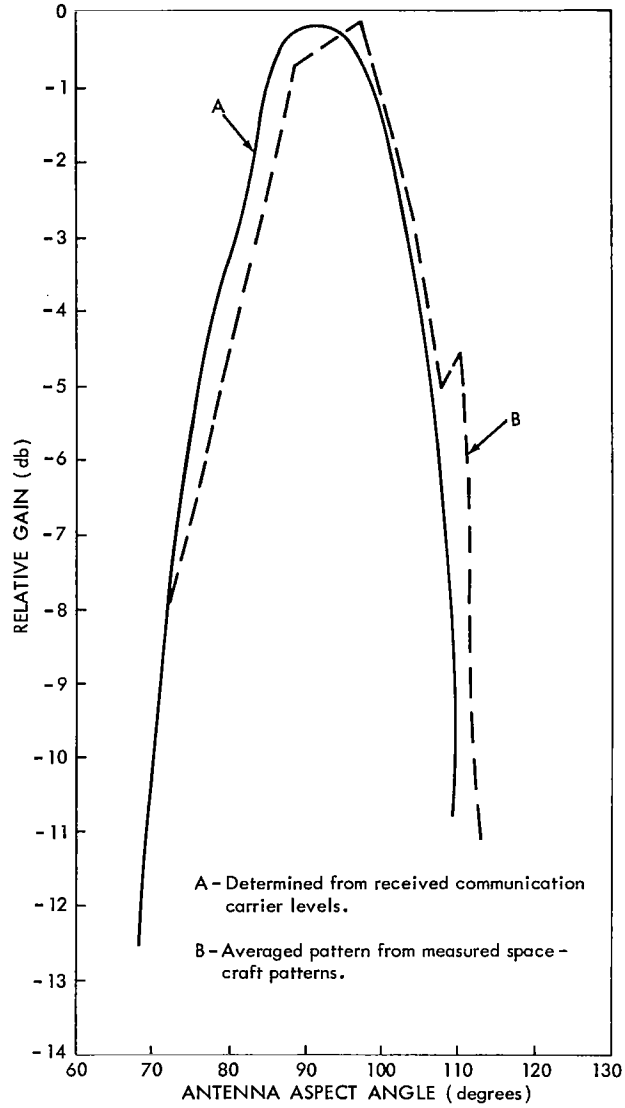

Figure IV-45—Syncom communication experiment, spacecraft antenna pattern, data from measurements made on 29 Jul 63.

the total change in antenna angle as Syncom goes from the high point to the low point in its inclined orbit.

Transmission of Real-Time Telemetry Data

On 21 October 1963, real time telemetry data was transmitted from Syncom II to the USNS Kingsport underway in the Mediterranean Sea and then relayed to Hughes Aircraft Company in Culver City, California, via the Lakehurst telemetry and command station. The test demonstrated the feasibility of relaying telemetry data via the spacecraft and land telephone line.

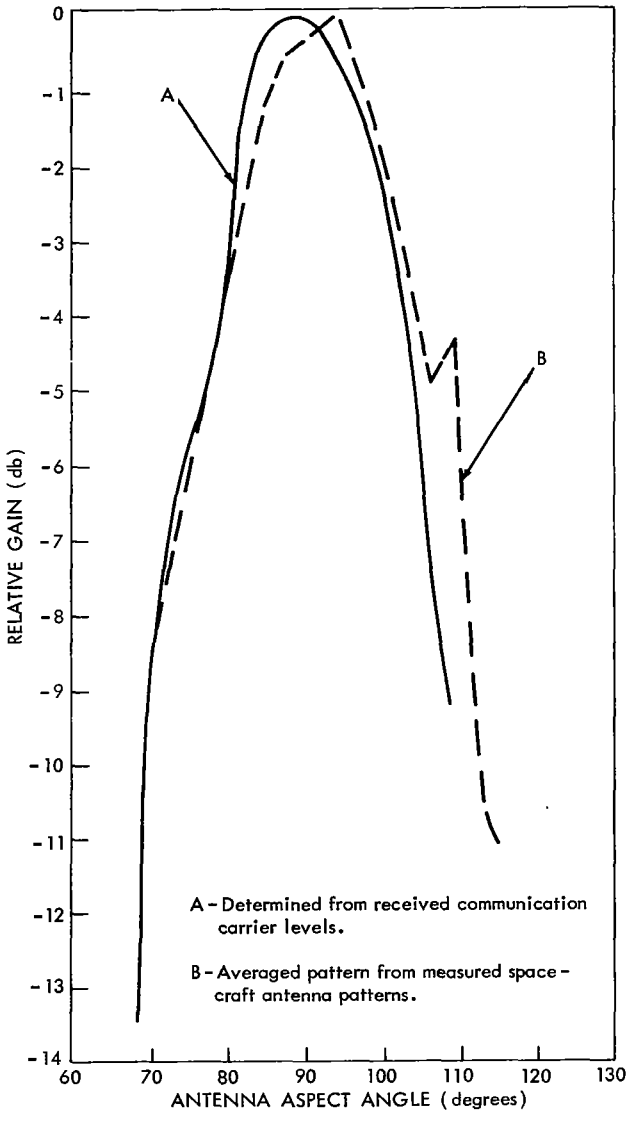

Figure IV-46—Syncom communication experiment, spacecraft antenna pattern, data from measurements made on 28 Jul 63.

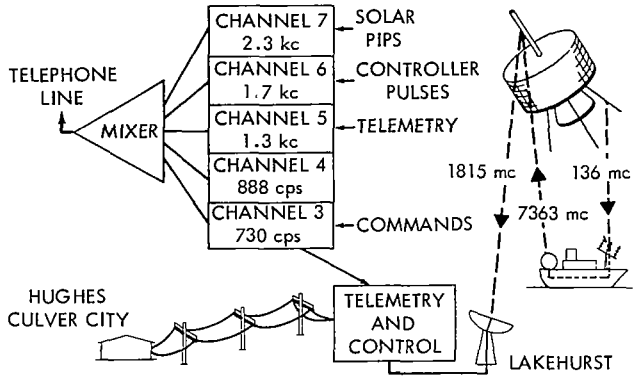

Figure IV-47—Real-time telemetry experiment.

The operation is shown schematically in Figure IV-47. The telemetry signal received at the ship, consisting of a 14.5 kc frequency-modulated subcarrier, was patched into the communications transmitter and relayed over the wide-medium (WM) modem communications link back to the spacecraft at 7363 mc. The 1815 mc signal from the spacecraft was received at the communications receiving terminal at Lakehurst, New Jersey and demodulated down to the 14.5 kc subcarrier. The subcarrier was patched into the telemetry and command trailer at Lakehurst and demodulated down to the original commutated level consisting of a pulse train of four channels per second. This low frequency telemetry data next frequency-modulated a 1.3 kc subcarrier oscillator (IRIG channel 5). A total of five subcarrier oscillators was used in the experiment, as shown in Figure IV-47. The solar pip signals were those received directly from the spacecraft by the Lakehurst telemetry and command station. The controller pulses and command signals were synthesized at the station.

A block diagram of the system is shown in Figure IV-48. Tape recordings and strip chart recordings of the telemetry data were made on the ship, at Lakehurst, and at Culver City. All tapes and strip charts were sent to Hughes for analysis after the test was completed. The ship receiver was in the wide-medium FM feedback (WM/FMFB) modem. In this modem, the baseband is 20 kc, and the peak carrier deviation is 50 kc. It is evident that the 20 kc baseband was required to pass the 14.5 kc subcarrier.

A standard leased telephone line designated FDA-7268-274 was installed by American Telephone and Telegraph Co. between Lakehurst, New Jersey and Culver City, California. No specific requirements were imposed on the telephone company to keep the rate at a minimum. The designation FDA (Full period data) implies a data line, but it was not specially conditioned for data service. The line was in service between 20 September and 22 October 1963 (32 days) and was equipped with a manual transfer key at each end of the line to switch between the talk and data

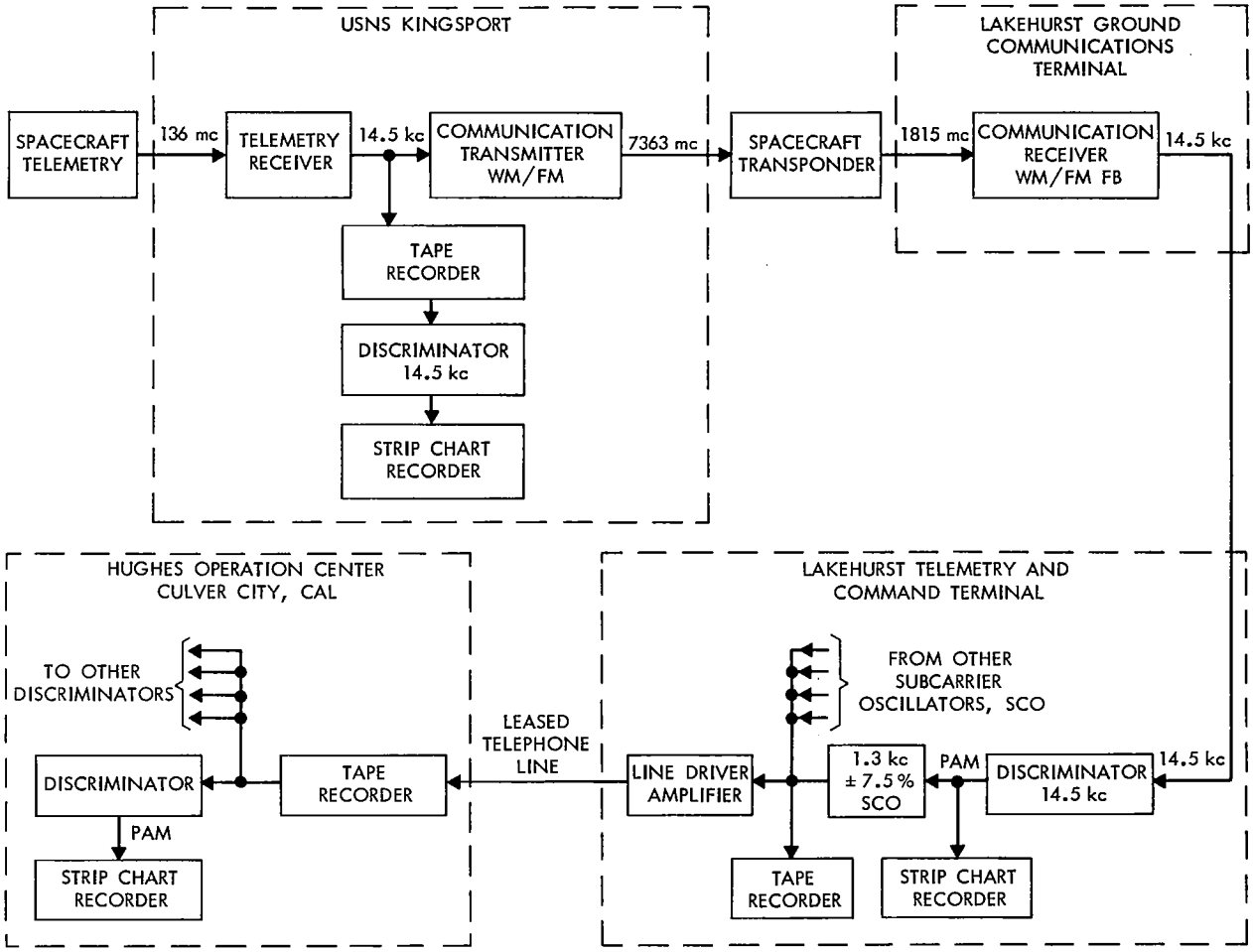

Figure IV-48—Overall system block diagram.

mode of operation. Electrical characteristics of the line were measured on 24 September and 20 October. All measured parameters were the same except frequency response beyond the upper and lower 15 db points, which was due to inconsistent signal generator sending levels. The measured frequency response of the line is shown in Figure IV-49. Other line characteristics were as follows:

Noise level at Culver City	-36 dbm
Bandwidth at 3 db points	200 to 2825 cps
Net loss at 1 kc	5.5 db

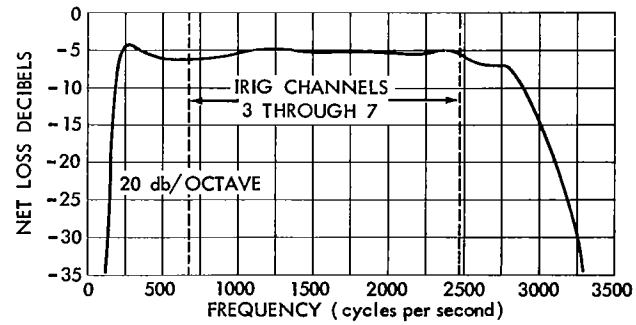

Figure IV-49—Telephone line frequency response.

(S+N)/N with -8 dbm send level in above bandwidth	28 db at Culver City at 1 kc
Send line impedance	1000 ohms
Receive line impedance	1000 ohms
Frequency translation	Lakehurst to Culver City: -0.3 cps

Other characteristics such as regulation (day to day net loss variations), absolute delay, and envelope delay were not pertinent to the demonstration, and were not measured. The combined sending level of the five subcarrier oscillator (SCO) tones was set at -8 dbm by adjusting each SCO output level to -15 dbm. A graph of "Combined Level" versus "Per Tone Level" for five and seven channel systems is given in Figure IV-50. This graph was based on coincident peaks of the five channels not exceeding the ordinate values more than 1 percent of the time.

Figure IV-51 shows the strip chart results of the real time telemetry demonstration. These strip charts are typical samples covering the same period of time. The Kingsport and Lakehurst charts were made from the 14.5 kc discriminators at these locations. The Culver City chart is the output of a 1.3 kc discriminator that was driven from a tape recorder. The ripple on the Culver City data is probably due to wow and flutter components added to the 1.3 kc signal by the Culver City recorder, contributing less than 0.5 percent error. Data values of eleven channels of the first data frame following 0544Z on the 294th day were read on the Telecomputing Corporation "Telereader". The amplitudes, percent of full scale and differences relative to the Kingsport values are shown in Table IV-12. The maximum difference in the values between Kingsport and Lakehurst is 0.7 percent, and between Kingsport and Culver City is 1 percent. The rms difference in percent for Lakehurst is 0.35 and for Culver City is 0.47. The comparison shows a high degree of accuracy for the transmission of analog data between widely separated locations on the earth. The fact that one station was mobile (on the high seas) is particularly significant to future applications of this data transmission system.

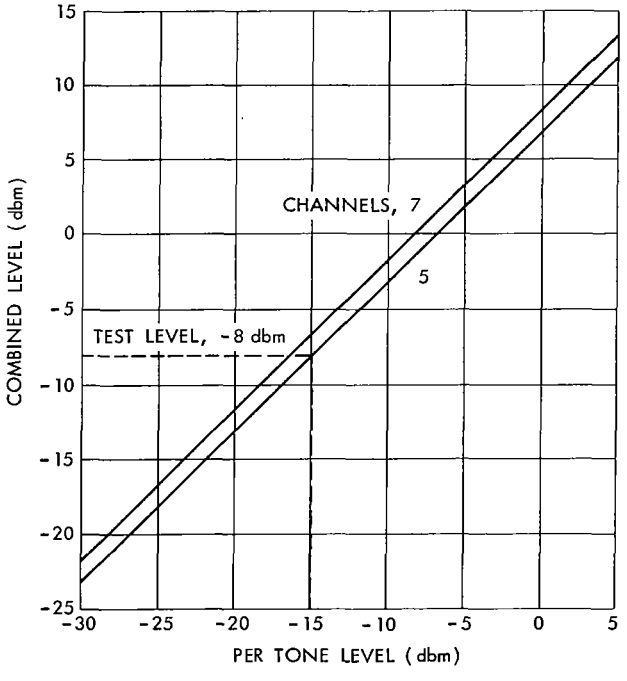

Figure IV-50—Combined output levels for 7 and 5 channels.

Concurrent with the transmission of telemetry data over the 1.3 kc (channel 5) SCO, Lakehurst added four SCO's to transmit locally generated commands on 730 cps (channel 3), a reference frequency of 888 cps (channel 4), controller pulses on 1.7 kc (channel 6) and solar pips on 2.3 kc (channel 7). All channels were

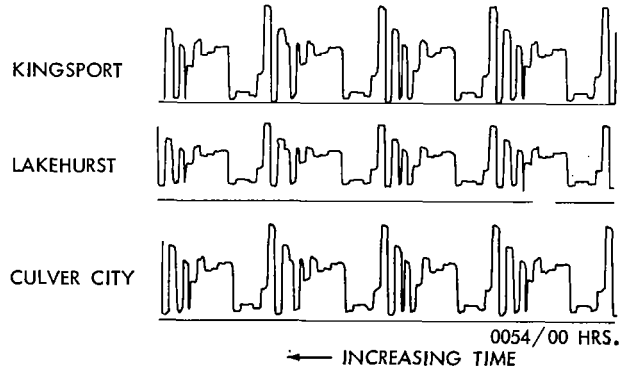

Figure IV-51—Telemetry strip charts.

Table IV-12
Comparison of Data Values

KINGSPORT		LAKEHURST			CULVER CITY		
AMPLITUDE, (cps)	PERCENT OF FULL-SCALE	AMPLITUDE, (cps)	PERCENT OF FULL-SCALE	DIFFERENCE IN PERCENT	AMPLITUDE, (cps)	PERCENT OF FULL-SCALE	DIFFERENCE IN PERCENT
0	0	0	0	0.0	0	0	0.0
1327	100.0	844	100.0	0.0	1216	100.0	0.0
376	28.3	236	28.0	-0.3	336	27.6	-0.5
89	6.7	51	6.0	-0.7	70	5.7	-1.0
145	10.9	90	10.7	-0.2	129	10.6	-0.3
145	10.9	90	10.7	-0.2	129		
54	4.1	32	3.8	-0.3	41	3.4	-0.7
763	57.5	488	57.8	+0.3	700	57.6	+0.1
754	56.8	482	57.1	+0.3	689	56.7	-0.1
683	51.5	433	51.3	-0.2	622	1.2	-0.3
652	49.1	413	48.9	-0.2	597	49.1	0.0

mixed in an amplifier and electrically coupled into the leased telephone line. Figure IV-52 shows typical portions of commands on track 1, reference voltage on track 2, telemetry on track 3, controller pulses on track 4 and psi pulses on track 5. The controller pulses and psi pulses are very distinct. The reference and command channels were disturbed by noise from undetermined sources modulating the SCO's in Lakehurst. Received level of the five tones was approximately -20 dbm each, which was sufficient to drive the electronics of the Culver City tape recorder without additional amplification.

Echo Suppression and Delay Tests

One of the advantages of the numerous and varied demonstrations conducted with the Syncom system was that it provided an excellent opportunity to evaluate the effects of delays encountered in long-distance transmission circuits. To date, delays of .5 to .6 seconds have been considered by many authorities to constitute an unacceptable by-product of synchronous satellite communications. This opinion has been based on the fact that a) in a two-wire system, the delay will provide intolerable echo and b) the effects of delay will so disturb the psyche of the average talker as to render the circuit unacceptable for normal use.

To date numerous and varied tests have been performed using the Syncom system. Four-wire system operation has been excellent, supporting previous theories that echo would not present any problems in this mode. In all operations of the Syncom system involving two-wire circuits, echo suppressors were employed

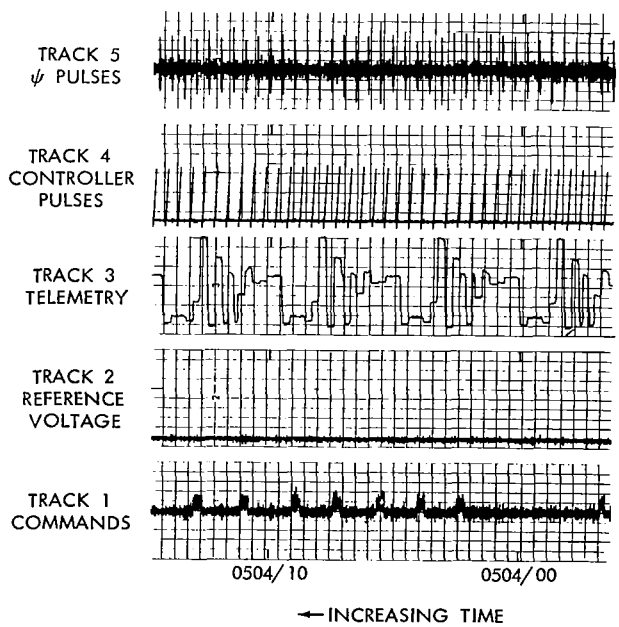

Figure IV-52—Culver City discriminator outputs.

to overcome the effects of delay. Two types of suppressors were used, the Lenkurt 931A and the Stelma FTA-15. Figure IV-53 shows a simplified block diagram of the 931A for uni-directional operation. If Station A is talking and Station B listening, the voice signal present at A switches the transmit control circuit to "set". However, since the lower control portion of Station A is isolated by a variable gain amplifier, the receive control switch remains "reset". The net effect at Station A is that both the transmit and receive loss switches and the echo control switch are closed. Hence, with the loss switch closed, the gain control amplifiers each have unity gain. At Station B, the received signal switches the receive control circuit to "set" causing the receive loss switch to close, resulting in unity amplifier gain. In addition, the echo control and transmit loss switches are opened. A portion of the received signal, due to hybrid leakage or reflection in the two-wire line, would be returned to the speaker at Station A if the echo control switch were closed. The same leakage signal could "set" the transmit control circuit at Station B. However, the variable reference bias is proportional to the received voice signal and is greater than the leakage or return signal. Thus, with the echo control switch open at Station B, the return or echo is blocked. If the talker at Station B interrupts by talking loud enough to override the reference bias, this switches the transmit control circuit at Station B to "set" and also closes the echo control switch. At this point, both parties are talking at the same time, resulting in the transmit and receive control circuits being "set" at both stations, and all gain amplifiers have a loss of approximately 6 db each. Therefore, each voice signal is attenuated 12 db, while the echo is attenuated 24 db. However, when both parties are speaking at the same time, the echo is unnoticed by the talkers. When one party stops talking, the echo suppressor recycles and returns to its unidirectional mode.

The Stelma FTA-15 is a voice operated break-in (VOX) type of echo suppressor which provides effective transmit-receive switching by means of in-band voice-operated signaling. The system uses two control signals: One for standby (1225 cps), and one for function (1310 cps). When either station employing an FTA-15 is in the standby condition, each continuously transmits the standby

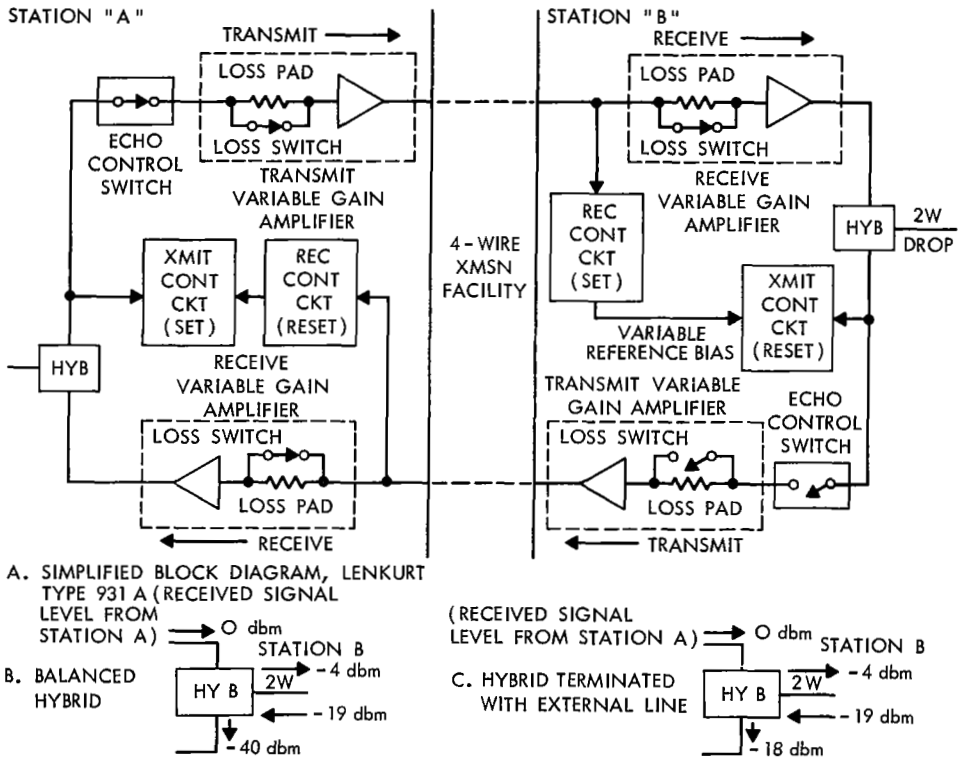

Figure IV-53—Syncom echo suppressor operation.

signal. When either station attempts to pass voice signal, its standby signal output automatically changes to the function signal which is continuously transmitted simultaneously with the voice signal. Reception of the function signal locks the distant station in the receive mode and prevents transmission of the function tone, thus break-in is not possible. The disadvantages of the FTA-15 are (a) break-in is not possible due to the nature of the voice-operated type of action; (b) there is a tendency to lose the first syllable at the start of transmission and (c) the hang time associated with VOX operation adds a total of 1/4 of a second to the overall transmission delay. Primarily, due to the break-in feature of the Lenkurt 931A, it was used the majority of the time for echo suppression.

The major problem encountered with two-wire circuits employing the 931A echo suppressor has not been with the satellite link or the echo suppressor, but has been directly associated with the extremely low levels encountered on telephone lines. The problem can best be illustrated by referring to Figure IV-53. Figure IV-53 shows an external, two-wire telephone line connected to hybrid preceding the echo suppressor. The desired signal transmitted from Station A is received at Station B at a 0 dbm level. If it is assumed that the hybrid is properly balanced either by employing internal balancing resistors or an input loss pad, then the reflected signal at Station B due to leakage will be in the order of -40 dbm. If the desired signal coming into Station B for transmission to Station A is -19 dbm or greater, there is no problem in adjusting the echo suppressor at Station B to distinguish between reflected and desired signals and thus prevent echo. However if the hybrid is not properly balanced, Figure IV-53 (which would be the case when connecting an ordinary two-wire phone line across a hybrid), tests have indicated that the hybrid leakage will increase to approximately -18 dbm. If the desired signal remains at a -19 db level, the echo suppressor cannot properly operate since the reflected signal levels exceed the desired. The levels encountered during many of the demonstration tests have been -19 dbm and below. In addition the hybrid associated with the echo suppressor did not contain balancing controls. However, with incoming phone line levels in excess of -15 dbm, absolutely no trouble has been encountered using the 931A. In short, under these conditions results have been excellent.

The next question to be answered is what, if any, are the psychological effects of delay on an average talker. In the past much has been written on this subject. Theories have been put forth indicating the possibility that circuits possessing delays of up to .6 of a second in conjunction with echo suppressors would be unacceptable a substantial portion of the time. In addition, much discussion has taken place concerning the relative merits of so called "casual laboratory trials" versus controlled laboratory tests under the guidance of trained psychologists. The test method provided by the Syncom system appears to be ideal, particularly from the psychological standpoint. What would be more desirable than to place the subject under evaluation in the actual environment to be studied and observe his reactions? This was the case with the more than 1000 people who have spoken through the spacecraft. In as many cases as possible, the talkers were asked to express their opinions on what they thought of the circuit. Only two cases have been noted where talkers were unable to speak through the spacecraft due to the effects of delay. In both cases the talkers involved happened to be women. Their difficulty was that they demanded an instantaneous reply and thus kept repeating the word "hello" as rapidly as possible. These were considered rare and extreme cases. What the tests have indicated is that if a psychological adjustment is required, the average talker makes this adjustment unconsciously in a matter of a few seconds. This has been observed without any prior briefing of the talker.

In summation, results of the tests to date clearly indicate that delays of 5/10 of a second definitely do not provide psychological blocks, or any other type of blocks, that will hinder satisfactory duplex communications by an average telephone user.

Data Transmission Experiments

A limited investigation of the data transmission capabilities of the "Syncom" satellite was conducted at the Fort Dix SATCOM Terminal. The test program was formulated to determine the

transmission performance of the normal Syncom ground equipment and also variations of this equipment tied into an NSA mod-demod along with a portion of the "ADVENT" system. Tests were conducted through the ground simulator and the orbiting satellite. Transmission performance of these test setups were measured in terms of binary error rate for various coding methods.

Description of Test Set Up

Envelope delay measurements were made with an Acton delay measuring set fed into the mod-demod terminals of the ground equipment as shown in Figure IV-54. Frequency response measurements were made in the same manner except that a Waveforms oscillator in conjunction with a counter and Ballentine voltmeter were used. This test set up is shown in Figure IV-55.

Quantitative error performance at the low bit rates was measured using the stored reference correlation detection scheme shown in Figure IV-55. A locally generated binary NRZ pattern at the transmit end was processed by the variable transmission system (which will be discussed later) into a form that made it suitable for transmission through the ground equipment and satellite. The processed data were then transmitted through the Syncom equipment and demodulated to NRZ by the receive transmission unit. The receiver clock information was automatically corrected for any transmission delay or drift so that each received bit transition lined up with each locally generated transition. Also each received bit was automatically framed with each locally generated bit and the two patterns were then compared and disagreements tallied on an error counter. Provisions were also made for generating a random signal which would closely simulate a true data signal. The received signal was then observed and photographed on an oscilloscope. The variable transmission system was capable of generating and detecting shaped baseband, dipulse, *vestigial sideband, double sideband AM, double sideband suppressed carrier* (biphase), dicode, bipolar, duo-binary, olympic fix, and unipolar at speeds up to 100 kc. (The italicized modulation techniques are the only ones that gave any degree of success).

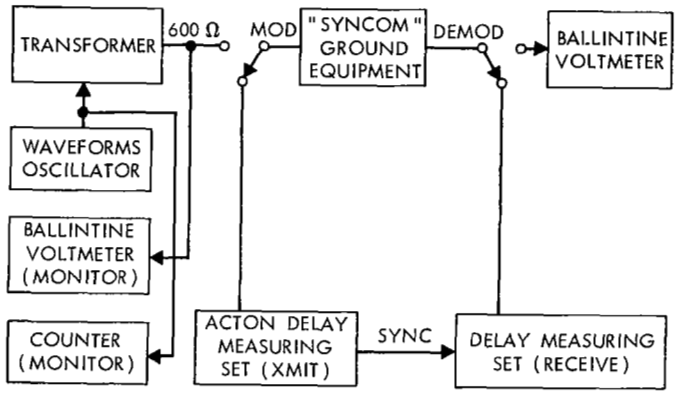

Figure IV-54—Delay and frequency response measurement test set up.

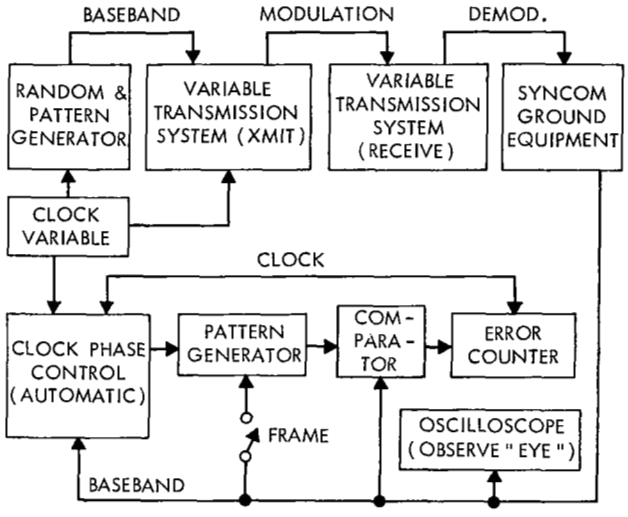

Figure IV-55—Test set up for quantitative error measurement and "eye" observation at low bit rates.

Error performance at high speeds was measured by similar methods employed at the low speeds with variations in mod-demod, and clock circuits. Figure IV-56 shows a block diagram of this test set up. A 1 mc frequency standard in conjunction with multipliers and dividers gave standard frequencies between 50 kc and 20 mc which drove the transmit pattern generator. The amplitude of the baseband output from the pattern generator was used to control the deviation of a 60 MC FM modulator. The FM output signal was fed directly into the transmitter exciter by passing

the normal Syncom modulator circuits. The receiver signal was taken from the 60 Mc IF output by passing the demodulator circuits and fed to a wideband FM receiver. The detected baseband signal was again lined up with the local clock, compared and error counts were made using a method similar to the low speed method.

Test Results - Ground

The envelope delay and frequency response of the Syncom ground configuration (Figure IV-35) are shown in Figures IV-57 through IV-61 for the seven different modes. The transmit video amplifier has been removed in Figures IV-62 and IV-63 and the signal applied directly to the phase modulator.

Table IV-13 shows the results of the pattern generator tests. The receiver signal input to the paramp was set to -115 dbm except in dicode and biphase operation. The data transmission level was lowered until no visual distortion occurred or the error rate was lowest at the receiver except in the last two tests of Table IV-14 where the effect of signal overloading is evidenced by errors. The test results show that 4 kilobits could be transmitted error free.

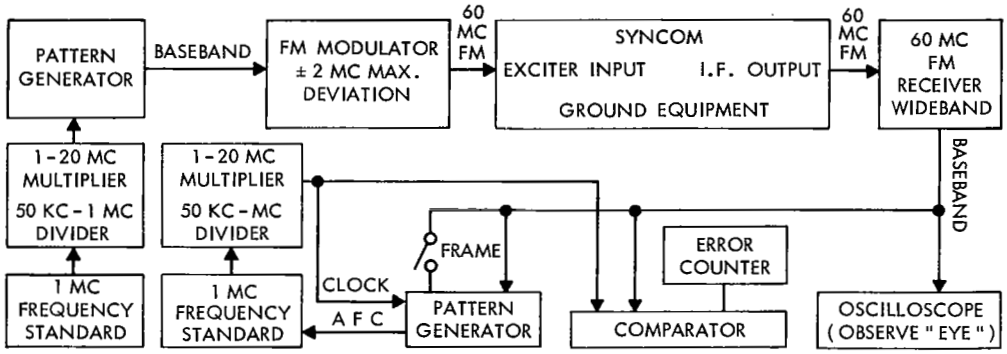

Figure IV-56—Test set up for quantitative error measurement and "eye" observation at high bit rates.

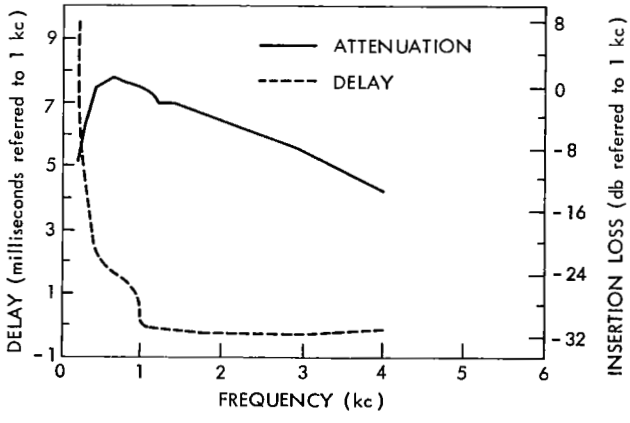

Figure IV-57—Envelope delay and frequency response of Syncom ground equipment (narrow-narrow).

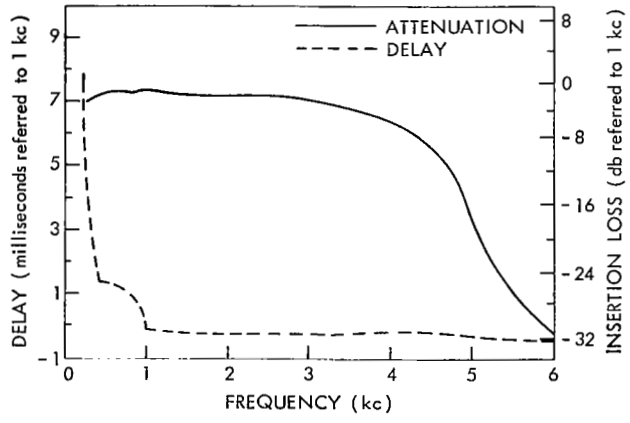

Figure IV-58—Envelope delay and frequency response of Syncom ground equipment (wide-narrow).

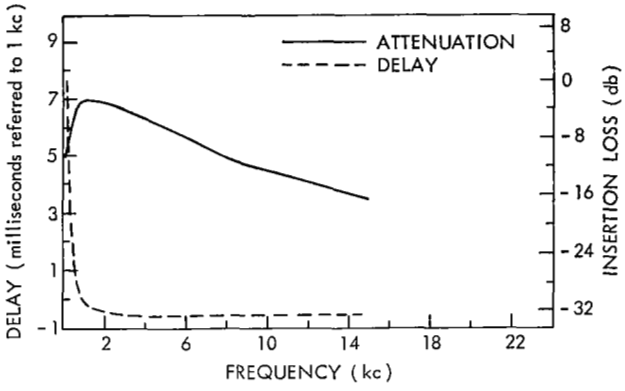

Figure IV-59—Envelope delay and frequency response of Syncom ground equipment (medium-medium).

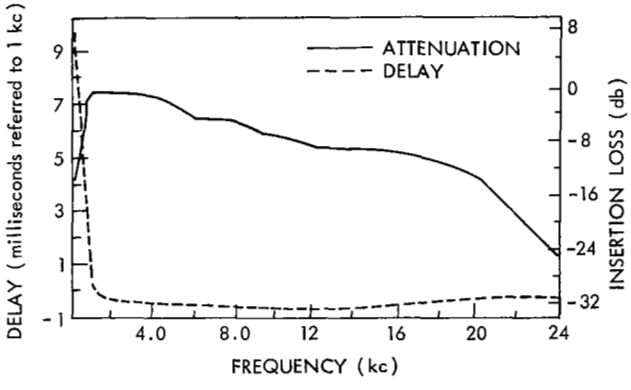

Figure IV-60—Envelope delay and frequency response of Syncom ground equipment (wide-medium).

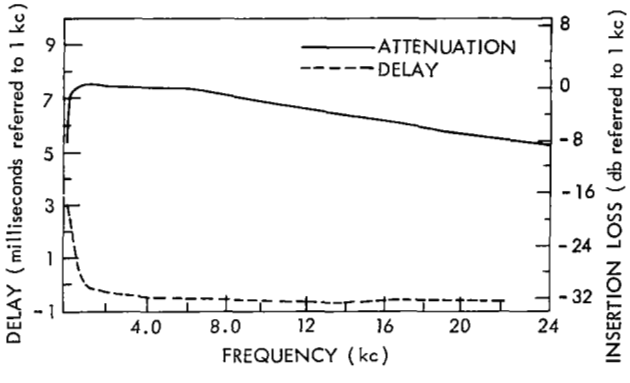

Figure IV-61—Envelope delay and frequency response of Syncom ground equipment (wide-wide).

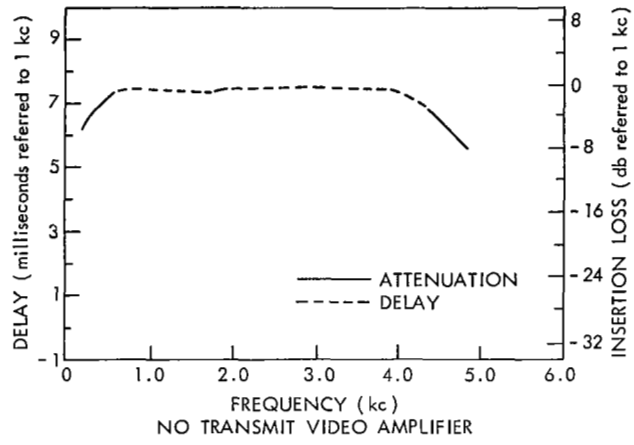

Figure IV-62—Envelope delay and frequency response of Syncom ground equipment (wide-narrow).

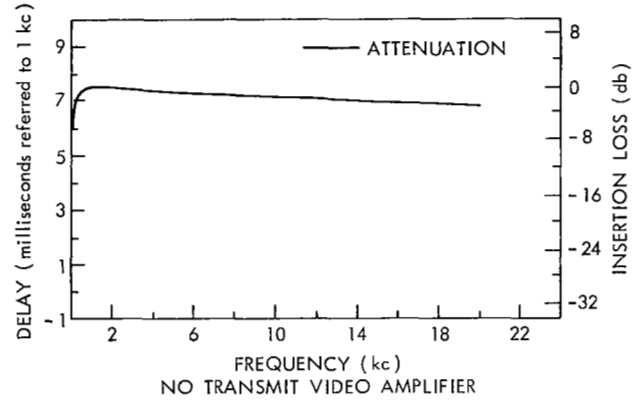

Figure IV-63—Envelope delay and frequency response of Syncom ground equipment (wide-narrow).

Table IV-15 shows the results of transmitting 50 kilobits through the "ADVENT" system using biphase modulation and varying the IF bandwidth. The 100 kc IF bandwidth gave an acceptable error rate.

Test Results - Satellite

It was determined from the ground tests that the best modes of operation were on wide-narrow, wide-medium and biphase so these were the only ones used on the satellite. Figure IV-64 shows a block diagram of the "live bird" system utilized while Tables IV-15 and 16 show the test results. The satellite will easily support a 3 kilobit data stream with an inexpensive transmission system

Table IV-13

Results of the Pattern Generator Tests

MODE	MOD INPUT LEVEL (mv)	DEMOD INPUT LEVEL (mv)	NOISE (mv)	S/N (db)	ERRORS (Per/sec.)	BIT ERRORS	REC COMM LEVEL (dbm)	DATA RATE	CARRIER	TRANSMISSION SYSTEM
Narrow Narrow	205	96.0	17.2	14.92	0	0	-115	2.4 kc	2.6 kc	Vestigial Sideband
Wide Narrow	510	175	9.0	25.8	0	0	-115	4.0 kc	4.2 kc	Vestigial Sideband
Medium Medium	150	80	12.5	16.12	-	-	-115	4.0 kc	4.2 kc	Vestigial Sideband
Wide Medium	89	87	22.5	11.74	-	-	-115	4.5 kc	10.0 kc	Double Sideband
Wide Medium	139	122	22.5	14.67	.6	7.5×10^{-5}	-115	8.0 kc	10.0 kc	Vestigial Sideband
Wide Wide	900	150	17.5	18.65	92	1.84×10^{-3}	-109.5	50 kc	-	DICODE Mod Direct
Wide Wide	900	150	31.0	13.69	1,500	$.3\times10^{-1}$	-115	50 kc	-	DICODE MOD. DIRECT
Wide Narrow	900	96	9.2	20.36	.1	2.5×10^{-5}	-115	4.0 kc	4.2 kc	Vestigial Sideband
Wide Medium	700	53	13.5	10.88	2.0	2.67×10^{-4}	-115	7.5 kc	8.0 kc	Vestigial Sideband

Table IV-14

Data Transmission Levels and Error Rates

MODE	BIT RATE	ERRORS PER/SEC	BIT ERRORS	REC COMM LEVEL	TRANSMISSION SYSTEM
ADVENT	25 KC	15 25 16 18 24 24	8.6×10^{-4}	-118 -9	BIPHASE
ADVENT	10 KC	8 9 8.1 10.9	9.3×10^{-4}	-118 -9	BIPHASE
ADVENT	5 KC	6 30 Burst 7	1.3×10^{-3}	-119.9	BIPHASE
ADVENT	32 KC	62	2×10^{-3}	-118.9	BIPHASE
ADVENT	38.4 KC	5	1.3×10^{-4}	-117	BIPHASE
ADVENT	50 KC	32	6.4×10^{-4}	-117	BIPHASE
ADVENT	19.2 KC	4.2 3.5 4.7	2.13×10^{-4}	-117	BIPHASE

Table IV-15
Fifty Kilobit Data Transmission

MODE	ERRORS PER/SEC.	BIT ERRORS	SIGNAL LEVEL	DATA RATE	CARRIER	BANDWIDTH
ADVENT BIPHASE	2	4×10^{-5}	DBM -117	50 kc	-	100 kc BW
ADVENT BIPHASE	10	2×10^{-4}	-117	50 kc	-	1.5 Mc BW

and 50 kilobits with a more sophisticated scheme. The error rates would have been much lower if the 20 kw ground transmitter had been available. This would have resulted in full limiting in the satellite receiver and less interference from the beacon transmitter. The transmitter power was only 2 kw and the received communications signal was -117 to -119 dbm.

Conclusions

The Syncom satellite with a 20 kw ground transmitter, the normal ground equipment and a suitable data modem should support 3 to 4 kilobits with a very low error rate. With a more sophisticated modem such as Phase Shift Keying, this rate could be doubled.

Using portions of the "ADVENT" biphase system with a properly phase locked receiver bit rates as high as 50 kc should be usable with PCM or delta-mod voice systems.

PERFORMANCE TESTS

Discussion

The Syncom II Communication System contains a great many variables and parameters which require evaluation and analysis. In order to arrive at meaningful conclusions on the overall system capabilities (or deficiencies) it has been necessary to isolate these characteristics and measure their individual effect upon the system. This approach has necessarily resulted in a fragmentation of what, on the surface, appears to be an excessive amount of data, but which in reality is insufficient in many cases for the formulation of final type conclusions. The best way to illustrate this predicament is with examples. Take the case of relating such variables as intelligibility and teletype error rate to signal-plus-noise to noise (S+N/N) ratios. During the period covered by this report (days 212 through 297), a total of 2964 valid S+N/N readings was recorded. Now, this figure includes the data of all stations, for all tests run under all operating modems; when we break out the data for a specific case, say, the S+N/N readings recorded by a particular station operating in a given equipment configuration for a specific test code (type of experiment), we find that we have, on the average, less than 10 readings. Hardly enough to permit significant statistical comparisons. On most occasions where the data are broken down to the third echelon, there are not enough data for statistical analysis.

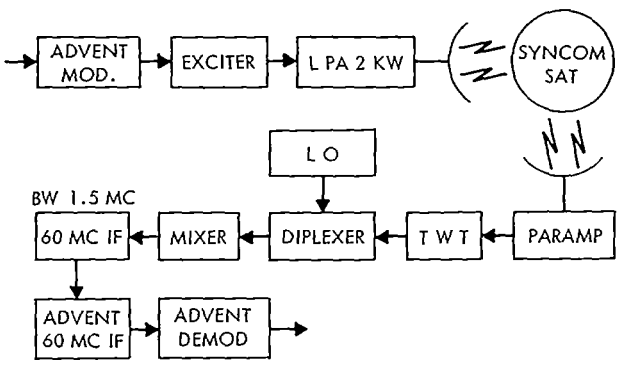

Figure IV-64—Advent Syncom test setup.

Table IV-16
Low Rate Data Transmission

MODE	MOD-INPUT LEVEL (mv)	DEMOD OUTPUT LEVEL (mv)	NOISE (mv)	S/N (db)	ERRORS PER/SEC	BIT ERRORS	REC COMM LEVEL (dbm)	DATA RATE	CARRIER	TRANSMISSION SYSTEM
WIDE	500	700	14.2	33.8	0	0	-119	2.4 kc	2.6 kc	Vestigial Sideband
NARROW										
WIDE	350	480	14.0	30.7	.7	2.36×10^{-5}	-119	3.0 kc	3.1 kc	
NARROW					0	0	-117	3.0 kc	3.1 kc	Vestigial Sideband
WIDE NARROW	350	400	14.0	29.2	1.4	3.5×10^{-4}	-117	4.0 kc	4.3 kc	Vestigial Sideband
WIDE NARROW	350	400	14.0	29.2	2	4×10^{-4}	-117	5.0 kc	4.3 kc	Vestigial Sideband
WIDE MEDIUM	380	400	28.0	23.18	4.3	1.43×10^{-3}	-117	3.0 kc	3.1 kc	Vestigial Sideband
WIDE NARROW	123	128	25.0	14.18	31	6.2×10^{-3}	-117	5.0 kc	6.0 kc	Vestigial Sideband
WIDE NARROW	123	128	25.0	14.18	34	5.6×10^{-3}	-117	6.0 kc	6.1 kc	Vestigial Sideband

Unfortunately, the evaluation has also been hampered by a poor spread of data. In most cases, such as limited range of elevation angles due to fixed station location and fixed satellite orbit, the conditions causing this situation are uncontrollable. The remaining cases were those which became apparent only after the data of the first 90 days of operation had been reduced and examined. Additional tests have been initiated to fill the gaps. An illustration of the ramifications of a poor spread in the data is presented when we attempt to define the mathematical relationship between multi-channel teletype (separated by channel and modem) and signal-plus-noise to noise ratio. It has been determined that the mathematical equation which best fits this relationship is that of a modified exponential known as a Gompertz curve (to be discussed later). The technique which must be employed to derive the Gompertz equation requires that the data be spread evenly over the range, and in addition, that they portioned in three equal increments. As can be seen from the scatter diagram (Figure IV-65) of teletype error vs signal-plus-noise to noise, the data are not spread evenly necessitating some subjective interpolating to fill in the gaps. Furthermore, multi-channel teletype tests have produced very little data in the region of S+N/N threshold; the data have invariably clustered at either 100 percent or 0 percent error. This indicates a very narrow threshold range, but because of the bias introduced by the uneven spread of data, the curve derived does not indicate the narrow threshold with a steep slope, but tends to average out and give a gradual slope. In order to provide more meaningful curves, a new series of controlled multi-channel teletype tests has been initiated with emphasis placed on obtaining data in the threshold region.

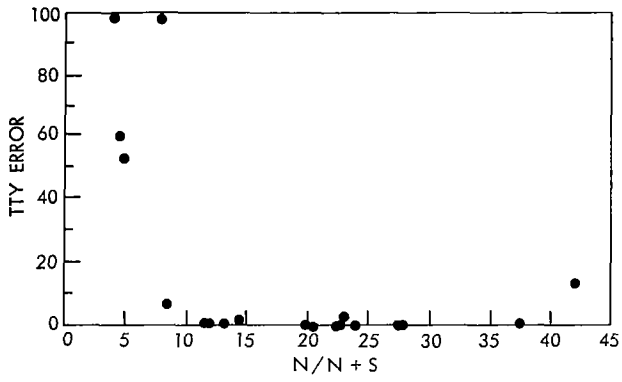

Figure IV-65—Stations 1, 2, 3, & 4 channel 11 modem 2.

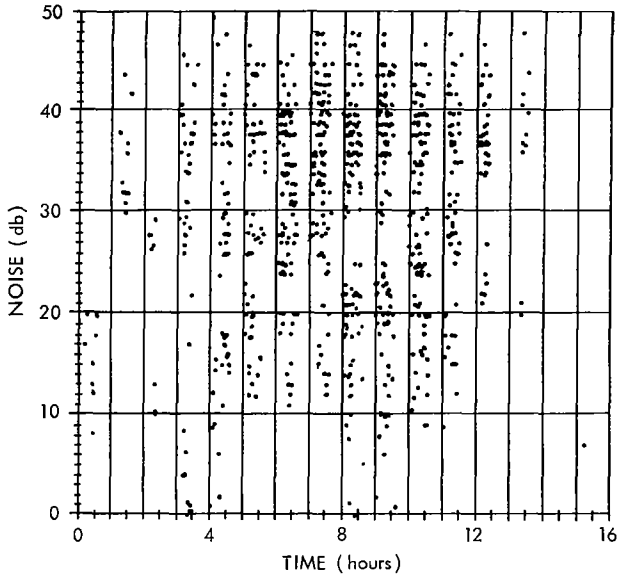

Figure IV-66—Correlation of analysis of pairs of matrix characteristics. Combinations are shown after little or no correlation.

These examples are cited here as a warning to the reader *not* to interpret the test results to be presented as final. This is an interim report and the results and conclusions contained herein are based upon data that are far from conclusive.

The nature of the Syncom II system dictates that the statistical analysis be performed at three levels: fitted frequency distributions, non-linear two variable and multivariable regression (or correlation) analysis and trend analysis. The frequency distribution curves have been fitted to the signal-plus-noise to noise ratio readings for each operating modem in order to provide statistical estimates of the expected frequency of occurrence. Since practically all system characteristics can be related to S+N/N, and since this expression can also be used for comparisons with other systems, these frequency distributions are most important and will be discussed in detail below.

For the correlation portion of the analysis, each of the pairs of characteristics indicated in matrices above were examined. The initial manipulation of the data is performed at Franklin Institute Laboratories where the computer does the appropriate sorting and the automatic plotter produces a scatter diagram for each pair. These diagrams are visually examined to screen out those combinations which offer little or no correlation as is shown in Figure IV-66. Where it is established that the degree of correlation is significant, the next step is to define the relationship between the values in terms of a mathematical expression. This is accomplished by a least squares fit of the data at hand to the appropriate type of equation. The choice of equation type (straight line, exponential curve, etc.) is made upon the basis of experience in eliminating those which obviously are not appropriate fits and then, by trial and error, fitting the data to the equations of the form which appears to be a good fit. Figure IV-67 shows a scatter diagram of Intelligibility Score (percent) versus Signal-Plus-Noise to Noise Ratio (DB). It is obvious from the scatter of the data that the best fit curve will be of the exponential family. Figure IV-68 shows three types of exponential curves fitted to the same scatter data. The Log Growth Curve is of the form $Y = 100\ (1 - e)\ KX + A$; the Logit Curve is $\log (y/100 - y) = KX + A$ and the Gompertz curve is $Y = Ka^{bx}$ or $\text{Log } L = \text{Log } K + (\log a)b^x$. Each of these curves appears to be a satisfactory fit, but in order to determine the best fit, a test must be made. For this particular test the Y error bias has been determined for each of the curves by taking the algebraic sum of the vertical distances between each data point and the computed Y value of the curve and dividing by N, the total number of data points. (Y error bias = $\Sigma Y_c - Y_i/N$). As shown by the results in Figure IV-68, the Gompertz curve is the best fit.

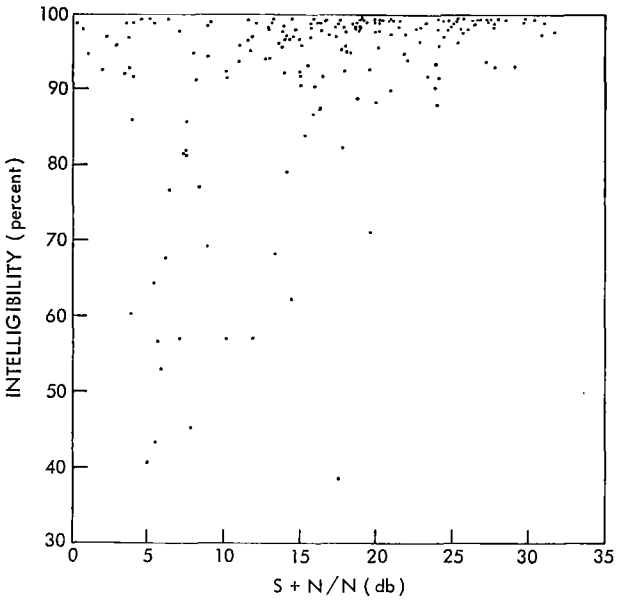

Figure IV-67—Scatter diagram of intelligibility score (%) versus signal-plus-noise to noise ratio (db). The best curve will be of the exponential family.

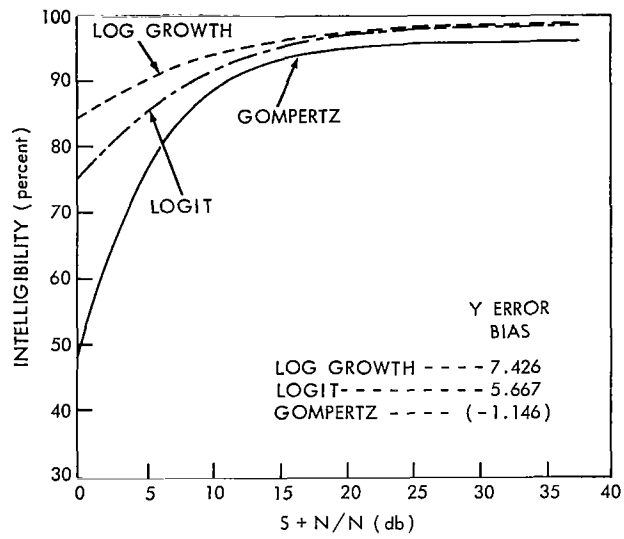

Figure IV-68—Three types of exponential curves fitted to the scatter diagram (a Log Growth Curve, a Logit Curve, and a Gompertz Curve).

The fitting of the curves to data and the subsequent testing for goodness of fit has proven to be a long and tedious process when performed by hand for the very large number of relationships in this evaluation program. Therefore, a series of computer programs has been, and is being, written to expedite the statistical analysis. To date, only the programs for frequency distributions and two-variable correlation and goodness of fit testing are operational.

Signal-Plus-Noise to Noise Distribution

Signal-Plus-Noise to Noise

One of the basic system performance measurements is that of signal-plus-noise to noise since, ultimately, almost all of the operating characteristics are related to this quantity. For this reason, the communication experiment tapes have been recorded (on the C.E.C. GR-2800 Recorder-Reproducer) such that, during testing periods, test tones for the measurement of received signal-plus-noise to noise are transmitted at least once every fifteen minutes. In addition, a separate test (Test Code 13) has been included to measure this quantity in all seven operating modes. The Test Code 13 tones are not pre-recorded, but are fed "live" directly into the modulator from a test tone generator. The significance in differentiating between the two types of test (pre-recorded vs. "live") is that the pre-recorded signal-plus-noise to noise levels are limited by the GR-2800 tape recorder and not the Syncom II System. The GR-2800, and hence, the pre-recorded test tapes are capable of producing a maximum 35 db signal-plus-noise to noise ratio. Therefore, all signal-plus-noise to noise statistics for test codes other than TC-13 will be biased by this upper limit of 35 db. This has necessitated the initiation of two independent examinations of signal-plus-noise to noise. The first is based upon signal-plus-noise to noise ratios from all tests run. The objective here is to provide an early analysis of the relative performance of the various operating modes and stations, and to make predictions (on a qualified basis) of future system performance. The second examination will be to analyze signal-plus-noise to noise ratios from Test Code 13 only, for it is here that we will receive an indication of system effectiveness bounded only by the limitations of the Syncom II System and not by the limitations of terminal equipment.

The data reduction of the taped signal-plus-noise to noise values became available prior to that of Test Code 13 data, therefore, it has been analyzed first. Figure IV-69 shows the skewed normal distribution curves which have been fitted by least squares techniques to the taped signal-plus-noise to noise measurements. The curves include all data from day 212 (the day of final orientation) to day 297 for all stations plotted by operating mode. Since the surface stations were located at various geographic locations, with differing relationships of satellite aspect angles, weather conditions, etc., the fitted curves offer the possibility of allowing general predictions of future results, provided that it is understood that there is a definite downward bias associated with the data used to derive these curves. (The bias is introduced by the terminal equipment and the fact that no attempt was made to attain optimum conditions during every test transmission.) Table IV-17 lists the means, lower standard deviations and lower 1.282 standard deviation points (indicating performance expected 90 percent of time) derived from the pre-taped data for various combinations of stations and modes. From Figure IV-69 and the corresponding columns of Table IV-17, it can be seen that, on the average, the wide-narrow with feedback (WNFB), mode has yielded the best results with the wide-medium with feedback (WMFB), narrow-narrow (NN), wide-medium (WM), wide-narrow (WN), medium-medium (MM), and wide-wide (WW) following in descending order. It should also be noted that these results were obtained for a 1 kc/s test tone and are not necessarily valid for the higher frequencies of the several modes. Nevertheless, several interesting conclusions may be drawn. It would appear that for the carrier levels encountered,

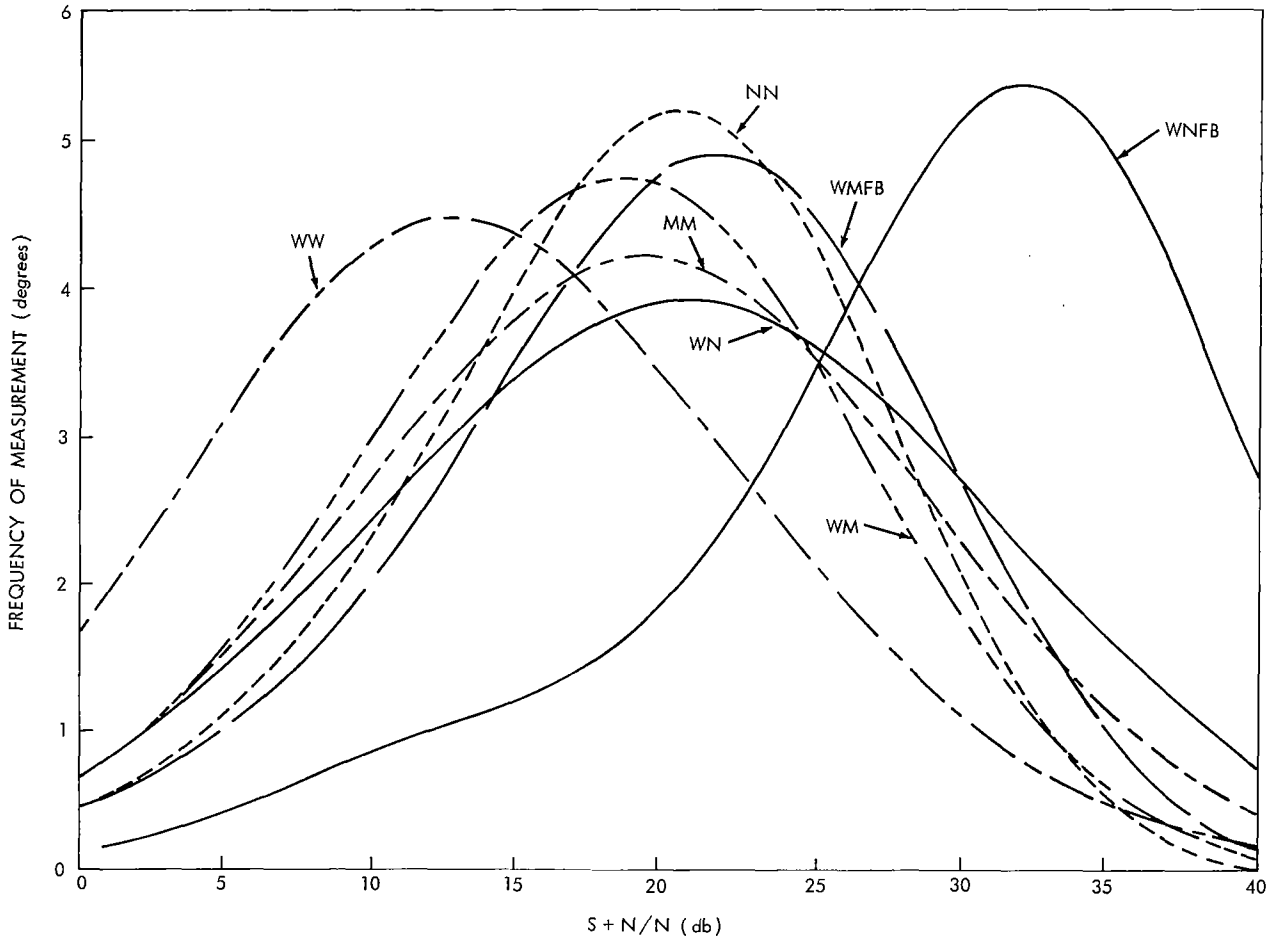

Figure IV-69—Syncom II communication experiment, frequency distribution signal-plus-noise to noise for all stations.

Table IV-17
Signal-Plus-Noise to Noise Distributions

MODE	STATION	MEAN (db)	STANDARD DEVIATION (db)	STANDARD DEVIATION X 1.282 (db)	84% (db)	90% (db)
All	All	19.7	10.0	12.8	9.8	7.0
NN	All	18.7	7.8	10.1	10.9	8.7
WN	All	20.3	10.8	13.8	9.6	6.5
WNFB	All	28.5	8.8	11.2	19.7	17.3
WW	All	13.9	9.6	12.3	4.3	1.6
WMFB	All	20.0	8.3	10.7	11.6	9.3
WM	All	17.5	8.6	11.0	9.0	6.5
MM	All	18.9	9.8	12.5	9.2	6.4
All	KSPT	17.7	10.0	12.9	7.7	4.8
All	LHST	19.1	10.9	14.0	8.2	4.2
All	DIX	19.4	11.7	15.0	7.6	4.3
All	RBTS	20.6	9.3	12.0	11.3	8.7

FM with feedback receivers offer advantages over straight FM receivers. It would also appear that the noise improvement advantages of wide deviation exist below threshold, since the received carrier levels all indicate below threshold operation.

The analysis of Test Code 13 data has been impeded by its format which prohibits utilization of the automated procedures applied to other data. It is expected that this portion of the analysis will illustrate that the system performance is significantly better then the results shown in Table IV-17.

Telephony

A good overall indicator of telephony performance is provided by intelligibility measurements. While these are somewhat subjective and dependent upon listener panel composition, training, and experience, this is a time-honored method of measuring communication system performance. As a means of verifying listener panel results as well as a means of investigating the possibility of replacing the listener panel, tests utilizing Voice Interference Analysis Set (VIAS) equipment have also been devised and evaluated. Comparison of the two results is most interesting.

Intelligibility

The objectives of the intelligibility analysis is a) to provide the mathematical relationship between Intelligibility Score and Signal-Plus-Noise to Noise Ratio; b) to provide a comparison of the intelligibility capabilities of the three narrow baseband equipment configurations; c) to show the relative comparison of intelligibility ratings for signal channel telephony as opposed to the telephony portion of simultaneous voice and teletype. The function of the mathematical equation, derived by statistically fitting the appropriate curve to the reduced data, is to allow predictions of voice intelligibility ratings based upon estimated or anticipated S+N/N levels.

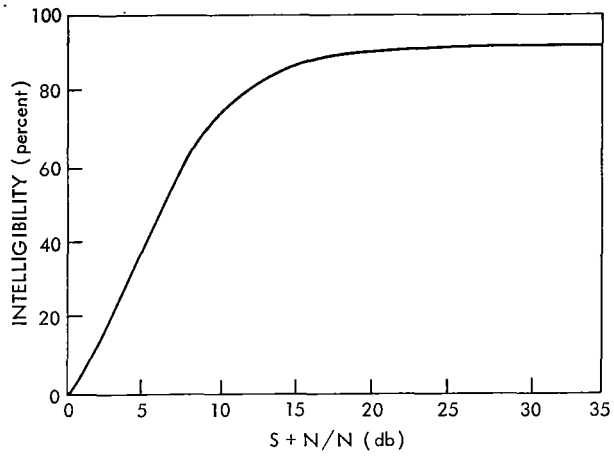

Figure IV-70—Mode 1-all stations, days 207-297.

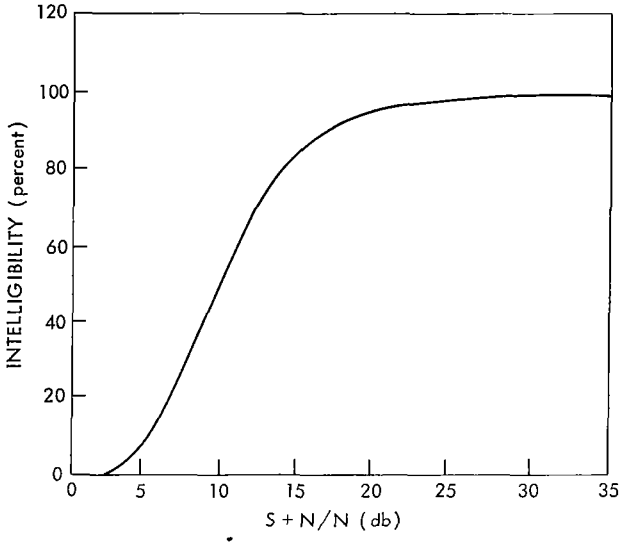

Figure IV-71—Mode 2-all stations, days 207-297.

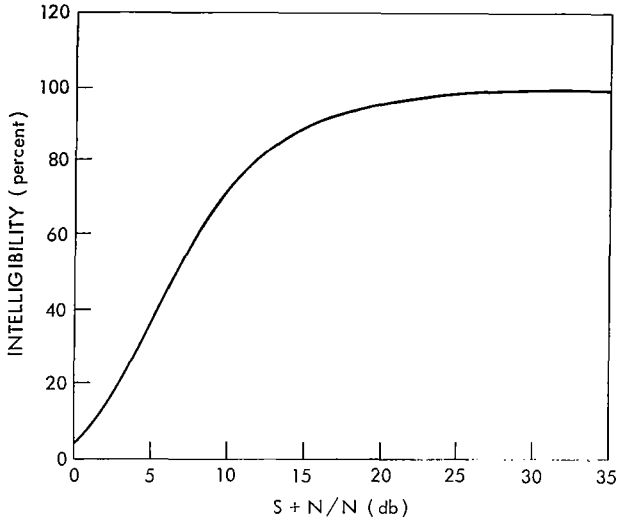

Figure IV-72—Mode 3-all stations, days 207-297.

The equations, and associated curves of intelligibility score versus S+N/N, for the narrow-narrow, wide-narrow, and wide-narrow with feedback modes are shown in Figures IV-70, 71 and 72.

An examination of the three curves reveals that at high S+N/N ratios the performance of the wide-narrow mode is superior to that of the narrow-narrow mode. This is attributed to the better frequency response (fidelity) of the wide-narrow mode (see Figures IV-36 and IV-37) which will have a significant psychological effect on the listener panel at good S+N/N levels. The differences existing among the three modes at low S+N/N values are attributed to a lack of data at the low S+N/N ratios.

Utilizing the curves in Figures IV-70, 71 and 72 in conjunction with those in Figure IV-69, we can make our predictions of expected intelligibility of word lists pre-recorded on magnetic tape. The performance values expected 90% of the time are listed in Table IV-18 under the "word" column. These values are word intelligibility which, through significant, are of lesser importance than total speech intelligiblity (which may be approximated closely by sentence intelligibility). Corresponding values of sentence intelligibility can be derived by using Kryter's curves for 256 phonetically balanced words (the word lists used in the Syncom II experiments employ 250 words). The listener panel sentence intelligibility results of Table IV-18 indicate that the WNFB mode provides a voice channel with the excellent intelligibility, the NN mode with somewhat lesser capability, and the WN mode very poor capability. These conclusions must be qualified, however, by the following facts: a) the data used to derive the curves include a goodly portion processed during the period, early in the program, which preceded the attainment of peak proficiency of the listener panel (discussed below); and b) the terminal equipment utilized in the experiments produced a significant downward bias to the expected S+N/N levels.

Table IV-18

Listener Panel Intelligibility and Vias—
Derived Articulation Index and Intelligibility

MODE	LISTENER PANEL INTELLIGIBILITY		VIAS	
			ARTICULATION INDEX	INTELLIGIBILITY
	90% WORD (%)	90% SENTENCE (%)	90% AI (%)	90% SENTENCE (%)
NN	61	81	41	97
WN	20	28	38	96
WNFB	86	94	78	99

In comparing the curve of Intelligibility versus S+N/N for single-channel telephone (Figure IV-73) with that obtained from the voice portion of simultaneous voice and teletype (Figure IV-74) it can be seen that, as expected, the single-channel offers the better results. However the differences are slight. This indicates that the small amount of speech power removed by the filter of AN/TCC-14 to provide the teletype channel does not significantly affect the performance of the voice channel.

Articulation Index

Another measure of voice communication performance is the articulation index. Briefly, this is a measure of intelligibility determined by calculating or measuring the contributions to articulation index in each of a number of narrow frequency bands (theoretically, twenty bands), and summing the contributions of each band. In practice, the Voice Interference Analysis Set, measured by General Electronics Laboratories, Incorporated, of Cambridge, Massachusetts, sums noise-to-signal ratios measured in fourteen bands, using a specially modulated signal. Provisions are made for adjusting the contributions of the bands according to the audio bandwidth of the system under

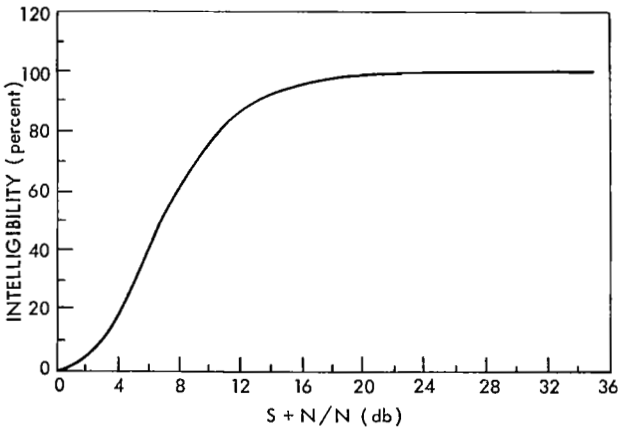

Figure IV-73—Signal-noise vs intelligibility, T. C. 05, all modes (1, 2, and 3), all stations.

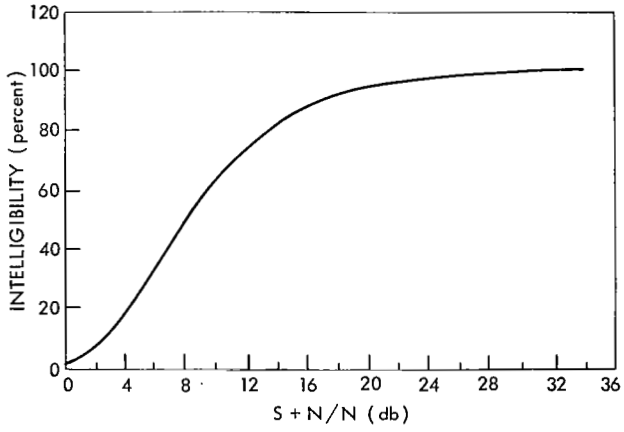

Figure IV-74—Signal-noise vs intelligibility, T. C. 07, all modes (1, 2, and 3), all stations.

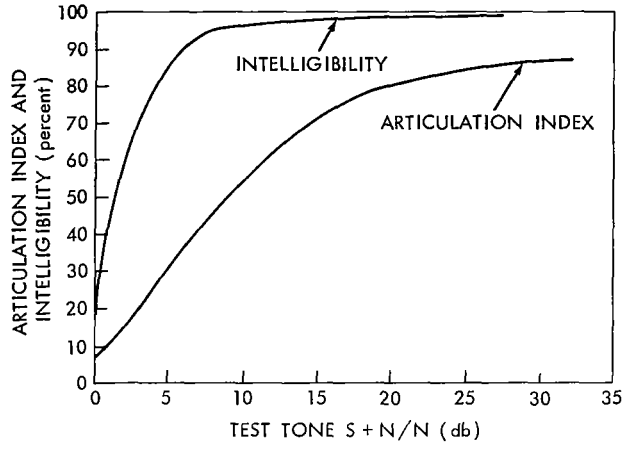

Figure IV-75—Syncom II communication experiment, wide-narrow mode.

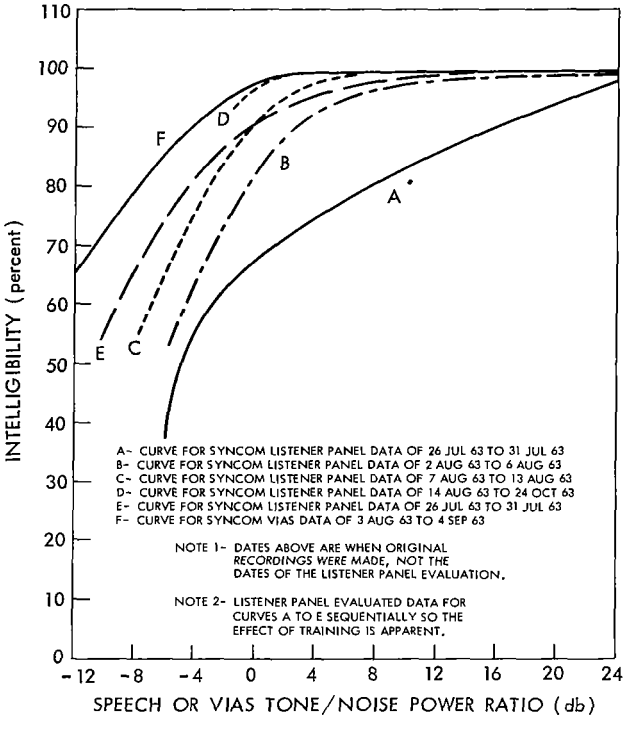

Figure IV-76—Syncom II communication experiment, comparison of intelligibility and VIAS.

test. Results, both for articulation index and corresponding sentence intelligibility are illustrated in Figure IV-75 and summarized in Table IV-18. It will be noted that the same relative intelligibility capabilities are indicated by both the listener panel scores and the VIAS scores, but that the absolute ratings differ.

Several possible explanations for the difference in measurements may be offered. Some question has been raised by people experienced with the VIAS as to the validity of VIAS measurements in an FM system which, to the best of the authors' knowledge, has not been answered; previous experience with the VIAS has been with the AM systems where the character of the system noise is somewhat different. On the input magnetic tapes, the rms level of the VIAS tones is recorded approximately 3 db higher than the rms level of the intelligibility word lists. Apparently, the most significant effect is related to the listener panel's state of training. Figure IV-76 shows a comparison between listener panel scores for data taken during subsequent weeks and the VIAS score. The curve clearly shows the effects of listener training. As a check, the listener panel scores plotted as Curve A were remeasured by playing the word lists through the panel again and the results are shown as Curve E. Note that with training, the listener panel scores approach the VIAS scores, but whether they coincide will require additional testing, particularly at low signal-plus-noise to noise levels where data are scarce. The objectives and approach employed in the statistical analysis of teletype are virtually identical to those employed in the telephony analysis.

Teletype

Single Channel Teletype

The results of single channel teletype testing have been excellent. For signal-plus-noise to noise (S+N/N) ratios of 9 db and above there have been no significant character errors. Even at the extremely low S+N/N ratio of 5 db, the character error rate is less then 3 percent. Figure IV-77 shows the relationship of single channel teletype error as a function of signal-plus-noise to noise.

The results of teletype multiplexed with voice are shown in Figure IV-78. A comparison of single channel and multiplexed data reveals that at signal-plus-noise to noise ratios above 2 db

the single channel teletype provides better performance. This is to be expected since for simultaneous teletype and telephony, the available transmitter power is divided between the two signals. The fact that the multiplexed teletype appears to be superior at signal-plus-noise to noise ratios below 2 db is due to the shortage of data at these points which distorts the statistical analysis.

Utilizing the frequency distribution curves of S+N/N as we did for intelligibility we can make predictions of minimum expected teletype performance 90 percent and 84 percent of the time. These values are summarized in Table IV-19.

Attempts have been made to compare the teletype performance of the Syncom II system with other transmission systems; unfortunately serious roadblocks have been encountered. Most of the Syncom II teletype tests have been run with very good S+N/N ratios which has resulted in a lack of data at the low or critical range of S+N/N where teletype errors first start to appear. Because of this, it is difficult to place much confidence in the low S+N/N portions of the curves in Figures IV-79 to -93, and it is in this area that meaningful comparisons should be made. Another factor in comparing to other systems is the non-standardized method of counting errors. For Syncom II each character deviation is counted as one error. Errors which cause erroneous figure shifts or carriage returns are considered one error in themselves, although they would result in many apparent errors in the copy. Some systems investigated for comparison do not count an error unless there are at least two correct characters between errors. Still others will discard all mistakes if they find that the measured noise in the system changes significantly from the start of test to the finish. Because of these shortcomings, no comparisons will be made at this time. Plans have been made, however, to run additional teletype tests with degraded signal-plus-noise in order to more accurately define the point and the rate at which teletype performance degrades.

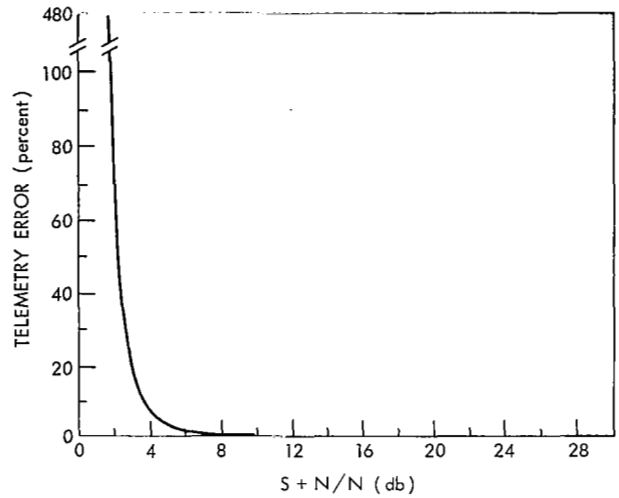

Figure IV-77—Signal-noise vs telemetry error T. C. 08, 2-12-64.

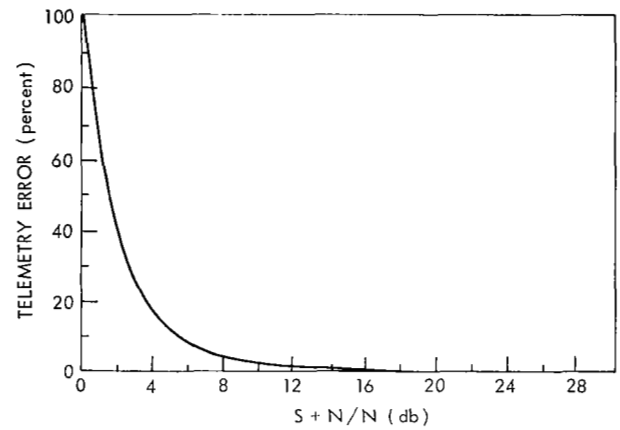

Figure IV-78—Signal-noise vs telemetry error T. C. 07, 2-12-64.

Multi-Channel Teletype

The analysis of multi-channel teletype, in order to be meaningful, should be made on a "by channel" basis, i.e., a separate curve for each channel at each operating mode. As mentioned earlier, this approach has fragmented the data to such a degree that little statistical confidence can be claimed for the curves of teletype error versus signal-plus-noise to noise for multi-channel teletype at this time. Additional tests are being run to supplement existing data. Nevertheless, the curves for 16 channel teletype for the WNFB mode (except Channel 5) are included for comparative purposes.

Table IV-19

Teletype Error Rate From Single-Channel Teletype and From Teletype Portion of Simultaneous Telephony and Teletype

MODE	ERROR RATE			
	MEAN		90%	
	SINGLE CHANNEL %	SIMULT. %	CHANNEL %	SIMULT. %
NN	0.1	1.9	0.3	3.3
WN	0.1	2.7	1.2	6.5
WNFB	0.1	0.1	0.1	0.2

It should be noted that the even numbered, low frequency channels are in general inferior in performance to the odd numbered, higher frequency channels. In order to understand the reason for this, it should be mentioned that the amplitude versus frequency response tests were run for Syncom II. It was found that below 1 kc the amplitude chopped off appreciably. This was apparently caused by the video shaper in the modulator (the section on Amplitude Response on page 98). If the video shaper is removed amplitude response rises in the lower frequencies. This is significant because the even numbered channels (No. 2, No. 4, etc.) start at 425 cycles. In order to confirm that the video shaper has been a cause of low frequency degradation, additional tests will be run without this equipment in the circuit. In addition, it has been determined that the low frequency channels are also degraded by spin modulation to a greater extent than the high frequency channels. Spin modulation is explained in considerable detail in connection with facsimile transmission; therefore, no attempt will be made to describe it here.

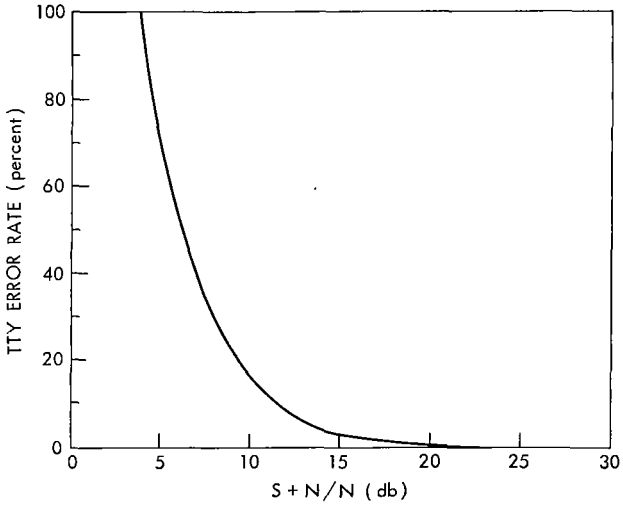

Figure IV-79—Modem 3 TTY channel 1 of 16 channels.

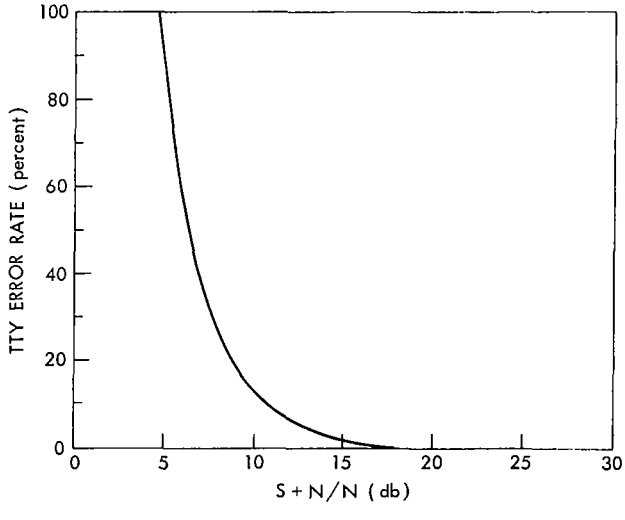

Figure IV-80—Modem 3 TTY channel 2 of 16 channels.

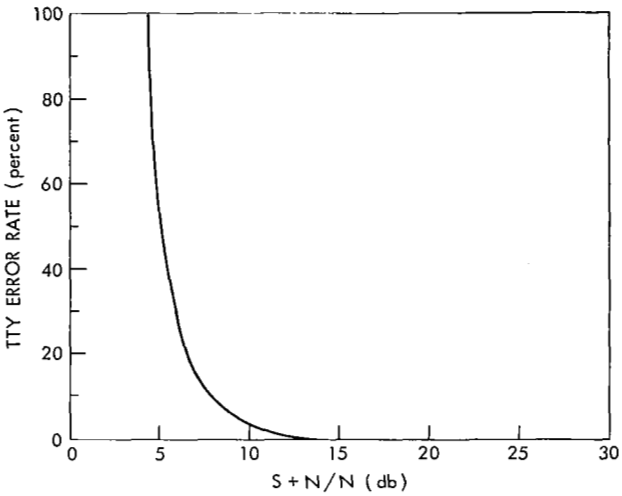

Figure IV-81—Modem 3 TTY channel 3 of 16 channels.

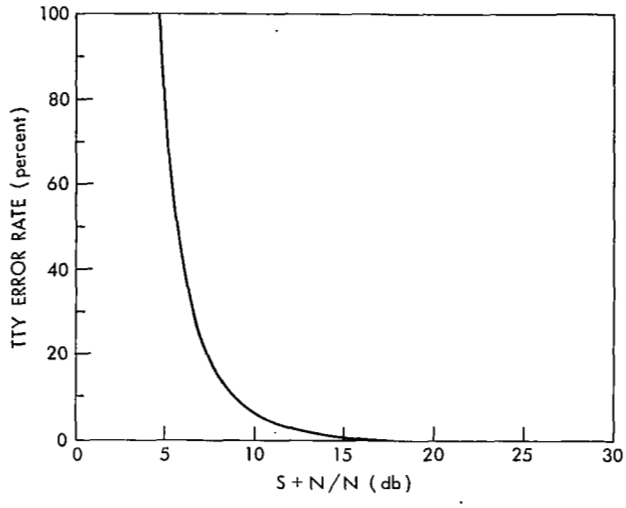

Figure IV-82—Modem 3 TTY channel 4 of 16 channels.

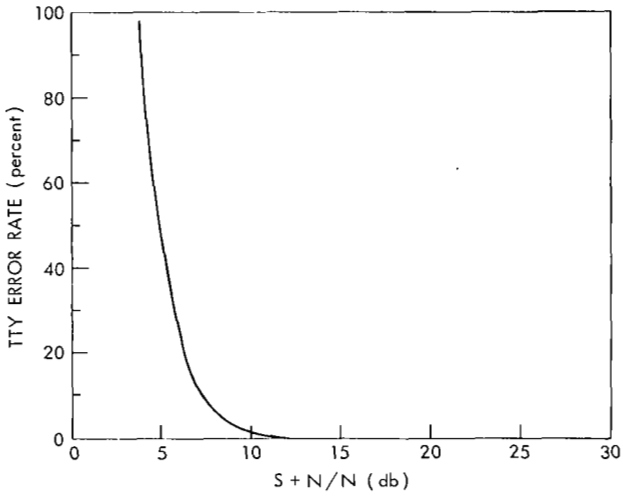

Figure IV-83—Modem 3 TTY channel 6 of 16 channels.

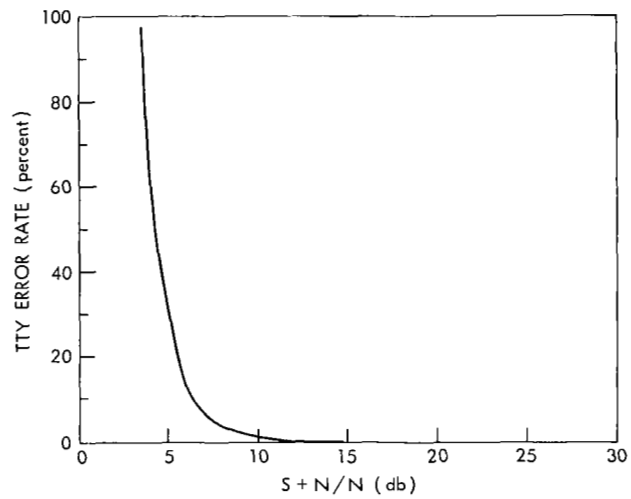

Figure IV-84—Modem 3 TTY channel 7 of 16 channels.

Facsimile

As of this reporting period, 113 facsimile pictures have been evaluated and numerically rated. A systematized numerical rating system was designed for use in evaluating the facsimile capability of the Syncom system and for use in the computer program for statistical analysis. The numerical rating system devised gives a rating of zero to ten (10) for the following three categories: a) Gray tone, b) Resolution, c) Overall Picture Quality. An overall picture value figure is determined by averaging the ratings of the above three categories. The numerical ratings are as follows: Superior -10; Excellent 8 or 9; Good -3 through 7; Poor 1 or 2; No Good -0. Additional information such as a fault indicator and a remarks column gives an indication as to why the rating was degraded. It can be seen that the above numerical rating is very subjective, and therefore, its usefulness or

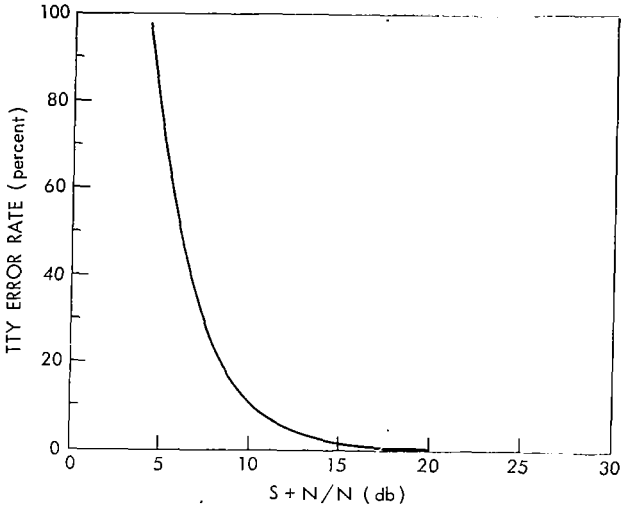

Figure IV-85—Modem 3 TTY channel 8 of 16 channels.

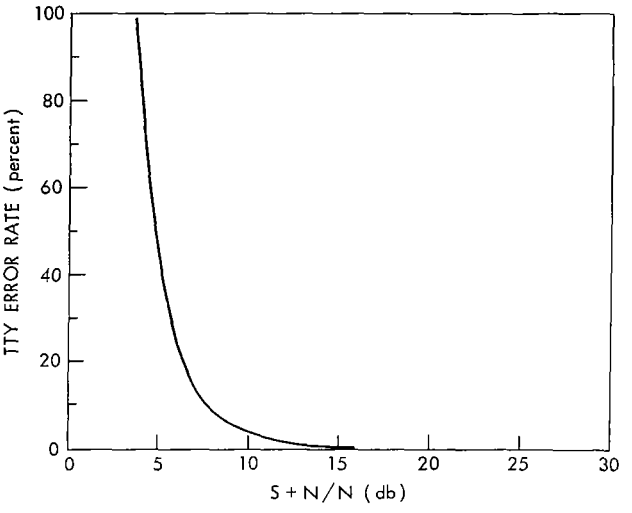

Figure IV-86—Modem 3 TTY channel 9 of 16 channels.

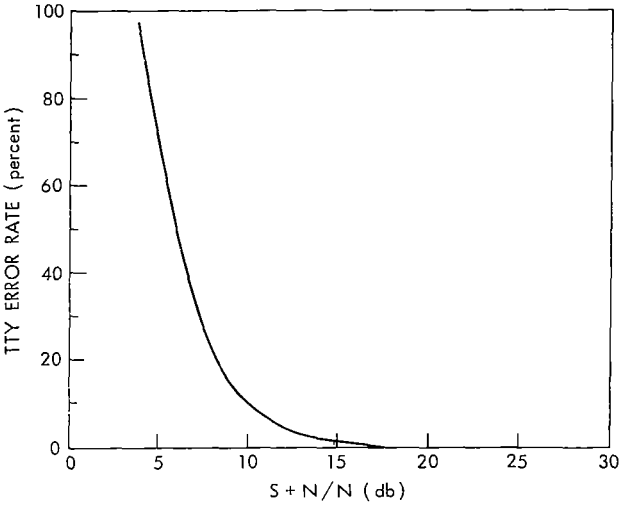

Figure IV-87—Modem 3 TTY channel 10 of 16 channels.

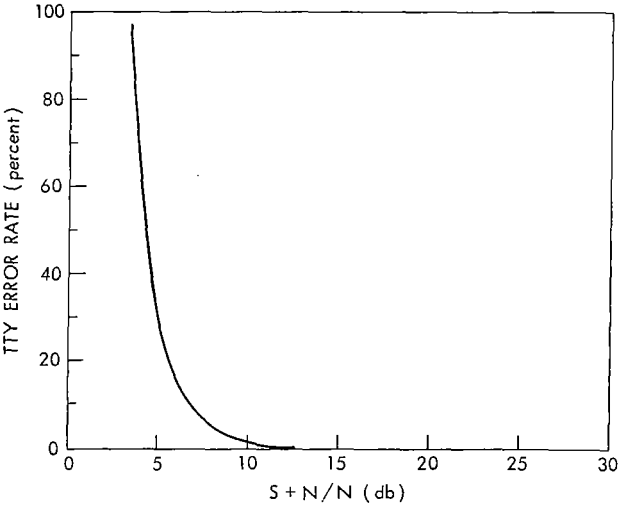

Figure IV-88—Modem 3 TTY channel 11 of 16 channels.

effectiveness must be proved. The two methods which are used to prove the validity of the rating system are a) comparison or ratings by several knowledgeable people in the field of facsimile, and b) re-evaluation of the same picture after a long period to show the effects of learning. Evaluation of pictures by two people have shown very close agreement in numerical ratings.

The numerical rating system described above can be less subjective if standards can be devised on which ratings can be based. These standards can only be devised if standard facsimile pictures are used. The standard photograph used in our tests is the IRE Facsimile Test Chart prepared by the Institute of Radio Engineers Technical Committee on Facsimile. A standard gray bar reproduction in which the third step from maximum black and from maximum white can be distinguished is considered superior and is given a rating of ten. Degradation in gray tone may be due to compression (machine or circuit), developing time, film quality, etc. Each shade of gray

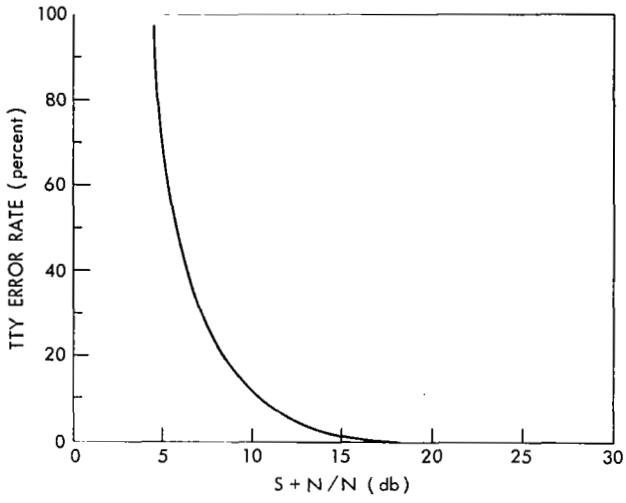

Figure IV-89—Modem 3 TTY channel 12 of 16 channels.

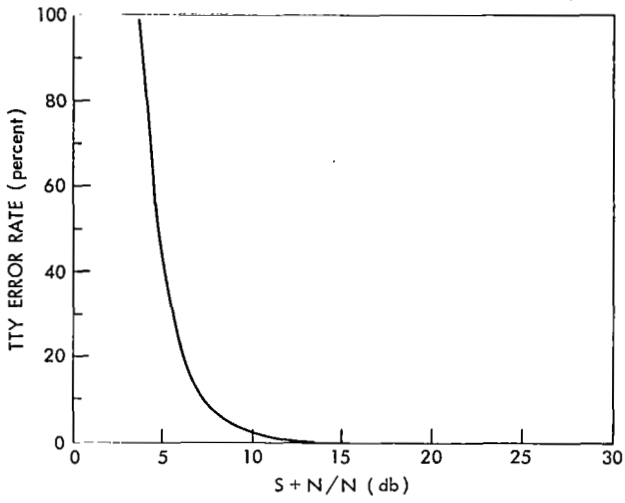

Figure IV-90—Modem 3 TTY channel 13 of 16 channels.

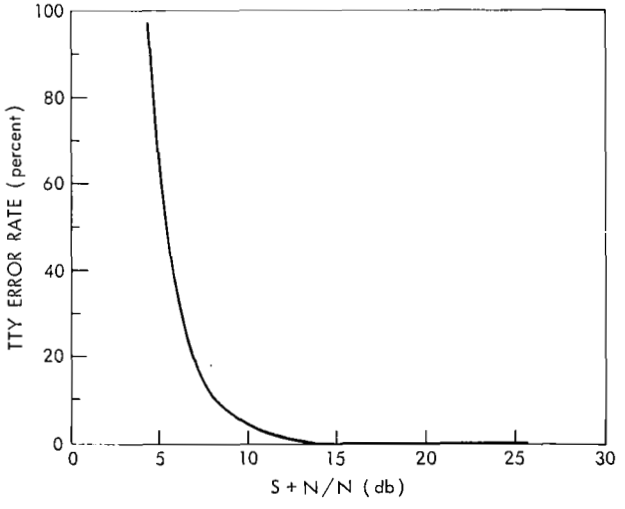

Figure IV-91—Modem 3 TTY channel 14 of 16 channels.

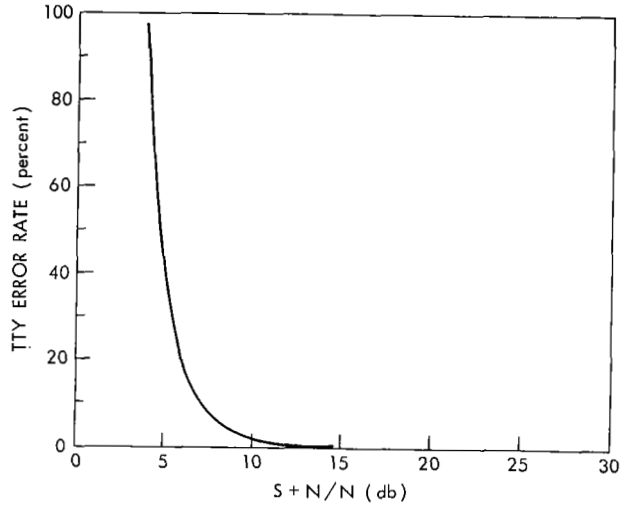

Figure IV-92—Modem 3 TTY channel 15 of 16 channels.

represents approximately 1.6 db change in level. A picture in which the standard resolution chart can be resolved below .004 is considered superior. Degradation in the resolution may be due to: a) Bandwidth limitations; b) Phase delay distortion; c) Doppler shift, etc. A picture with a superior numerical rating for picture quality must not exhibit any operator errors, equipment malfunction or system link deficiencies such as improper phasing, level changes, interference, noise, etc.

It should not be implied that only standard photographs can be adequately evaluated using the numerical rating system described above. The evaluation becomes more difficult when

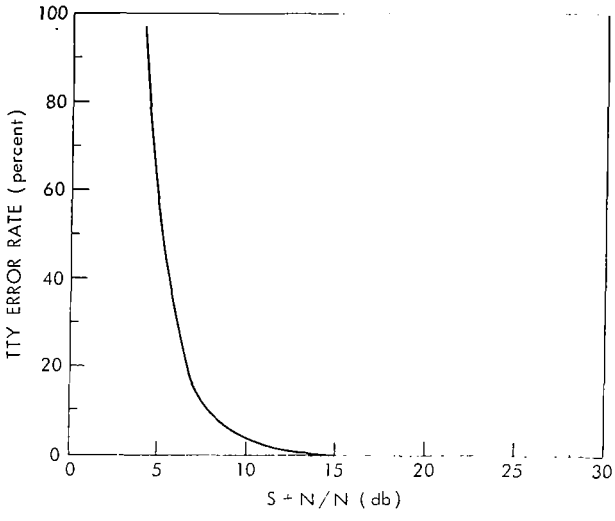

Figure IV-93—Modem 3 TTY channel 16 of 16 channels.

non-standard photographs are used, and thus, the rating becomes more subjective. In most cases the original of the non-standard is not available for comparison pusposes. The gray tone is usually rated by comparing the darkest black and the whitest white to the standard gray tone scale or comparing the darkest black to the phasing bar. Resolution is evaluated by denoting the amount of detail that can be distinguished or the sharpness of lines or sharp contrast areas.

Some of the more common effects and how they may be identified are listed below.

a) Improper recording current - improper record current results in compression of the blacks on the gray bar chart or a washout of the whites. This is the same as reducing the dynamic range.

b) Incorrect developing time - incorrect development time results in a picture which is overprinted or underprinted.

c) Level change - level change results in more than one shade of gray on the reproduced picture for one shade of gray on the original.

d) The picture was allowed to set on the roller - this results in a white streak across the entire picture (including the phasing bar).

e) False starts or machine not started - this results in all or part of the film not being exposed. A white spot will usually appear in the top portion of the picture.

f) Salt and pepper - the salt and pepper effect is due to the recorder being misaligned. The craddle lamp fires on ripples resulting in spots on the picture.

g) Poor signal plus noise-to-noise - this results in white and black streaks or hash appearing in the picture.

h) Jitter - jitter results in a wavy streak perpendicular to the scan.

i) Modeling - this is due to the film aging or the film degrading due to improper storage. This effect is similar to that obtained if haze tones are scanned (spotty).

j) Hum - coherent bars diagonally across the picture at the repetition rate of the frequency of hum.

k) Coherent noise - this appears as black and white streaks or hash parallel to the scan lens at evenly spaced intervals.

l) Phase delay distortion - phase delay distortion results in the convergence and spreading of the lines in the standard resolution wedge. This also results in echos near lettering, etc.

m) Bandwidth limitation - bandwidth limitation results in convergence of the lines of the standard resolution. Transient effects may also be present when a rapid transition from full black to full white occurs.

14. Spin modulation - spin modulation results in bars diagonally across the picture at a repetition rate which is related to the spin rate. (See example of calculation of spin modulation frequency.)

Figure IV-94 shows the above types of effects and percent occurrence for all stations. It should be noted that one picture may exhibit several effects (see Figure IV-99). Other effects such as spin modulation may show a large percent of occurrences, however this is due mainly to the fact that a large number of pictures were transmitted under conditions which would exhibit spin modulation for the purpose of analysis. System effects are as follows: a) Hum; b) Coherent noise; c) Phase delay distortion; d) Bandwidth limitation; e) Noise; f) Spin Modulation. Operator effects are as follows: a) Improper record current; b) Incorrect developing time; c) Level change; d) Picture set on roller. Equipment effects are as follows: a) False starts; b) Salt and pepper; c) Jitter; d) Modeling; e) Improper phasing. One of the more interesting results, directly related to the Syncom system, is the effect of spin modulation. This effect is most pronounced when the satellite antenna aspect angle is poor and the input to the satellite does not fully saturate the transponder. Since the spin rate is close to the scan rate, or a sub-multiple thereof, this effect appears as a herringbone pattern. As an example, assume that the spin rate is exactly the same as, or is exactly a sub-harmonic of the scan rate of the facsimile set. Under these conditions, a bar would appear lengthwise of the picture (see Figure IV-95). By knowing the scan rate, therefore, and measuring the angle between the scan line and the diagonal bar due to spin modulation, the spin rate can be calculated. For example, for one picture, a spin rate of 124.1 rpm was calculated; for that same time, the spin rate determined from telemetry was 126.3 rpm. Example of spin modulating is shown in Figure IV-99c. Under normal operating conditions, the effects of slight spin modulation on the overall picture quality is very minute.

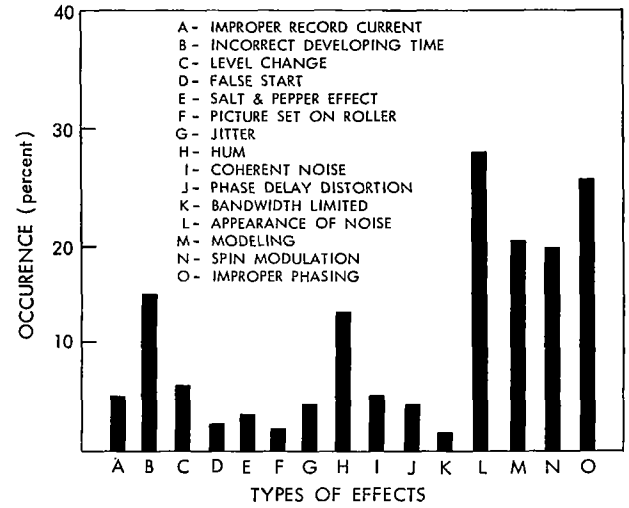

Figure IV-94—Syncom II communication experiment, facsimile test effects for 113 pictures from all stations.

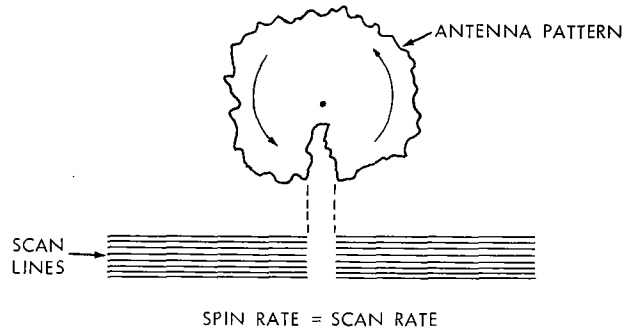

Figure IV-95—TV picture transmitted when spacecraft spin rate is equal to, or a submultiple of, the facsimile set picture scan rate.

It is possible to determine with a reasonable degree of accuracy the bandwidth of the circuit from the standard resolution wedge. One scan across the resolution wedge produces a series of square waves (see Figure IV-97). If the circuit bandwidth is sufficient to pass all the components of the square wave, the resolution is preserved and if the circuit bandwidth is insufficient to pass all the components of the square wave, the resolution is poor. By knowing the highest frequency which is resolved, the bandwidth can be determined as twice the frequency.

EXAMPLE:

Assume the lowest point that can be resolved is .004 inches. The total width of the wedge at this point is .004 inches x 29 = .116 inches. At 240 scans per minute, each scan is equal to .25 seconds. The time required to scan .116 inches is therefore equal to

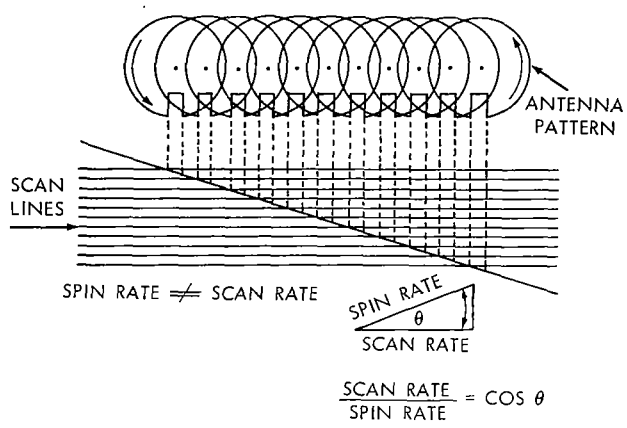

Figure IV-96—TV picture transmitted when spacecraft spin rate is not equal to picture scan rate.

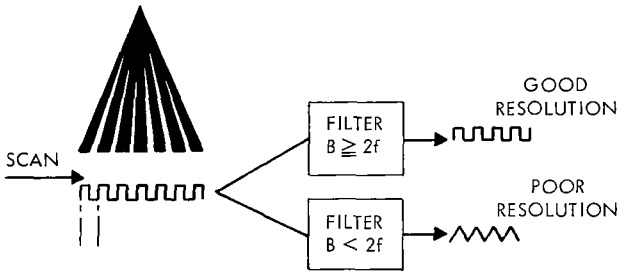

Figure IV-97—Determination of circuit bandwidth from a scan across the resolution wedge.

$$\frac{.95 \text{ sec}}{3.25 \text{ inches}} = \frac{x}{.076 \text{ inches}} ,$$

$$x = \frac{.25 \text{ sec} \times .116}{3.25} = \frac{.029}{3.25} = .0089 \text{ seconds} .$$

The period of one square wave cycle = .0088/14.5 = .000614,

$$f = \frac{1}{P} = \frac{1}{.000614} = 1628, \text{ and}$$

$$B \square 2f = 3256 \text{ cps} .$$

In the narrow-narrow mode the 3 db bandwidth is 1.7 kc for a particular station. Therefore the lowest point that can be resolved on the resolution wedge is as follows:

$$B = 2f = 1700 \text{ cps} ,$$

$$f \square 850 \text{ cps} ,$$

$$P = \frac{1}{f} = \frac{1}{850} = .001175$$

The time required to scan 14.5 cycles $\doteq$ .001175 × 14.5 = .017 × = 3.25 In. × .017/.25 = 222 □ total width of lowest point on the resolution wedge that can be resolved.

.222/29 = .00765 = lowest point on the resolution wedge that can be resolved with a bandwidth of 1.7 kc.

Figure IV-98 shows normal skewed distribution curves which have been fitted by at least squares techniques to the numerical ratings for gray tone, resolution, picture quality and overall picture value. The mean numerical ratings and standard deviations for the different categories are shown in the following manner.

CATEGORY	MEAN	84%
Gray tone	7.3	4.4
Resolution	8.5	6.0
Picture Quality	6.9	4.1
Overall Picture Value	7.7	4.7

Examples of perfect copy and some of the more common system, machine, and operational effects are shown in the following figures.

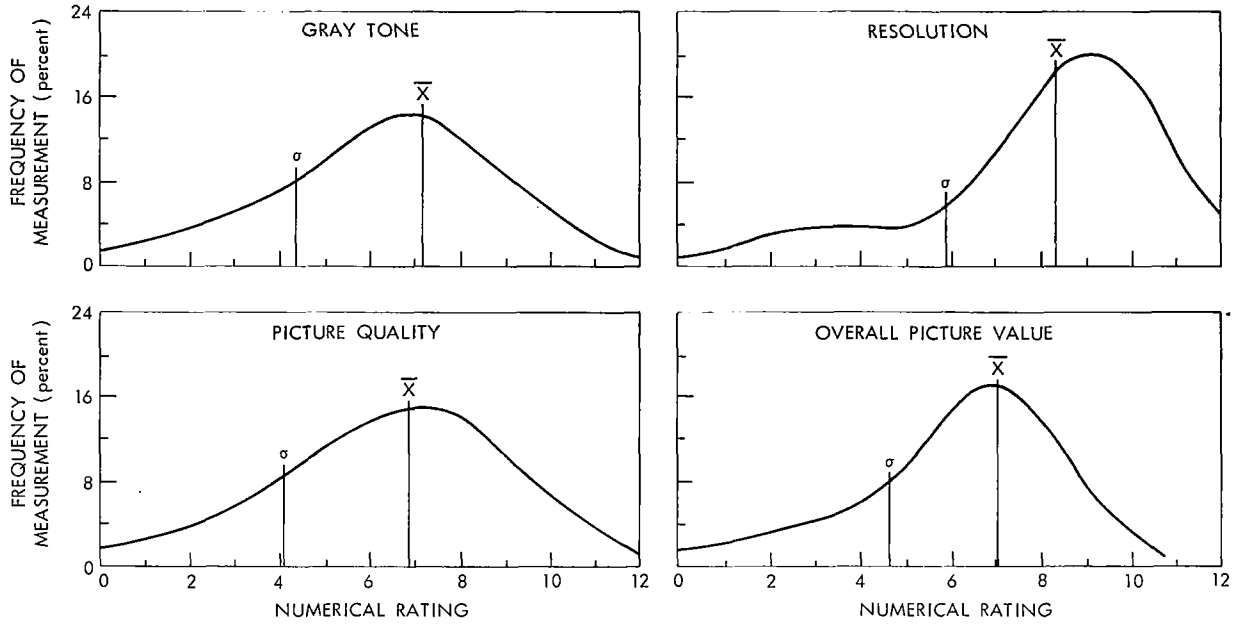

Figure IV-98—Syncom II communication experiment, facsimile distributions, frequency of measurement vs. numerical rating.

Figure IV-99a shows a perfect resolution wedge reproduction. Note that the wedge can be resolved below the .004 inch point.

Figure IV-99b shows perfect gray tone reproduction. Note that differences in shades of gray can be distinguished at the third level from maximum white and maximum black.

Figure IV-99c shows the effects of spin modulation.

Figure IV-99d shows a combination of effects. The picture is out of phase. There is a loss of signal near the end of the picture. The effects of modeling are pronounced and the picture is underprinted.

Figure IV-100a shows good reproduction received under moderate signal-plus-noise to noise conditions.

Figure IV-100b shows a picture received under extremely poor ratios of signal plus noise to noise.

Figure IV-101a shows an example of the receiver breaking lock.

Figure IV-101b shows the effect of hum.

Figure IV-102 shows the effects of phase decay distortion. Note the convergence and spreading of the resolution wedge. Also note ghost images near the lettering.

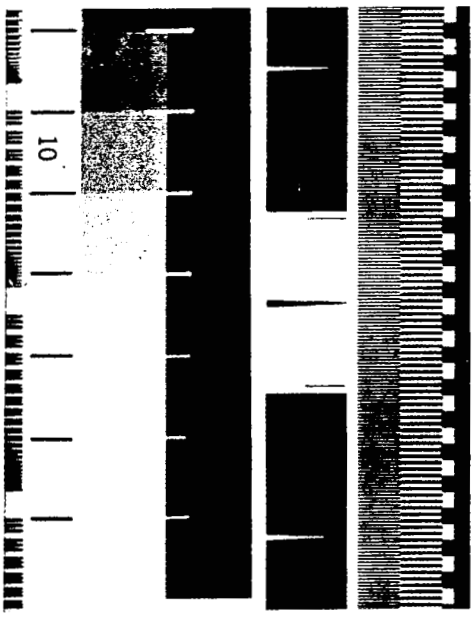

a. Perfect Resolution Chart-Rating
10-10-10

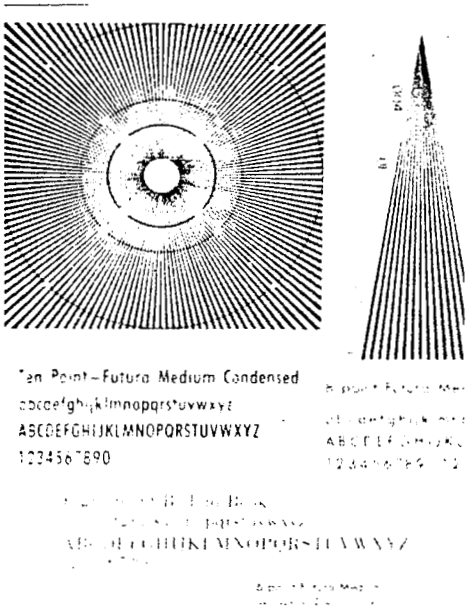

b. Perfect Gray Tone Chart-Rating
10-10-10

c. Gray Tone Chart showing Spin
Modulation Rating 8-9-8

d. Various System Faults-Rating 8-8-6

Figure IV-99—Syncom II communication experiment, facsimile pictures.

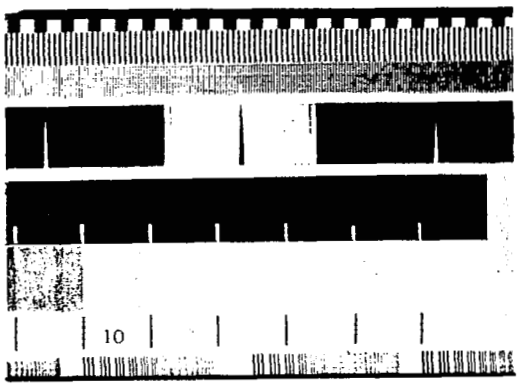

Rating - 7 - 9 - 6
Mode - 2
Signal-Plus-Noise to Noise - 13 db
Communication Carrier Level - -122
Transmitter Power - 4 kw
Elevation Angle - 43
Receive Station - 1
Transmit Station - 1
Good Reproduction Under Medium
Signal-Plus-Noise to Noise Conditions

A

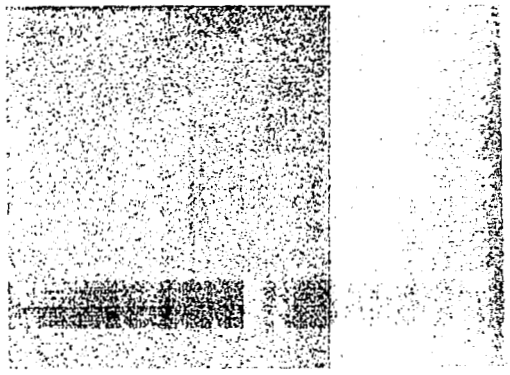

Rating - 1 - 1 - 1
Mode - 1
Signal-Plus-Noise to Noise - 4 db
Communication Carrier Level - -135
Transmitter Power - 4 kw
Elevation Angle - 62.2°
Receive Station - 3
Transmit Station - 1
Very Poor Signal-Plus-Noise to Noise; Out of Phase;
Loss of Signal

B

Figure IV-100—Facsimile pictures. (a) Good reproduction received under medium signal-plus-noise to noise conditions. (b) Picture received under extremely poor ratios of signal-plus-noise to noise.

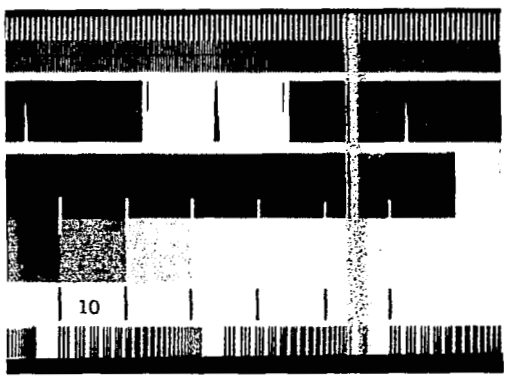

Rating - 10 - 10 - 9
Mode - 3
Signal-Plus-Noise to Noise - 37
Communication Carrier Level - 113
Transmitter Power - 5 kw
Elevation Angle - 64.3°
Receive Station - 2
Transmit Station - 4
Loss Lock; Slightly Overprinted

A

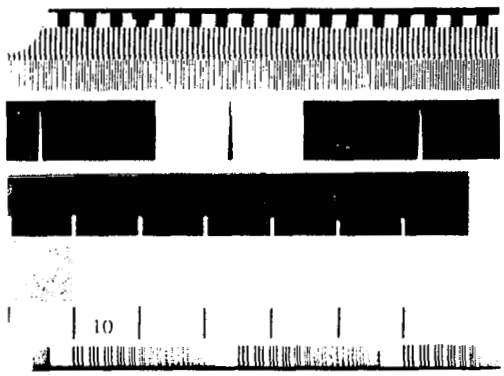

Rating - 9 - 10 - 9
Mode - 3
Signal-Plus-Noise to Noise - 32 db
Communication Carrier Level - -117
Transmitter Power - 10 kw
Elevation Angle - 14.7°
Receive Station - 2
Transmit Station - 1
Hum; Improper Spreading of Developing Fluid

B

Figure IV-101—Facsimile pictures. (a) An example of the receiver breaking lock. (b) The effect of hum.

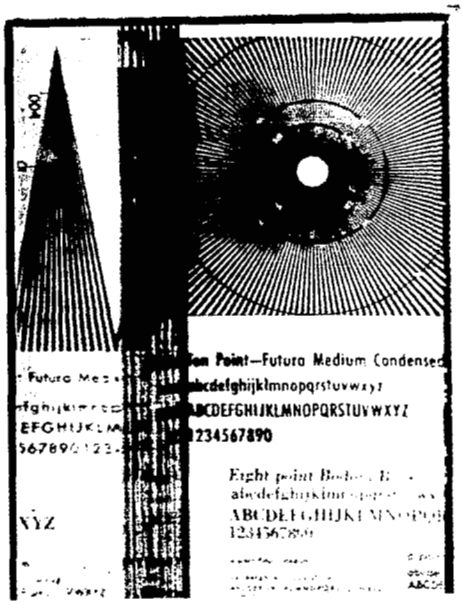

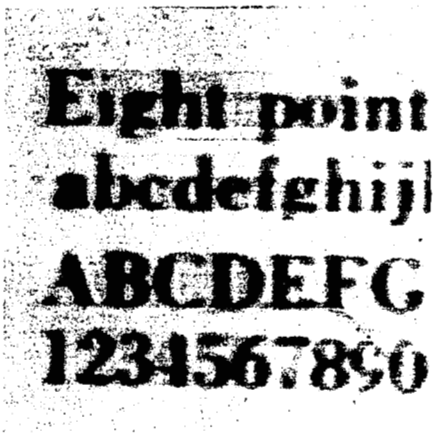

Rating - 7 - 6 - 7
Mode - 3
Signal-Plus-Noise to Noise - 33 db
Communication Carrier Level - -108.5
Transmitter Power - 10 kw
Elevation Angle - 37.8°
Receive Station - 3
Transmit Station - 3
Phase Delay Distortion; Dirty Phasing Contacts

Figure IV-102—The effects of phase decay distortion.

CHAPTER V

SPACECRAFT PERFORMANCE

The performance of Syncom II is satisfactory. Close correlation exists between the actual and the predicted performance. This conclusion is based on telemetered information, results of communications experiments, and spacecraft attitude and position data.

The accumulated information has been analyzed and compared with prelaunch predictions. Based upon this analysis, the following conclusions are offered:

a) All mission objectives have been met.
b) All spacecraft systems have been utilized successfully.
c) The telemetered data has shown no evidence of degradation in any of the spacecraft electronics.
d) The ambient spacecraft internal temperature (65° to 75° F) is near that expected.
e) The station keeping capacity of the hydrogen peroxide control system remaining after the latest orbital correction (November 24, 1963) is equivalent to at least eight more years of controlled operation if required corrections are limited to corrections of triaxiality disturbances only.
f) Spacecraft operational longevity appears to be limited by its power supply, but it is estimated that from 2 to 5 years of full transponder operation can be expected.
g) A leak in the nitrogen control system has been apparent since the first week in orbit. A decrease in spin speed is believed to be a direct result of the N_2 leak.
h) The eclipse period has had no apparent detrimental effect on spacecraft operation. To the contrary, the solar array voltage has increased since entering the shadowing cycle.

TELEMETRY DATA ACCURACY

The telemetered data are, of course, the prime source of information concerning the spacecraft performance. Analysis of all the error factors involved results in the conclusion that the Syncom II telemetered data is accurate within ±2 percent (based on root-mean-square evaluation of the contributing errors).

Telemetry data analysis is conducted primarily with magnetic and paper strip chart recordings of data recorded at the various ground stations. In addition, the "quick-look" telemetry data or VCO (voltage-controlled-oscillator) frequency readings, representing telemetry quantities, have been utilized. The magnetic tapes have been processed to allow each decommutated segment of the telemetry pulse train to be plotted separately on scaled paper at low speeds. With the use of calibrated overlays; the telemetry data can be read out directly. The accuracy with which the spacecraft parameters can be determined is limited, to a degree, by the following:

a) circuitry tolerances relating to calibration or reference voltages,
b) stability of the subcarrier oscillator,
c) effect of various load and voltage conditions on reference voltages,
d) calibration and accuracy of the transducers, and
e) ability to accurately read and reduce the telemetry data.

A theoretical analysis of the reference voltage circuitry and the subcarrier oscillator was made to determine the effects of the first three factors on telemetry accuracy. It was concluded that the contribution is about ±1 percent; this conclusion is based on the data that follow.

Error Magnitudes in Reference Voltage Circuitry

The circuitry related to the -9 volt reference voltage is shown in Figure V-1. The -9 voltage reference depends upon the current through the zener diode CR1, which is a 9 volt zener ± 0.45 volt at 25° C, 7.5 milliamperes. The voltage temperature coefficient is 0.001 percent/°C, and its zener impedance at 7.5 milliamperes is 20 ohms. The zener voltage will change a maximum of 0.001 percent/°C × ±25° C × 9 volts = ±2 millivolts. This means that the -5 volt supply could change by 5/9 × ±2 millivolts = ±1 millivolt. The voltage at the anode of CR2 can change approximately ±66 millivolts. The gas pressure transducer voltage could then change by a maximum of

$$\frac{2 \text{ kilohm}}{4.25 \text{ kilohm}} = \frac{5 \text{ kilohm}}{10.5 \text{ kilohm}} \ (\pm 66 \text{ millivolts}) = \pm 32 \text{ millivolts} ,$$

or approximately 0.8 percent of reading.

Figure V-1 shows that as an input source is sampled, the commutator switch loads the source by 25 to 45 microamperes, depending on the voltage level. The loading is primarily determined by the 510-kilohm base resistor and the input resistance of the subcarrier oscillator. Since the telemetry encoder is calibrated while the inputs are loaded, only changes in loading will cause loading errors. If component drift should cause the load current to change by even as much as 10 microamperes, the maximum loading errors are tabulated in Table V-1. When a data source is not being sampled, the commutator switch is cut off and the source is not loaded. Thus, motion of the pressure transducer pickoffs has absolutely no effect on the -5 volt reference level. As the temperature changes, the temperature sensor load on the -9 volt line also changes. Typical variation of current through R12 for 50 degrees change is

$$\frac{3.991 \text{ volts} - 1.972 \text{ volts}}{4.99 \text{ kilohms}} = 0.405 \text{ milliamperes} .$$

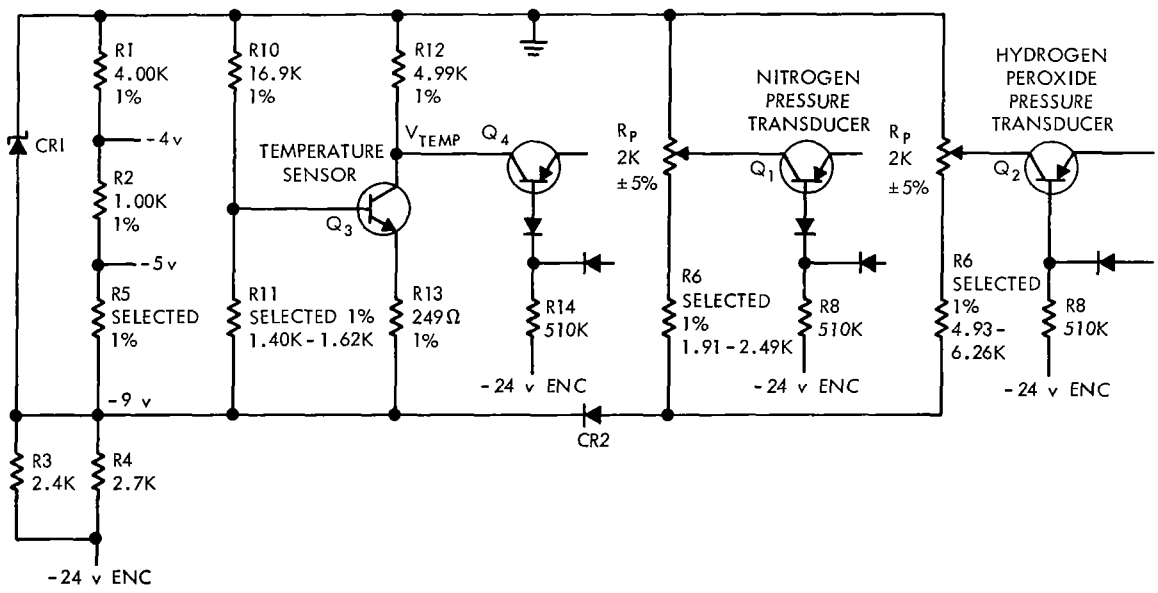

Figure V-1—9 volt reference circuitry.

Table V-1

Loading Errors of the Telemetry Encoder

SOURCE	R OUT (kilohms)	LOADING ERROR (millivolts)	PERCENT OF FULL SCALE
-5 volt reference	2.3	23	0.46
H_2O_2 pressure	1.1	11	0.28
N_2 pressure	2.8	28	0.70
Temperature	4.99	50	1.67

The change in the zener voltage would be 0.405 milliamperes × 20 Z_z = 8 millivolts. The change in the -5 volt reference would be 5/9 × 8 millivolts = 5 millivolts.

Tests performed on the remaining flight spacecraft indicate that transponder operation is not affecting subcarrier frequencies in that spacecraft. However, the following telemetry data received from Syncom II on 27 July 1963 show the effect of transponder operation.

Table V-2

Effect of Transponder Operation from Syncom II on 27 July 1963.

SOURCE	AVERAGE FREQUENCY (kcps)	
	TRANSPONDER OFF	TRANSPONDER ON
-5-volt	15.58	15.61
0-volt	13.47	13.47
Hydrogen Peroxide	14.57	14.58
Nitrogen	14.32	14.325
Temperature	14.66	14.71

Assuming that the -9 volt reference had increased because of RF pickup, the frequency shift is in the correct direction. To have the frequency shift in the -5 volt frequency would mean that the -5 volts had shifted

$$(15.61 - 15.58) \times \frac{5.00 \text{ volts}}{2.11 \text{ kilocycles}} = 71 \text{ millivolts} ,$$

and the -9 volt reference would have had to change

$$71 \text{ millivolts} \times \frac{9.0}{5.0} = 128 \text{ millivolts} .$$

Because the temperature frequency change is larger than the -5 volt frequency change, it is almost certain that the -9 volt reference voltage changes when the transponder goes on or off. As the

pressure transducers were calibrated with the transponders off, the readings taken with only the telemetry system on would be the most accurate.

The power supply regulated -24 volt $_{ENC}$ can change by ± 3 percent so the current through R3 and R4 can change

$$\frac{24.72-9}{2.4 \text{ kilohms}/2.7 \text{ kilohms}} - \frac{23.23-9}{2.4 \text{ kilohms}/2.7 \text{ kilohms}} = 1.2 \text{ milliamperes} .$$

The change in the -9 volt reference supply would then be 1.2 milliamperes × 20 ohms = 24 millivolts. The change in the -5 volt reference would be 5/9 × 24 millivolts = 13 millivolts. Examination of the predicted maximum deviations shows that none are as large as one percent of the 5-volt analog information range (50 millivolts). The largest deviations are caused by the temperature variation of CR2, but since this variation is quite repeatable, it can be calibrated out. Not calibrating it out, the error introduced is still only 0.8 percent of reading. Variations in the -5 volt supply of 5 millivolts constitute a frequency change of 2 cps. If for some reason the -9 volt reference voltage did change by some radical amount, it could be estimated by the shift in the -5 volt synchronous frequency and the pressures and temperatures could still be accurately determined since the voltage divider ratios would remain the same. This accuracy, however, could never be more than ±1 percent of 5 volts (±2 cps).

Error Magnitudes in Subcarrier Oscillator

The stability of the subcarrier oscillator is also important in determining telemetry data accuracy. Some of the key requirements in the procurement specification for the subcarrier oscillator are

Linearity: Output frequency versus input voltage shall be within 0.25 percent of bandwidth from best straight line,
Power supply variation: ± 5 percent power supply variation shall produce a frequency change less than ±1 percent of bandwidth, and
Temperature: Output center frequency variation shall be less than 2 percent of bandwidth over the range 0 to +105° F.

The major sources of telemetry errors, described above, are small enough that the accuracy of the telemetry data can be confidently taken as within the design limits of ±2 percent.

Interaction of Spacecraft Parameters

While the theoretical analysis was being conducted to determine spacecraft telemetry accuracies to be expected, another investigation was begun to observe the interaction of the various spacecraft parameters. These tests were conducted on the remaining flight spacecraft at Hughes' El Segundo facilities.

The first test was made to determine the effects on various system parameters of a changing unregulated bus voltage. All telemetry channels were monitored as the bus voltage was decreased, in steps, from 35 to 20 volts. Between bus voltage ranges of 25 to 33 volts, the range so far experienced by Syncom II, no changes were observed in other telemetered data. The second test was made to determine the possible line loading effect of the nitrogen transducer on the telemetered unregulated bus voltage. The unregulated bus voltage was monitored while the nitrogen pressure was lowered from 1000 to 500 psi; no change in telemetered bus voltage was noticed.

Accuracy of Telemetry Transducers

The telemetry transducers are accurate within ± 2 percent of full scale indications. The accuracy, however, is not as important as the repeatability, since inaccuracies are calibrated out. Prior test results indicate that the transducers will generally repeat within approximately 0.5 percent. The calibration of each transducer is performed with precision test equipment, but is regarded as being no better than one percent of full scale.

Accuracy of Data Reduction

The telemetry data cannot be read, either in strip chart form or VCO form, to an accuracy greater than one percent. If the pulse amplitude-modulated signal is noisy, the inaccuracy is certainly increased. In reading the telemetry data in VCO form, the least significant digit represents approximately one percent of the total possible change. For example, the smallest nitrogen pressure change that can be noted is 30 psia.

SPACECRAFT TEMPERATURE

An analysis of telemetered temperature data shows that spacecraft temperatures generally agree with predicted temperatures. Temperatures measured at a point in the spacecraft near one of the communication traveling-wave tubes show a variation of approximately 25° F as the traveling-wave tube is turned on and off. It is estimated that the temperature in the interior of the spacecraft near the hydrogen peroxide and nitrogen tanks is staying within the range of 65 to 70° F. The temperatures measured at the point near the traveling-wave tube should vary seasonally between 75 and 104° F (with the traveling-wave tube operating) because of changes in the sun angle and the distance to the sun.

Since the temperature varies throughout the spacecraft, no ideal location exists for locating a sensor to measure a single representative spacecraft temperature. The two sensors were located at points near two representative varying spacecraft loads, as shown in Table V-1. Since telemetry subsystem 1 us used most of the time, the data presented here are from temperature sensor 2. Data obtained from temperature sensor 1 show that under comparable operating conditions the data received from the two temperature sensors agree within 2° F. (Data from sensor 2 with the traveling-wave tube off were compared with data from sensor 1 after telemetry transmitter 1 had been off for at least 40 minutes.)

Table V-3
Location of Temperature Sensors

TEMPERATURE SENSOR	LOCATION	TELEMETRY SUBSYSTEM
1	Near telemetry transmitter 1	2
2	Near traveling-wave tube 2	1

Analysis of Telemetered Data

Temperatures telemetered from temperature sensor 2 are shown in Figure V-2. The marked effect of transponder 2 operation on the temperature is evident. The transponder-off temperature, 75° F at launch, decreased to 50° F prior to apogee motor firing. The effect of apogee motor firing

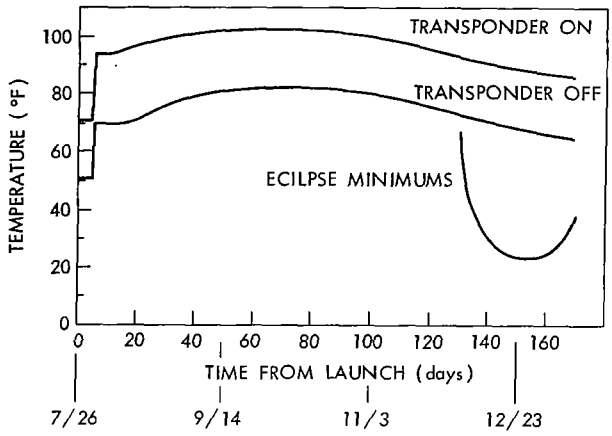

Figure V-2—Temperature (sensor 2).

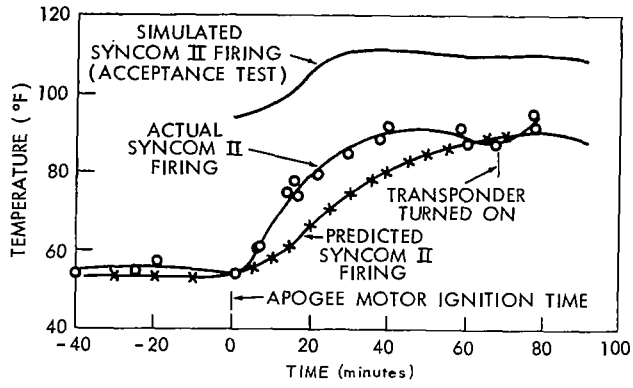

Figure V-3—Actual and predicted spacecraft temperatures during apogee motor firing.

is not evident on the figure; it is shown on an expanded scale in Figure V-3. After the thermal environment stabilized following apogee motor firing, the temperature was approximately 50° F with transponder 2 off, and 73° F with transponder 2 on.

Spacecraft reorientation on 31 July (5 days after launch) changed the sun angle, θ, from 64 degrees to approximately 101 degrees (measured from the positive roll axis). The increase in sun angle allowed partial solar illumination of the antenna end of the spacecraft and resulted in 20° F increases for both the on and off operational modes. A second reorientation on 18 August increased the solar angle from 103 to 106 degrees, which correspondingly increased the temperature levels from 71 and 96° F to 75 and 98° F for nonoperating and operating conditions.

Actual and predicted temperatures during apogee motor firing are given in Figure V-3. Also shown are temperatures that were recorded during simulated motor firing in the spacecraft acceptance tests. The maximum temperature actually reached following apogee motor firing agreed with the prediction, but its increase was faster than predicted.

Syncom II Spacecraft Thermal Control Evaluation

The available telemetry data received from the Syncom II spacecraft has been analyzed for the purpose of correlation to an existing detailed analytical thermal model in the hope that ultimate temperature prediction of all areas within the vehicle can be achieved. The data analysis has been directed toward discussions of

a) Evaluation of the Analytical Thermal Model
b) Predicted Satellite Temperature Distributions
c) Eclipse Temperature Predictions
d) Correlation of Prediction to Telemetry

Evaluation of the Analytical Thermal Model

During the first two months of spacecraft operation, an effort has been made to correlate the existing flight data to the total vehicle thermal model so that reliable estimates may be made of temperature of other portions of the vehicle. The data to be matched by the analytical model consists of essentially four points: i.e., operating and nonoperating rib (S-2) temperatures with the sun on the apogee motor end of the spacecraft, and operating and nonoperating rib (S-2) temperatures with solar illumination on the antenna end.

Initial comparison of prediction and actual flight data indicated a 20° F error, greatly in excess of the established ±11° F prediction tolerance. After adjustments were made in both the effective solar absorptance and infrared emittance of the antenna mechanism cavity, correlation of flight data and analytical prediction was achieved for transponder-off operation. However, subsequent to these analytical modifications, transponder-off data correlation was still not achieved, thus indicating further analytical model error.

Since it was observed that the lack of correlation occurred during the high-power operation mode (TWT on) where localized hot spots exist and internal component and structure modeling is of prime importance, it was decided to re-examine, in detail, the entire analytical model.

For direct comparison of the analytical model and the flight spacecraft, the Y-1 prototype spacecraft and the T-4 structure were made available for use as visual aids. Each nodal point of the thermal model was located and labeled on either the Y-1 or the T-4 structure. The interconnecting radiation and conductance coefficients were then estimated and compared with the previously assigned values. Several discrepancies were noted and the thermal model was modified to correct these variations.

Predicted Satellite Temperature Distributions

The modified analytical thermal model has been utilized to predict spacecraft temperature distribution of sun angles of 70°, 90°, and 110°. Both high-power (TWT No. 2 and Telemetry System No. 1) and low-power predictions (Telemetry System No. 1) have been made. Figures V-4a through V-4d, V-5a through V-5d, and V-6a through V-6d are for sun angles of 70°, 90°, and 110°, respectively. The assumed electrical power dissipations are given in Table V-2.

A comparison of the present analytical model predictions and the temperatures observed from the telemetry data is presented in Table V-2.

It is interesting to note (Figure V-4a) that with the sun on the apogee motor end (β = 70°), that the apogee motor case is at approximately 90° F or 20° F above the vehicle bulk temperature. The motor case is apparently receiving energy from the nozzle attach ring which is predicted to be at 116-119° F for this solar angle. Fortunately, exploratory analyses have indicated that a 10° F change in motor case temperature results in only a 1° F of change in vehicle bulk temperature.

Table V-4

Comparison of Predictions and Actual Flight Data

MODE/SOLAR ANGLE	PREDICTION	TELEMETRY
Telemetry System No. 1 on		
β = 70°	56° F	52° F
β = 90°	67	66
β = 110°	79	81
Telemetry System No. 1 and TWT No. 2 on		
β = 70°	76	74
β = 110°	97	101

Table V-5
Spacecraft Current Requirements

SPACECRAFT SUBSYSTEM ON	CURRENT REQUIREMENTS (milliamperes)
Telemetry Subsystem 1	370
Telemetry Subsystem 1 and Communication Receiver 1	480
Telemetry Subsystem 1, Communication Receiver 1, and Traveling-wave Tube 1 Filament	565
Telemetry Subsystem 1, Communication Receiver 2, and Traveling-wave Tube 1 Filament	580
Communication Receiver 2 and Traveling-wave Tube 2 Filament And High Voltage	610
Telemetry Subsystem 1, Communication Receiver 1, and Traveling-wave Tube 2 Filament And High Voltage	910
Telemetry Subsystem 1, Communication Receiver 2, and Traveling-wave Tube 2 Filament And High Voltage	925
Telemetry Subsystem 1, Receiver 2, and Traveling-wave Tube 1 Filament And High Voltage	1010

For the condition with the sun on the antenna end of the vehicle ($\beta = 110^\circ$), Figure V-6a, it is noted that the motor case is predicted to be 60-65° F or 15-20° F below the bulk vehicle temperature. In this orientation, the nozzle attach ring is at 43-48° F and is acting as a radiator drawing energy from the motor case.

Eclipse Temperature Predictions

In early December, 1963, Syncom II entered the first eclipse period. Eclipses have ranged in time from 5 to 70 minutes. Transient temperature predictions have been made and are presented for the maximum eclipse time of 70 minutes. Figures V-7 through V-11 indicate the expected vehicle temperature response to the eclipse transient for the 90° solar angle. The solar angle during the current eclipse is very close to 90° and it is felt that the transient predictions made are directly applicable to these eclipses.

Correlation of Prediction to Telemetry

An evaluation of the predictability of the current analytical thermal model is shown in Table V-2. Five different modes of operation have been compared for correlation between actual telemetry and analytical prediction. It can be seen that for all three of the low power cases, the difference between the analytical prediction and S-2 telemetry data is from 2-4° F. This close correlation has lent confidence in the ability of the analytical model to account for the external energy input to

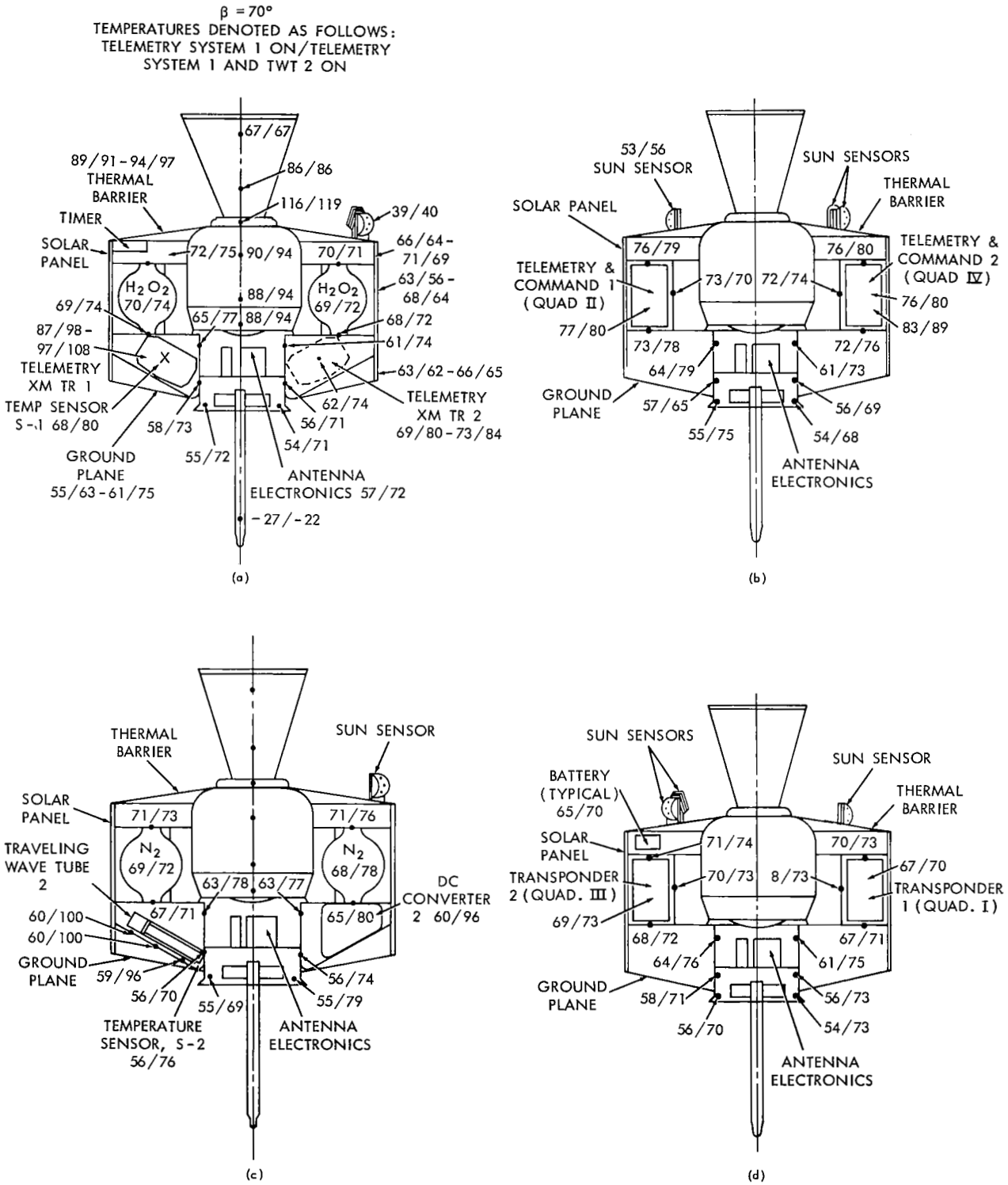

Figure V-4—Syncom 1 temperatures. The sun angle is 70 degrees.

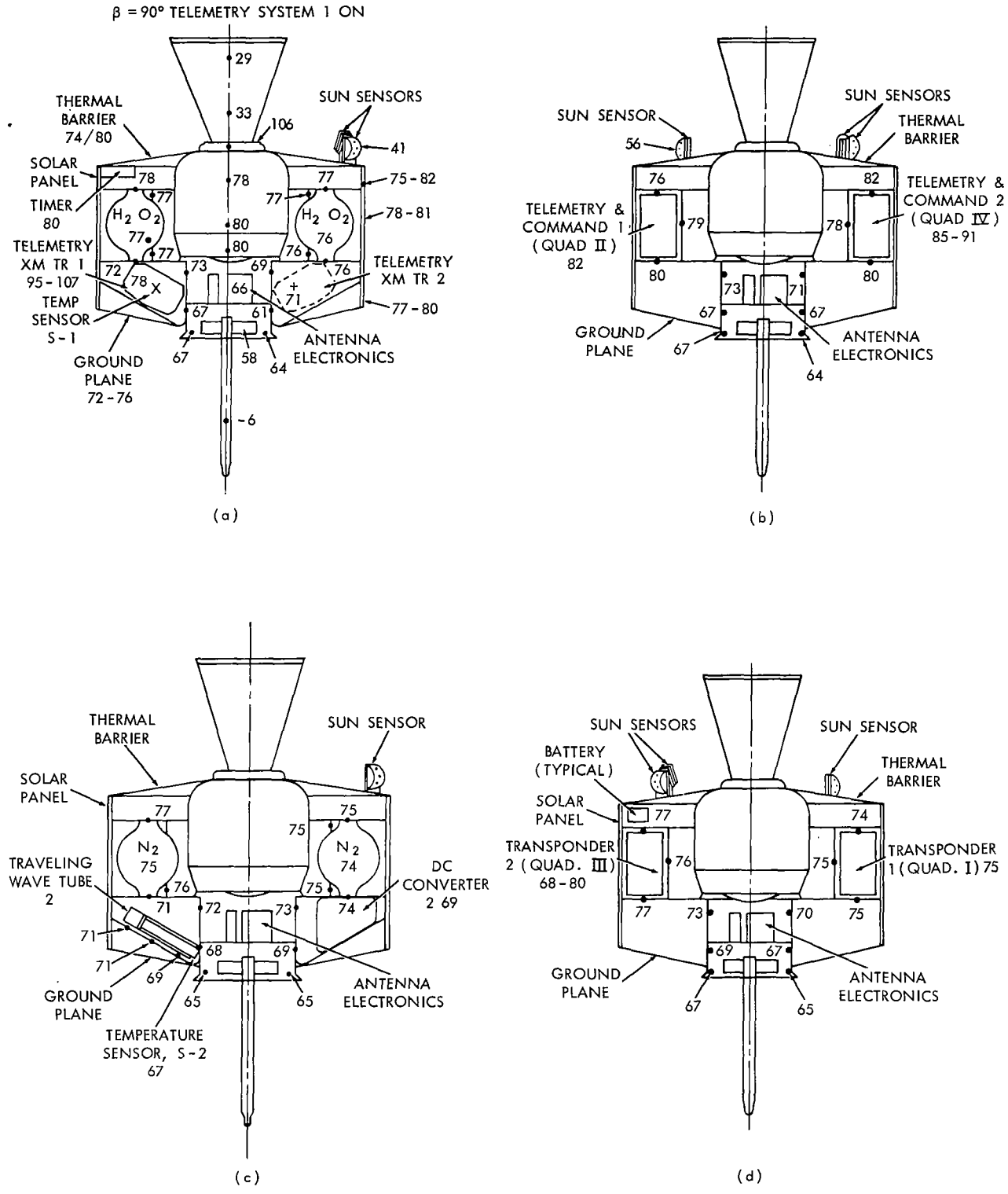

Figure V-5—Syncom 1 temperatures. The sun angle is 90 degrees.

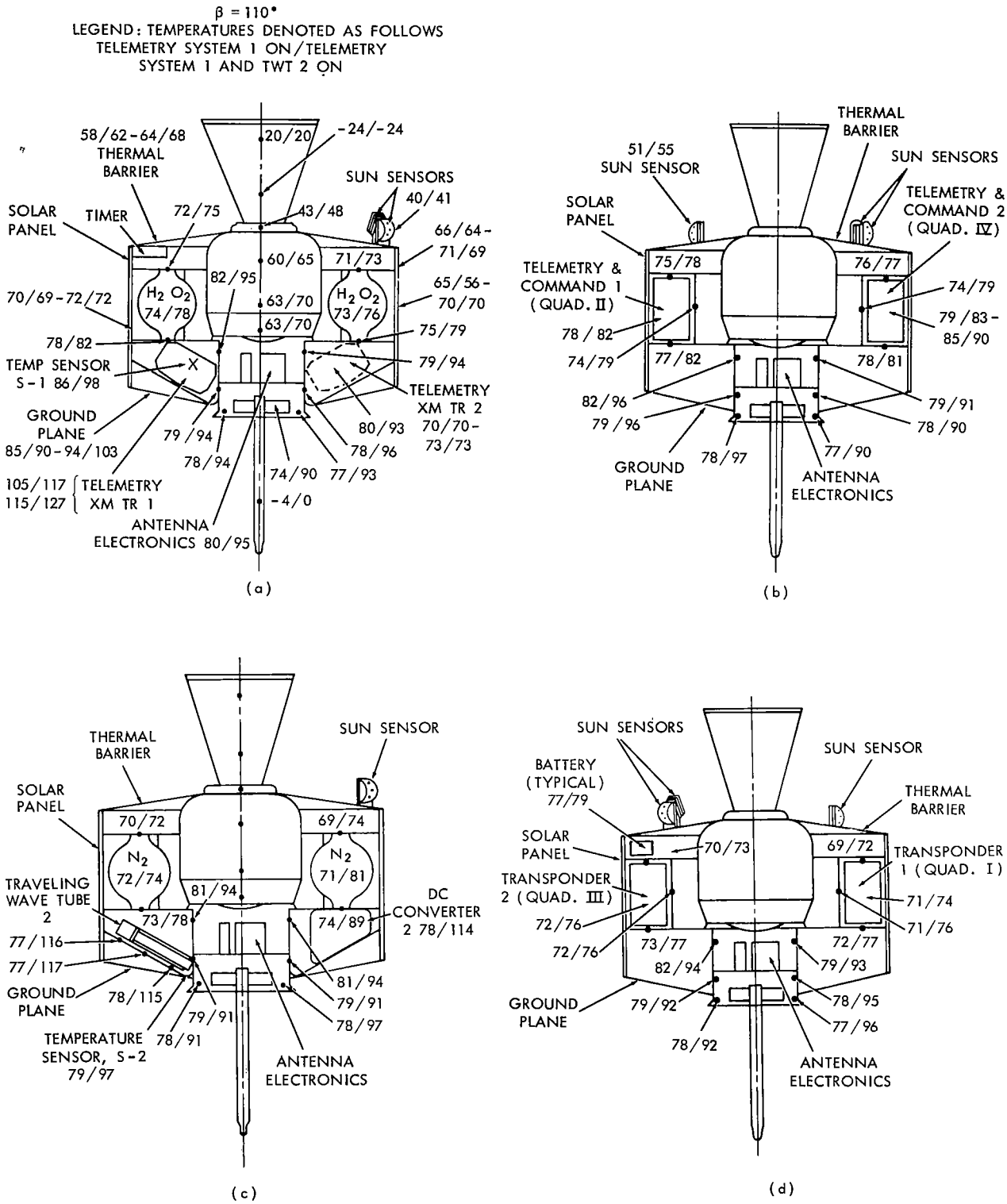

Figure V-6—Syncom 1 temperatures. The sun angle is 110 degrees.

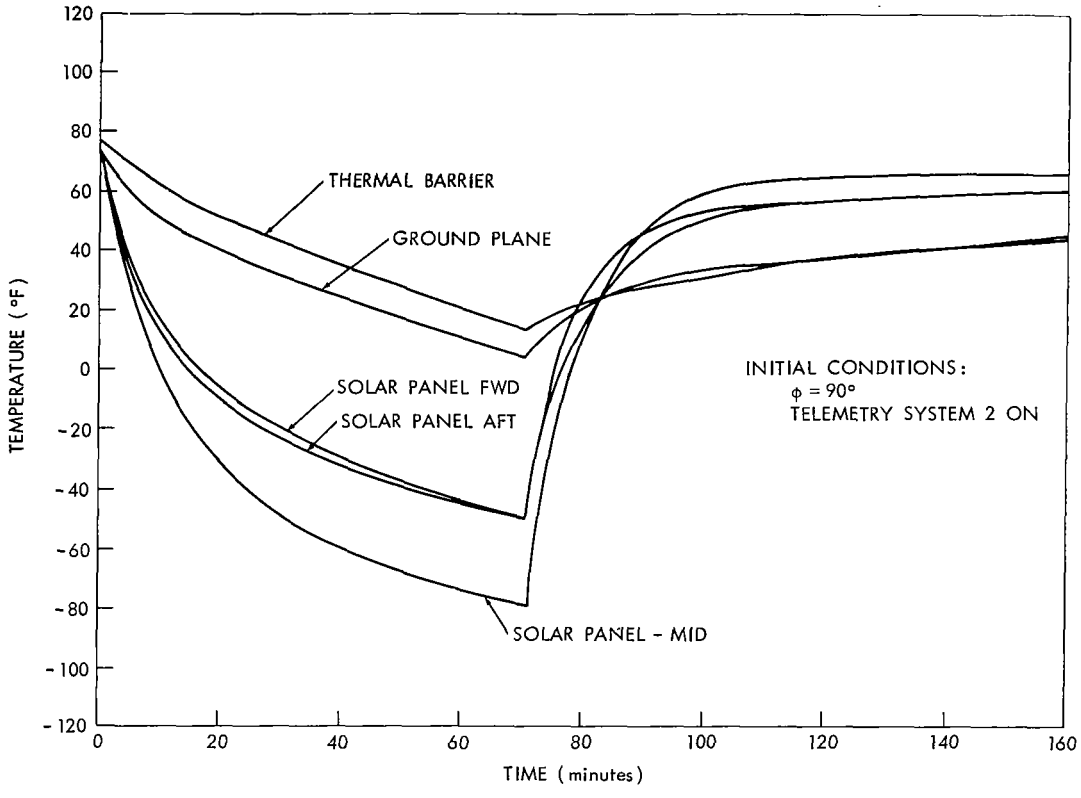

Figure V-7—Typical Syncom II eclipse responses with command receiver on.

the satellite over the complete range of solar angles. The difference between prediction and analysis at the high power modes of operation has also been shown to be in the 2-4° range. This close correlation indicates that correct modeling techniques have been utilized in the region of the TWT's and hopefully throughout the complete interior regions of the spacecraft. It is now felt that the predicted temperatures for other specific locations within the spacecraft are within the accepted engineering tolerance of ±11° F of the actual temperatures.

The comparison of the S-2 sensor transient response prediction and telemetry data is shown in Figure V-12 for the 70 minute eclipse of the 90° solar angle. The drop in temperature during the eclipse is seen to be identical for the prediction and the telemetry, although displaced by approximately 1° F due to that difference in orbital steady state temperature. It can be seen from the comparison of the curves in Figure V-12 that the predicted time for temperature drop does not conform exactly with telemetry; however, the temperature correlation here is again considered satisfactory enough to insure that eclipse temperatures in other portions of the spacecraft are within the allowed engineering tolerance.

SPACECRAFT POWER SUPPLY PERFORMANCE

During the first 170 days of spacecraft operation, the capacity of the spacecraft power supply decreased approximately 20 percent. This decrease was probably caused by a combination of the following factors:

a) normal degradation caused by expected radiation, and
b) unexpected degradation caused by solar flare activity.

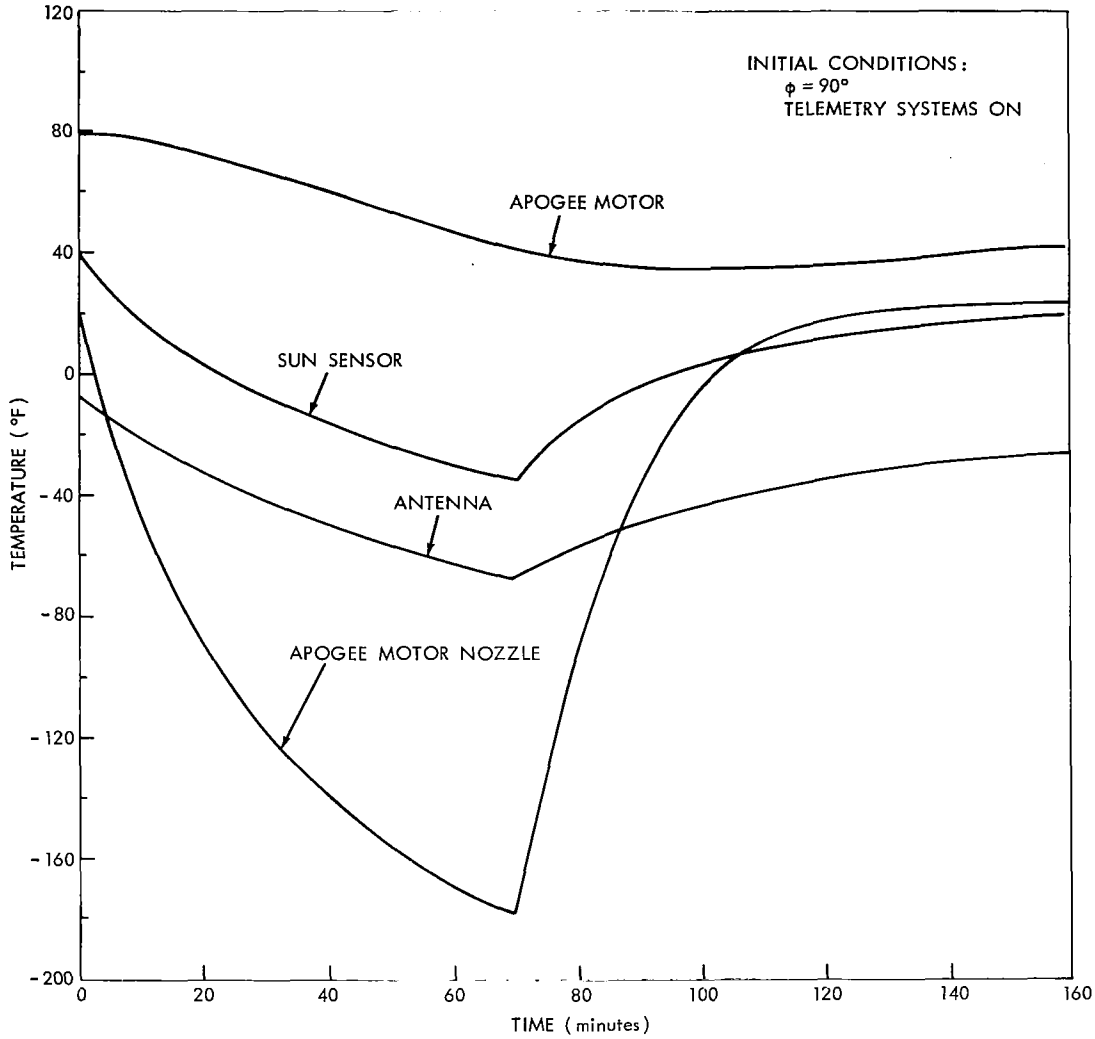

Figure V-8—Typical Syncom II eclipse temperature response with command receiver on.

It is predicted that the power supply performance will be adequate for two years of full time transponder operation.

There are three (3) direct spacecraft telemetered parameters that can be used to determine the power available from the solar array, the state of battery charge, and the solar panel degradation. These parameters are solar string voltage, unregulated bus voltage, and battery voltage. Indirect parameters that can be utilized are traveling-wave tube and telemetry transmitter power outputs. A loss of transmitted power can be converted to an approximate reduction in current drain.

The solar string voltage is not too useful in determining power supply characteristics because it is a measure of the performance of only 1 of 64 strings. Also, the accuracy of the solar string voltage reading is somewhat less than that of the unregulated bus voltage. The solar string data has been useful, however, in determining the intensity and direction of earth illumination.

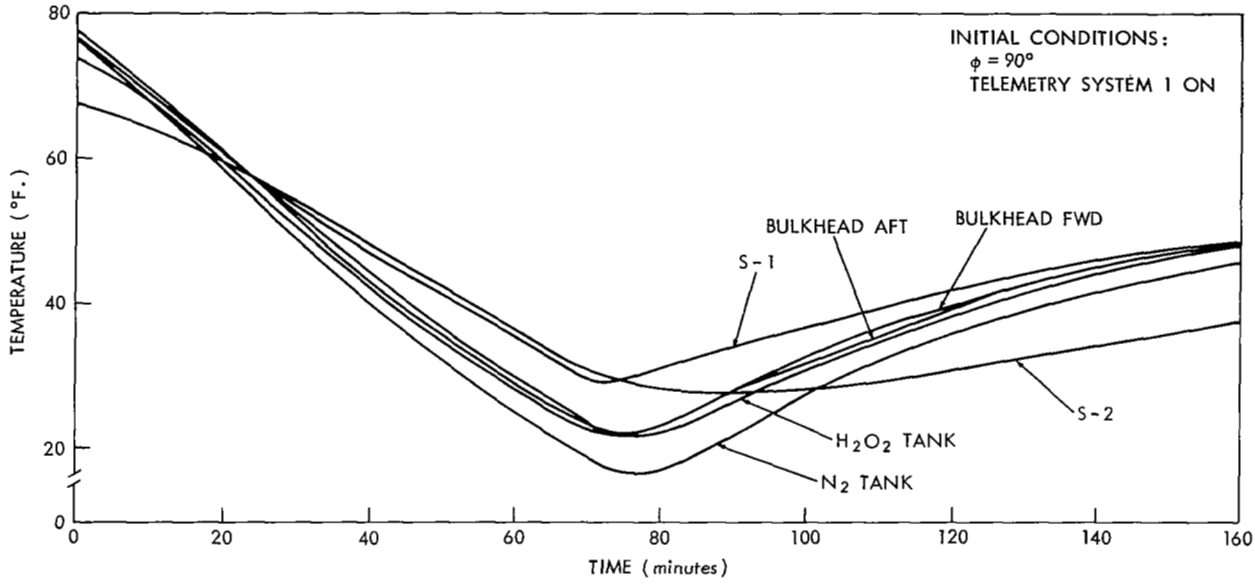

Figure V-9—Typical Syncom II eclipse temperature responses with command receivers on.

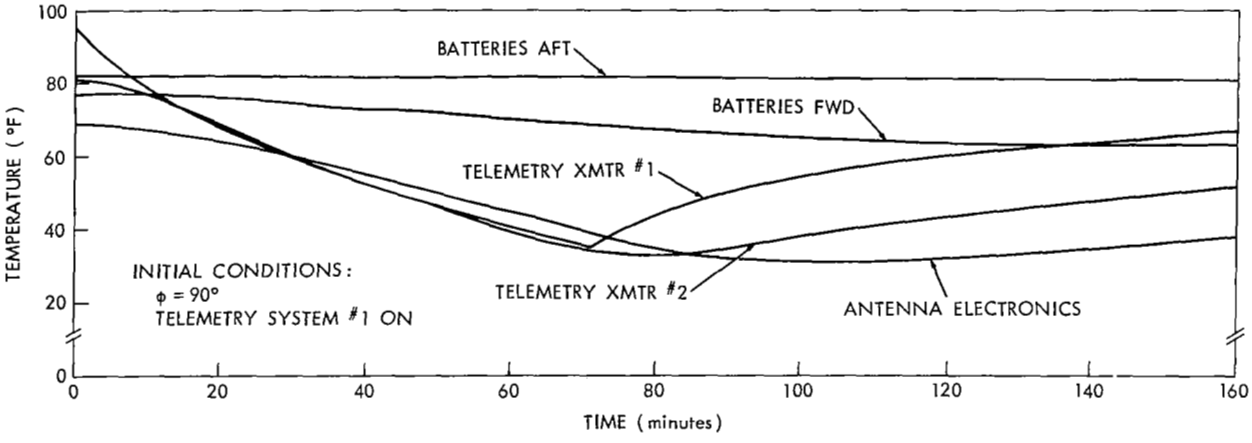

Figure V-10—Typical Syncom II eclipse temperature responses with command receiver on.

Analysis of Telemetry Data

The spacecraft unregulated bus voltage during the first 170 days is shown in Figure V-13; the points represent daily averages rather than continuous data. These data are presented as actually recorded and do not take into account changes in load, duty cycle, sun angle, or sun proximity. Since transponder operation uses the major portion of the available power, the data are presented for transponder-on and transponder-off conditions. The general slope of both curves is approximately the same, indicating only that the available power has decreased.

Investigation of the pulse amplitude-modulated telemetry train from Syncom II reveals a dip in the unregulated bus segment under high power loads (simultaneous transponder and telemetry operation). This dip, very nearly the same as seen on Syncom I telemetry under similar conditions,

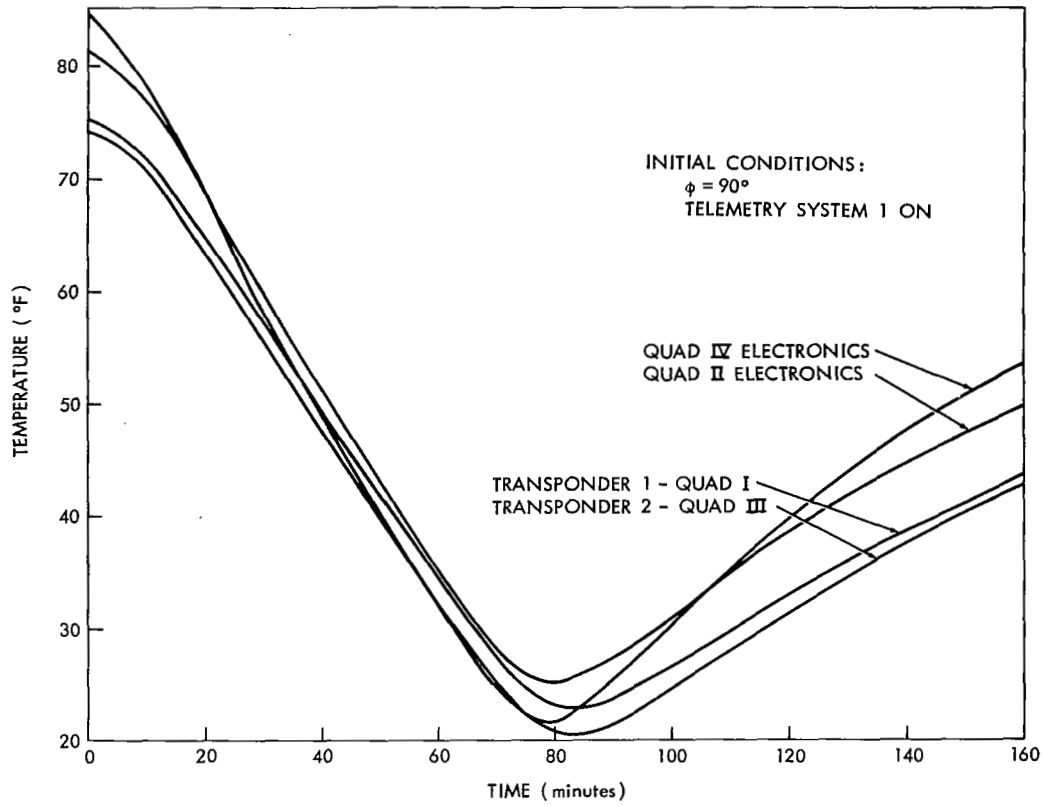

Figure V-11—Typical Syncom II eclipse temperature responses with command receiver on.

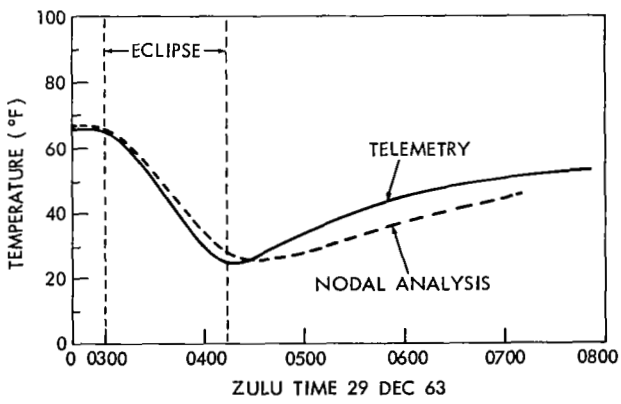

Figure V-12—Syncom II eclipse temperature response prediction vs. S-2 telemetry.

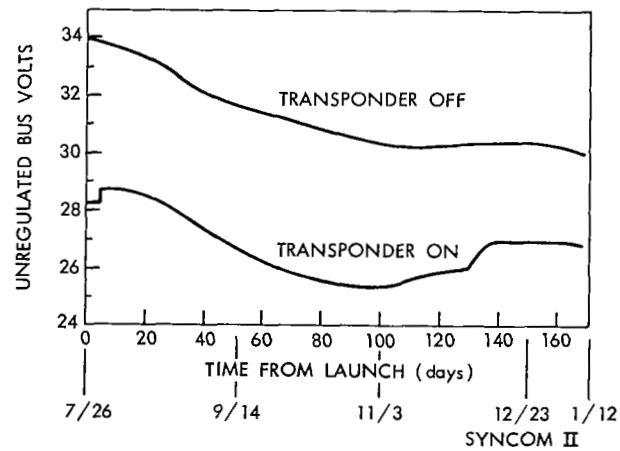

Figure V-13—Unregulated bus voltage.

appears to drop 0.4 volt below the battery voltage. This is equal to the differential that appears when the batteries are supplying the load. From power considerations alone, it is estimated either that 2 of the 64 solar strings are open or damaged, or that one solar panel is contributing less

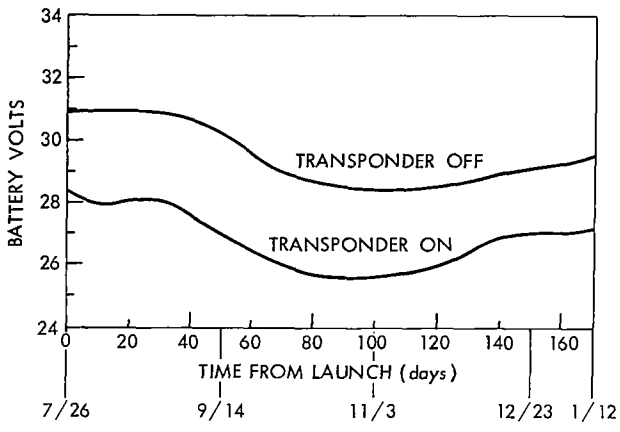

Figure V-14—Battery voltage.

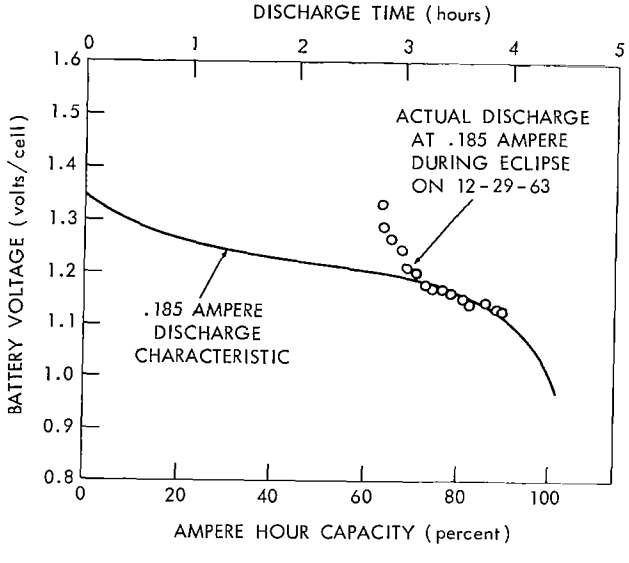

Figure V-15—Syncom II (F-3 spacecraft) battery performance.

power than the other three. The reason for this damage is unknown. The center of this dip is located 60 degrees clockwise from the solar sensor.

The spacecraft battery voltage during the first 170 days is shown in Figure V-14. The batteries were in a fully charged condition before launch and had only to support telemetry operation for 3 minutes without solar power between liftoff and Delta nose fairing removal. The general slope is the same as that of the unregulated bus curves. Although the batteries have not had a full charge since the first 30 days of operation, they have been partially charged on numerous occasions when the transponders have been off. The batteries have supplied a portion of the power when transponder and telemetry operations are simultaneous since the first thirty days in orbit. During the interval following this time, the transponder and telemetry load could not be sustained by the solar array. Since the eclipse season started, it has again been possible to operate transponders and telemetry simultaneously for extended periods of time. The battery state-of-charge is directly dependent on a) the unregulated bus voltage, and b) battery charge regulator characteristics.

The unregulated bus voltage available has been reduced (as a function of time) due to the particulate radiation damage to the solar array encountered since launch. Under current conditions (command receivers only operating) the voltage at the bus is expected to be approximately 31.5 volts. With a 1.2 volt threshold loss across the battery charging regulator only 30.3 volts (1.37 volts/cell) is available for battery charging. Based on Advanced Syncom tests (potential limit charging), approximately 33 percent of the battery capacity could be returned with this charging potential. Figure V-15 represents the battery discharge telemetered data of 12-29-63 showing only 35 percent of the battery capabity had been returned by the previous day of charging.

The initial voltage (at start of discharge) of 1.33 volts/cell indicates no battery cell failures have occurred.

Solar Array Performance

Since precise solar panel temperatures are not telemetered from the spacecraft, only an approximation of the panel operating temperatures is available. This has been calculated to be 77 ±5 °F. This temperature, together with the spacecraft component electrical load demands (measured during acceptance testing), has been used to determine the solar array performance from the telemetered voltages. Spacecraft current requirements are indicated in Table V-3.

Special solar array characteristics tests have been conducted weekly since 27 September 1963; their purpose being the determination of solar array degradation. Spacecraft loads, ranging from 370 ma to 910 ma, are selected by command. For each of these load conditions, bus and battery voltages are monitored for a sufficient period of time to allow the two voltages to come into equilibrium as indicated by a steady bus voltage. At equilibrium it is assumed that the battery is neither charging nor discharging. Using several load points it is then possible to plot a voltage current curve similar to that shown in Figure V-16. From this curve the maximum available power on that particular day can be estimated. The results of a series of weekly estimations are shown in Figure V-17. Plots are shown for measured and normalized power and for the pre-launch power prediction. Based on the results of Figure V-17, it is predicted there will be sufficient spacecraft power available for two years operation of the transponder.

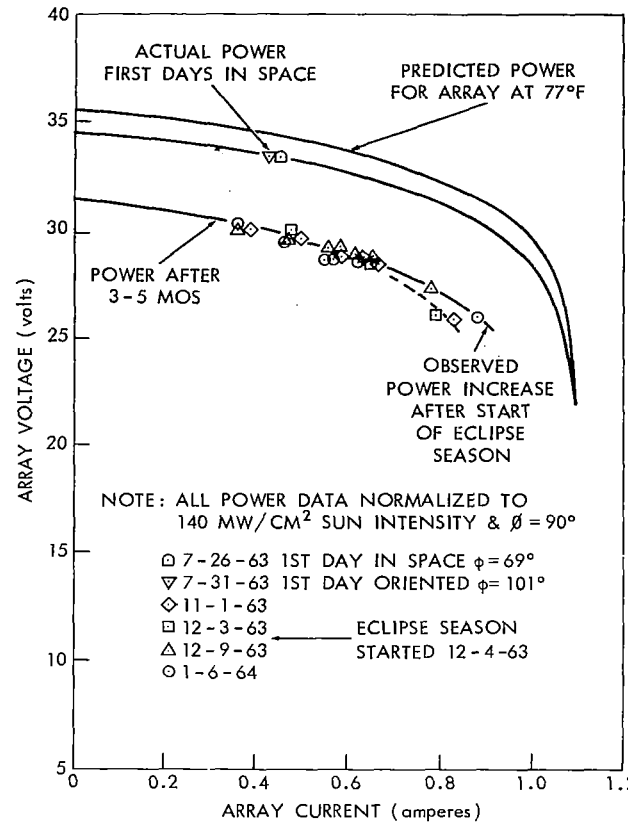

Figure V-16—Syncom II (F-3 spacecraft) solar array electrical power performance.

CONTROL SUBSYSTEM

All functions of the spacecraft control subsystem have been exercised and have performed in a satisfactory manner. The hydrogen peroxide (H_2O_2) unit has performed its mission in both continuous and pulsed modes. The nitrogen (N_2) unit has been utilized in the pulsed mode (ground commanded) and in the quadrant mode (self-contained). The solar sensors are monitored daily for attitude determination. They were used, also, to actuate the quadrant mode jet-pulsing sequences. The accelerometer, nutation damper, and apogee motor timer have also performed as expected.

Hydrogen Peroxide Unit

While the H_2O_2 unit was intended primarily for coarse adjustments of the orbital velocity, it has given excellent performance as a vernier correction system and has satisfactorily performed delicate velocity and attitude corrections. It has been demonstrated that the H_2O_2 system can perform all the intricate maneuvers normally required of the cold gas system. It is therefore reasonable to assume that future Syncom type spacecraft can be equipped with redundant H_2O_2 systems. This is advantageous because the total impulse to weight ratio will be increased.

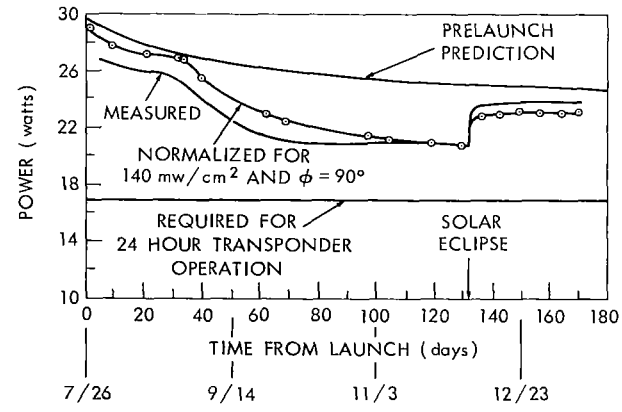

Figure V-17—Solar array power (maximum).

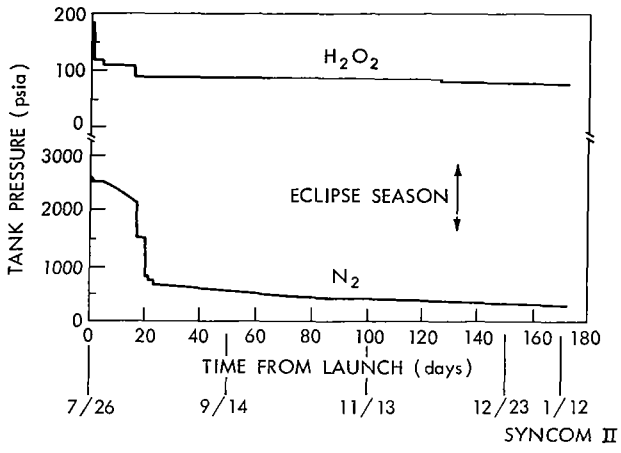

Figure V-18—Hydrogen peroxide and nitrogen pressure.

The Syncom II unit was charged with 4.9 pounds of 90 percent H_2O_2 (98 percent stability) and clean dry nitrogen containing 1 percent helium gas three days prior to the actual launching. Initially the N_2 pressure was 185 psig (charge kit gauge). Approximately 1.5 hours later a reading of 195 psi absolute was obtained from the telemetry subsystem, and 12 hours later the telemetered pressure reading was 178 psi absolute. Intensive leak checks were made, and since no evidence of leakage was found, it was assumed that a leak in the pressure transducer had occurred, accounting for the 1 atmosphere change. Because this problem was not serious enough to forestall launch, the countdown was continued. During the transfer orbit, the pressure appeared to increase to 195 psi absolute, supporting the assumption above.

The hydrogen peroxide pressure as a function of time is shown in Figure V-18. Except for changes caused by pulsing of the jets, no change in pressure is evident (prior to eclipse period). Because decomposition of the hydrogen peroxide would have resulted in a pressure increase, it has been concluded that the hydrogen peroxide is stable. Since the velocity correction on the sixteenth day, the indicated tank pressure has been quite steady at approximately 87 psia. With this pressure, and with an estimated 1.65 pounds of hydrogen peroxide remaining, the unit can provide a calculated total velocity correction of 64 fps, far more than the 6.0 fps required for stationkeeping for one year.

The predicted hydrogen peroxide unit impulse values of 157 seconds continuous operation and 111 seconds in the pulse-spin mode have been verified within the accuracy of orbital tracking and telemetered tank pressure data.

Nitrogen Unit

To realize a pressure in orbit of 2500 psia at 50°F, the nitrogen unit was initially charged to 2620 ± 50 psia at 75°F. The nitrogen pressure as a function of time is shown in Figure V-18. The pressure remained fairly constant at 2550 psia until the fourth day, one day before the orientation maneuver. From this time on, the nitrogen pressure continually decreased, although the leak rate declined after the seventeenth day, when the nitrogen jets were fired for the first time. The leak rate during this 14-day interval was approximately 30 psia per day. From the twenty-third day, the last day the nitrogen unit was used, the leak rate has been decreasing at what appears to be an exponential rate.

Although the rate of leakage can be determined, it is difficult to determine the leak location. It may be in either the jet nozzle or the solder that seals the valve assembly.

Specific emphasis was placed on eliminating nitrogen leaks before launch. Both jet nozzles were checked with a water manometer, with neither showing a sign of leakage. For this reason, plus the lack of pressure change for four days in orbit, a large leak in the jet nozzle is not considered probable.

It is more reasonable to assume that a leak occurred on one of the solder seals. The internal pressure plus launch vibrations could have caused a nitrogen bubble to start working through the solder. Such a bubble could erupt at any time and at any circumferential location. Both of the Syncom II nitrogen valves experienced similar leaks during environmental testing. In each case,

heating the solder resealed it. The leak direction and magnitude can also change as a function of both time and nitrogen pressure. A direction change was indicated by the reversal of spin rate that occurred on the tenth day.

Spacecraft Nutation

An effort was made to determine the effect of pulsing control system jets on spacecraft nutation. There are two possible methods of obtaining this information, neither being sensitive enough to reveal a nutation. The first method involves observing a systematic change in the frequency of the ψ pulses (frequency of spacecraft revolution). Because of the uncertainty of the nutation frequency, long lists of spacecraft spin speeds were compiled for the times in question. The natural dispersion of the data prevented extraction of nutation information. The second course of information was the telemetered accelerometer data. Since the acceleration forces caused by the pulsing of a jet were on the order of 0.01 g, the 0.5 g noise on the acceleration channel prevented any meaningful analysis. There is no reason to believe, however, that any significant nutation exists.

Jet Misalignment

Misalignment of the hydrogen peroxide and nitrogen jets in roll will produce a change in spin speed. Misalignment of the jets in pitch will change spacecraft attitude. Both effects have been noted in Syncom II.

All four jets in Syncom II were unintentionally aligned with a slight bias in the negative spin direction, although the measured alignment was well within the performance requirements.

Corrections executed through the hydrogen peroxide axial jet produced spin rate changes very nearly as predicted. Nitrogen axial jet use has been so limited that no real conclusions can be drawn as to its behavior regarding spin rate. Corrections executed through the two lateral jets, however, produce much greater changes in spin speed than were predicted. The reason for this apparent misalignment is not completely understood. Several possibilities are

a) misalignment of the jets prior to launch by error or improper procedures,
b) jarring or vibration during shipment or launch, or
c) assumption that alignment data obtained prior to Syncom I launch regarding optical versus dynamic alignment of hydrogen peroxide jets holds true for all Syncom spacecraft.

During ground system check of Syncom II, all four jets were aligned in roll by aligning the spacecraft on the spacecraft assembly fixture, which is a precision indexing head on a level tooling plate. Machined jet mandrels were then inserted into the jet nozzle. A theodolite was leveled and its crosshairs aligned on the spacecraft spin axis. In the case of the lateral jets, the jet was aligned in roll until the tip of the alignment mandrel fell in line with the nozzle throat center. In the case of the axial jets, the jets were aligned so that two machined sections of the mandrel were perfectly vertical as seen through the theodolite. Any residual misalignment,and its sense, was determined by rotating the spacecraft on the indexing head until the mandrel was aligned exactly on the theodolite crosshairs. The misalignment angles were then read on the indexing head.

The nitrogen jet roll alignment was then checked by placing the spacecraft on a level, near-frictionless air bearing in a vacuum chamber. The jets were fired with the spacecraft spinning in each direction. The jets were realigned so that a given jet impulse caused an equal spin decrease in each direction, taking into account the drag in each direction. Before the launch of Syncom I, the hydrogen peroxide jets were also aligned in this manner. The optical alignment showed good correlation (0.1 degree) with the air bearing alignment on the three spacecraft tested. Because the Syncom II tanks were not loaded with hydrogen peroxide until immediately before launch, the air bearing alignment check was not made on the hydrogen peroxide jets.

The pitch misalignment of the lateral jets, affecting spacecraft attitude, was within specifications. It does appear, however, that both were aligned through a longitudinal center of gravity slightly below (toward the negative z axis) the nominal center of gravity.

It is believed that, by exercising proper procedures and care in aligning the hydrogen peroxide jets by optical means, accurate jet alignment can be achieved without having to fill the tanks for dynamic alignment. A further refinement in jet alignment may be obtained by balancing those jet biases that cannot be removed.

Hydrogen Peroxide Control System Performance

Orbital operation and performance of the hydrogen peroxide control system were highly satisfactory. The successful orbital velocity control and precession maneuvers completed are an historic first and proved the feasibility of using a hot gas control system to do the job.

The vacuum specific impulse attained in the continuous jet mode of operation was 157 seconds as predicted. Spin pulse jet operation was at an effective specific impulse of 106 seconds in the velocity vector direction (for pulse trains exceeding 900 pulse cycles). For stationkeeping operations (pulse trains from 50 to 100 pulse cycles), the spin pulse specific impulse reduces to about 100 seconds because the jet catalyst bed has not reached equilibrium temperature; therefore, the peroxide decomposition efficiency is low.

The orbital experience with this system is invaluable in providing data for improved accuracy of operation in future Syncom spacecraft.

The control system performance is summarized in Table V-6.

Table V-6
Summary of H_2O_2 Control System Performance

ITEM	ENGINE	ON-TIME, (seconds)	PREDICTED CORRECTION	INDICATED CORRECTION	ESTIMATED FROM TANK PRESSURE	INITIAL H_2O_2 TANK PRESSURE (psia)	FINAL TANK PRESSURE (psia)	PREDICTED EFFECTIVE SPECIFIC IMPULSE (sec)	EFFECTIVE SPECIFIC IMPULSE (sec)
First velocity correction	Axial (continuous)	140	124 fps	110.5 cps	110.5 cps	186	119	157	157
Precession First-step	Axial (pulsing)	56	30 deg	29 to 31 deg		119	115.8		
Second step		87*	54 deg	52 to 53 deg		115.8	110	111	104
Total		143	84 deg	83 deg	88.6				
ΔV			15.5 fps	30 fps	16.3 fps				
Second velocity correction	Radial (pulsing)	393	44 fps	37.5 fps	39.1 fps	106	91	110.8	106.3
Third velocity correction	Radial (Pulsing)	31.5	2.79 fps	*** 2.54 fps		87	86	110	*** 100

*On-time was approximated on: 1) reduced precession angle remaining and 2) distance indicated on reorientation diagram.
**The effective specific impulse (mission) is based on observed orbital corrections and initial and final tank pressure data.
***Insufficient orbital data to predict accurately.

Performance Data

The four orbital maneuvers completed using the H_2O_2 control system consisted of the following:

a) An incremental velocity correction by the axial engine to change the eastward drift rate from 7.01 degrees per orbit to a westward rate of 4.53 degrees per orbit,
b) A precession correction, suing the axial engine in the pulse mode to reorient the spacecraft through 83 degrees,
c) An incremental velocity correction by the pulsed radial engine to reduce the westward drift from 6.82 to 2.67 degrees per orbit, and
d) An orbital correction by the pulsed radial engine to stop the spacecraft at about 59 West longitude and to make the orbit perfectly circular

The first maneuver resulted in a 'V = 110.5 fps (orbital data) after 140 seconds of continuous axial engine operation. Initial ON-time calculations based on average engine flow rate data indicated that a 'V = 124 fps should have been attained. Examination of tank pressure data showed final pressures higher than expected, indicating that the propellant expelled was less than expected. Performance evaluation based on corrected initial and final stabilized tank pressures confirmed a 'V = 110.5 fps and a vacuum specific impulse of 157 seconds.

The second (reorientation) maneuver was made in two steps using the axial engine. An initial precession angle of 29 to 31 degrees was achieved by pulsing the axial engine for 56 seconds (135 pulses). The predicted initial precession angle was 30 degrees. The second precession angle of between 52 and 53 degrees was achieved in 87 seconds (215 pulses). The predicted precession angle of the second step or reorientation was 54 degrees. Thus, the total precession angle predicted was 84 degrees; however, the actual precession angle appears to be about 83 degrees. During the precession maneuver, an increase in westward drift rate of 2.29 degrees per orbit also occurred.

From an analysis of the precession maneuver from initial and final tank pressures and an assumed pulsing specific impulse of 111 seconds, a total precession angle of 88.6 degrees was predicted. Using the actual precession angle and the propellant consumption based on initial and final tank pressures, a precession specific impulse of 104 seconds was calculated.

After reorientation, a reduced orbital drift rate from 6.82 to 2.67 degrees per orbit was attained by pulsing the radial engine for 393 seconds (906 pulses). The corresponding velocity increment was 37.5 fps versus the initially predicted 44 fps. A calculation based on tank pressure data indicates that a 'V = 39.1 fps should have been attained. The effective specific impulse achieved was 106.3 seconds versus 110.8 seconds predicted.

The fourth (or stationkeeping) maneuver provided an approximate 'V = 2.54 fps versus the V = 2.79 fps expected. However, this correction was sufficient to reduce the drift rate to about 0.01 degrees per orbit. The calculated effective specific impulse for the stationkeeping maneuver was about 100 seconds versus the expected specific impulse of 110 seconds. The lower specific impulse results largely because the engine catalyst bed doesn't reach equilibrium temperature and maximum efficiency until over 900 pulses in a pulse cycle are completed.

The differences between the initially predicted and finally calculated pulsing specific impulses can be attributed to the following sources of error:

a) pressure transducer,
b) telemetry,
c) orbital data,
d) engine calibration,
e) jet misalignment,
f) correction factors for variation in spin speed, and the ratio of pulsing-to-continuous values of specific impulse for various pulse durations,

g) pulse lead-time provided by the synchronous controller, and
h) unknown hydrogen peroxide temperature variations and temperature levels.

It is difficult to assess the contribution of any and all of these potential sources of error to the total. However, with the orbital data and analysis results obtained so far, it is probable that predictions of future maneuvers will be within 5 percent of actual results.

Propellant Utilization

The calculated total weight of hydrogen peroxide consumed is 3.237 pounds versus 3.556 pounds predicted. However, the total of velocity corrections and precession angles initially desired were not all achieved with the hydrogen peroxide system.

The propellant utilization is summarized in Table V-7. In arriving at the results, an initial propellant loading of 4.89 pounds was assumed and an initial spacecraft weight (after apogee injection) of 85.53 was used. Neglecting propellant used for jet warming pulses, and assuming zeroperoxide leakage, about 1.65 pound of propellant remains.

Table V-7

Hydrogen Peroxide Utilization

ITEM	ENGINE	SECONDS	NUMBER OF PULSES	PREDICTED W_p, (lb)	ACTUAL* W_p, (lb)	H_2O_2 REMAINING (lb)
First Velocity Correction	Axial (continuous)	140	-	2.067	1.84	3.05
Precession	Axial (pulsing)	57 87	135 215	0.396	0.418	2.632
Second Velocity Correction	Radial (pulsing)	393	906	1.03	0.909	1.723
Third Velocity Correction	Radial (pulsing)	31.5	65	0.063	0.07	1.653

*Based on initial and final tank pressures from telemetry data.
**Initial propellant load of 4.89 pounds; initial spacecraft weight of 85.53 pounds.
Propellant used during warming pulses neglected. Zero system leakage assumed.

Hydrogen Peroxide Storage

Hydrogen peroxide storage capability of the control system has far exceeded expectations. The tank pressure transducer data indicate the exceptional storability of hydrogen peroxide in the passivated 1060 aluminum system, since there has been no detectable long-term pressure rise. Apparently, the system has stabilized at a temperature considerably lower than the 75° F at which a pressure rise of about 2-1/2 percent per year could be expected due to active oxygen loss from the propellant.

Examination of the pressure versus time plot for the peroxide tank indicates that pressure generally held steady except where maneuvers or temperature variations occurred. However, it is difficult to explain wholly the approximate 6 psi drop in pressure since the last maneuver. Part of the drop can definitely be attributed to a lower average peroxide temperature level during the shadow phase of spacecraft operation. Possibly there was a slight temporary leakage through the peroxide valve. The pressure has remained steady over the past three weeks at 79° to 80° F, indicating that peroxide or gas leakage, if it ever occurred, has stopped.

Remaining Control Capability

Assuming the remaining propellant to be 1.65 pounds, an initial spacecraft weight of 80.81 pounds, and a pulsing specific impulse of 100 seconds, the ΔV capability of the peroxide control system is about 64 feet per second. For a stationkeeping requirement of 6 fps per year, the system could theoretically provide stationkeeping for over 10 years, assuming no propellant leakage.

If propellant leakage corresponding to a 6 psi pressure drop after the last maneuver is assumed (about 0.42 pounds), the remaining ΔV capability is 47.7 fps, or about 8 years stationkeeping. This is far in excess of any stationkeeping requirement for Syncom II.

Conclusions

The following conclusions are drawn from the first 160 days of H_2O_2 control system operation:

a) all spacecraft maneuvers were satisfactorily completed,
b) the effective engine specific impulse in the continuous operation mode was 157 seconds,
c) the effective engine specific impulse in the spin pulsing mode varied between 100 and 106 seconds over the pulse mode range of 65 to 906 pulses per maneuver, and
d) the hydrogen peroxide storability in the 1060 aluminum control system has been outstanding. Negligible active oxygen loss is apparent from tank pressure data.

Future performance predictions before spacecraft maneuvering can be more accurate by using the following:

a) improved engine calibration data for pulse-mode operation, particularly over the range of pulse-cycles from 50 to 900 pulses,
b) a hydrogen peroxide tank temperature indicator, and
c) present operational data from Syncom II.

Recommendations

It is recommended that future Syncom spacecraft provide telemetry for monitoring hydrogen peroxide temperature in addition to the tank pressure so as to improve the accuracy of maneuvers and assessment of propellant utilization.

SPACECRAFT SPIN SPEED

The spacecraft spin speed has decreased from 146 rpm at launch to 123.5 rpm at the end of 170 days. This decrease of 22.5 rpm has been attributed to

a) jet misalignment (7.0 rpm),
b) loss of energy associated with the expenditure of hydrogen peroxide and nitrogen (2.5 rpm),
c) apparent leaks in the nitrogen unit (14 rpm), and
d) magnetic effects (negligible).

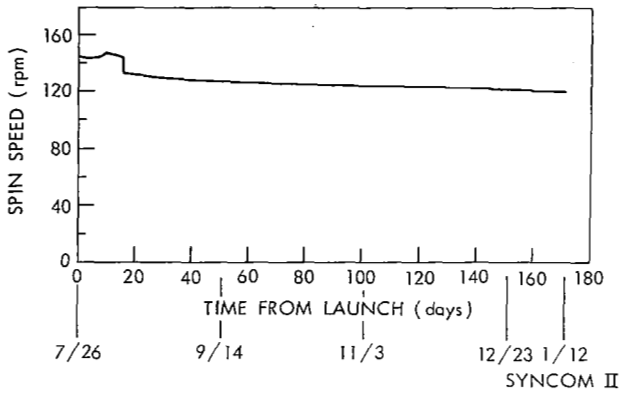

Figure V-19—Spin speed.

The nominal spin speed is 150 rpm, with an operating range from 80 to 200 rpm. This range has been established on the low end by the capability of the ground control equipment in its present configuration and on the high end by acceleration loading on the solar panels.

It is predicted that spin speed will continue to decrease, but the lower operational limit of 80 rpm will not be reached during the operational life of the spacecraft.

The spacecraft spin speed as a function of time is shown in Figure V-19. The effect of apogee motor firing is not evident in the figure because the change was only 0.2 rpm. Significant decreases in spin speed were noted at the times that control jets were operated for velocity corrections. These decreases have been attributed to jet misalignment and loss of energy associated with the expenditure of hydrogen peroxide and nitrogen. The spin speed continued to change, however, when the control jets were not in operation. These changes have been attributed to the effect of the leak in the nitrogen unit.

Effect of Jet Misalignment

Jet misalignment has been discussed in the control subsystem subsection. Spin speed changes caused by jet misalignment, plus that caused by loss of energy, are shown in Table V-8.

A portion of the jet roll misalignment can be accounted for by the law of the conservation of momentum. As fuel is transferred from the tanks through the jet nozzles, energy is extracted from the system. The calculation for the change in spin speed is as follows:

$$I_i \omega_i = I_f \omega_f + M_p R^2 \left(\frac{\omega_i + \omega_f}{2} \right),$$

where

I_i = roll moment of inertia before correction;

I_f = roll moment of inertia after correction;

ω_i = initial angular velocity;

ω_f = final angular velocity;

M_p = mass of propellant expelled;

R = radius of jet exhaust.

For the hydrogen peroxide case, using the lateral jet, the following values are used:

I_i = 1.964 slug-ft^2.

I_f = 1.938 slug-ft^2.

ω_i = 15 rad/sec.

M_p = 0.031 slugs

R = 1.21 feet (exhaust port)

then

$$I_i\omega_i = I_f\omega_f + \frac{M_pR^2\omega_i}{2} + \frac{M_pR^2\omega_f}{2} ,$$

$$\omega_f = \frac{I_i\omega_i - \frac{M_pR^2\omega_i}{2}}{I_f + \frac{M_pR^2}{2}} ,$$

$$\omega_f = \frac{(1.964)(15) - \frac{(0.031)(1.21)^2(15)}{2}}{1.938 + \frac{(0.031)(1.21)^2}{2}} ,$$

$$\omega_f = 14.852 \text{ Rad/sec} .$$

Table V-8

Spin Speed Caused by Jet Firing

CORRECTION	JET USED	FUEL EXPENDED, (Pounds)	$\Delta\omega$ (rpm*)		MISALIGNMENT ANGLE (degrees**)	
			Predicted	Actual	Measured	Apparent
Velocity	H_2O_2 axial	1.80	-1.37	-1.3	-0.055	-0.052
Orientation	H_2O_2 axial	0.38	-0.29		-0.055	
Velocity	H_2O_2 lateral	1.00	-0.74	-5.0	-0.05	-0.33
Orientation	N_2 axial	0.08	-0.013	-0.2	-0.03	-0.45
Velocity	N_2 lateral	1.03	-0.55	-3.0	-0.09	-0.48

*rpm = $\frac{Ia\theta}{6I_z}$

θ deg = $\frac{6I_z}{Ia}$

where

I = portion of total impulse expended;

a = radius of jet;

θ = misalignment angle, degrees;

I_z = roll moment of inertia

= change in spin speed, rpm.

**This figure does not take into account the jet effect of conservation of momentum.

The spin speed decrease is 15-14.852 = 0.148 rad/sec 1.4 rpm, or $1.4/5.0 \times 100 = 28$ percent of total decay.

For the nitrogen case, using the lateral jet (sum of three corrections), the following values are used:

$I_i = 1.938$ slug-ft^2

$I_f = 1.908$ slug-ft^2

$\omega_i = 14.03$ rad/sec

$M_p = 0.032$ slugs

$R = 1.18$ feet

then

$$\omega_f = \frac{I_i\omega_i - \frac{M_pR^2\omega_i}{2}}{I_f + \frac{M_pR^2}{2}} ,$$

$$\omega_f = \frac{(1.938)(14.03) - \frac{(0.032)(1.18)^2(14.03)}{2}}{1.908 + \frac{(0.032)(1.18)^2}{2}} ,$$

$$\omega_f = 13.91 \text{ rad/sec} .$$

The spin speed decrease is 14.03-13.92 = 0.11 rad/sec = 1.05 rpm or $1.05/3 \times 100 = 35$ percent of total decay.

The calculations and the resultant spin speed decay as determined on the basis of the conservation of momentum principle are only approximations. Many variables especially the initial and final moments of inertia, preclude a more accurate calculation.

In summary, the jet misalignment caused a spin speed decrease of 7.0 rpm, and the loss of energy associated with the expenditure of hydrogen peroxide and nitrogen caused a spin speed decrease of 2.5 rpm.

Effect of Leak in Nitrogen Unit

In the period of 18 August to 16 September (29 days), the spin speed dropped from 130.8 rpm to 128.3 rpm, or 2.5 rpm. The roll moment of inertia is approximately 1.90 slug-ft^2 with the amounts of propellants remaining, indicating an angular momentum change of 0.50 ft-lb$_f$/sec. During the same period, nitrogen pressure had dropped from 680 psia to 570 psia, a drop of 110 psia, corresponding to leakage of 0.0834 pound of gas. Assuming a specific impulse, here taken as 60 seconds, a roll moment arm can be calculated that would account for the spin decay thus

$$= \frac{0.50}{0.0834 \times 60} = 0.10 \text{ (foot)}.$$

If the gas escapes at a radius of 1.1 foot, this moment arm will result if there is an angle of 5.2 degrees between the resulting force and the plane containing the spin axis and the point of gas escape. This amount of deviation seems reasonable for a leak on one side of a valve seat, or even for gas escaping around one of the inlet fittings. The same was also true earlier when the leak rate was 35 psia per day and the spin rate decay was 0.86 rpm per day.

On the fifth day following launch, the spin speed started to increase, and at the same time, the nitrogen pressure started to decrease. This condition was maintained for five days, at which time the spin speed started to decrease - the N_2 pressure continuing to decrease. From that time on, the spin rate has continually declined, the decay being exponential when not affected by jet operation. The rate of decay of the N_2 pressure follows a similar curve. It is assumed, therefore, that the N_2 leak has produced a spin rate decay, and furthermore, that the increase in spin rate was also caused by this leak. It has been shown that a leak vector of only 5 degrees could produce such a spin rate decay. The change in tank pressure could cause this thrust vector to shift across the centerline or zero roll moment plane, thereby producing a torque of the opposite sense. While there is no positive proof that this did happen, it is the most reasonable explanation of the spin rate reversal.

Magnetic Effects

The possibility that magnetic effects, rather than or in addition to a roll moment caused by gas leakage, might be a significant factor causing the decrease of spin rate was examined. It was concluded that magnetic effects could account, at most, for 1 percent of the observed rate of spin decrease.

Eddy Current Effect

A lower bound on the spin damping time constant is

$$\tau = \frac{1.50 \times 10^{-4} \text{ kg ohm/m}^2}{B_\perp^2} ,$$

where $B_\perp$ is the magnetic field normal to the spin axis. If $B_\perp$ is substituted in webers per square meter, the resulting τ is in seconds. The radial component of the earth's magnetic field (equal to $B_\perp$ for nominal attitude) is given approximately by

$$0.630 \sin \lambda_m \frac{R^3}{R_e} \text{ (gauss)} ,$$

where λ_m is the magnetic latitude, R the radius, and R_e the radius of the earth. At the synchronous radius with λ_m = 90 degrees, this field is 0.00218 gauss (218 gamma, or 2.18×10^{-7} weber/m_2). Using this conservative value, it is found that τ cannot be less that 3.15×10^9 seconds (3.65×10^4 days or 100 years). This estimate is probably low by a factor of 3 or 4 because of the geometry for the orbit of Syncom II, and low by perhaps a factor of 10^2 because of the spacecraft configuration as compared to the model used. On the other hand, if the observed decay is exponential, the time constant must be about

$$\frac{129.5 \text{ rpm}}{2.5 \text{ rpm}} \times 29 \text{ days} = 1500 \text{ days, or } 4.1 \text{ years.}$$

Therefore, eddy current damping fails to account for the spin decay by at least two, and probably four or more, orders of magnitude.

"Motor" Effect

Because the spacecraft is illuminated from essentially a fixed spatial direction, it is possible for the current drawn from the solar power supply to flow so that it generates a space-fixed

component of magnetic moment normal to the spin axis; that is, the power supply wiring can act as an armature winding, and the current in this "winding" can be effectively "commutated" by the illumination of the solar panels. In the earth's magnetic field, this effect would result in a net roll moment. Consideration of the geometry of the orbit relative to the earth's magnetic field shows that this roll moment would have a non-zero average value over an orbital revolution.

The roll moment is given by $G = BM$, where M is the magnetic moment. Again using the maximum B from the earth's field, the torque is

$$G = 2.18 \times 10^{-7} \frac{\text{newton-meters}}{\text{ampere-turn/m}^2} \cdot M ,$$

$$= 1.60 \times 10^{-7} \frac{\text{ft-lb}_f}{\text{ampere-turn/m}^2} \cdot M .$$

The average torque observed for Syncom II is

$$G = \frac{0.50 \text{ ft-lb}_f/\text{sec}}{(29 \times 85,400)} = 2.0 \times 10^{-7} \text{ ft-lb}_f$$

This means that even with the favorable assumptions regarding geometry, a magnetic moment of 1.25 ampere-turn/m^2 would be required. The result is probably low by a factor of 3 because of the crude assumption. As a result of careful examination, it has been concluded that the magnetic moment should not exceed about 0.04 ampere-turn/m^2 at full power drain. It has also been concluded that the "motor" effect is too small by two orders of magnitude to account for the observed spin rate decrease.

Spin Speed Predictions

Although the magnetic effects have contributed to spin speed decay, the major portion of the decay has been attributed to the nitrogen leak. It appears that the nitrogen leak and the spin decay are following similar exponential curves.

Considering only the following effects and neglecting any additional abnormalities, the spin rate will remain above the minimum operational limit of 80 rpm for many years.

a) The nitrogen unit will not be used. The nitrogen leakage will account for an additional spin decay of 8 rpm until the nitrogen unit is depleted.
b) The hydrogen peroxide unit will be pulsed for stationkeeping purposes once every 2 months. This will account for a spin rate decay of 0.05 rpm per month.
c) Magnetic effects will account for a spin rate decay of 0.1 rpm per month. While this assumption is not necessarily correct, it does appear to be an upper limit of the magnetic effects.

SUN SENSOR OPERATION

Five of the seven sun sensors are known to have functioned properly. This includes the redundant pair of ψ, ψ_2 sensors which are utilized for attitude determination and one of the three single sensors which has been used in a successful quadrant mode maneuver. The two remaining single sensors have yet to be used.

The spacecraft attitude with respect to the sunline is a parameter that must be determined to enable proper orientation of the spacecraft for optimum antenna beam coverage. The sun angle, ϕ, measured from the positive spin axis is also used in determining solar power available to the spacecraft power supply. The sun angle, ϕ, is calculated from the equation: $\cot \phi = \sin \psi_2 \cot I$, where I is the fixed angle of 35 degrees between the ψ and ψ_2 beam planes, ψ and ψ_2 being the nomenclature for the set of solar sensors. The angle ψ_2 is measured using the ratio of the separation of the ψ and ψ_2 pulses and the separation of adjacent ψ pulses. The separation of the ψ pulses represents the spacecraft period of revolution.

Based upon a root-mean-square distribution the ψ_2 readings appear to be accurate to ±.15 degrees. Residual bias errors, such as sensor misalignment, appear to be negligible, and they tend to cancel out over extended periods of time. Of the two parameters required to determine spacecraft attitude, the ψ_2 reading is considerably more accurate than is the polarization angle measurement.

The sun angle as a function of time is shown in Figure V-20. The ϕ angle during the transfer orbit was 69 ± 0.2 degree. After apogee boost, the ϕ angle decreased daily until the initial orientation maneuver on the fifth day. This maneuver resulted in a ϕ angle shift from 64 to 101 degrees. With the exception of slight changes resulting from additional velocity and orientation corrections, the ϕ angle steadily increased to 111 degrees on 24 September. On 29 September, the ϕ angle started to decrease toward the minimum value of 68.4 degrees, which should occur six months later.

Maximum solar power (ϕ = 90 degrees) was available during the months of December 1963 and January 1964 when the power demand was at a maximum because of the eclipse period.

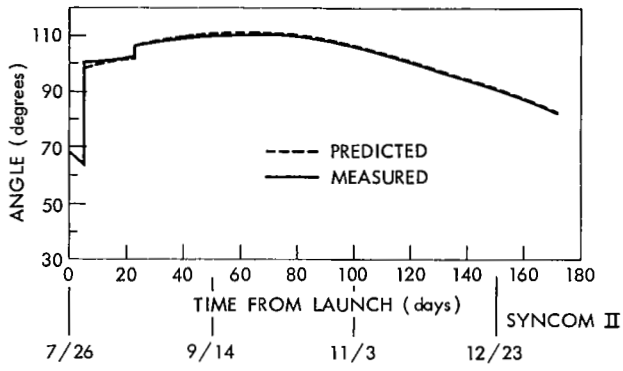

Figure V-20—Sun angle, ϕ, from spin axis.

APOGEE MOTOR TIMER

The apogee motor was ignited automatically by the onboard timer five hours and twenty-four minutes after third stage separation. The nominal time of five of this timer, as determined by environmental testing, was five hours and twenty minutes at an average temperature of +60° F. The actual firing time corresponds to an average temperature of +70° F. The allowable deviation from nominal is plus or minus ten minutes.

ACCELEROMETER OPERATION

Figure V-21 shows a plot of the spacecraft acceleration during first-, second-, and third-stage burning as monitored by the spacecraft accelerometer. Figure V-22 shows a similar plot of the acceleration experienced during apogee motor boost. As initial accelerometer calibration data at high acceleration levels was only an approximation, the calibration on the

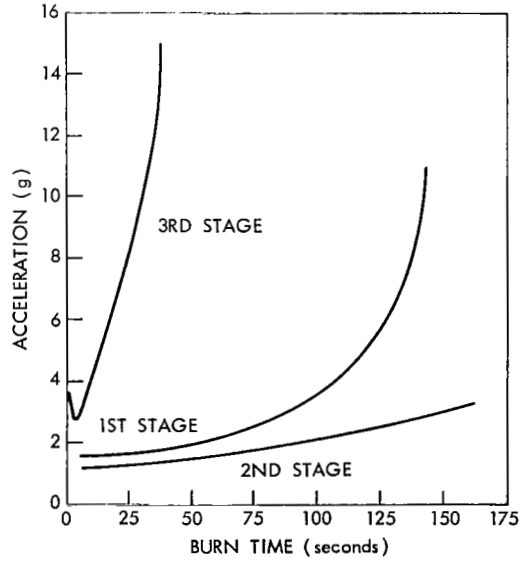

Figure V-21—Spacecraft acceleration from Thor-Delta booster.

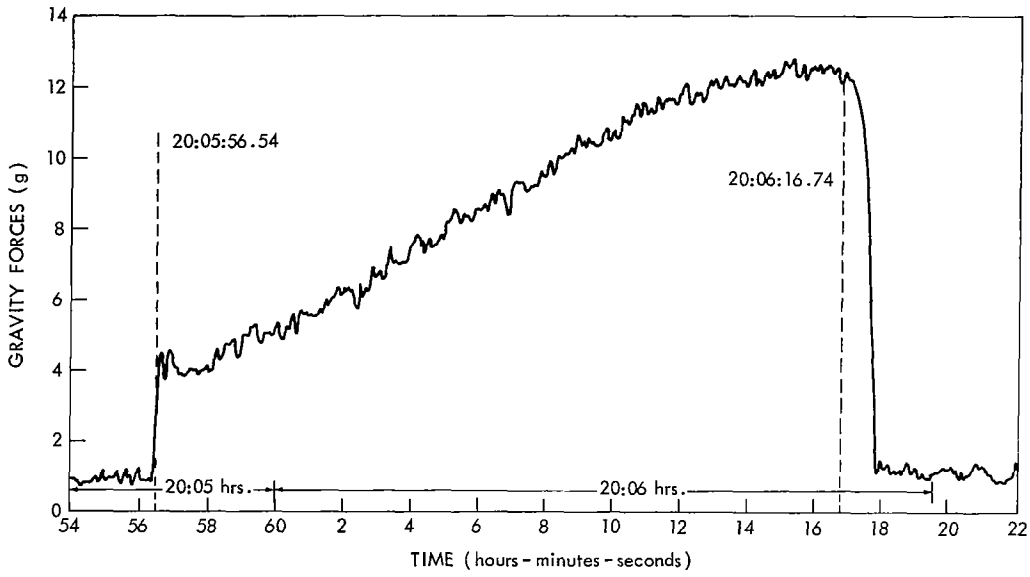

Figure V-22—Spacecraft acceleration during apogee motor boost.

depicted curves was determined by comparing the maximum point on the apogee motor boost curve with that calculated from nominal conditions. The error in this calibration is considered to be small because the injection orbit parameters and conditions are accurately known. One factor affecting the accuracy of the accelerometer calibration is the limiting of the ground receiver which begins at 12 g.

The 0.8 g acceleration before apogee motor boost is caused by spacecraft spin. The slightly higher level following boost is possibly caused by noise, as the level returns to 0.8 g after approximately five seconds. The apogee motor acceleration time is 20.2 seconds. While this is not necessarily the total burning time, the burning time would not be less than 20.2 seconds.

TELEMETRY AND TRAVELING-WAVE TUBE POWER

Telemetry transmitter 1 power output (referenced to the output of the telemetry bias unit) is shown in Figure V-23. Shown in the same figure is a plot of the power output of traveling-wave tube 2, referenced to the antenna input. The indicated power from the telemetry transmitter is approximately 1 db higher than the average recorded during 15 systems tests made before launch. Telemetry transmitter 2 has been used only briefly, with an indicated power output of 29.8 dbm, 1 db below the ground test indication.

The traveling-wave tube 2 telemetered power output, 32.3 dbm, is 0.7 db greater than that measured on the ground. Traveling-wave tube 1, when used, has indicated a power output 1 db greater than that recorded during ground testing. These

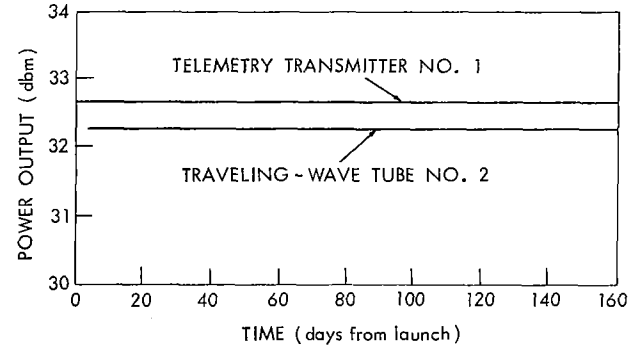

Figure V-23—Telemetry transmitter and traveling-wave tube power.

differences between ground and space performance are not significant, since they are of the same order of magnitude as the telemetry accuracy.

The power stability of each transmitter has been good. The only power changes noted to date have been caused by loading the power supply to point where the voltage to the telemetry transmitter has dropped out of regulation. This situation does not exist when a low duty cycle of telemetry operation is used in conjunction with full-time transponder operation.

TELEMETRY AND COMMUNICATION SUBSYSTEM OPERATING CYCLES

The telemetry and communications subsystems have operated for long periods of time and have been repeatedly turned off and on (see Table V-9). No apparent degradation has resulted from this use.

Table V-9

Operating Cycles of Telemetry and Communication Subsystems

SUBSYSTEM ELEMENT	HOURS OF OPERATION	ON-OFF CYCLES
Telemetry transmitter 1	1380	1079
Telemetry encoder 1	1380	1079
Telemetry transmitter 2	5.8	20
Telemetry encoder 2	6.5	28
Communications transmitter 1 filament	35.7	47
Communications transmitter 2 filament	2120	173
Communications transmitter 1 high voltage	25	22
Communications transmitter 2 high voltage	2101	152
Communications receiver 1	910	175
Communications receiver 2	1224	152

COMPARISON OF ACTUAL AND EXPECTED TELEMETRY SIGNAL LEVELS

In Table V-10 the parameters related to the telemetry spacecraft-to-ground link are listed. The transmitter power level of 1.7 watts was measured just before launch. This power level is one of the telemetered channels and no measurable change has resulted since launch, except on specific occasions when the battery voltage was unusually low.

A nominal value of 0.0 db was used for the spacecraft antenna gain and 20.0 db for the gain of the ground receiving antenna. Since telemetry carrier signal levels are usually recorded when the telemetry subcarrier is on, and therefore suppressing the carrier level due to the phase modulation index of 1.2, a carrier loss of 3.4 db is shown. The resulting expected carrier level is 123.6 dbm.

In Table V-11 the telemetry signal parameters measured at the Lakehurst telemetry and command station on 8 January 1964 are listed. Here it is noted that the carrier levels varied from a minimum of -127 dbm to a maximum of -122 dbm. The ground antenna was in the right circular polarization mode throughout the period. The spacecraft signal transmitted is elliptically polarized. The signal level variations in Table V-11 are caused by changes in the apparent spacecraft antenna gain due to changes in the antenna angle, slant range variation changes in polarization angle, and ground receiver gain fluctuations. The received carrier level calibration accuracy for the ground station is approximately ±2 db and the tolerance on the ground antenna gain is about

Table V-10

Telemetry Link-Spacecraft to Ground .136 Mc

CHARACTERISTIC	VALUE
Transmitter power 1.7 watts	2.3 dbw
Cable loss	0.1 db
Attenuator loss	1.5 db
Diplexer loss	0.7 db
Hybrid-balum loss	0.5
Radiated power	-0.5 dbw
Spacecraft antenna gain	0.0 db
Propagation loss	167.4 db
Ground antenna gain	20.0 db
Line loss preceding paramp	0.3 db
Filter loss	2.0 db
Carrier suppression due to mod. index	3.4 db
Expected received carrier level	-123.6 dbm

Table V-11

Telemetry Signal Parameters Measured at Lakehurst Telemetry and Command Station on 8 January 1964

TIME (Zulu)	AZIMUTH	ELEVATION	RECEIVED CARRIER LEVEL
0300	131°	61°	-123 dbm
0400	141	55	-124
0500	150	48	-124
0600	158	40	-124
0700	164	32	-124
0800	168	24	-125
0900	170	17	-125
1000	170	12	-126
1100	169	8	-125
1200	166	7	-127
1300	164	8	-127
1400	161	11	-125
1500	159	17	-122
1600	158	24	-127
1700	157	33	-123
1800	157	42	-123
1900	157	51	-123
2000	155	60	-123
2100	150	68	-122
2200	139	73	-123
2300	125	74	-122

±1.5 db. It is therefore evident that the calculated value of the received carrier level (-123.6 dbm) is in good agreement with the arithmetic mean of the extremes of the measured signal levels (-124.5 dbm).

COMMAND SYSTEM PERFORMANCE

Some problems have been experienced from time to time with the spacecraft commands. These problems have followed no definite pattern and have not been repeatable.

The general nature of the problems has been a) no verification or improper verification of transmitted commands b) apparently no response to executed commands c) response to command different from the command transmitted to the spacecraft.

None of the problems associated with the command function can be attributed with certainty to spacecraft malfunction.

Each of the above problems has been studied at the time of the occurrence and has been classified into one of the following categories:

a) Operational errors - during the early phase of the in-orbit tests there were cases of erroneous commands sent to the spacecraft. The problems could be isolated to operational techniques at the station or improper instructions from the communication space operations center.

b) Weak signal resulting from low elevation angle - the schedule operation for the telemetry and command stations has been such that in numerous cases the spacecraft has been at a relatively low elevation angle at the time that commands have been sent. Under such conditions the transmitted signal to the spacecraft is affected by multipaths, attenuation, and polarization shifts. The exact character of the signal may be altered to the extent that the command train does not reach the spacecraft in the same format as that generated by the ground equipment.

c) Improper polarization of the transmitted signal - In determining which antenna polarization to use when commands are sent to the spacecraft, it is operational procedure to use the polarization producing the best signal from the spacecraft-to-ground telemetry link as the polarization for transmission of command signals to the satellite. The procedure is satisfactory when the telemetry is in continuous use. Recently the telemetry is put in use only intermittently at times when telemetry data are desired or commands must be sent to the spacecraft. In this situation, turn-on procedures are normally "blind"; that is, no received telemetry signal is available from the satellite on which to base a beforehand choice of polarization to be used in issuing a turn-on command. Throughout the day the polarization shifts. No reliable pattern has been established which represents the daily shift. Failure resulting in the wrong choice of polarization is presumed but cannot be verified, except that switching to another polarization after observance of a command anomaly invariably produced correct command response.

d) Lack of command verification - Lack of a telemetry signal prior to blind turn-on prevents operational personnel from taking advantage of the command verification feature of the telemetry and command system to verify turn-on commands. If the spacecraft does not receive the programmed command there is no way for determining so until the command executions start and the spacecraft does not respond as intended. Where the spacecraft has failed to respond or has responded incorrectly, the presumption can be made that it received no command or the wrong command but the actual difficulty cannot be established with certainty. Notwithstanding, the many varied conditions under which commands are sent to the spacecraft including the blind turn-on, the confidence factor for proper response to a properly sent command is in excess of 99 percent.

e) Radio frequency interference (RFI) - The Kingsport experienced considerable RFI. It appears that this RFI causes the command verification to report receipt or erroneous commands by the spacecraft. Conceivably, this RFI could affect the command sent to the

spacecraft, but, more likely, it interfered with receipt of the command verification causing the receiving system to display an erroneous verification.

f) The Triax antenna aboard ship did not appear to be as effective as the TACO antenna for transmitting commands. The poorer performance of the Triax is believed to be traceable to its lower transmission gain and polarization selection problems. Limit stops on the Triax also hampered its effectiveness at low-horizon positions of the spacecraft (also a problem with the TACO antenna).

Since the launch of the Syncom II spacecraft on 26 July 1963, approximately 8400 commands have been sent to the spacecraft from the three ground stations. The major command responsibility has been shared by the T and C station aboard the USNS Kingsport and by the T and C station at Lakehurst, New Jersey. The Johannesburg T and C station, which served as backup to the Kingsport during the transfer orbit and initial drift orbit phase, was relieved of T and C responsibility on 16 August because, at this time, the periods of spacecraft visibility due to the westward drift toward final orbit position were too short to justify continued manning of this station.

Between launch day, 26 July 1963 and 31 December 1963, 8400 commands were sent to the spacecraft. The total includes enable, command, and execute tones transmitted via the ground-to-spacecraft link on the 148 mc carrier.

During this period the problems encountered with ground-to-spacecraft commands represented less than 1.5 percent of the total commands sent.

An analysis of the particular environment and conditions at each of the ground stations could rationalize 78 percent of the 119 improper responses or actions; the most serious area being attributable to ground antennas, particularly to the proper selection of polarization.

Of particular note were the RFI problems encountered by the ship. These problems were generated by equipments external to the T and C equipment, but did contribute to this reduction of effectiveness of the ground-to-spacecraft command link or the spacecraft-to-ground verification link.

Even though the T and C operations scheduled were based to some degree on periods of best visibility, there were numerous occasions, particularly during the early phases or late phases of the tracking period, when the spacecraft was low on the horizon with respect to the ground station. The TACO antenna used for T and C has limit stops at +10 degrees elevation, therefore the ground to spacecraft signal is significantly degraded at spacecraft elevation angles low on the horizon.

There were 26 cases where no action or erroneous action was taken on the spacecraft that cannot be positively assessed into one of the categories discussed. Due to the fact that no command problems have reoccurred to establish a pattern or trend, Hughes Aircraft has an extremely high confidence that the random sampling could be properly categorized if all of the influencing factors were available and cannot be attributed to any spacecraft degradation or malfunction. At no time has a command problem cancelled, delayed, or compromised any of the critical operations on the spacecraft, viz. velocity or orientation maneuvers. The command problems have occurred randomly during routine operations.

EFFECT OF ECLIPSE ON SPACECRAFT PERFORMANCE

Syncom II entered its first semi-annual eclipse period on 4 December 1963. This eclipse phase will continue daily until 18 January 1964, with the maximum eclipse of seventy (70) minutes occurring on 26 December (see Figure V-24). Special tests have been conducted to monitor telemetry data through the eclipse and for a sufficient number of hours following the eclipse to determine voltage, temperature transients and time constants.

The eclipse phase has apparently had no ill effects on spacecraft performance. To the contrary, in some areas a definite improvement has been noted. Observations of telemetered data reveal the following information regarding spacecraft performance during the eclipse phase.

The solar array has exhibited an increase of approximately two watts (as determined by weekly solar array tests) since entering the eclipse period. Attainment of this extra power by thermal means would require the solar array average temperature to be 16° F below pre-eclipse phase ambient, two hours following the daily eclipse when the power tests are conducted. Thermal considerations indicate that this is not probable. The temperature at sensor 2 returns to ambient in approximately six hours. (See Figure V-25.)

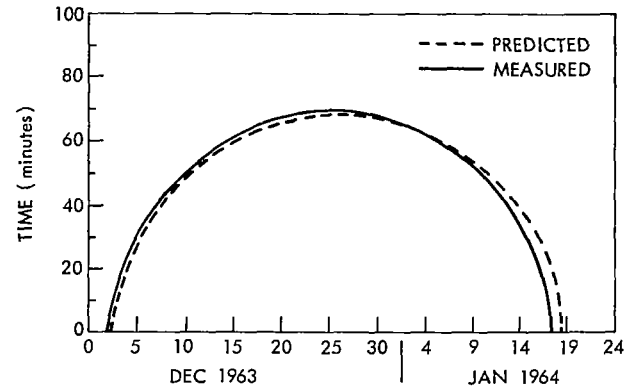

Figure V-24—Solar eclipse.

A changing power load, brought about by thermal shock, could also cause the available power to show an increase. This possibility has been examined by comparing transmitted powers before and after the apparent increase. No sign of any power variation is in evidence from either of the four transmitters. An abnormal current drain of approximately 100 milliamperes during the first few months in orbit would have been apparent. The loss of this drain, however, at the beginning of the eclipse phase, would have been required to show the apparent two watt increase.

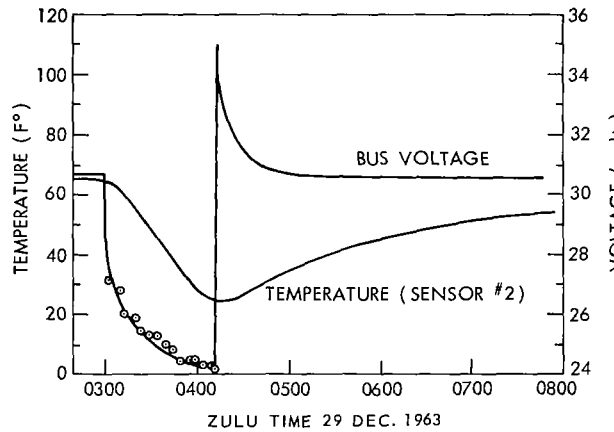

Figure V-25—Spacecraft temperature and bus voltage through eclipse.

If radiation damaged solar cells and glass cover slides are exposed to temperatures in the order of several hundred degrees, an annealing process takes place to restore a portion of the lost power capability. Thermal analysis reveals that temperatures of this magnitude were not encountered, although thermal shocks of 100°-150° F are felt each time the spacecraft passes through an eclipse. There is a possibility that this thermal shock treatment could have restored at least a fraction of the observed power increase.

Until solar cell radiation tests are completed and/or the eclipse period comes to an end it must be assumed that some combination of the aforementioned possibilities accounts for the apparent two watt increase.

The hydrogen peroxide pressure has decreased by 4 to 6 psia since the eclipse season began, with the greater fraction of the decrease taking place in the first two weeks. This pressure change is equivalent to approximately a 30° F temperature decrease, a situation which does not match the thermal model. As a matter of fact, the telemetry (both encoders) indicates that the H_2O_2 pressure returns to ambient in three hours (see Figure V-26). Because the H_2O_2 system was used one week prior to the eclipse phase a small leak in the system cannot be ruled out at this time. This uncertainty will be clarified following the completion of the eclipse period. The N pressure does not appear to be greatly affected by the shadowing cycles.

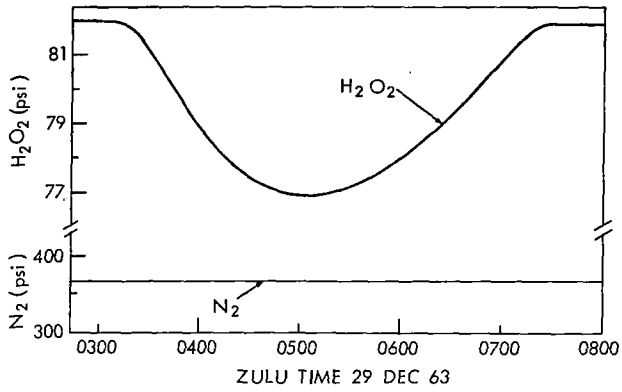

Figure V-26—Spacecraft H_2O_2 and N_2 pressures through eclipse.

The remaining spacecraft parameters have followed predicted patterns throughout the eclipsing. As previously mentioned, the transmitter powers have not changed. The temperatures monitored during and following the eclipses and associated thermal time constants have been close to that expected. The transponders have not been operated during periods of shadowing, but have operated successfully only forty minutes following the eclipse. In general, it can be said that the spacecraft has easily survived its first encounter with the eclipse cycle.

RELIABILITY

Although the accumulated communication time of over 2100 hours after 170 days in orbit is an outstanding achievement, no correlation of reliability predictions has been attempted due to the long expected life of the components and systems used.

Every system has been used successfully at least once.

The only known degradation is that of the solar array (this was predicted) and a small nitrogen leak which has contributed to the reduction of spin speed and reduced orbit correction capacity of the nitrogen gas control system.

"The aeronautical and space activities of the United States shall be conducted so as to contribute . . . to the expansion of human knowledge of phenomena in the atmosphere and space. The Administration shall provide for the widest practicable and appropriate dissemination of information concerning its activities and the results thereof."

—NATIONAL AERONAUTICS AND SPACE ACT OF 1958

NASA SCIENTIFIC AND TECHNICAL PUBLICATIONS

TECHNICAL REPORTS: Scientific and technical information considered important, complete, and a lasting contribution to existing knowledge.

TECHNICAL NOTES: Information less broad in scope but nevertheless of importance as a contribution to existing knowledge.

TECHNICAL MEMORANDUMS: Information receiving limited distribution because of preliminary data, security classification, or other reasons.

CONTRACTOR REPORTS: Technical information generated in connection with a NASA contract or grant and released under NASA auspices.

TECHNICAL TRANSLATIONS: Information published in a foreign language considered to merit NASA distribution in English.

SPECIAL PUBLICATIONS: Information derived from or of value to NASA activities. Publications include conference proceedings, monographs, data compilations, handbooks, sourcebooks, and special bibliographies.

TECHNOLOGY UTILIZATION PUBLICATIONS: Information on technology used by NASA that may be of particular interest in commercial and other nonaerospace applications. Publications include Tech Briefs; Technology Utilization Reports and Notes; and Technology Surveys.

Details on the availability of these publications may be obtained from:

SCIENTIFIC AND TECHNICAL INFORMATION DIVISION

NATIONAL AERONAUTICS AND SPACE ADMINISTRATION

Washington, D.C. 20546